

BYPASSING TRANSDOMINANT INHIBITION WITH
CHIMERIC p53 FOR CANCER GENE THERAPY

by

Abood Okal

A dissertation submitted to the faculty of
The University of Utah
in partial fulfillment of the requirements for the degree of

Doctor of Philosophy

Department of Pharmaceutics and Pharmaceutical Chemistry

The University of Utah

August 2014

Copyright © Abood Okal 2014

All Rights Reserved

The University of Utah Graduate School

STATEMENT OF DISSERTATION APPROVAL

The dissertation of Abood Okal
has been approved by the following supervisory committee members:

Carol S. Lim, Chair April 22, 2014
Date Approved

David W. Grainger, Member April 22, 2014
Date Approved

Jindřich Kopeček, Member April 22, 2014
Date Approved

James N. Herron, Member April 22, 2014
Date Approved

Philip J. Moos, Member April 22, 2014
Date Approved

and by David W. Grainger, Chair/Dean of
the Department/College/School of Pharmaceutics and Pharmaceutical Chemistry

and by David B. Kieda, Dean of The Graduate School.

ABSTRACT

It is well documented that more than 50% of all human cancers have a mutated p53 gene status, rendering it inactive. The resulting tumor-derived p53 variants, similar to wild-type (wt) p53, retain their ability to oligomerize via the tetramerization domain. Upon hetero-oligomerization, mutant p53 enforces a dominant negative effect over active wt-p53 in cancer cells. To overcome this barrier, we have designed a chimeric superactive p53 (p53-CC) with an alternative oligomerization domain (CC) from breakpoint cluster region (Bcr). This approach led to the hypothesis that *swapping the oligomerization domain of p53 with an alternative oligomerization domain will prevent hetero-oligomerization and transdominant inhibition by mutant p53 in cancer cells.*

The tumor suppressor activity of the chimeric p53-CC was evaluated *in vitro* and found to be similar to that of wt-p53 regardless of cancer type or endogenous p53 status. However, co-immunoprecipitation and viral transduction of p53-CC and wt-p53 into a breast cancer cell line that harbors a tumor derived transdominant mutant p53 validated that p53-CC indeed evades sequestration and consequent transdominant inhibition by endogenous mutant p53. Following proof-of-concept studies, the superior tumor suppressor activity of p53-CC and its ability to cause tumor regression of the MDA-MB-468 aggressive p53-dominant negative breast cancer tumor model was demonstrated *in vivo*. In addition, the underlying differential mechanisms of activity for p53-CC and wt-p53 delivered using viral-mediated gene therapy approach in the MDA-MB-468 tumor

model were investigated. Finally, since domain swapping to create p53-CC could result in p53-CC interacting with endogenous Bcr, which is ubiquitous in cells, modifications on the CC domain were necessary to minimize potential interactions with Bcr. Hence, the possible design of mutations that will improve homo-dimerization of CC mutants and disfavor hetero-oligomerization with wild-type CC (CCwt) were investigated, with the goal of minimizing potential interactions with endogenous Bcr in cells. Indeed, the resulting lead candidate p53-CCmutE34K-R55E avoided binding to endogenous Bcr and retained p53 tumor suppressor activity.

Although breast cancer was the main focus of this dissertation, the application of this research extends to many other types of cancer, including the deadliest cancers (pancreatic, lung, and ovarian), which currently lack effective treatments.

TABLE OF CONTENTS

ABSTRACT.....	iii
LIST OF FIGURES.....	ix
LIST OF TABLES.....	xii
LIST OF ABBREVIATIONS.....	xiii
ACKNOWLEDGEMENTS.....	xvi
Chapter	
1. INTRODUCTION AND BACKGROUND	1
1.1 Introduction	1
1.2 Rationale of Study	2
1.3 Summary of Thesis.....	3
1.4 Background	4
1.4.1 Cancer.....	4
1.4.2 Breast Cancer.....	5
1.4.3 Triple Negative Breast Cancer	6
1.4.4 The Tumor Suppressor p53	7
1.4.5 Dominant Negative Effect of Mutant p53	13
1.4.6 Alternative TD: Coiled-Coil Domain	16
1.4.7 Break Point Cluster Region (Bcr).....	17
1.4.8 Gene Therapy	18
1.5 Statement of Objectives.....	21
1.6 References	23
2. CANCER BIOLOGY: SOME CAUSES FOR A VARIETY OF DIFFERENT DISEASES	35
2.1 Abstract	35
2.2 Introduction	36
2.3 Origins of Cancer	36
2.3.1 Cancer Stem Cells	36
2.3.2 Cancer Stem Cell vs. Stochastic Model.....	40
2.4 Pathways that Lead to Cancer	40
2.4.1 Genetic Changes.....	41

2.4.2 Epigenetic Alterations	50
2.5 miRNA in Cancer Diagnosis	52
2.6 Nutrients and Metabolic Characteristics of Cancer	53
2.6.1 Organic Players: How Tumors Feed and Grow	55
2.6.2 Inorganic Compounds	64
2.7 The Cancer Microenvironment	66
2.7.1 The Stroma and its Components	67
2.7.2 The Invasion-Metastasis Cascade	70
2.8 Conclusion	74
2.9 References	74
3. A CHIMERIC P53 EVADES MUTANT p53 TRANSDOMINANT INHIBITION IN CANCER CELLS	91
3.1 Abstract	91
3.2 Introduction	92
3.3 Materials and Methods	95
3.3.1 Construction of Plasmids (Figure 3.1A)	95
3.3.2 Cell Lines and Transient Transfection	96
3.3.3 Microscopy	97
3.3.4 qRT-PCR	97
3.3.5 Western Blotting	98
3.3.6 TUNEL Assay	98
3.3.7 Annexin-V Assay	99
3.3.8 7-AAD Assay	99
3.3.9 Colony Forming Assay (CFA)	100
3.3.10 Reporter Gene Assay	100
3.3.11 Coimmunoprecipitation (co-IP)	101
3.3.12 Overexpression of Mutant p53	102
3.3.13 Recombinant Adenovirus Production	102
3.4 Results	103
3.4.1 p53-CC Localizes to the Nucleus	103
3.4.2 Wt p53 and p53-CC Show Similar Gene Expression Profiles	103
3.4.3 p53-CC Exhibits Tumor Suppressor Activity	107
3.4.4 p53-CC Maintains Transcriptional Activity of p53 Target Genes	111
3.4.5 p53-CC Avoids Interaction with Endogenous p53	111
3.4.6 Bypassing the dominant negative effect	113
3.5 Discussion	116
3.6 References	120
4. RE-ENGINEERED p53 ACTIVATES APOPTOSIS IN VIVO AND CAUSES PRIMARY TUMOR REGRESSION IN A DOMINANT NEGATIVE BREAST CANCER XENOGRAFT MODEL	125
4.1 Abstract	125
4.2 Introduction	126
4.3 Materials and Methods	128
4.3.1 Recombinant Adenovirus Production	128
4.3.2 Cell Lines and Viral Transductions	129
4.3.3 7-AAD Assay	129

4.3.4 TMRE Assay	130
4.3.5 Caspase-3/7 Assay.....	130
4.3.6 Annexin-V Assay	131
4.3.7 <i>In Vivo</i> Study	131
4.3.8 Histology	132
4.3.9 Western Blotting.....	132
4.3.10 Statistical Analysis	133
4.4 Results	134
4.4.1 p53-CC Induces Higher Levels of Cell Death Compared to Wt-p53	134
4.4.2 p53-CC Caused Cell Death via the Apoptotic Pathway	134
4.4.3 <i>In vivo</i> Efficacy in a Dominant Negative Breast Cancer Animal Model.....	137
4.4.4 Histopathological Evaluation of Tumor Tissues and Evidence for Tumor Suppressor Activity	140
4.4.5 Detection of Pathway-Specific Markers for Cell Cycle Arrest and Apoptosis	143
4.5 Discussion	144
4.6 References	149
5. A RE-ENGINEERED p53 CHIMERA WITH ENHANCED HOMO-OLIGOMERIZATION THAT MAINTAINS TUMOR SUPPRESSOR ACTIVITY	154
5.1 Abstract	154
5.2 Introduction	155
5.3 Materials and Methods	160
5.3.1 Computational Modeling and Simulation.....	160
5.3.2 Cell Lines and Transient Transfections	162
5.3.3 Plasmid Construction.....	162
5.3.4 7- AAD Assay	164
5.3.5 Mammalian Two-Hybrid Assay	164
5.3.6 Coimmunoprecipitation (Co-IP).....	165
5.3.7 Statistical Analysis	166
5.4 Results	166
5.4.1 <i>In Silico</i> Modeling of Coiled-Coil Structure and Estimation of Binding Free Energies	166
5.4.2 Initial Screening for <i>In Vitro</i> Activity	169
5.4.3 Global Stability of p53-CCmutE34K-R55E.....	171
5.4.4 Binding Assay Validates Design	173
5.4.5 p53-CCmutE34K-R55E Interaction with Endogenous Bcr.....	175
5.4.6 p53-CCmutE34K-R55E Induces Apoptosis Regardless of the p53 Status or Cancer Cell Type	177
5.4.7 p53-CCmutE34K-R55E Induces Apoptosis Regardless of the p53 Status or Cancer Cell Type	177
5.4.8 p53-CCmutE34K-R55E Induces Apoptosis Regardless of the p53 Status or Cancer Cell Type	177
5.5 Discussion	177
5.5.1 Explanation of the Potential Deviation between Results Obtained <i>In Silico</i> and <i>In Vitro</i>	181
5.6 Supporting Information	184
5.7 References	185
6. CONCLUSIONS AND FUTURE WORK.....	190
6.1 Conclusions	190
6.1.1 Chimeric p53-CC Maintains Tumor Suppressor Function.....	191
6.1.2 Validation of p53-CC Tumor Suppresspr Function <i>In Vivo</i>	192

6.1.3 Altering the Design of the p53-CC Chimera to Minimize Interaction with Bcr	193
6.2 Future Studies.....	194
6.2.1 Exploring the Differential in Target Gene Regulation by p53-CC vs Wt p53	194
6.2.2 Further Optimizations of Our Chimeric p53	195
6.2.3 Test the Activity of the Enhanced Version of p53-CC <i>In Vivo</i>	197
6.2.4 Combinational Gene Therapy with Proteasomal Protein Switch and Chimeric p53- CC.....	199
6.2.5 Using Chimeric p53-CC for Treatment of Cancers in Patients with Li-Fraumeni Syndrome.....	200
6.3 References	201

LIST OF FIGURES

<u>Figure</u>	<u>Page</u>
1.1 Schematic structure of wild-type p53	8
1.2 p53-dependent induction of apoptosis	12
1.3 A representation of the most frequently mutated residues of p53 in cancers	14
1.4 Bypassing the dominant negative effect with p53-CC	15
1.5 A ribbon diagram with the corresponding helical wheel of the coiled-coil domain of Bcr	17
2.1 Certain genetic changes or mutations can transform normal stem cells or progenitor cells into cancer stem cells	37
2.2 According to the “two-hit hypothesis,” both alleles of a tumor suppressor gene must be mutated prior to malignant transformation.....	42
2.3 Retinoblastoma tumor suppressor function in cell cycle progression	44
2.4 Reprogramming carbohydrate metabolism in cancer	57
2.5 The major steps in cancer.	70
3.1 p53 domains and translocation to the nucleus	104
3.2 p53-CC is capable of transactivating several p53 target genes	106
3.3 Apoptotic and cell proliferation assays were performed in T47D cells 48 h after transfection.	108
3.4 7-AAD assay was conducted in four different cell lines with varying p53 status (A) HeLa, (B) MDA-MB-231, (C) MCF-7, and (D) H1373.....	110
3.5 Relative luminescence represents the activation of (A) the p53-cis reporter, (B) the p21/WAF1 reporter, and (C) the PUMA reporter in T47D cells	112

3.6 p53-CC circumvents transdominant inhibition by mutant p53.....	114
3.7 Proposed mechanism of p53-CC activity	118
4.1 Schematic representation of the fates of wt-p53 and p53-CC in the presence of endogenous mutant p53 in cancer cells.	127
4.2 7-AAD staining of apoptotic and necrotic cells was performed.....	135
4.3 Induction of apoptosis is measured by (A) TMRE, (B) Caspas-3/7, and (C) Annexin-V.....	137
4.4 Effect of viral gene therapy using p53-CC and wt-p53 on induced the aggressive p53-dominant negative MDA-MB-468 human breast adenocarcinoma in female athymic nu/nu mice	139
4.5 Representative photomicrographs showing the effects of the different treatment groups on tumor tissues visualized via H&E staining, p21 immunohistochemistry staining, and ZsGreen1 fluorescence	141
4.6 Representative cropped western blots of MDA-MB-468 (A-C) <i>in vitro</i> cell lysates and (D-F) homogenized tumors from the <i>in vivo</i> study treated with Ad-p53-CC, Ad-wt-p53, Ad-ZsGreen1, or untreated	145
4.7 Schematic representation of the outcomes of wt-p53 and p53-CC activation.....	148
5.1 Helical wheel diagrams of wild-type CC homo-dimers (CCwt) (A), CCmutS41R homo-dimers (B), CCmutQ60E homo-dimers (C), CCmutE34K-R55E homo-dimers (D), and CCmutE46K-R53E homo-dimers (E)	158
5.2 Tumor suppressor activity screening using the 7-AAD assay was conducted in T47D cells 48 h post transfection.	169
5.3 Ribbon diagrams with corresponding helical wheels of CCwt homo-dimer (A), CCwt-CCmutE34K-R55E hetero-dimer (B), and CCmutE34K-R55E homo-dimer (C)	171
5.4 Time course of the deviation of the MD structures of the Bcr coiled-coil region (CCwt) and CCmut E34K-R55E to the experimental reference structure.....	172
5.5 Binding of CCmutE34K-R55E homo- and hetero-dimers with CCwt tested using the mammalian two-hybrid assay.....	174
5.6 Interaction of p53-CCmutE34K-R55E and p53-CC with endogenous Bcr was investigated in T47D cells via co-IP.....	176
5.7 7-AAD assay was conducted in three different cell lines with varying p53 status (A) SKOV 3.ip1, (B) MCF-7, and (C) T47D cells.....	178

Supporting Information 5.1 MM-PBSA energetic analysis at 5 ns snapshots.....	184
Supporting Information 5.2 Atomic positional fluctuations of the E34K-R55E compound mutant relative to the wild-type homo-dimer	185

LIST OF TABLES

<u>Table</u>	<u>Page</u>
1.1 Some of the p53 target genes involved in different cellular signaling pathways	11
1.2 Comparison of mainly used viral vectors for gene therapy	20
2.1 Markers of cancer stem cells in different cancers	39
2.2 A summary of some miRNAs in different cancers.....	54
3.1 Comparison of the native TD from wt-p53 to the CC domain from Bcr	94
3.2 Comparison of the four different cell lines (HeLa, MDA-MB-231, MCF-7 and H1373) in terms of p53 status and cancer type.....	109
5.1 Mutant candidates and the rationale of the design for each mutation	160
5.2 Energetic analysis of p53-CC wild type and mutants coiled-coil dimers as obtained by MM-PBSA.	167
5.3 Relative helicity of the modified coiled-coil region CCmutE34K-R55E relative to the native coiled-coil from Bcr (CCwt)	173

LIST OF ABBREVIATIONS

Ad	Adenovirus
AKT/PKB	Protein Kinase B
AML	Acute myeloid leukemia
ARF	Alternative reading frame protein
ATM	ataxia-telangiectasia mutated protein
ATR	ataxia-telangiectasia and Rad3-related protein
Bax	Bcl-2 associated X protein
Bcl-2	B-cell lymphoma 2
Bcl-XL	B-cell lymphoma-extra large
Bcr	Breakpoint cluster region
BRCA1	breast cancer type 1 susceptibility protein
BRCA2	breast cancer type 2 susceptibility protein
CAF	Cancer associated fibroblasts
CC	Coiled-coil
CCmut	Mutant coiled-coil
CCwt	wild type coiled-coil
CD	Cluster of differentiation
CKI	Cyclin-dependent kinase inhibitor
c-kit	Mast/stem cell growth factor receptor
CML	Chronic myeloid leukemia
Co-IP	Co-immunoprecipitation
CSC	Cancer stem cells
CTC	Circulating tumor cells
DBD	DNA binding domain
DR5	Death receptor 5
E	Nuclear export signal
ECM	Extracellular matrix
EGFP	Enhance green fluorescent protein
EGFR	Epidermal growth factor receptor
EMT	Epithelial to mesenchymal transition
ER	Estrogen receptor
ERK	extracellular signal-regulated kinases
Fas	Apoptosis antigen 1
FDA	Food and Drug Administration
FDG	2-fluoro-2-deoxy-D-glucose
FSP1	Fibroblast-specific protein 1
GADD45	Growth arrest and DNA damage gene

H&E	Hematoxylin and eosin
H1373	non-small cell lung carcinoma
HAUSP	Herpes virus-associated ubiquitin-specific protease
HeLa	Human epithelial cervical adenocarcinoma
HER-2	Human epidermal growth factor receptor 2
HIF-1 α	Hypoxia inducible factor 1
HRP	Horseradish Peroxidase
LDH	Lactate dehydrogenase
LFS	Li-Fraumeni syndrome
MBD	MDM2 binding domain
MCF-7	Human breast adenocarcinoma
MCT	Monocarboxylate transporter
MD	Molecular dynamics
MDA-MB-231	Metastatic triple negative breast carcinoma
MDA-MB-468	Human triple negative breast adenocarcinoma
MDM2	Mouse double minute 2 homolog
MEK	Mitogen-activated protein kinase kinase
MOI	Multiplicity of infection
MSC	Myeloid suppressor cells
mTOR	Mechanistic target of rapamycin
MTS	Mitochondrial targeting signal
Myc	Myelocytomatosis oncogene
NK	Natural killer cells
NLS	Nuclear localization signal
Noxa	Phorbol-12-myristate-13-acetate-induced protein 1
PARP	Poly ADP ribose polymerase
PDGF	Platelet-derived growth factor
PDH	Pyruvate dehydrogenase
PERP	p53 apoptosis effector related to PMP22
PET	Positron emission tomography
PIP3	Phosphatidylinositol (3,4,5)-trisphosphate
PK M2	Pyruvate kinase M2
PML	polymorphonuclear leukocytes
pRb	Retinoblastoma protein
PRD	Proline rich domain
PTEN	Phosphatase and tensin homolog
PUMA	p53 upregulated modulator of apoptosis
Ras	Rat sarcoma
SGK	Serum-and glucocorticoid-regulated kinase
SKOV-3.ip1	Human ovarian adenocarcinoma
SLC2A1	Solute-linked carrier gene member 2A1
T47D	Human ductal breast epithelial carcinoma
TA	Transactivation domain
TAM	Tumor-associated macrophages
TD	Tetramerization domain
TNBC	Triple negative breast cancer

TSG	Tumor suppressor gene
TSP-1	Thrombospondin-1
VEGF	Vascular endothelial growth factor
Wt	Wild type
α -SMA	Smooth muscle α -actin

ACKNOWLEDGEMENTS

Foremost, I would like to thank my parents for their support during my graduate school years. I would not be where I am today if it were not for their support and guidance over the years. They never stopped caring and calling every time there is an exam, a presentation, or even a quiz. Their visits helped me stay strong during graduate school, and my mother's cooking made me feel as if I was home in Palestine.

I am also grateful for my siblings. I am thankful for my brother Mohamed, who was always there for support and made me laugh even on rough days. I am also thankful for my older brother Ahmad, who has always been there for me with his wisdom and kindness. My youngest brother, Anas, has always been caring and considerate. I am also extremely blessed and thankful for my sisters. Ala'a always makes me laugh during our long calls, and her sons' fun stories never end. I will always be grateful for my sister Asma'a for taking care of me in school for as long as I remember. She always got me out of trouble during our elementary school years. I would also like to thank my year-a-part twin sister, Eman, for all the memories, laughs, and support over the years. I would also like to thank my youngest sister Haneen, who is a sweetheart, for her support over the years, and all the snacks and sandwiches she used to make for me. I would like to thank my uncle Ahab and his wife Sheila, as well as my cousins Abraham and Nadia. If it were not for their support, and weekly visits, being away from home would have been much harder.

I am very grateful for having Dr. Carol Lim as a mentor. She offered me a position in her lab even though she was not looking to hire any graduate students. If it were not for her, my career life would not be where it is today. She is an outstanding and caring mentor. I know I am blessed to have her as a mentor. Her perfection and attention to details, yet nourishment and loving nature brings the best out of us. She encouraged me throughout graduate school to exceed even my own expectations. Without her guidance, I would not have accomplished anything in my graduate career.

I would also like to thank everyone in the Lim Lab for their support and for providing the best lab environment anyone could wish for in graduate school. I would like to thank Andy Dixon, Jonathan Constance, Rian Davis, David Wossner, Ben Bruno, Geoff Miller, and Shams Reaz. Special thanks go to Mohanad Mossalam and Karina Matissek in the p53 group. Mohanad trained me during the beginning of my graduate career, and Karina helped me with many experiments. I would also like to acknowledge all the students who worked directly under my mentorship specially Steffan Matissek.

I would like to thank my supervisory committee members, Dr. David Grainger, Dr. James Herron, Dr. Jindřich Kopeček, and Dr. Philip Moos. They were always helpful during committee meetings, and provided me with overwhelming recommendation letters. Finally, I am thankful to God for having all these people in my life.

CHAPTER 1

INTRODUCTION AND BACKGROUND

1.1 Introduction

With more than 200 different types of cancer identified to date, the large heterogeneity observed among the different types of cancers makes it challenging to develop effective therapeutics to treat cancer patients. In fact, it is commonly observed that even patients with the same type of cancer respond differently to the same drugs. Thus, demand for personalized medicine has increased in the last few years, which has proven effective in treatment of cancer patients (1-3). However, personalized medicine usually comes with high costs that render it inaccessible to the majority of cancer patients. Therefore, there is an urgent need for a therapeutic approach that can benefit a large subset of cancer patients. With that in mind, we searched for common molecular features and abnormalities in different types of cancers that can be targeted for development of effective therapeutics.

The tumor suppressor p53 is one of the most well-studied and commonly abrogated self-defense mechanisms of normal cells prior to malignant transformation. It is well documented that more than 50% of all human cancers have a mutated p53 gene status, rendering it inactive. In addition, the majority of the remaining cancers, although harboring wild-type copies of the gene, have an inactivated p53 pathway via mechanism

other than mutational inactivation. Hence, *we pursued a p53-based gene therapeutic approach in order to reactivate the p53 pathway in cancer cells*. Although breast cancer is the main focus of this work, the application of this research extends to many other types of cancer, including the deadliest cancers (pancreatic, lung, and ovarian), which currently lack effective treatments.

1.2 Rationale of Study

p53 is a transcription factor that can activate multiple pathways such as DNA repair, cell cycle arrest, and apoptosis (4-6). Current targeting of p53 as a therapeutic is mainly focused on introducing the wild-type (wt) p53 gene into cancer cells using various delivery vehicles (7-9). However, many cancer cells contain endogenous mutant p53 that has a squelching effect over wt-p53 upon hetero-oligomerization. The hetero-tetramers have a significantly reduced transcriptional activity compared to homo-tetramers of wt-p53. Such a phenomenon gives rise to a great barrier that limits the utility of p53 for cancer therapy (10-12). This work focuses on investigating a chimeric p53 with an alternative oligomerization domain, which can offer an improved approach to using wt-p53 for cancer gene therapy.

p53 relies on its oligomerization or tetramerization domain (TD) to form tetramers, a step that is essential for its transcriptional activity and activation of signaling pathways. It is well established that p53 lacking its TD is transcriptionally inactive (13). However, the presence of the TD allows for mutant p53 found in most cancer cells to oligomerize with exogenous wt-p53, leading to diminished efficacy of p53 gene therapy. This is known as the “dominant negative effect” of mutant p53 in cancer cells (9). Thus,

we investigated possible swapping of the native TD with an alternative oligomerization domain to prevent hetero-oligomer formation. The oligomerization domain of breakpoint cluster region (Bcr) protein, a coiled-coil (CC) that tetramerizes in a similar orientation to the TD of wt-p53 (antiparallel dimer of dimers) (14-17), was chosen as the alternative oligomerization domain. Thus, replacing the native TD of p53 with CC from Bcr to create p53-CC should sustain the transcriptional and tumor suppressor activity of p53, while preventing hetero-oligomer formation and transdominant inhibition of our chimeras by mutant p53 in cancer cells.

1.3 Summary of Dissertation

This introductory chapter provides an overview of the dissertation in brief, followed by background and rationale for the work presented. In addition, three different hypotheses under investigation are presented along with the specific aims for each subproject. Chapter 2 (our published book chapter) reviews cancer biology. The different theories explaining how cancers originate (cancer stem cell hypothesis vs stochastic clonal model) are described in detail. In addition, the genetic and epigenetic pathways that lead to cancer are delineated, and the alterations of nutrient and metabolic pathways as well as tumor physiology and the cancer microenvironment are examined in this chapter.

While Chapter 3 describes the proof-of-concept studies for the chimeric p53-CC conducted *in vitro* (18), Chapter 4 focuses on validating its activity in a p53-dominant negative orthotopic breast tumor model in mice (under review, *Gene Therapy*). Chapter 5 describes a set of rationally and computationally designed modifications that can be

introduced in the coiled-coil domain of p53-CC chimera to enhance its binding specificity, and minimize any possible interactions with endogenous Bcr in the cells (submitted, *Molecular Pharmaceutics*). Finally, Chapter 6 provides conclusions, limitations, and future directions.

1.4 Background

1.4.1 Cancer

The oldest identification and description of cancer dates back to 1600 BC in Egypt (19). Since then, different theories have been proposed to explain the origins for cancer development and survival. While the word *cancer* itself refers to the blood vessels that feed the tumors, cancerous cells develop from normal cells that eventually acquire the ability to proliferate aberrantly and grow uncontrollably into malignant tumors that can metastasize (20). In addition, cancerous cellular growth can take place in any organ or tissue anywhere in the body, with more than 200 different types of cancers identified so far. Furthermore, different types of cancers usually have distinct molecular features and abrogated pathways that make them respond differently to varying treatment regimens. This heterogeneity in the nature of the disease adds to the complexity of the diagnosis, treatment, and overcoming drug resistance in cancer (21-23). Furthermore, a certain cancer type can vary significantly from one patient to another. Even within the same patient, the tumor tissue may contain several heterogeneous types of cancer cells (24, 25). Therefore, cancer is commonly viewed as a collection of different diseases, often with one treatment approach insufficient for remission. Hence, it is extremely challenging to find a single drug that can be effective in more than one type of cancer. In

Chapter 2, a review is presented to offer a better fundamental understanding of cancer biology, and to shed the light on some of the causes for the heterogeneity of the disease.

1.4.2 Breast Cancer

The focus of this work is breast cancer, which remains the most common cancer and the second leading cause of cancer death among women, owing to the high and increasing incidence rate (26). According to the American Cancer Society, the lifetime risk of a woman developing breast cancer is 13% or almost 1 in 8. Even though patients with noninvasive cancers have a good treatment prognosis and high survival rates, invasive cancer (invading the fat tissue) remains a deadly form of the disease. For instance, approximately 80% of all breast cancers are invasive ductal carcinomas in which the cancer moves into the lymphatic system and metastasizes to regional lymph nodes, which helps it spread to different tissues (27, 28). A breast-conserving surgical approach benefits some patients, while others receive neoadjuvant (presurgery) chemotherapy or hormone therapy to downstage large tumors, thus potentially allowing conservative surgery (26). Moreover, adjuvant therapy (chemotherapy given after surgery) is used to eradicate micro-metastases, to improve survival rate, and to delay tumor recurrence (29). Anthracycline (doxorubicin or epirubicin) and taxane-based agents have been the standard chemotherapy for breast cancer (30, 31). However, most chemotherapeutic agents are known to have serious side effects (32-35). In addition, certain patients may be eligible for hormonal breast cancer therapy (e.g., tamoxifen, which blocks the activity of estrogen in the body), or targeted drugs such as trastuzumab (Herceptin™) based on the molecular features of their cancer cells (e.g., HER-2 receptor)

(36, 37). Furthermore, there is no one therapy currently that can be used for treatment of all breast cancers, and some breast cancers do not even have combination therapies that address their particular molecular status. One such indication is triple negative breast cancer (TNBC), which lacks molecular targets that can be utilized for therapy. Hence, a universal approach such as our chimeric p53-CC that does not depend on the molecular features of a cell would be a highly significant approach for TNBC.

1.4.3 Triple Negative Breast Cancer

Triple negative breast cancer (TNBC) accounts for about 15 to 20% of the 1.5 million cases of breast cancers diagnosed per year, but is responsible for a disproportionate number of deaths (38, 39). The challenge of treating TNBC originates from the absence of molecular targets (including estrogen receptor (ER), progesterone receptor (PR), and human epidermal growth factor receptor 2 (HER2)) (40) and disease heterogeneity. This heterogeneity stems from the numerous subtypes of TNBC, the variable status of other receptors (such as BRCA1, BRCA2, EGFR, c-kit, PARP) and other genetic mutations present in TNBC, further complicating targeted treatment options. Standard chemotherapy (41) (such as platinum and anti-tubulin agents) and anti-angiogenic therapy (bevacizumab) are the only currently available FDA-approved treatment options for TNBC, but both response to treatment and prognosis are poor (42, 43). Additionally, TNBC responds 10-100 fold less to platinum agents when the p53 pathway is damaged (44). TNBC generally occurs in women less than 50 years old, and is linked to recurrence and death, particularly in the first 3-5 years of follow up (45). Triple negative tumors are also more likely to form lung or brain metastases (46). Up to

10,000 women die per year from TNBC in the U.S. alone. While much progress has been made against many types of breast cancer, the same cannot be said for TNBC, mainly due to the lack of molecular targets for this disease (40, 43, 47-49). Gene expression profiling of TNBC has identified 5 main clusters with a remarkable heterogeneity (50). While existing chemotherapeutics/dosing regimens may be effective for a minority of patients (51), it is thought that development of new targeted therapeutics are an urgent medical need for these patients (52). Targeted therapies against EGFR, c-kit, or PARP, multi-tyrosine kinase inhibitors, and adjuvant anti-angiogenic agents are being currently tested (41, 53), but their success will hinge on the clinicians' ability to discover distinct molecular features for stratification of breast cancer subtypes and for identifying triple negative breast cancer in patients (54). Clinical trials for some of these agents have been somewhat disappointing to date (55), and no single drug can be used for all types of TNBC. However, mutation of the tumor suppressor p53 has been reported in 60-88% of TNBC (56, 57); likewise, loss of p53 function is known to be associated with metastasis (58, 59). Therefore, a universal approach such as our chimeric p53 that does not depend on the molecular features of a cell would be a highly significant approach for TNBC treatment.

1.4.4 The Tumor Suppressor p53

The tumor suppressor p53 is encoded by the *TP53* gene mapped on the short arm of chromosome 17. Its structure and function have been highly preserved over one billion years of evolution (60). p53 is a 393 amino acid sequence-specific transcription factor (Figure 1.1) (61), and is commonly divided into three regions: an acidic N-terminal

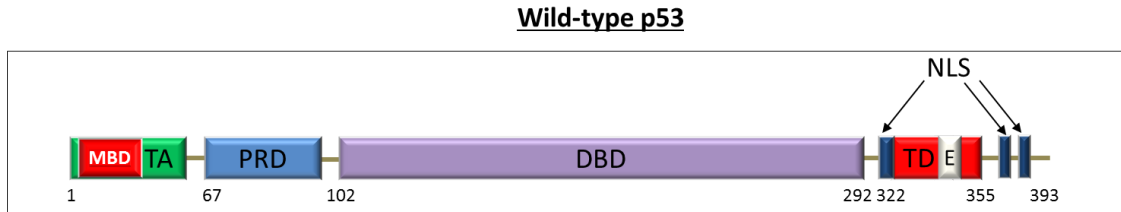


Figure 1.1 Schematic structure of wild-type p53. The amino terminus contains the MDM-2 binding domain (MBD) and the transactivation domain (TA). The DNA binding domain (DBD) spans from amino acids 102-292. The C-terminus consists of three nuclear localization signals (NLS), a nuclear export signal (E), and the tetramerization domain (TD).

region (codons 1-101), a DNA binding domain (DBD, codons 102-292), and a basic C-terminal region (codons 293-393). The N-terminal region contains a transactivation domain (TA, codons 1-42), a MDM2 binding domain (MBD, codons 17-28) and a proline rich domain (PRD, codons 67-97). The C-terminus contains three nuclear localization signals (NLSs, with the strongest NLS spanning on codons 305-322), a nuclear export signal (E, codons 340-351), and a tetramerization domain (TD, codons 323-355).

p53 is commonly referred to as the “guardian of the genome” (62) due to its pivotal role in suppressing malignancy (63, 64). In fact, inactivation of p53 pathway is reported in more than half of all human tumors and can be achieved via several mechanisms including nuclear exclusion and hyperactivation of MDM2, the main regulator of p53 function (65-67). Therefore, disruption of the MDM2-p53 complex has been targeted for its potential to restore p53 activity in cancers that harbor a wild type copy of the gene. MDM2 targeting by small molecules (such as Nutlin-3a) achieved significant success in restoring p53 functionality in cancer cells (68). Although effective, the outcomes of preventing p53 degradation by MDM2 remain limited to cancers that retain a wild-type p53 status, which includes only a small subset of cancer patients.

Acquisition of missense mutations in one or both alleles of the *TP53* gene remains one of the most common mechanisms of p53 inactivation (21, 69). Although there have been countless efforts to ‘reactivate’ mutant p53 in cancer cells, the diversity of p53 mutations precludes finding a single drug that hits all possible variants of the protein (55). Hence, recent drug development was aimed to reactivate specific types of p53 mutants, such as the small molecule drugs PRIMA and MIRA. While PRIMA reactivates DNA-contact p53 mutants as well as structural mutants via forming adducts with thiols in mutant p53 core domain (70, 71), MIRA relies on its maleimide group to interact with thiol and amino groups and restore the native folding state of p53 (71, 72).

To exert its tumor suppressor function, p53 acts as a transcription factor that responds to various cellular stimuli including, and not limited to, DNA damage, hypoxia, and oncogenic activation. Upon activation, p53 regulates the expression of several genes involved in different cellular signaling events including DNA repair, cell cycle arrest, and programmed cell death (apoptosis) (73). While p53 is able to induce apoptosis when targeted to the mitochondria (74-76), its tumor suppressor function mainly depends on localization to the nucleus and formation of p53 tetramers leading to its function as a transcription factor of several target genes. The role of p53 at the nucleus and mitochondria is further examined below.

1.4.4.1 Nuclear p53

The cellular levels of p53 are tightly regulated in normal cells at the protein level (77). This regulation is carried out via the MDM2 negative feedback loop. MDM2 is an E3 ubiquitin ligase that acts as the main regulator of p53 via nuclear exclusion and

proteasomal degradation of the tumor suppressor. Upon activation, the MDM2-p53 complex is disrupted and the half-life of the p53 protein is rapidly increased from minutes to hours (78), which facilitates tetrameric formation and binding to the response elements of target genes. At the nucleus, tetrameric p53 regulates the expression of hundreds of target genes involved in several signaling pathways (see Table 1.1) (79). The outcome of nuclear p53 activation is highly dependent on the type and intensity of cellular stimuli detected in the cell. For instance, upon DNA damage caused by UV radiation, p53 forces the cells to undergo p21-dependent cell cycle arrest to allow time for repair, and up-regulates the expression of the GADD45 and p48XPE proteins involved in the DNA repair machinery (80, 81). However, if the damage is too extensive and cannot be repaired, or if cell cycle arrest lasts for too long, then p53 activates the apoptosis pathway (82).

p53 can activate apoptosis via two distinct pathways: the extrinsic or intrinsic apoptosis pathways (Figure 1.2). The extrinsic apoptosis pathway relies on p53 up-regulation of death receptor genes, including Fas, DR5, and PERP, which upon binding to their corresponding ligand can activate the caspase cascade terminating in apoptosis. p53 can also mediate apoptosis via the intrinsic apoptosis pathway following the induction of several pro-apoptotic proteins that act at the mitochondria. PUMA, Noxa, and Bax are some of the key players in inducing the intrinsic apoptosis pathway. Upon expression, these pro-apoptotic proteins and others translocate to the mitochondrial and induce mitochondrial outer membrane disruption, resulting in the release of cytochrome C to the cytoplasm, which in turn leads to activation of the caspase cascade and apoptosis.

Table 1.1 Some of the p53 target genes involved in different cellular signaling pathways (adapted from (83)).

Symbol	Description	Symbol	Description
APAF1	Apoptotic peptidase activating factor 1	KRAS	V-Ki-ras2 Kirsten rat sarcoma viral oncogene homolog
ATM	Ataxia telangiectasia mutated	PIDD	P53-induced death domain protein
TR	Ataxia telangiectasia and Rad3 related	MCL1	Myeloid cell leukemia sequence 1
BAI1	Brain-specific angiogenesis inhibitor 1	MDM2	Mdm2 p53 binding protein homolog
BAX	BCL2-associated X protein	MDM4	Mdm4 p53 binding protein homolog
BCL2	B-cell CLL/lymphoma 2	MYC	V-myc myelocytomatosis viral oncogene homolog
BCL2A1	BCL2-related protein A1	MYOD1	Myogenic differentiation 1
BID	BH3 interacting domain death agonist	NFKB1	Nuclear factor of kappa light polypeptide gene enhancer in B-cells 1
BIRC5	Baculoviral IAP repeat containing 5	TP53AIP1	Tumor protein p53 regulated apoptosis inducing protein 1
BRCA1	Breast cancer 1, early onset	PCNA	Proliferating cell nuclear antigen
BRCA2	Breast cancer 2, early onset	PTEN	Phosphatase and tensin homolog
CASP2	Caspase 2, apoptosis-related cysteine peptidase	PTTG1	Pituitary tumor-transforming 1
CASP9	Caspase 9, apoptosis-related cysteine peptidase	RB1	Retinoblastoma 1
CDK1	Cyclin-dependent kinase 1	RPRM	Reprimo, TP53 dependent G2 arrest mediator candidate
CDK4	Cyclin-dependent kinase 4	STAT1	Signal transducer and activator of transcription 1, 91kDa
CDKN1A	Cyclin-dependent kinase inhibitor 1A (p21, Cip1)	TNF	Tumor necrosis factor
CDKN2A	Cyclin-dependent kinase inhibitor 2A (melanoma, p16, inhibits CDK4)	TNFRSF10D	Tumor necrosis factor receptor superfamily, member 10d
E2F1	E2F transcription factor 1	TP53	Tumor protein p53
E2F3	E2F transcription factor 3	TP53BP2	Tumor protein p53 binding protein, 2
EGR1	Early growth response 1	TP73	Tumor protein p73
EI24	Etoposide induced 2.4 mRNA	TP63	Tumor protein p63
ESR1	Estrogen receptor 1	TRAF2	TNF receptor-associated factor 2
FADD	Fas (TNFRSF6)-associated via death domain	TSC1	Tuberous sclerosis 1
FASLG	Fas ligand (TNF superfamily, member 6)	XRCC5	X-ray repair (double-strand-break rejoining)
GADD45A	Growth arrest and DNA-damage-inducible, alpha	IGF1R	Insulin-like growth factor 1 receptor
HDAC1	Histone deacetylase 1	IL6	Interleukin 6 (interferon, beta 2)

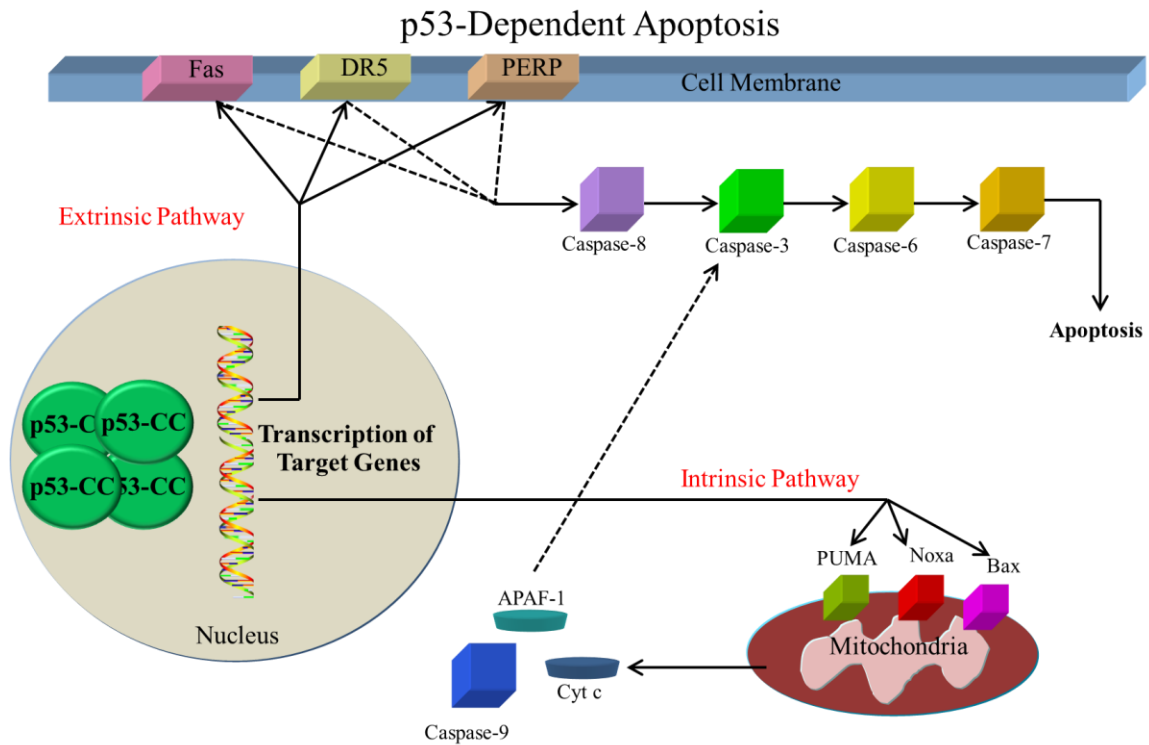


Figure 1.2 p53-dependent induction of apoptosis requires transcriptional activation of pro-apoptotic target genes. Tetrameric p53 transactivates genes involved in the extrinsic apoptotic pathway (Fas, DR5, and PERP) which in turn activates the caspase cascade via cleavage of procaspase-8. In addition, p53 transactivates genes involved in the intrinsic apoptotic pathway (PUMA, Noxa, and Bax), which lead to mitochondrial outer membrane permeabilization and release of cytochrome-C. Similarly, the intrinsic apoptotic pathway is dependent on activation of the caspase cascade.

1.4.4.2 Mitochondrial p53

Although p53 is a transcription factor, and hence, achieves its tumor suppressor function at the nucleus, it is known that p53 can directly translocate to the mitochondria and cause transcriptionally independent activation of the intrinsic apoptosis pathway (84-87). Under certain stress conditions (e.g., radiation), p53 is translocated to the mitochondria; first, p53 must be mono-ubiquitinated to achieve nuclear export to the cytoplasm, followed by shuttling via the herpes virus-associated ubiquitin-specific protease (HAUSP) (88, 89). At the mitochondrial outer membrane, p53 can then directly either inhibit anti-apoptotic proteins such as Bcl-2 and Bcl-XL, or activate pro-apoptotic proteins including Bak and Bax (90-92). Moll et al. were the first to show that due to the ability of p53 to mediate apoptosis directly at the mitochondria, mitochondrial targeting of p53 has a therapeutic potential for cancer gene therapy (93-95). However, for optimal mitochondrial targeting without causing unintentional toxicity to cells, a mitochondrial targeting signal (MTS) must be fused to the p53 protein. Furthermore, therapeutic p53 can be targeted to different mitochondrial subcompartments based on the MTS used, which results in different toxicity profiles and has been recently reported by our lab (86, 87).

1.4.5 Dominant Negative Effect of Mutant p53

Acquisition of missense mutations in the *TP53* gene results in aberrant p53 that is transcriptionally inactive (96-98). More than 50% of solid tumors contain mutated p53, whereas the majority of the remaining tumors have inactive p53 via other mechanisms. Such mutations mainly take place in the DNA binding domain (DBD) and are divided

into two main classes: class I contains mutations that can cause p53 to lose DNA binding contact sites, and class II contains mutations that lead to significant changes in the structural conformation of the protein (Figure 1.3) (10, 99). Consequently, mutated p53 is unable to regulate its target genes. Since the negative regulator MDM2 is one of the target genes for p53, tumor cells with mutated p53 tend to accumulate relatively high concentrations of the dysfunctional protein (100, 101). Such mutant proteins retain their tetramerization capabilities since their tetramerization domain (TD) remains intact, and can form inactive p53 hetero-tetramers with wild type (wt) p53 in cancer cells (Figure 1.4). Tetramer inactivity is due to the dominant negative effect of mutant p53 upon hetero-oligomerization with wt-p53 (102, 103). This sequestration of wt-p53 into inactive tetramers is commonly known as the dominant negative effect of mutant p53, and forms a critical barrier to the efficacy of introducing active p53 into tumor cells for cancer therapy (10-12, 104). Furthermore, the dominant negative effect of mutant p53 has been shown to be operative *in vivo* using knock-in mice expressing mutant p53 (105). To bypass this dominant negative effect, we suggested that a coiled-coil domain could be used as an alternative oligomerization due to its dimerization capability.

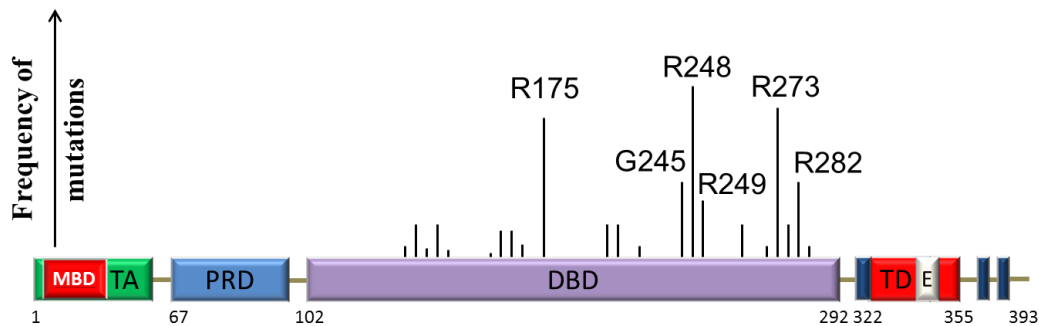


Figure 1.3 A representation of the most frequently mutated residues of p53 in cancers.

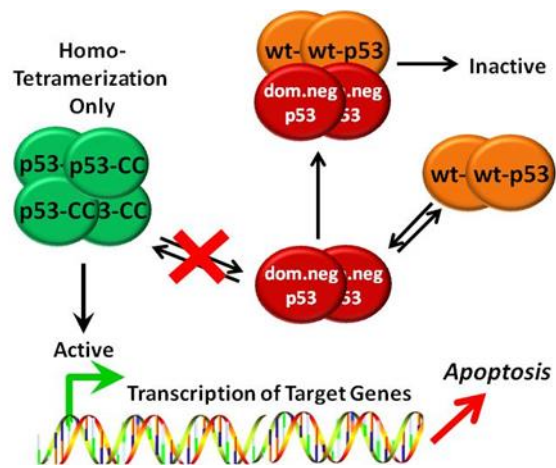


Figure 1.4 Bypassing the dominant negative effect with p53-CC. Wt-p53 interacts with dominant negative p53 in cancer cells, and is inactivated. On the other hand, p53-CC cannot tetramerize with dominant negative p53 in cancer cells. Instead, p53-CC can only form tetramers with itself, bind to target DNA, and activate apoptosis.

1.4.6 Alternative TD: Coiled-Coil Domain

In general, coiled-coil domains are characterized by heptad repeats of amino acids (denoted by letters for each residue, **(abcdefg)_n**, for n repeats) that control the specificity and orientation of the oligomerization motif (106, 107). Furthermore, distinct interaction profiles exist between the different residues based on the orientation (parallel or antiparallel) of the coiled-coil (106, 108). Residues **a** and **d** are usually occupied by hydrophobic residues while residues **e** and **g** are usually hydrophilic. Surface interactions between positions **e** to **e'** (where the prime refers to a residue on the opposite helix) and **g** to **g'** are known to be essential in antiparallel coiled-coils, whereas interactions between positions **g** to **e'** are the most critical for parallel coiled-coils (106, 108). Hence, coiled-coils thermodynamically favor association in cells in order to bury the hydrophobic residues of each coiled-coil from the hydrophilic environment, forming an amphipathic structure. This association is usually very strong and stable, which qualifies coiled-coils as extremely efficient oligomerization domains as observed in many transcription factors and proteins that require oligomerization to achieve their functions (109, 110).

The coiled-coil domain from break point cluster region (Bcr) protein is assembled as two 36-residue helices antiparallel to each other (see Figure 1.5) (111, 112). This antiparallel orientation gives rise to the aforementioned **e** to **e'** and **g** to **g'** interactions that can be utilized to potentially create more salt bridges within a dimer. The potential design of enhanced coiled-coil mutants to achieve higher binding specificity is further explored in Chapter 5.

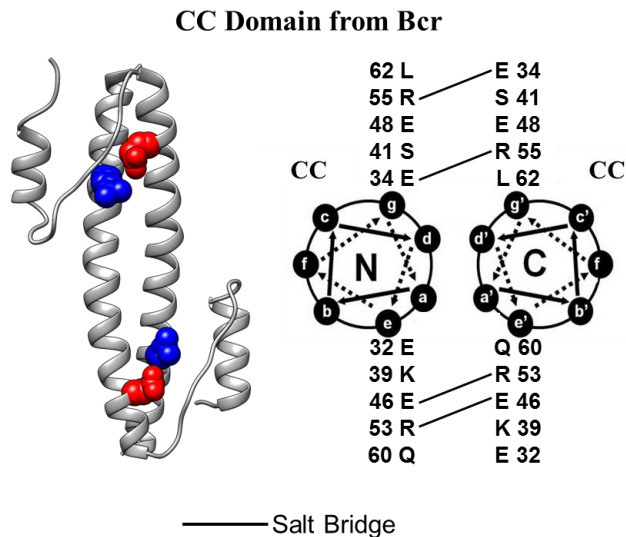


Figure 1.5 A ribbon diagram with the corresponding helical wheel of the coiled-coil domain of Bcr. The side chains of key residues are shown as red (acidic) or blue (basic). Solid lines indicate salt bridges.

1.4.7 Break Point Cluster Region (Bcr)

Since the CC domain was obtained from Bcr, it may be important to minimize any possible cross-interaction with Bcr found in most cells. Bcr is a ubiquitous eukaryotic phosphotransferase protein that may have a role in general cell metabolism. Bcr-knockout mice still survive; the major defect in these mice was reduced intimal proliferation in low-flow carotid arteries compared to wt mice (113). Bcr has mostly been studied in the context of chronic myeloid leukemia (CML) where a reciprocal chromosomal translocation with Abl results in the fusion protein Bcr-Abl, the causative agent of CML (114, 115). The activity of Bcr-Abl is largely due to the constitutive activation of the Abl portion of the molecule (116). In addition, Bcr plays a role in arterial proliferative disease *in vivo* as well as differentiation and inflammatory responses of vascular smooth muscle cells (113, 117). Hence, optimizing the CC domain to prevent possible interaction

with Bcr is essential, and is further investigated in Chapter 5.

1.4.8 Gene Therapy

The main theme for this work is to utilize p53-based therapeutics in cancer gene therapy. Gene therapy entails introduction of gene(s) in the forms of therapeutic DNA to correct a cellular dysfunction or replace a mutated gene (118-120). Since proteins encoded within the genome carry out all biological events in cells, gene therapy has enormous therapeutic potential to cure many diseases. Hence, identifying the molecular features or the aberrant proteins within a certain disease is a prerequisite for gene therapy. For instance, cancers often develop following acquisition of mutations in tumor suppressor genes, which renders their protein products inactive. Once the inactive or dysfunctional protein is identified within the context of the cancer cells, either the native corresponding gene, or an enhanced version of it, is delivered to cancer cells to restore normal function. Recent advances in the Human Genome Project and the Hap Map Project have accelerated identification of genes and proteins involved in several diseases (121). Although many clinical trials utilize gene therapy approaches for certain diseases such as neurodegenerative, cardiovascular, and infectious diseases, cancer remains to be the largest target for gene therapy clinical trials (122). As of 2012, there have been over 1843 clinical trials approved, undergoing, or completed for several diseases worldwide, 64.4% of which are focused on cancer diseases (123). Cancer gene therapy usually aims towards introduction of tumor suppressor genes (such as p53), immunotherapy, and oncolytic virotherapy (124-126). In fact, introduction of the tumor suppressor p53 gene into cancer cells was the first clinically approved cancer gene therapeutic worldwide.

Approved in 2004 by the State Food and Drug Administration in China (SFDA) for head and neck squamous cell carcinoma, p53 delivered using an adenovirus was marketed under the brand name Gendicine™. One year later (2005), another p53-based gene therapeutic was also approved in China under the brand name Oncorine™. However, using wt-p53 for cancer gene therapy has moderate success so far for many types of cancers due to several barriers that must be overcome, such as the dominant negative effect of mutant p53 commonly found in cancer cells. In addition, delivery of wt-p53 and any therapeutic DNA genes in general into cells represents one of the major barriers in utilizing gene therapy approaches for many diseases. Hence, great research efforts are aimed towards designing a carrier system that can successfully deliver its gene loads efficiently and specifically to target cells. These carrier systems are commonly referred to as vectors, and can range from simple plasmids or natural gene carriers such as viruses to very complex nonviral delivery systems.

1.4.8.1 Viral vs. Nonviral Vectors

Viral gene delivery takes advantage of the evolutionary design and evolution of viruses to efficiently deliver genes of interest into host cells. The concept behind using viral vectors is to harness the viral infection pathway and expression of genes without subsequent toxicity (127). This is often achieved by reengineering the viral genome to eliminate certain coding regions that are responsible for viral toxicity, while preserving viral genes responsible for desired functions such as packaging the capsid of the viral vector or integration into the host cell genome (128). Table 1.2 summarizes the main features of the viral vectors commonly used in clinical trials for gene therapy.

Table 1.2 Comparison of mainly used viral vectors for gene therapy (adapted from (129, 130))

Virus	Gene Material	Packaging Capacity	Chromosome Integration	Limitations	Applications
Adenovirus	dsDNA	30kb	No	Capsid mediates a potent inflammatory response	Cancer therapy, angiogenesis induction, DNA vaccine production
Adeno-associated virus	ssDNA	5kb	No	Small packaging capacity	Genetic diseases, cancer, neurological, ocular and cardiovascular diseases
Retrovirus	RNA	8kb	Yes	Only transduces dividing cells; integration may cause oncogenesis	Genetic diseases of T cells, hematological diseases, HIV/AIDS
Lentivirus	RNA	8kb	Yes	Integration may cause oncogenesis	Genetic diseases of T cells, hematological diseases, HIV/AIDS
Herpes simplex virus-1	dsDNA	40kb	No	Inflammatory; transient expression in cells other than neurons	Neurological diseases

Although initial use of viral vectors for gene therapy was rapidly criticized for lack of safety and efficacy, better understanding of how to safely harness the advantages of viruses as biological delivery vehicles over the last 15 years has resulted in promising clinical successes. In addition, the use of viral vectors is approved for clinical trials, and comprises more than 70% of gene therapy clinical trials (131). One of the most common viral vectors used in clinical trials is adenoviral Ad5, derived from a serotype 5 adenovirus. Adenovirus is the most efficient in terms of delivering their genetic cargo to the nucleus (131-134). Adenoviral vectors will transduce both dividing and nondividing cells and transfer to a target cell nucleus in an epi-chromosomal location with rare integration into chromosomes (135).

Therefore when the target cell divides, only one daughter cell will receive the transferred gene. In addition, the immunogenicity of adenovirus has improved recently enhancing its prospects for long-term gene transfer in a wide range of different tissues (128). Although not without issues, adenovirus will be used in this proposal as a means to validate our model as a high efficiency vector. Alternatively, nonviral delivery systems have steadily gained their place as gene delivery vectors due to their safety and ease of large-scale production (136-138). However, different concerns must be addressed for the design of optimal nonviral delivery vehicles such as optimizing uptake by cells and intracellular release of the vector and/or the gene load (139-141). While the actual delivery of our candidate gene therapeutics is not the focus of this work, they can be delivered virally or nonvirally as DNA encoded products.

1.5 Statement of Objectives

The long-term objective of this work is to develop and optimize a p53-based therapeutic that can be used for cancer gene therapy. This study describes the design of a novel chimeric p53 by swapping the TD from p53 with the coiled-coil (CC) tetramerization domain from Bcr protein (142) to create p53-CC. These 2 domains are structurally analogous in that they both form antiparallel dimer of dimers (tetramers). The choice to replace the TD of p53 with the CC from Bcr is entirely novel, and has never been attempted before. Hence, extensive proof-of-concept experiments and preliminary work was carried out to validate the tumor suppressor function of our constructs. Breast cancer was mainly chosen as the disease model to test the efficacy of our constructs. *In vitro* work showed that as hypothesized, p53-CC was able to bypass

hetero-oligomerization with endogenous mutant p53 and prevent any consequent transdominant inhibition *in vitro* (Chapter 3). Once the tumor suppressor activity of our lead construct was validated, we initiated efficacy studies in a mouse breast cancer model to test if the activity of p53-CC translates *in vivo* (Chapter 4). Indeed, p53-CC demonstrated superior tumor suppressor activity compared to wt-p53 and caused tumor regression of an aggressive p53-dominant negative orthotopic breast cancer xenograft tumor model (using MDA-MB-468 TNBC cells) *in vivo*. In addition, the underlying differential mechanisms of activity for p53-CC and wt-p53 delivered using viral-mediated gene therapy approach were investigated in the MDA-MB-468 tumor model. Finally, the chimeric p53-CC construct was further optimized to increase specificity and reduce any potential off-target effects (Chapter 5). Since domain swapping to create p53-CC could result in p53-CC interacting with endogenous Bcr, modifications on the CC domain were necessary to minimize potential interactions with Bcr. These approaches lead to the hypothesis that *swapping the oligomerization domain of p53 with an alternative oligomerization domain will prevent hetero-oligomerization and transdominant inhibition by mutant p53 in cancer cells*. In this study, three major hypotheses were proposed with their corresponding aims, as follows:

Hypothesis 1: *The chimeric p53-CC can bypass the dominant negative effect of mutant p53, while retaining the tumor suppressor function of p53 in cancer cells.*

Aim: To design the chimeric p53-CC by swapping the TD of p53 with the CC domain from Bcr, and investigate its transcriptional and tumor suppressor activity *in vitro*.

Hypothesis 2: *The tumor suppressor function of p53-CC is superior to wt-p53 activity,*

and will demonstrate significant efficacy in a p53-dominant negative breast cancer tumor model.

Aim: To test if the activity of p53-CC translates *in vivo* in a p53-dominant negative orthotopic breast tumors in mice.

Hypothesis 3: *Rationally designed mutations in the coiled-coil domain of p53-CC will reduce potential interactions with endogenous Bcr without affecting the tumor suppressor function.*

Aim: To introduce the designed mutations on the CC domain and create an enhanced version of the p53-CC chimera that has minimal interactions with endogenous Bcr.

These hypotheses and aims have been discussed in detail in Chapters 3, 4, and 5, respectively. Chapter 2 reviews topics regarding cancer biology and some causes for the complexity of the disease, and has been published as a book chapter by Springer (21). The results in the studies described in Chapter 3 have also been peer-reviewed and published by *Molecular Pharmaceutics*. In addition, the work from Chapter 4 and 5 has been submitted to *Gene Therapy* and *Molecular Pharmaceutics*, respectively.

1.6 References

1. S.D. Ramsey, D. Veenstra, S.R. Tunis, L. Garrison, J.J. Crowley, and L.H. Baker. How comparative effectiveness research can help advance 'personalized medicine' in cancer treatment. *Health Aff (Millwood)*. 30:2259-2268 (2011).
2. A.M. Gonzalez-Angulo, B.T. Hennessy, and G.B. Mills. Future of personalized medicine in oncology: a systems biology approach. *J Clin Oncol*. 28:2777-2783 (2010).
3. J.S. Ross, E.A. Slodkowska, W.F. Symmans, L. Pusztai, P.M. Ravdin, and G.N. Hortobagyi. The HER-2 receptor and breast cancer: ten years of targeted anti-HER-2 therapy and personalized medicine. *Oncologist*. 14:320-368 (2009).

4. O.D. Staples, R.J.C. Steele, and S. Lain. p53 as a therapeutic target. *The Surgeon*. 6:240-243 (2008).
5. J.L. Abrahamson, J.M. Lee, and A. Bernstein. Regulation of p53-mediated apoptosis and cell cycle arrest by Steel factor. *Molecular and Cellular Biology*. 15:6953-6960 (1995).
6. A.J. Wagner, J.M. Kokontis, and N. Hay. Myc-mediated apoptosis requires wild-type p53 in a manner independent of cell cycle arrest and the ability of p53 to induce p21waf1/cip1. *Genes & Development*. 8:2817-2830 (1994).
7. A. El-Aneed. An overview of current delivery systems in cancer gene therapy. *Journal of Controlled Release*. 94:1-14 (2004).
8. F.F. Lang, J.M. Bruner, G.N. Fuller, K. Aldape, M.D. Prados, S. Chang, M.S. Berger, M.W. McDermott, S.M. Kunwar, L.R. Junck, W. Chandler, J.A. Zwiebel, R.S. Kaplan, and W.K.A. Yung. Phase I Trial of Adenovirus-Mediated p53 Gene Therapy for Recurrent Glioma: Biological and Clinical Results. *Journal of Clinical Oncology*. 21:2508-2518 (2003).
9. M.V. BLAGOSKLONNY. p53 from complexity to simplicity: mutant p53 stabilization, gain-of-function, and dominant-negative effect. *The FASEB Journal*. 14:1901-1907 (2000).
10. J. Milner and E.A. Medcalf. Cotranslation of activated mutant p53 with wild type drives the wild-type p53 protein into the mutant conformation. *Cell*. 65:765-774 (1991).
11. S. Srivastava, S. Wang, Y.A. Tong, Z.M. Hao, and E.H. Chang. Dominant negative effect of a germ-line mutant p53: a step fostering tumorigenesis. *Canc Res*. 53:4452-4455 (1993).
12. S.E. Kern, J.A. Pietenpol, S. Thiagalingam, A. Seymour, K.W. Kinzler, and B. Vogelstein. Oncogenic forms of p53 inhibit p53-regulated gene expression. *Science*. 256:827-830 (1992).
13. R. Kulikov, M. Winter, and C. Blattner. Binding of p53 to the central domain of Mdm2 is regulated by phosphorylation. *The Journal of Biological Chemistry*. 281:28575-28583 (2006).
14. M.J. Waterman, J.L. Waterman, and T.D. Halazonetis. An engineered four-stranded coiled coil substitutes for the tetramerization domain of wild-type p53 and alleviates transdominant inhibition by tumor-derived p53 mutants. *Cancer Res*. 56:158-163 (1996).
15. P.D. Jeffrey, S. Gorina, and N.P. Pavletich. Crystal structure of the tetramerization domain of the p53 tumor suppressor at 1.7 angstroms. *Science*. 267:1498-1502 (1995).
16. W. Lee, T.S. Harvey, Y. Yin, P. Yau, D. Litchfield, and C.H. Arrowsmith. Solution structure of the tetrameric minimum transforming domain of p53. *Nat Struct Biol*. 1:877-890 (1994).

17. C. Wichmann, Y. Becker, L. Chen-Wichmann, V. Vogel, A. Vojtkova, J. Herglotz, S. Moore, J. Koch, J. Lausen, W. Mantele, H. Gohlke, and M. Grez. Dimer-tetramer transition controls RUNX1/ETO leukemogenic activity. *Blood*. 116:603-613 (2010).
18. A. Okal, M. Mossalam, K.J. Matissek, A.S. Dixon, P.J. Moos, and C.S. Lim. A Chimeric p53 Evades Mutant p53 Transdominant Inhibition in Cancer Cells. *Mol Pharm*. 10:3922-3933 (2013).
19. J.E. Visvader. Cells of origin in cancer. *Nat*. 469:314-322 (2011).
20. N.A. Lobo, Y. Shimono, D. Qian, and M.F. Clarke. The Biology of Cancer Stem Cells. *Annu Rev Cell Dev Biol*. 23:675-699 (2007).
21. A. Okal, S. Reaz, and C. Lim. Cancer Biology: Some causes for a variety of different diseases. In Y.H. Bae, R.J. Mersny, and K. Park (eds.), *Cancer Targeted Drug Delivery*, Springer New York, 2013, pp. 121-159.
22. N.C. Turner and J.S. Reis-Filho. Genetic heterogeneity and cancer drug resistance. *The Lancet Oncology*. 13:e178-185 (2012).
23. T.A. Yap, M. Gerlinger, P.A. Futreal, L. Pusztai, and C. Swanton. Intratumor heterogeneity: seeing the wood for the trees. *Sci Transl Med*. 4:127ps110 (2012).
24. D.L. Dexter, H.M. Kowalski, B.A. Blazar, Z. Fliigel, R. Vogel, and G.H. Heppner. Heterogeneity of tumor cells from a single mouse mammary tumor. *Cancer Research*. 38:3174-3181 (1978).
25. C.E. Meacham and S.J. Morrison. Tumour heterogeneity and cancer cell plasticity. *Nature*. 501:328-337 (2013).
26. N.C. Turner and A.L. Jones. Management of breast cancer—Part I. *BMJ*. 337: (2008).
27. S.E. Singletary, L. Patel-Parekh, and K.I. Bland. Treatment trends in early-stage invasive lobular carcinoma: a report from the National Cancer Data Base. *Ann Surg*. 242:281-289 (2005).
28. E.A. Rakha, J.S. Reis-Filho, F. Baehner, D.J. Dabbs, T. Decker, V. Eusebi, S.B. Fox, S. Ichihara, J. Jacquemier, S.R. Lakhani, J. Palacios, A.L. Richardson, S.J. Schnitt, F.C. Schmitt, P.H. Tan, G.M. Tse, S. Badve, and I.O. Ellis. Breast cancer prognostic classification in the molecular era: the role of histological grade. *Breast Cancer Research : BCR*. 12:207 (2010).
29. N.C. Turner and A.L. Jones. Management of breast cancer—Part II. *BMJ*. 337: (2008).
30. M. De Laurentiis, G. Canello, D. D'Agostino, M. Giuliano, A. Giordano, E. Montagna, R. Lauria, V. Forestieri, A. Esposito, L. Silvestro, R. Pennacchio, C. Criscitiello, A. Montanino, G. Limite, A.R. Bianco, and S. De Placido. Taxane-Based Combinations As Adjuvant Chemotherapy of Early Breast Cancer: A Meta-Analysis of Randomized Trials. *Journal of Clinical Oncology*. 26:44-53 (2008).

31. Effects of chemotherapy and hormonal therapy for early breast cancer on recurrence and 15-year survival: an overview of the randomised trials. *Lancet*. 365:1687-1717 (2005).
32. D. Greene, L.M. Nail, V.K. Fieler, D. Dudgeon, and L.S. Jones. A comparison of patient-reported side effects among three chemotherapy regimens for breast cancer. *Cancer Pract*. 2:57-62 (1994).
33. A.H. Partridge, H.J. Burstein, and E.P. Winer. Side effects of chemotherapy and combined chemohormonal therapy in women with early-stage breast cancer. *J Natl Cancer Inst Monogr*:135-142 (2001).
34. R.R. Love, H. Leventhal, D.V. Easterling, and D.R. Nerenz. Side effects and emotional distress during cancer chemotherapy. *Cancer*. 63:604-612 (1989).
35. C.L. Shapiro and A. Recht. Side effects of adjuvant treatment of breast cancer. *New England Journal of Medicine*. 344:1997-2008 (2001).
36. C.L. Vogel, M.A. Cobleigh, D. Tripathy, J.C. Gutheil, L.N. Harris, L. Fehrenbacher, D.J. Slamon, M. Murphy, W.F. Novotny, M. Burchmore, S. Shak, S.J. Stewart, and M. Press. Efficacy and safety of trastuzumab as a single agent in first-line treatment of HER2-overexpressing metastatic breast cancer. *J Clin Oncol*. 20:719-726 (2002).
37. P.E. Goss, J.N. Ingle, S. Martino, N.J. Robert, H.B. Muss, M.J. Piccart, M. Castiglione, D. Tu, L.E. Shepherd, K.I. Pritchard, R.B. Livingston, N.E. Davidson, L. Norton, E.A. Perez, J.S. Abrams, P. Therasse, M.J. Palmer, and J.L. Pater. A randomized trial of letrozole in postmenopausal women after five years of tamoxifen therapy for early-stage breast cancer. *N Engl J Med*. 349:1793-1802 (2003).
38. L.A. Carey, C.M. Perou, C.A. Livasy, et al. Race, breast cancer subtypes, and survival in the carolina breast cancer study. *JAMA*. 295:2492-2502 (2006).
39. T. Sørli, R. Tibshirani, J. Parker, T. Hastie, J.S. Marron, A. Nobel, S. Deng, H. Johnsen, R. Pesich, S. Geisler, J. Demeter, C.M. Perou, P.E. Lønning, P.O. Brown, A.-L. Børresen-Dale, and D. Botstein. Repeated observation of breast tumor subtypes in independent gene expression data sets. *Proceedings of the National Academy of Sciences*. 100:8418-8423 (2003).
40. C.A. Hudis and L. Gianni. Triple-negative breast cancer: an unmet medical need. *Oncologist*. 16 Suppl 1:1-11 (2011).
41. O. Gluz, C. Liedtke, N. Gottschalk, L. Pusztai, U. Nitz, and N. Harbeck. Triple-negative breast cancer--current status and future directions. *Ann Oncol*. 20:1913-1927 (2009).
42. J. Crown, J. O'Shaughnessy, and G. Gullo. Emerging targeted therapies in triple-negative breast cancer. *Ann Oncol*. 23 Suppl 6:vi56-65 (2012).
43. O. Gluz, C. Liedtke, N. Gottschalk, L. Pusztai, U. Nitz, and N. Harbeck. Triple-negative breast cancer--current status and future directions. *Ann Oncol*. 20:1913-1927 (2009).

44. C.O. Leong, N. Vidnovic, M.P. DeYoung, D. Sgroi, and L.W. Ellisen. The p63/p73 network mediates chemosensitivity to cisplatin in a biologically defined subset of primary breast cancers. *The Journal of Clinical Investigation*. 117:1370-1380 (2007).
45. C. Oakman, G. Viale, and A. Di Leo. Management of triple negative breast cancer. *Breast*. 19:312-321 (2010).
46. N.U. Lin, A. Vanderplas, M.E. Hughes, R.L. Theriault, S.B. Edge, Y.N. Wong, D.W. Blayney, J.C. Niland, E.P. Winer, and J.C. Weeks. Clinicopathologic features, patterns of recurrence, and survival among women with triple-negative breast cancer in the National Comprehensive Cancer Network. *Cancer*. 118:5463-5472 (2012).
47. R. Santana-Davila and E.A. Perez. Treatment options for patients with triple-negative breast cancer. *J Hematol Oncol*. 3:42 (2010).
48. S. Cleator, W. Heller, and R.C. Coombes. Triple-negative breast cancer: therapeutic options. *The Lancet Oncology*. 8:235-244 (2007).
49. B.P. Schneider, E.P. Winer, W.D. Foulkes, J. Garber, C.M. Perou, A. Richardson, G.W. Sledge, and L.A. Carey. Triple-negative breast cancer: risk factors to potential targets. *Clinical Cancer Research : an official journal of the American Association for Cancer Research*. 14:8010-8018 (2008).
50. J.S. Reis-Filho and A.N. Tutt. Triple negative tumours: a critical review. *Histopathology*. 52:108-118 (2008).
51. C. Liedtke, C. Mazouni, K.R. Hess, F. Andre, A. Tordai, J.A. Mejia, W.F. Symmans, A.M. Gonzalez-Angulo, B. Hennessy, M. Green, M. Cristofanilli, G.N. Hortobagyi, and L. Pusztai. Response to neoadjuvant therapy and long-term survival in patients with triple-negative breast cancer. *J Clin Oncol*. 26:1275-1281 (2008).
52. R. Dent, M. Trudeau, K.I. Pritchard, W.M. Hanna, H.K. Kahn, C.A. Sawka, L.A. Lickley, E. Rawlinson, P. Sun, and S.A. Narod. Triple-negative breast cancer: clinical features and patterns of recurrence. *Clinical cancer research : an official journal of the American Association for Cancer Research*. 13:4429-4434 (2007).
53. D.P. Silver, A.L. Richardson, A.C. Eklund, Z.C. Wang, Z. Szallasi, Q. Li, N. Juul, C.O. Leong, D. Calogrias, A. Buraimoh, A. Fatima, R.S. Gelman, P.D. Ryan, N.M. Tung, A. De Nicolo, S. Ganesan, A. Miron, C. Colin, D.C. Sgroi, L.W. Ellisen, E.P. Winer, and J.E. Garber. Efficacy of neoadjuvant Cisplatin in triple-negative breast cancer. *J Clin Oncol*. 28:1145-1153 (2010).
54. B.D. Lehmann, J.A. Bauer, X. Chen, M.E. Sanders, A.B. Chakravarthy, Y. Shyr, and J.A. Pietenpol. Identification of human triple-negative breast cancer subtypes and preclinical models for selection of targeted therapies. *The Journal of Clinical Investigation*. 121:2750-2767 (2011).
55. N. Turner, E. Moretti, O. Siclari, I. Migliaccio, L. Santarpia, M. D'Incalci, S. Piccolo, A. Veronesi, A. Zambelli, G. Del Sal, and A. Di Leo. Targeting triple negative breast cancer: Is p53 the answer? *Cancer Treat Rev*. 39:541-550 (2013).

56. W.J. Irvin Jrand L.A. Carey. What is triple-negative breast cancer? *Eur J Cancer*. 44:2799-2805 (2008).
57. T. Sorlie, C.M. Perou, R. Tibshirani, T. Aas, S. Geisler, H. Johnsen, T. Hastie, M.B. Eisen, M. van de Rijn, S.S. Jeffrey, T. Thorsen, H. Quist, J.C. Matese, P.O. Brown, D. Botstein, P.E. Lonning, and A.L. Borresen-Dale. Gene expression patterns of breast carcinomas distinguish tumor subclasses with clinical implications. *Proceedings of the National Academy of Sciences of the United States of America*. 98:10869-10874 (2001).
58. A.M. Davidoff, B.J. Kerns, J.D. Iglehart, and J.R. Marks. Maintenance of p53 alterations throughout breast cancer progression. *Cancer Res*. 51:2605-2610 (1991).
59. R.M. Elledge and D.C. Allred. The p53 tumor suppressor gene in breast cancer. *Breast Cancer Res Treat*. 32:39-47 (1994).
60. V.A. Belyi, P. Ak, E. Markert, H. Wang, W. Hu, A. Puzio-Kuter, and A.J. Levine. The origins and evolution of the p53 family of genes. *Cold Spring Harb Perspect Biol*. 2:a001198 (2010).
61. M. Lacroix, R.A. Toillon, and G. Leclercq. p53 and breast cancer, an update. *Endocr Relat Cancer*. 13:293-325 (2006).
62. A. Efeyan and M. Serrano. p53: guardian of the genome and policeman of the oncogenes. *Cell Cycle*. 6:1006-1010 (2007).
63. W.S. el-Deiry, T. Tokino, V.E. Velculescu, D.B. Levy, R. Parsons, J.M. Trent, D. Lin, W.E. Mercer, K.W. Kinzler, and B. Vogelstein. WAF1, a potential mediator of p53 tumor suppression. *Cell*. 75:817-825 (1993).
64. T. Miyashita and J.C. Reed. Tumor suppressor p53 is a direct transcriptional activator of the human bax gene. *Cell*. 80:293-299 (1995).
65. A.J. Levine, J. Momand, and C.A. Finlay. The p53 tumour suppressor gene. *Nature*. 351:453-456 (1991).
66. U.M. Moll, G. Riou, and A.J. Levine. Two distinct mechanisms alter p53 in breast cancer: mutation and nuclear exclusion. *PNAS*. 89:7262-7266 (1992).
67. P.H. Kussie, S. Gorina, V. Marechal, B. Elenbaas, J. Moreau, A.J. Levine, and N.P. Pavletich. Structure of the MDM2 oncoprotein bound to the p53 tumor suppressor transactivation domain. *Science*. 274:948-953 (1996).
68. S. Shangary and S. Wang. Small-molecule inhibitors of the MDM2-p53 protein-protein interaction to reactivate p53 function: a novel approach for cancer therapy. *Annu Rev Pharmacol Toxicol*. 49:223-241 (2009).
69. U.M. Moll, M. LaQuaglia, J. Benard, and G. Riou. Wild-type p53 protein undergoes cytoplasmic sequestration in undifferentiated neuroblastomas but not in differentiated tumors. *Proceedings of the National Academy of Sciences of the United States of America*. 92:4407-4411 (1995).

70. C.B. Piantino, S.T. Reis, N.I. Viana, I.A. Silva, D.R. Morais, A.A. Antunes, N. Dip, M. Srougi, and K.R. Leite. Prima-1 induces apoptosis in bladder cancer cell lines by activating p53. *Clinics (Sao Paulo)*. 68:297-303 (2013).
71. M.N. Saha, L. Qiu, and H. Chang. Targeting p53 by small molecules in hematological malignancies. *J Hematol Oncol*. 6:23 (2013).
72. V.J. Bykov, N. Issaeva, N. Zache, A. Shilov, M. Hultcrantz, J. Bergman, G. Selivanova, and K.G. Wiman. Reactivation of mutant p53 and induction of apoptosis in human tumor cells by maleimide analogs. *The Journal of Biological Chemistry*. 280:30384-30391 (2005).
73. L.J. Koand C. Prives. p53: puzzle and paradigm. *Genes & Development*. 10:1054-1072 (1996).
74. N.D. Marchenko, A. Zaika, and U.M. Moll. Death signal-induced localization of p53 protein to mitochondria. A potential role in apoptotic signaling. *J Biol Chem*. 275:16202-16212 (2000).
75. M. Mihara, S. Erster, A. Zaika, O. Petrenko, T. Chittenden, P. Pancoska, and U.M. Moll. p53 has a direct apoptogenic role at the mitochondria. *Mol Cell*. 11:577-590 (2003).
76. M. Mossalam, K.J. Matissek, A. Okal, J.E. Constance, and C.S. Lim. Direct induction of apoptosis using an optimal mitochondrially targeted p53. *Mol Pharm*. 9:1449-1458 (2012).
77. M. Oren. Regulation of the p53 tumor suppressor protein. *The Journal of Biological Chemistry*. 274:36031-36034 (1999).
78. T. Riley, E. Sontag, P. Chen, and A. Levine. Transcriptional control of human p53-regulated genes. *Nature Reviews Molecular Cell Biology*. 9:402-412 (2008).
79. K.H. Vousden. Outcomes of p53 activation--spoilt for choice. *Journal of Cell Science*. 119:5015-5020 (2006).
80. M.L. Smith and Y.R. Seo. p53 regulation of DNA excision repair pathways. *Mutagenesis*. 17:149-156 (2002).
81. M.L. Smith, J.M. Ford, M.C. Hollander, R.A. Bortnick, S.A. Amundson, Y.R. Seo, C.X. Deng, P.C. Hanawalt, and A.J. Fornace, Jr. p53-mediated DNA repair responses to UV radiation: studies of mouse cells lacking p53, p21, and/or gadd45 genes. *Molecular and Cellular Biology*. 20:3705-3714 (2000).
82. B. Pucci, M. Kasten, and A. Giordano. Cell cycle and apoptosis. *Neoplasia*. 2:291-299 (2000).
83. <http://www.sabiosciences.com/genetable.php?pcatn=PAHS-027A>.
84. M. Schuler, E. Bossy-Wetzel, J.C. Goldstein, P. Fitzgerald, and D.R. Green. p53 induces apoptosis by caspase activation through mitochondrial cytochrome c release. *The Journal of Biological Chemistry*. 275:7337-7342 (2000).

85. M. Mihara, S. Erster, A. Zaika, O. Petrenko, T. Chittenden, P. Pancoska, and U.M. Moll. p53 has a direct apoptogenic role at the mitochondria. *Molecular Cell*. 11:577-590 (2003).
86. M. Mossalam, K.J. Matissek, A. Okal, J.E. Constance, and C.S. Lim. Direct induction of apoptosis using an optimal mitochondrially targeted p53. *Mol Pharm*. 9:1449-1458 (2012).
87. K.J. Matissek, M. Mossalam, A. Okal, and C.S. Lim. The DNA binding domain of p53 is sufficient to trigger a potent apoptotic response at the mitochondria. *Mol Pharm*. 10:3592-3602 (2013).
88. N.D. Marchenko, S. Wolff, S. Erster, K. Becker, and U.M. Moll. Monoubiquitylation promotes mitochondrial p53 translocation. *The EMBO Journal*. 26:923-934 (2007).
89. N.D. Marchenko and U.M. Moll. The role of ubiquitination in the direct mitochondrial death program of p53. *Cell Cycle*. 6:1718-1723 (2007).
90. F. Hagn, C. Klein, O. Demmer, N. Marchenko, A. Vaseva, U.M. Moll, and H. Kessler. BclxL changes conformation upon binding to wild-type but not mutant p53 DNA binding domain. *The Journal of Biological Chemistry*. 285:3439-3450 (2010).
91. Y. Tomita, N. Marchenko, S. Erster, A. Nemajerova, A. Dehner, C. Klein, H. Pan, H. Kessler, P. Pancoska, and U.M. Moll. WT p53, but not tumor-derived mutants, bind to Bcl2 via the DNA binding domain and induce mitochondrial permeabilization. *The Journal of Biological Chemistry*. 281:8600-8606 (2006).
92. J.L. Perfettini, R.T. Kroemer, and G. Kroemer. Fatal liaisons of p53 with Bax and Bak. *Nature Cell Biology*. 6:386-388 (2004).
93. F. Talos, O. Petrenko, P. Mena, and U.M. Moll. Mitochondrially targeted p53 has tumor suppressor activities in vivo. *Cancer Research*. 65:9971-9981 (2005).
94. S. Erster, M. Mihara, R.H. Kim, O. Petrenko, and U.M. Moll. In vivo mitochondrial p53 translocation triggers a rapid first wave of cell death in response to DNA damage that can precede p53 target gene activation. *Molecular and Cellular Biology*. 24:6728-6741 (2004).
95. U.M. Moll and A. Zaika. Nuclear and mitochondrial apoptotic pathways of p53. *FEBS letters*. 493:65-69 (2001).
96. T. Soussi. p53 alterations in human cancer: more questions than answers. *Oncogene*. 26:2145-2156 (2007).
97. T. Soussi, C. Ishioka, M. Claustres, and C. Beroud. Locus-specific mutation databases: pitfalls and good practice based on the p53 experience. *Nat Rev Cancer*. 6:83-90 (2006).
98. T. Soussi and K.G. Wiman. Shaping genetic alterations in human cancer: the p53 mutation paradigm. *Cancer Cell*. 12:303-312 (2007).

99. A. Willis, E.J. Jung, T. Wakefield, and X. Chen. Mutant p53 exerts a dominant negative effect by preventing wild-type p53 from binding to the promoter of its target genes. *Oncogene*. 23:2330-2338 (2004).
100. C.A. Midgley and D.P. Lane. p53 protein stability in tumour cells is not determined by mutation but is dependent on Mdm2 binding. *Oncogene*. 15:1179-1189 (1997).
101. G. Selivanova and K.G. Wiman. Reactivation of mutant p53: molecular mechanisms and therapeutic potential. *Oncogene*. 26:2243-2254 (2007).
102. W.M. Chan, W.Y. Siu, A. Lau, and R.Y. Poon. How many mutant p53 molecules are needed to inactivate a tetramer? *Molecular and Cellular Biology*. 24:3536-3551 (2004).
103. S. Rajagopalan, F. Huang, and A.R. Fersht. Single-Molecule characterization of oligomerization kinetics and equilibria of the tumor suppressor p53. *Nucleic Acids Res*. 39:2294-2303 (2011).
104. A.G. Zeimet and C. Marth. Why did p53 gene therapy fail in ovarian cancer? *The Lancet Oncology*. 4:415-422 (2003).
105. Ming K. Lee, Wei W. Teoh, Beng H. Phang, Wei M. Tong, Zhao Q. Wang, and K. Sabapathy. Cell-type, dose, and mutation-type specificity dictate mutant p53 functions in vivo. *Cancer Cell*. 22:751-764 (2012).
106. J.M. Mason and K.M. Arndt. Coiled coil domains: stability, specificity, and biological implications. *ChemBiochem*. 5:170-176 (2004).
107. A. Lupas. Coiled coils: new structures and new functions. *Trends Biochem Sci*. 21:375-382 (1996).
108. P. Burkhard, J. Stetefeld, and S.V. Strelkov. Coiled coils: a highly versatile protein folding motif. *Trends in Cell Biology*. 11:82-88 (2001).
109. R.A. Kammerer. Alpha-helical coiled-coil oligomerization domains in extracellular proteins. *Matrix Biol*. 15:555-565; discussion 567-558 (1997).
110. P. Burkhard, J. Stetefeld, and S.V. Strelkov. Coiled coils: a highly versatile protein folding motif. *Trends in Cell Biology*. 11:82-88 (2001).
111. C.M. Taylor and A.E. Keating. Orientation and oligomerization specificity of the Bcr coiled-coil oligomerization domain. *Biochemistry*. 44:16246-16256 (2005).
112. J.R. McWhirter, D.L. Galasso, and J.Y. Wang. A coiled-coil oligomerization domain of Bcr is essential for the transforming function of Bcr-Abl oncoproteins. *Molecular and Cellular Biology*. 13:7587-7595 (1993).
113. J.D. Alexis, N. Wang, W. Che, N. Lerner-Marmarosh, A. Sahni, V.A. Korshunov, Y. Zou, B. Ding, C. Yan, B.C. Berk, and J. Abe. Bcr kinase activation by angiotensin II inhibits peroxisome-proliferator-activated receptor gamma transcriptional activity in vascular smooth muscle cells. *Circ Res*. 104:69-78 (2009).

114. M.W. Deininger, J.M. Goldman, and J.V. Melo. The molecular biology of chronic myeloid leukemia. *Blood*. 96:3343-3356 (2000).
115. D.W. Woessner, C.S. Lim, and M.W. Deininger. Development of an effective therapy for chronic myelogenous leukemia. *Cancer J*. 17:477-486 (2011).
116. J.V. Melo and D.J. Barnes. Chronic myeloid leukaemia as a model of disease evolution in human cancer. *Nat Rev Cancer*. 7:441-453 (2007).
117. S.J. Yi, J. Groffen, and N. Heisterkamp. Bcr is a substrate for Transglutaminase 2 cross-linking activity. *BMC Biochem*. 12:8 (2011).
118. A.K. Lalwani, B.J. Walsh, P.G. Reilly, N. Muzyczka, and A.N. Mhatre. Development of in vivo gene therapy for hearing disorders: introduction of adeno-associated virus into the cochlea of the guinea pig. *Gene Ther*. 3:588-592 (1996).
119. I.M. Verma and N. Somia. Gene therapy -- promises, problems and prospects. *Nature*. 389:239-242 (1997).
120. A. Mountain. Gene therapy: the first decade. *Trends in Biotechnology*. 18:119-128 (2000).
121. R.R.B. Karina J. Matissek, James R. Davis and Carol S. Lim Choosing Targets for Gene Therapy. In P.Y. You (ed.), *Targets in Gene Therapy*, InTech, 2011.
122. M.L. Edelstein, M.R. Abedi, and J. Wixon. Gene therapy clinical trials worldwide to 2007—an update. *The Journal of Gene Medicine*. 9:833-842 (2007).
123. S.L. Ginn, I.E. Alexander, M.L. Edelstein, M.R. Abedi, and J. Wixon. Gene therapy clinical trials worldwide to 2012 - an update. *The Journal of Gene Medicine*. 15:65-77 (2013).
124. I.A. McNeish, S.J. Bell, and N.R. Lemoine. Gene therapy progress and prospects: cancer gene therapy using tumour suppressor genes. *Gene Ther*. 11:497-503 (2004).
125. S.A. Rosenberg, J.C. Yang, and N.P. Restifo. Cancer immunotherapy: moving beyond current vaccines. *Nature Medicine*. 10:909-915 (2004).
126. D. Kirn. Oncolytic virotherapy for cancer with the adenovirus dl1520 (Onyx-015): results of phase I and II trials. *Expert Opin Biol Ther*. 1:525-538 (2001).
127. M. Ali, N.R. Lemoine, and C.J. Ring. The use of DNA viruses as vectors for gene therapy. *Gene Ther*. 1:367-384 (1994).
128. C.E. Thomas, A. Ehrhardt, and M.A. Kay. Progress and problems with the use of viral vectors for gene therapy. *Nature Reviews Genetics*. 4:346-358 (2003).
129. M.L. Edelstein, M.R. Abedi, J. Wixon, and R.M. Edelstein. Gene therapy clinical trials worldwide 1989-2004-an overview. *The Journal of Gene Medicine*. 6:597-602 (2004).

130. J.A. Roth, S.F. Grammer, S.G. Swisher, R. Komaki, J. Nemunaitis, J. Merritt, T. Fujiwara, and R.E. Meyn, Jr. Gene therapy approaches for the management of non-small cell lung cancer. *Semin Oncol.* 28:50-56 (2001).
131. C.A. Gerdes, M.G. Castro, and P.R. Lowenstein. Strong promoters are the key to highly efficient, noninflammatory and noncytotoxic adenoviral-mediated transgene delivery into the brain in vivo. *Molecular therapy : the Journal of the American Society of Gene Therapy.* 2:330-338 (2000).
132. F.R. Khuri, J. Nemunaitis, I. Ganly, J. Arseneau, I.F. Tannock, L. Romel, M. Gore, J. Ironside, R.H. MacDougall, C. Heise, B. Randlev, A.M. Gillenwater, P. Bruso, S.B. Kaye, W.K. Hong, and D.H. Kirn. a controlled trial of intratumoral ONYX-015, a selectively-replicating adenovirus, in combination with cisplatin and 5-fluorouracil in patients with recurrent head and neck cancer. *Nature Medicine.* 6:879-885 (2000).
133. A.P. Cotrim and B.J. Baum. Gene therapy: some history, applications, problems, and prospects. *Toxicol Pathol.* 36:97-103 (2008).
134. A. Jacobs, X.O. Breakefield, and C. Fraefel. HSV-1-based vectors for gene therapy of neurological diseases and brain tumors: part I. HSV-1 structure, replication and pathogenesis. *Neoplasia.* 1:387-401 (1999).
135. R.d.S. Coura and N.B. Nardi. A role for adeno-associated viral vectors in gene therapy. *Genetics and Molecular Biology.* 31:1-11 (2008).
136. S. Li and L. Huang. Nonviral gene therapy: promises and challenges. *Gene Ther.* 7:31-34 (2000).
137. T. Niidome and L. Huang. Gene therapy progress and prospects: nonviral vectors. *Gene Ther.* 9:1647-1652 (2002).
138. G.D. Schmidt-Wolf and I.G. Schmidt-Wolf. Non-viral and hybrid vectors in human gene therapy: an update. *Trends in molecular medicine.* 9:67-72 (2003).
139. C. Conwell and L. Huang. Recent Progress in Non-viral Gene Delivery. In K. Taira, K. Kataoka, and T. Niidome (eds.), *Non-viral Gene Therapy*, Springer Tokyo, 2005, pp. 3-10.
140. S.D. Li and L. Huang. Gene therapy progress and prospects: non-viral gene therapy by systemic delivery. *Gene Ther.* 13:1313-1319 (2006).
141. R.G. Vile, S.J. Russell, and N.R. Lemoine. Cancer gene therapy: hard lessons and new courses. *Gene Ther.* 7:2-8 (2000).
142. A.S. Dixon, S.S. Pendley, B.J. Bruno, D.W. Woessner, A.A. Shimpi, T.E. Cheatham, 3rd, and C.S. Lim. Disruption of Bcr-Abl coiled coil oligomerization by design. *J Biol Chem.* 286:27751-27760 (2011).

CHAPTER 2

CANCER BIOLOGY: SOME CAUSES FOR A VARIETY OF DIFFERENT DISEASES

2.1 Abstract

Advances and integration of biochemistry, cell biology, molecular biology, and genetics have led to a better fundamental understanding of cancer biology and the causes for many types of cancer. Cancer is now thought to originate following either the "cancer stem cell hypothesis" or the "stochastic clonal model." The pathways that lead to cancer have been delineated genetically and epigenetically. In addition, post-translational players such as miRNA are now known to have a significant role in cancer diagnosis. To meet the high demands of rapidly proliferating cancer cells, alterations of nutrient and metabolic pathways are required. Accordingly, tumor physiology and the cancer microenvironment have been extensively studied due to their significant role in malignancy. This chapter will discuss these topics and provide a detailed investigation of cancer biology including identification of many of the genes, proteins, signals, and other

Reprinted by permission from *Springer "Cancer Targeted Drug Delivery: An Elusive Dream"* 121-69 (2013).

Okal A., Reaz S., Lim C.S.

A.O. wrote sections on origins of cancer, pathways that lead to cancer, and miRNA in cancer diagnosis. S.R. wrote sections on nutrients and metabolic characteristics of cancer. C.S. wrote sections on the cancer microenvironment.

factors involved in tumorigenesis.

2.2 Introduction

The oldest identification and description of cancer dates back to 1600 BC in Egypt (1). Since then, different theories have been proposed to explain the origins for cancer development and survival. While the word *cancer* itself refers to the blood vessels that feed the tumors, cancerous cells develop from normal cells that eventually acquire the ability to proliferate aberrantly and grow uncontrollably into tumors that can metastasize (2). From the most common initiating events that lead to malignant transformation, the diverse modifications in tumor metabolic pathways that give cancerous cells a clear proliferative advantage, and terminating in the dynamics of the cancer microenvironment, this comprehensive cache of knowledge can be used for effective drug delivery of existing and novel cancer therapeutics.

2.3 Origins of Cancer

2.3.1 Cancer Stem Cells

Based on data obtained from both *in vitro* and *in vivo* studies, only a small population of tumor cells are capable of self-renewal, commonly identified as cancer stem cells (CSCs) (3, 4). Characterized by their ability to proliferate indefinitely, these tumorigenic cells drive malignancy in a similar manner to the way normal stem cells construct organs. As with normal organs and tissues, tumors are formed from heterogeneous populations of cells with different levels of differentiation and proliferation capacities. Therefore, tumors have been viewed as aberrant organs that

originate from cancer stem cells that have acquired mutations allowing them to proliferate abnormally (4). However, cancer stem cells are only a small subset of cells in a given tumor. For instance, 1-4% of leukemic cells were capable of forming spleen colonies when introduced *in vivo* (5, 6), and only 0.0001% to 0.01% of leukemic mouse myeloma cells, separated from normal hematopoietic cells, were able to form colonies *in vitro* (7). Although cancer stem cells are very similar in nature and function to normal stem cells, cancer stem cells are not necessarily aberrant counterparts of normal stem cells (8). In certain cases, genetic modifications of normal stem cells can lead to their transformation into cancer stem cells (Figure 2.1).

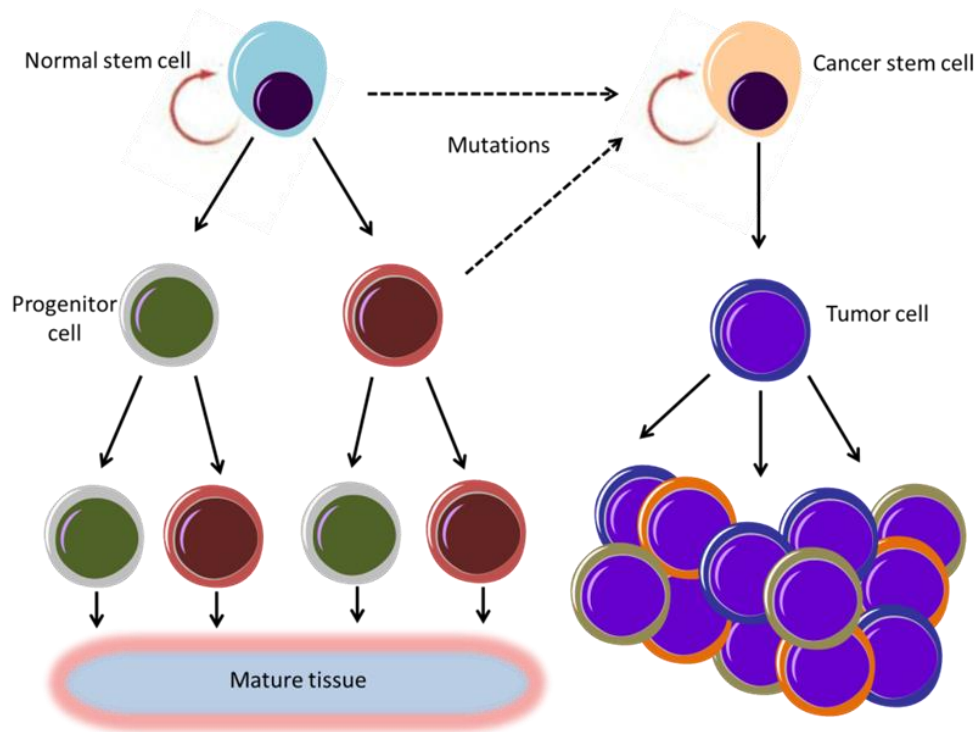


Figure 2.1 Certain genetic changes or mutations can transform normal stem cells or progenitor cells into cancer stem cells. Such an event allows malignant tumors to divide and differentiate indefinitely. Adapted from (9)

For example, it is well accepted that the reciprocal translocation between chromosomes 9 and 22 [t(9;22)(q34;q11)] in chronic myelogenous leukemia (CML), which leads to the formation of the Bcr-Abl oncogene, can transform normal hematopoietic stem cells into cancer stem cells that propagate in the bone marrow (10, 11). However, it is often difficult to establish a link between normal stem cells and cancer stem cells. It is well accepted now that CSCs can also originate from progenitors that have acquired the ability to self-renew as well as from normal stem cells (Figure 2.1). Therefore, identifying proper markers and techniques to isolate a homogenous population of CSCs remains challenging and is considered to be the rate-limiting step in understanding the nature and function of CSCs.

In addition, proper isolation of CSCs could lead to identification of the specific molecular characteristics of such cells for cancer targeted therapy (12). Some success has been achieved in isolating CSCs often in a heterogeneous mixture with normal stem cells. For instance, it has been demonstrated that cells defined by the phenotype CD34⁺/CD38⁻ contain a subset of cells that were capable of initiating human acute myeloid leukemia (AML) when transplanted into murine models (13). Table 2.1 illustrates some of the well-established definitions of CSCs in different cancer types and their origins (8). Similar work has led to the identification of cancer stem cells in breast cancer (14), gliomas (15, 16), melanoma (17), prostate cancer (18), and osteosarcoma (19). These observations have led to an increased interest in the “cancer stem cell hypothesis” (4) due to the therapeutic potential that could be translated clinically upon proper identification of CSCs.

Table 2.1 Markers of cancer stem cells in different cancers (adapted from (8))

Cancer	Definition	Fraction	Origin	References
AML	CD34 ⁺ CD38 ⁻	0.2-1%	Myeloid progenitors	(20)
B-ALL (p190 BCR-ABL1)	CD34 ⁺ CD38 ⁻ CD19 ⁺	1.1%	B progenitors	(21)
Medulloblastomas	CD133 ⁺	6-21%	Stem cells/ progenitors	(22)
Glioblastomas	CD133 ⁺	19-29%	Stem cells/ progenitors	(22)
Ependymomas	CD133 ⁺ Nestin ⁺ RC2 ⁺ BLBP ⁺	0.001- 1.5%	Radial glia cells	(23)
Breast cancer	ESA ⁺ CD44 ⁺ CD24 ^{-/low} LIN ⁻	0.5-5%	Stem cells/ progenitors	(24)
Melanomas (metastatic)	CD20 ⁺ MCAM ⁺	20.0%	N/A	(25)

2.3.2 Cancer Stem Cell vs. Stochastic Model

While the “cancer stem cell hypothesis” suggests a hierarchical organization in which a) tumors originate in cancer stem cells niches or their progeny through dysregulation of self-renewal process, and b) tumors contain a subset of cells that have stem cell characteristics (26), other models have been suggested to describe tumor development. One such model is the *stochastic* model for cancer origins in which tumors are thought to develop as a consequence of random somatic mutations and develop the capability to self-renew and differentiate similar to stem cells. According to the stochastic model, any cell has the potential to activate carcinogenesis implying that tumor initiation is no longer exclusive to a rare subset of cells. In other words, every cell in the tumor bulk will have an equal probability to develop cancer stem cell-like characteristics and recapitulate the tumor (27, 28). Some of the major arguments supporting the stochastic model are the high heterogeneity, genomic instability, and epigenetic alterations observed in tumors (29). Nevertheless, it is well-established now that not all cancers follow one model or another. Even though *in vivo* studies suggest that leukemias (15, 30), breast cancer (31-33), and squamous cell carcinoma (34) in mice follow the cancer stem cell model, it remains dangerous to generalize that cancers in mice follow a hierarchical CSC model rather than a stochastic clonal evolution model for tumor development.

2.4 Pathways that Lead to Cancer

Following vast advances in the field of genetics, the stochastic genetic model for cancer development has predominated other models, supported by the discovery of dominantly acting oncogenes, recessively acting tumor-suppressor genes, and diverse

molecular changes observed in cancer that lead to the highly heterogeneous nature of the disease (35). Nevertheless, recent correlations between cancer development and the pathological epigenetic changes commonly observed in cancers such as global DNA methylation, chromatin alterations, and genomic imprinting suggest that such events can serve as surrogates for genetic mutations (35, 36). In this section, an overview of the main changes that take place during cellular transformation in cancer cells will be discussed. In addition, a summary of the main pathways that lead to cancer cell survival will be presented.

2.4.1 Genetic Changes

First postulated by Carl O. Nordling in 1953, the multiple-hit hypothesis offered a clonal approach for explaining cancer development (37). Nordling suggested that accumulation of mutations in the DNA of cells leads to malignant development. In addition, Nordling emphasized that cancer susceptibility in industrialized nations can be correlated to the sixth power of age, implying that for cancer to develop, six mutations in the DNA must be acquired. However, Nordling's explanation for cancer development did not agree well with the fact that cells possess several defense mechanisms against acquiring mutations via the expression of tumor suppressors. Therefore, it was not until 1971 that the geneticist Alfred Knudson developed the concept of a "two-hit hypothesis" based on several studies of retinoblastoma patients. Between 1944 and 1969, Knudson studied 48 patients that had retinoblastoma due to either somatic or germ-line mutations. Interestingly, Knudson showed that for patients with somatic mutations, tumors took longer to develop in the eye compared to patients who inherited a mutation (38). He

concluded that for retinoblastoma to develop, a subject has to acquire a mutation in both alleles of a tumor suppressor gene (TSG) that encodes for the retinoblastoma protein (pRb). Thus, subjects who inherited a mutation in one of the two copies of the RB1 gene were more susceptible to developing tumors, since only one more mutation in the second copy of the tumor suppressor needed to be acquired. (39). Knudson’s hypothesis (Figure 2.2) forms the basis for understanding how mutations in tumor suppressor genes correlate to tumor development, where, for a tumor suppressor to become inactivated, both alleles need to be mutated or “hit” before a tumor can develop.

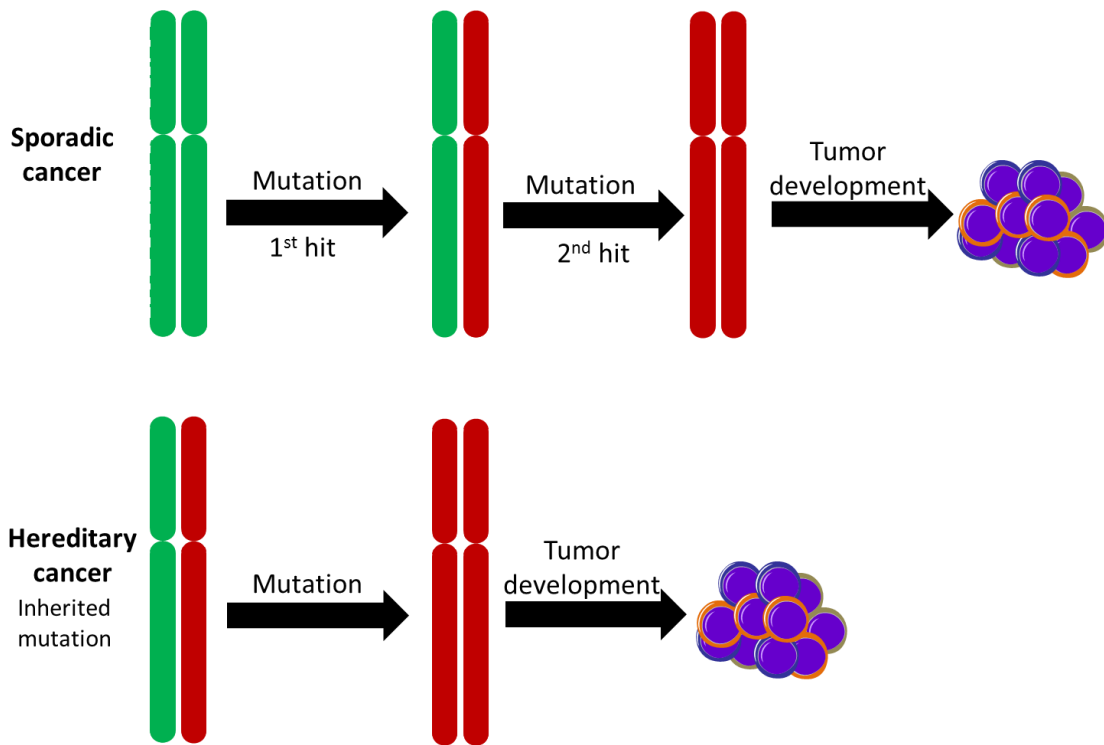


Figure 2.2 According to the “two-hit hypothesis,” both alleles of a tumor suppressor gene must be mutated prior to malignant transformation. In sporadic cancers, two mutations must be acquired before a complete inactivation of a tumor suppressor gene. In hereditary cancers, an inherited mutation exists and only one more “hit” is required before tumors develop.

2.4.1.1 Tumor Suppressor Genes in Cancer

Following Knudson's findings, aberrant function of tumor suppressor genes emerged as the leading cause for cancer development. It is well-documented now that activation of a proto-oncogene will not lead to cancer unless accompanied by an inactivation event of both alleles of a TSG. Therefore, it is important to examine tumor suppressor genes and understand the mechanisms by which they prevent uncontrolled cellular growth in normal cells. In this section, several key prototypical tumor suppressor genes will be discussed.

2.4.1.1.1 pRb

The retinoblastoma protein (pRb) was one of the first tumor suppressors to be identified during extensive studies on cancer-prone families in the 1940s (40). Even though pRb is important in all cells, its inactivation usually corresponds in most cases to tumor development specifically in the eye. Similar to other tumor suppressors, the pRb protein inhibits tumor growth by interfering directly with cell cycle progression, leading to arrest in G1 phase. To exert its tumor suppressor function, pRb inhibits the E2F transcription factor family known to be essential for transactivating a cohort of genes involved in DNA replication in S phase. Consequently, pRb prevents replication of damaged DNA commonly found in cancer cells. During pathogenesis and tumor progression, pRb function can be impaired via several mechanisms. In retinoblastoma, small cell lung carcinoma, and bladder carcinoma, the tumor suppressor gene is mutated leading to a loss of function of pRb (41). In cervical carcinomas, the human papillomavirus E7 oncoprotein can bind the active pocket of pRb causing the tumor

suppressor protein to become incapable of binding E2F transcription factors (42). Finally, in esophageal, breast, and squamous cell carcinomas, cyclin D is frequently overexpressed which then destabilizes the pRb-E2F complex by phosphorylating pRb resulting in the inhibition of the tumor suppressor (43, 44). Figure 2.3 summarizes the effects of pRb on the cell cycle.

2.4.1.1.2 p53

Encoded by the TP53 gene mapped on the short arm of chromosome 17, p53 is commonly referred to as the “guardian of the genome” (45). Its tumor suppressor function can be divided into two main categories: the first being a sensor for DNA damage that activates the DNA repair machinery in the cells, and the second being a “policeman” for oncogenic signaling and activation (45).

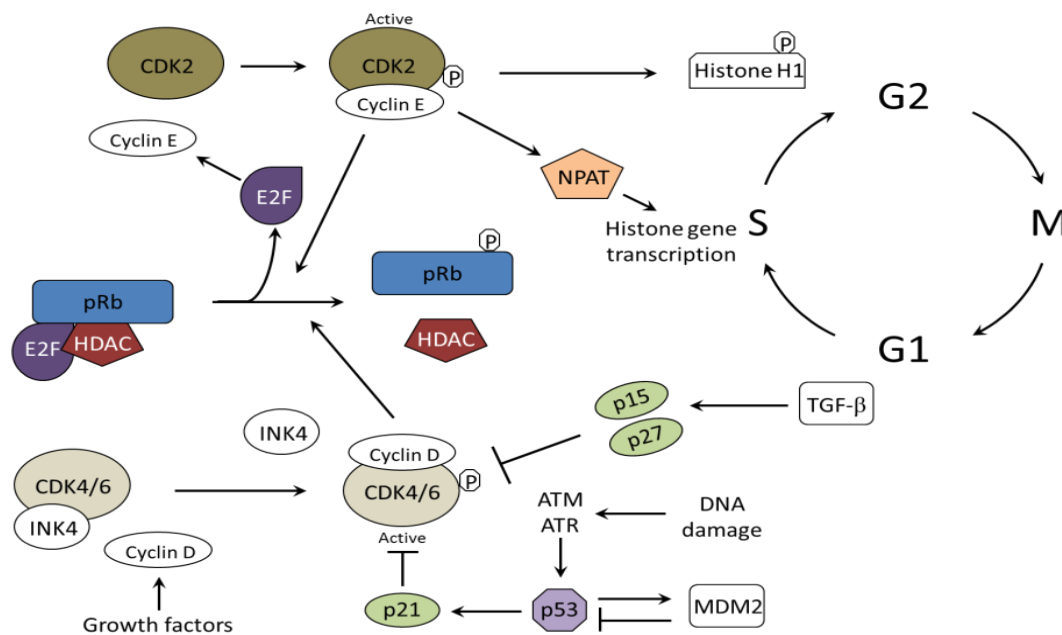


Figure 2.3 Retinoblastoma tumor suppressor function in cell cycle progression (adapted from (46)).

Known to be mutated in more than 50% of human cancers, the tumor suppressor p53 is a major player in several signaling pathways that are dependent on the context of the stimuli such as DNA repair, cell cycle progression, angiogenesis inhibition, and programmed cell death (apoptosis).

Similar to the tumor suppressor gene RB1, both alleles of TP53 must be inactivated for the protein to lose its function. According to Knudson's "two-hit hypothesis," subjects with an inherited mutation in one of the two copies of TP53 are predisposed to develop tumors in early adulthood since only one mutation needs to be acquired in the second copy of the gene to completely inactivate the tumor suppressor. This condition is rare and is known as Li-Fraumeni syndrome. Once activated in response to various cellular stimuli such as DNA damage (via UV, IR, or chemotherapy), hypoxia, or oncogene activation, the tumor suppressor, in its tetrameric form, acts as a transcription factor that regulates the expression of several genes involved in different cellular signaling events. This activity is mainly mediated by nuclear p53 which activates both the extrinsic and intrinsic apoptotic pathway. Furthermore, p53 can activate the extrinsic apoptotic pathway via the mitochondria as well (47). One of the most important signaling pathways controlled by p53 is DNA repair and its ability to induce apoptosis if cellular damage is too extensive to be repaired. Two of the main factors that control p53 activation upon DNA damage are ataxia-telangiectasia mutated (ATM) and ataxia-telangiectasia and Rad3-related (ATR) protein kinases. ATM and ATR are capable of rapidly degrading MDM2 (48), the main negative regulator protein of p53, as well as influencing the outcome of the p53 response to DNA damage by inducing various post-translational modifications on the tumor suppressor (49, 50). This is depicted in Figure

2.3, bottom right. In addition, p53 can be activated via the tumor suppressor ARF signaling pathway in response to sustained cellular proliferation. Similar to ATM and ATR, ARF can act as an inhibitor of MDM2 leading to the accumulation of p53 in the nucleus (51). Another major pathway by which p53 can regulate cell growth is via transactivation of the CDKN1A gene that leads to the expression of p21/WAF1 protein. As a member of the cyclin-dependent kinase inhibitor (CKI) family, p21 can inhibit the cyclin-CDK2 complex required for entry into G1 phase, causing an arrest in cell cycle progression (52). Therefore, p53 inactivation can be crucial during malignant transformation due to its ability to inhibit tumor growth via many different mechanisms.

Once activated in response to various cellular stimuli such as DNA damage (via UV, IR, or chemotherapy), hypoxia, or oncogene activation, the tumor suppressor, in its tetrameric form, acts as a transcription factor that regulates the expression of several genes involved in different cellular signaling events. This activity is mainly mediated by nuclear p53 which activates both the extrinsic and intrinsic apoptotic pathway. Furthermore, p53 can activate the extrinsic apoptotic pathway via the mitochondria as well (47). One of the most important signaling pathways controlled by p53 is DNA repair and its ability to induce apoptosis if cellular damage is too extensive to be repaired. Two of the main factors that control p53 activation upon DNA damage are ataxia-telangiectasia mutated (ATM) and ataxia-telangiectasia and Rad3-related (ATR) protein kinases. ATM and ATR are capable of rapidly degrading MDM2 (48), the main negative regulator protein of p53, as well as influencing the outcome of the p53 response to DNA damage by inducing various post-translational modifications on the tumor suppressor (49, 50). This is depicted in Figure 2.3, bottom right. In addition, p53 can be activated via the

tumor suppressor ARF signaling pathway in response to sustained cellular proliferation. Similar to ATM and ATR, ARF can act as an inhibitor of MDM2 leading to the accumulation of p53 in the nucleus (51). Another major pathway by which p53 can regulate cell growth is via transactivation of the CDKN1A gene that leads to the expression of p21/WAF1 protein. As a member of the cyclin-dependent kinase inhibitor (CKI) family, p21 can inhibit the cyclin-CDK2 complex required for entry into G1 phase, causing an arrest in cell cycle progression (52). Therefore, p53 inactivation can be crucial during malignant transformation due to its ability to inhibit tumor growth via many different mechanisms.

2.4.1.1.3 PTEN

PTEN is another tumor suppressor gene that is commonly found to be mutated in several human cancers. Although the PTEN gene product helps regulate cell cycle progression in a similar fashion to p53, this protein functions as a dual protein/lipid phosphatase. One of the major substrates for PTEN is PIP3, a crucial protein involved in the AKT/PKB signaling pathway. Upon dephosphorylation by PTEN, PIP3 can no longer recruit AKT to the cell plasma membrane, therefore disrupting the AKT/PKB pathway. This results in increased proliferation and activation of the growth regulatory factor mTOR (53). Similar to other tumor suppressor genes, PTEN can be inactivated by inheriting a mutation or by acquiring sporadic mutations that can render the protein inactive. Although PTEN knock-out models *in vivo* showed embryonic lethality, the tumor suppression functions of PTEN have been validated using heterozygous (PTEN^{+/-}) murine models where animals developed tumors in several organs (54, 55).

2.4.1.2 Proto-oncogenes and Oncogenes in Cancer

As part of the malignant transformation process, oncogene activation lies at the heart of tumor initiating mechanisms. Proto-oncogenes are normal genes involved in controlling cellular growth in normal cells that upon alteration (usually mutation or overexpression) can lead to the production of oncogenes, whose protein products induce cancer formation (40). Certain alterations of proto-oncogenes during tumorigenesis result in oncogene activation that allows cancer cells to exhibit abnormal proliferation. It has been suggested that the main mechanisms of proto-oncogene activation are a) point mutations that lead to gain-of-function, b) gene amplification resulting in growth advantage of cancer cells, and c) chromosomal rearrangement and fusion that can result in aberrant expression of growth-regulatory proteins (56). Since tumor suppressor proteins such as p53 respond rapidly and efficiently to oncoprotein activity in normal cells, it is frequently observed that oncogene activation is accompanied by inactivation of tumor suppressor genes. In this section, some examples of oncogenes and their activation mechanisms will be examined in the context of malignant progression.

2.4.1.2.1 Ras mutations

The Ras family of proto-oncogenes (H-ras, K-ras, N-ras and others) is known to be mutated in approximately 20% to 30% of human cancers (57). K-ras is mutated in about 30% of lung cancers, 50% of colon carcinomas, and 90% of pancreatic carcinomas (58). N-ras is known to be mutated in acute myeloid leukemias (59). The full function of ras proteins remains elusive. However, ras proteins are known to be monomeric membrane G proteins that can be activated in response to several extracellular stimuli

that control cellular proliferation and differentiation (60). Upon mutation, ras proteins are locked in the GTP-bound active state, resulting in constitutive activity. Consequently, oncogenic ras continuously activates downstream effectors such as the MAP-kinase Raf-1, which further activates the MEK/ERK gene regulation pathway that governs proliferation, differentiation and survival of cancer cells (61).

2.4.1.2.2 Myc amplification

The myc family of proto-oncogenes encodes transcription factors that are involved in several cellular pathways that control cell cycle, cell growth, differentiation, apoptosis and angiogenesis (62). C-myc is a myc family member that is commonly overexpressed in several carcinomas. Studies show that the gene encoding c-myc is amplified in about 20% to 30% of breast, ovarian and squamous cell carcinomas (63). N-myc is another member of the myc family that is amplified in neuroblastomas, where up to 300 copies of the gene can be found in a single cell (64, 65). Upon overexpression of Myc, several genes involved in cellular proliferation are altered. For example, cyclins (which promote cell cycle progression and division) (66) and ribosomal RNA and proteins (which increase global protein synthesis needed for cell division) (67) are upregulated, and p21 (a key factor in causing cell cycle arrest) is downregulated (68). Similarly, the proto-oncogene erbB is another example in which amplification of a normal gene that regulates cellular growth can contribute significantly to tumor development (69).

2.4.1.2.3 Bcr-Abl Chromosomal Translocation

Chromosomal rearrangements are another mechanism by which proto-oncogenes can be activated during pathogenesis. Such events are frequently detected in hematologic cancers and to a lesser extent in some solid tumors (70, 71). In chronic myelogenous leukemia, a reciprocal translocation between chromosome 9 and 22 results in the formation of the Philadelphia chromosome that encodes the Bcr-Abl oncogene. Capable of autophosphorylation (i.e., auto-activation), the Bcr-Abl oncogene does not require activation by other cellular signals which allows it to retain constitutive activity (72). As a result, Bcr-Abl can drive malignant transformation by activating several prosurvival signaling pathways such as Ras-Raf-ERK, JAK-STAT and PI(3)K pathways (73).

2.4.2 Epigenetic Alterations

Epigenetic alterations in cancers are mitotically and meiotically heritable phenotypes caused by changes in the gene expression profile of cells and not dependent on alteration of the primary DNA sequence in the nucleus. Such alterations during carcinogenesis involve events such as DNA methylation, histone modifications, and gene silencing. Unlike genetic changes during carcinogenesis, most of the epigenetic alterations that take place in cancer cells are clinically reversible by directly targeting the moieties that contribute to carcinogenesis (74).

It has become clear that epigenetic silencing of certain genes contributes significantly to pathogenesis. For instance, an alternative mechanism to gross or intragenic deletions and point mutations that lead to inactivation of tumor suppressor genes could be epigenetic silencing of the promoters that drive the expression of those

genes. Such an event can play a major role during malignant transformations since inactivation of one tumor suppressor allele via genetic alterations combined with silencing of the second allele can lead to a complete loss of function of the tumor suppressor. Although modifications of other parts of the genes can contribute to gene silencing, the main cause for epigenetic changes in the expression profiles of genes is methylation patterns in the promoter regions of those genes. DNA methylation in mammalian cells usually takes place on cytosine bases on cytosine-guanine (CpG) dinucleotide pairs. (75). Approximately half of all genes contain CpG rich regions, commonly referred to as CpG clusters or islands, in their promoters (74). It is estimated that up to 70% of the CpG pairs are methylated in humans. In addition to gene silencing in cancer, methylation of DNA can prompt point mutations in DNA and lead to general genomic instability in tumors. For instance, the “hot spot” mutations of the tumor suppressor gene TP53 at residues 248 and 273 are caused by cytosine to thymine (T) transition following the deamination of m⁵C, the methylated form of cytosine (76). Parallel to hypermethylation of cytosine residues in the CpG rich regions of many gene promoters is the global genomic hypomethylation phenotype observed in cancer cells. DNA hypomethylation is responsible for upregulating several genes such as the MDR1 (multiple drug resistance 1) gene (77). It has been well-established that tumors demonstrate large scale loss of DNA methylation (78-80). Furthermore, it has been suggested that DNA hypomethylation can reactivate silenced genes in normal cells (mostly genes involved in cell proliferation and survival signaling) and the transcription of intragenomic parasitic DNA (such as viral DNA) (81).

Additionally, chromatin methylation and histone modifications are another set of

epigenetic alterations that are frequently observed in many cancers. Histones are proteins around which the DNA wraps itself, and understanding histone modifications and how they alter the gene expression profile in cancer cells remains a major barrier in the field of epigenetic characterization of cancer (82). However, since histones represent the core building blocks for chromatin structures which can regulate gene expression, the variable posttranslational modifications that take place on histones can contribute to gene silencing or reactivation by changing chromatin structure depending on which amino acids are undergoing modification (83-85). Therefore, studies on epigenetic alterations in cancer have focused on validating the significance of the synergy between genetic and epigenetic alterations during malignant transformation, rather than attempting to prove whether cancer is a genetic or an epigenetic disease (86).

2.5 miRNA in Cancer Diagnosis

MicroRNAs (miRNAs) are short biological molecules (23 ribonucleotides on average) that are involved in interference with messenger RNAs (mRNAs) leading to post-translational repression (87). The rapid discovery and identification of new microRNAs have led to a better understanding of the complexity of cancers and the different biological processes underlying the disease. Indeed, the ability to detect miRNAs has required the development of sensitive and high-throughput screening methods such as microarrays that can screen hundreds of miRNA expression profiles at once. In the last few years, miRNA expression profiles have become one of the most powerful tools in cancer diagnosis. For instance, detection of miR-221 is considered to be a very specific and accurate diagnosis for human prostate cancer (88). Another example

for using miRNA as a signature for cancer diagnosis is the over-expression of miR-155 and downregulation of miR-141 in 97% of patients with renal malignancy (89). In addition, cancer-related miRNAs (known as oncomiRs) can serve not only as biomarkers for diagnosing malignant development, but also for progression, metastasis and response to therapy (90). In gastric cancer, it is currently established that downregulation of miR-451 correlates with poor prognosis. In gastric cancer, upregulation of miR-451 leads to repression of the oncogene MIF (macrophage migration inhibitory factor), leading to inhibition of cell growth and sensitization of cancer cells to radiotherapy (91, 92). Furthermore, miRNA expression profiles can serve as biomarkers for anticipating survival rates. In pancreatic cancer, patients who demonstrate overexpression of miR-155, miR-203, miR-210, and miR-222 have a 6-fold higher fatality rate from pancreatic malignancy compared to patients with lower levels of the miRNAs (93). Table 2.2 summarizes some of the well-defined miRNAs in different cancers. Finally, miRNAs have also been found to influence malignant transformation due to the fact that they can function as tumor suppressors (e.g., miR-15a and miR-16-1) or oncogenes (e.g., miR-17-92 cluster) (94). However, the utility of miRNAs in cancer diagnosis remains a largely underutilized field that requires more research before it can be implemented efficiently in the clinic.

2.6 Nutrients and Metabolic Characteristics of Cancer

One of the major issues with anticancer therapies is their lack of tumor specificity. Therefore, a fundamental understanding of the unique physiological properties of cancer is needed.

Table 2.2 A summary of some miRNAs in different cancers (adapted from (90))

miRNA	Alteration in cancer	Molecular mechanisms	Diagnostic biomarkers	References
miR-21	Upregulated in breast, bladder, laryngeal cancers, and tongue squamous cell carcinoma	Maintains a low level of BTG2 and inhibits apoptosis partly via TPM1	Overexpression indicates poor survival of tongue squamous cell carcinoma	(95-97)
miR-155	Upregulated in Hodgkin lymphoma, breast, pancreatic and clear cell renal cell cancers	N/A	Overexpression indicates poor prognosis in pancreatic cancer	(98-102)
miR-203 miR-210 miR-222	Upregulated in pancreatic cancer	Overexpressions of any of these three miRNAs correlate with poor prognosis	N/A	(100)

In normal cells, microvasculature develops with order, and exhibits regular blood flow. But, in tumors, these vessels are tortuous, leaky, and often sluggish with irregular blood flow, resulting in poor drug delivery due to high interstitial pressure (103). Selective cytotoxic studies revealed that cancer cells are highly heterogeneous with hypoxic regions that reduce tumor sensitivity to radiation therapy. Furthermore, necrosis (premature cell death) is more common in cancer than in normal cells (104). Understanding the causes underlying each of these distinctive features, together with cancer-associated metabolic pathways, may help to develop more cancer specific therapeutics. The most obvious feature that separates tumor cells from normal cells is their accelerated metabolic rate, resulting in uncontrolled growth (105) and proliferation (106). The elevated metabolism of cancer cells can be tracked back to their unique ability

to reprogram the traditional mechanisms of energy production, which leads to cellular stress (107).

Because metabolic pathways are connected, and therefore interdependent, alteration of a single pathway can have a significant impact on the regulation of others. These reprogrammed pathways not only widen the options to consume energy in different forms, but also facilitate utilization of inorganic nutrients to augment proliferation. Even though cancer cells are notorious for chaos and instability, metabolically they are very well-organized to satisfy their need for growth and support (105).

2.6.1 Organic Players: How Tumors Feed and Grow

2.6.1.1 Carbohydrates

Sugars such as glucose, fructose, and sucrose are primary sources of fuel for any cell. Moreover, glucose can coordinate gene transcription, hormone secretion, enzyme activity, and glucoregulatory neurons (108, 109).

2.6.1.1.1 Warburg Effect

Cancer cells develop several unconventional mechanisms to employ glucose and its downstream metabolites to dominate their functions for amplified cell growth. Warburg effect is one of the prime cancer reprogramming models associated with glucose and respiration. In the presence of adequate oxygen, normal cells produce energy by breaking down glucose into carbon dioxide and water, a process called aerobic respiration. Aerobic respiration begins with the conversion of glucose to pyruvate via glycolysis in the cytosol, followed by oxidative phosphorylation to yield a maximal

amount of ATP. When an adequate supply of oxygen is not available, cells break down glucose to lactate by fermentation at the expense of ~18 fold less energy production than aerobic respiration (105). However, the same rule does not apply to cancer cells. In the early 20th century, a German scientist named Otto Warburg first noticed an aberrant biochemical characteristic in cancer cell metabolism (107). Warburg observed that even under aerobic conditions, rat sarcomas and human tumors were generating copious amounts of lactate compared to normal cells (110). This finding together with others confirmed that cancer cells restrict their metabolic energy largely to glycolysis, leading to a condition termed “aerobic glycolysis,” more commonly known as Warburg effect. Warburg effect is depicted in Figure 2.4. In 1931, Warburg won the Nobel prize in Physiology or Medicine for the discovery of the hydrogen-transferring function of flavine and nicotinamide (107). Warburg’s finding changed the scientific perspective of cancer with his first step that distinguishes tumor metabolic features from normal cells. From this, numerous questions arise: Do cancer cells consume more glucose than normal cells? If they do, which proteins facilitate the high uptake of glucose? How does this overconsumption affect neighboring normal cells? Is glucose the only essential nutrient required for tumor growth and survival? What other metabolic characteristics can be unraveled to specify malignant transformation?

2.6.1.1.2 Glucose and its Transporters

To detect glucose uptake, positron emission tomography (PET) has been widely used to diagnose tumor staging and to monitor treatment progression (111). 2- fluoro-2- deoxy-D-glucose (FDG) labeled with ¹⁸F serves as a molecular probe for PET imaging.

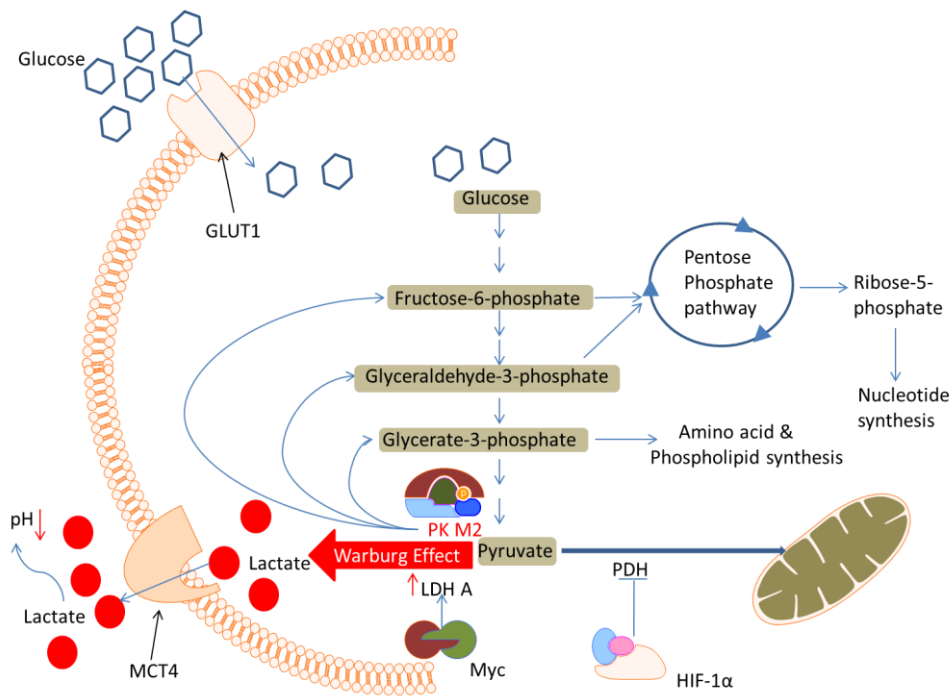


Figure 2.4 Reprogramming carbohydrate metabolism in cancer. Overexpression of glucose transporter 1 (GLUT1) facilitates import of excess glucose for accelerated glycolysis. Pyruvate kinase M2 (PK M2) favors accumulation of biosynthetic precursors fructose-6-phosphate and glyceraldehyde-3-phosphate for nucleotide synthesis, and glycerate-3-phosphate for amino acid and phospholipid synthesis. The oncoprotein myc upregulates lactate dehydrogenase A (LDH A) to alleviate Warburg effect, and hypoxia-inducible factor 1, alpha subunit (HIF-1 α) inhibits pyruvate dehydrogenase (PDH) to prevent cytosolic pyruvate export to the mitochondria. Monocarboxylate transporter 4 (MCT 4) exports lactate out of the cell to lower the surrounding pH for acidification.

Once inside the cell, FDG is catalyzed by hexokinase, and is converted to a 6-phosphate derivative which is chemically stable and resistant to further catalysis (112). Signal from the resultant compound correlates directly to the amount of glucose uptake in the cell. PET diagnosis of cancer patients reported increased uptake of FDG at the cancer site, confirming that cancer cells indeed consume more glucose than normal cells (113).

Because of limited passive diffusion through membranes, cells largely rely on specific transporters for the exchange of vital substances such as glucose to achieve high

glucose uptake (114). The uptake of glucose into cells is facilitated by the Glut family of transporters. Among the 14 members of this family, the Glut1 isoform is the most studied transporter due to its critical role in providing nutrients for cancer cells. Glut1, encoded by solute-linked carrier gene family member SLC2A1, is a facilitated glucose transporter ubiquitously expressed in human tissues (115). Since the brain depends solely on glucose as the energy source, Glut1 is more highly expressed in the blood-brain barrier compared to all other tissues (116). Cancer cells mimic the same strategy to meet their excessive glucose requirement by upregulating Glut1 expression via RAS and SRC oncogenes (117). Thus, Glut1 can be signified as a metabolic marker for malignant transformation. Clinical reports showed that Glut1 expression correlates reciprocally with cancer patient survival (118-120) and directly to tumor aggressiveness (121). With further advancement in modern technologies, overexpression of several other Glut family members in cancers have been identified, including Glut3 in cervical cancers (122) and Glut4 in thyroid carcinoma and alveolar rhabdomyosarcoma (117).

2.6.1.1.3 Pyruvate and its Regulatory Enzyme, Pyruvate Kinase M2

Besides glucose, pyruvate is at the heart of cellular metabolism. Despite being the final product of glycolysis, pyruvate plays a central role in interconnecting biosynthetic pathways. In cancer cells, HIF-1 α inactivates pyruvate dehydrogenase (PDH) to prevent mitochondrial matrix import, confining pyruvate to the cytosol (123). At the same time, oncogenic myc upregulates lactate dehydrogenase A (LDH A) expression for the conversion of cytosolic pyruvate to lactate, securing NAD⁺ regeneration for tumor propagation, and avoiding pyruvate-related cytotoxicity (124) as illustrated in Figure 2.4.

For the last decade, the pyruvate kinase M2 (PK M2) isoform has received attention as an indicator of malignant transformation. Pyruvate kinase is the rate-limiting enzyme in glycolysis for pyruvate generation, and therefore a major regulator of pyruvate-linked pathways. Depending on the tissue, different isoforms of PK are expressed to perform designated tasks. For instance, PK M1 is mostly found in brain and muscle for instant energy generation, whereas PK M2 is present mainly in multiplying cells such as embryonic cells, which require constant nucleic acid synthesis. Not surprisingly, tumor cells replace PK M1 with PK M2 for rapid cell proliferation (125, 126). Being the key glycolytic enzyme, PK M2 dominates glycolysis either directly or indirectly. By generating pyruvate, PK M2 favors pyruvate-alanine conversion via a glutamate intermediate to synthesize purines and pyrimidines (127), and simultaneously controls the glutaminolysis cycle (truncated Krebs cycle) for ATP production (128). Conversely, limiting pyruvate production results in accumulation of preceding metabolites such as fructose-6-phosphate, glyceraldehyde-3-phosphate, and glycerate-3-phosphate (precursors of biosynthetic pathways). PK M2 canalizes glyceraldehyde-3-phosphate and fructose-6-phosphate to the nonoxidative pentose phosphate cycle for ribose-5-phosphate production, necessary for nucleic acid synthesis. PK M2 also channels glycerate-3-phosphate to amino acid and phospholipid synthesis as depicted in Figure 2.4 (126). Further, the role of PK M2 is not limited to its glycolytic function in the cytosol. With the help of a nuclear localization signal (NLS) located at the C-terminus, PK M2 can translocate to the nucleus upon epidermal growth factor (EGF) receptor activation (129). Once inside the nucleus, PK M2 phosphorylates Stat3 for MEK5 transcription, leading to cell proliferation (130).

Since PK M2 is predominantly expressed in cancer cells, targeting it may provide tumor specificity with minimal cytotoxicity to normal cells. Theoretically, inhibition of PK M2 should deplete pyruvate production in cancer cells. Therefore, this precludes subsequent anabolic pathways such as amino acid and phospholipid biosynthesis, and hence could manifest anticancer activity. Lactate, the final product of “aerobic glycolysis,” is primarily associated with biosynthesis, metastasis, and immune suppression. Similar to pyruvate and glucose, lactate requires an efficient shuttling system to augment tumorigenic effects. Monocarboxylate transporters (MCT), encoded by SLC family genes, are transmembrane proteins responsible for lactate and pyruvate transport (131). Unlike glucose transporters, MCT isoforms are involved in both import and export of lactate, therefore expressed selectively in different cell types. Recent studies have established that cancer cells upregulate the proton-coupled MCT-4 isoform in a HIF-1 α -dependent fashion (132) for the export of excess lactate, and epigenetically suppress sodium-coupled MCT 1 (SMCT1) to prevent lactate import inside the cell (133). Moreover, MCT shuttles lactate to fibroblasts, and imports pyruvate back to the cancer cell. This conserves a high lactate to pyruvate ratio, which is proposed to be essential for tumor survival (134). Besides MCT, several other lactate shuttling proteins have been identified over the past few of decades, such as the lactate-alanine shuttle for amino acid synthesis (135, 136).

Release of excessive lactate into the extracellular milieu decreases the pH of the surroundings as shown in Figure 2.4, and thereby causes acidification of adjacent normal cells. Removal of normal cells reduces competition for nutrients and provides additional space for tumors to grow. This explains how overconsumption of glucose by cancer cells

can be pernicious to normal cells. Moreover, reduction in pH facilitates angiogenesis and metastasis through up-regulation of EGFR and HIF-1 α (137, 138), and inhibits T-cell proliferation via blockade of lactate efflux thus evading the immune response.

2.6.1.2 Protein: mTOR

Mammalian target of rapamycin, also known as mechanistic target of rapamycin (mTOR), is an atypical serine/threonine kinase at the border of cell growth and starvation. In presence of a plethora of nutrients, mTOR is advantageous to cells with uncontrolled growth and deregulated metabolism such as cancer cells. However, mTOR is unaffordable to nutrient-deprived cells due to its high energetic requirements. Since the first discovery in yeast (139), mTOR has gained a considerable reputation throughout the years for its reprogrammed expansive signaling array to fuel cancer cell growth, proliferation, survival, metabolism, and transcription (140). Structurally, mTOR has two distinct catalytic domains, mTOR complex 1 (mTORC1), and mTOR complex 2 (mTORC2), which may exist as dimers (141, 142). Regulatory-associated protein of mTOR (RAPTOR) and rapamycin-insensitive companion of mTOR (RICTOR) serve as a scaffold for mTORC1 and mTORC2, respectively, to form complexes with their substrates and regulators. Growth factors and amino acids such as insulin regulate mTORC1 activation. Another key protein, GTPase RHEB, when loaded with GTP can activate mTORC1 as well. In fact, overexpression of RHEB can maintain mTORC1 kinase activity even under starvation conditions (143). However, for mTORC2 regulation, emerging evidence suggests that the oncogene Ras may be necessary to link growth factors to mTORC2 (144).

Substrates of mTORC1, mainly S6 kinase (S6K) and initiation factor 4E binding protein 1 (eIF4E-BP1) are involved in strict regulation of mRNAs. Upon phosphorylation by mTORC1, eIF4E-BP1 dissociates from eIF4E, allowing incorporation of translation factors to initiate anti-apoptotic protein synthesis (145, 146). When phosphorylated by mTORC1, S6K binds to multiple proteins, including nuclear-capping binding protein (CPB) for mRNA translation initiation and progression (147). In addition, phosphorylated S6K initiates transcription of rRNA polymerase 1 (RNAP I), signifying that mTORC1 actively up regulates rRNA synthesis (148), which may contribute to oncoprotein translation. mTORC1 is also involved in autophagy, a process of self-degradation of damaged cells through the lysosomal machinery. mTORC1 phosphorylates the enzyme Atg-13, preventing autophagic action (149). Increasing evidence indicates that autophagy facilitates tumor suppression; thus, autophagic evasion implies mTORC1 may favor tumorigenesis (150). Unlike mTORC1, mTORC2 directly activates a group of signaling pathways that are already known for tumorigenesis. The primary substrates of mTORC2, predominantly Akt, serum- and glucocorticoid-regulated kinase (SGK), and protein kinase C (PKC) are responsible for cell cycle progression and cell survival (151, 152).

2.6.1.3 Lipids

To date, the majority of cancer metabolic research has focused on the catabolic process of glycolysis. Because cancer cells can proliferate faster than normal cells, they seemingly must have a shifted anabolic rate as well. For rapidly proliferating cells such as cancer cells, lipid synthesis can be vital for new membrane formation, energy storage, hormone production, and growth factor regulation.

2.6.1.1.4 Lactate and its Transporter MCT

Studies of ^{14}C -labeled glucose show that most of the esterified acids are derived from *de novo* synthesis (153, 154), confirming that a higher rate of lipid biosynthesis takes place in cancer cells. Two key enzymes, ATP citrate lysate (ACL), and most importantly, fatty acid synthase (FAS) have been identified as mandatory supporters for increased lipid synthesis (155). To stimulate lipid production, the P13/Akt pathway inhibits breakdown of fatty acids by blocking β -oxidation, and activates ACL (156) to channel oxaloacetate for lipid synthesis. Fatty acid synthase (FAS), encoded by the FASN gene, is downregulated in most normal tissues but highly upregulated in cancer cells, which makes it a possible candidate as a therapeutic biomarker. Functions of FAS include energy storage in liver and adipose tissue, reproduction, and lactation. As the name suggests, FAS synthesizes palmitate (16C) from acetyl- CoA (2C) (155) to serve as a precursor for longer fatty acid synthesis. Inhibition of FAS in promyelocytic leukemia caused cell accumulation in G1 phase, followed by reduction in cell proliferation (157), demonstrating the possible role of FAS in cell cycle regulation. Another lipid-associated marker protein, Spot-14 was found to be overexpressed in breast cancer cells, and its expression level correlates with aggressiveness of the disease state (158). However, the role and mechanistic pathway of Spot-14 in lipid synthesis are still unknown (156). Recently, Nomura and colleagues reported that monoacylglycerol lipase (MAGL) drives tumorigenesis through lipolytic release and remodeling of free fatty acids. Inhibition of overexpressed MAGL *in vitro* impaired cell migration and invasiveness (159). If MAGL is proven to be specific for cancer, this finding will add another enzyme to the existing list of lipid players in cancer.

2.6.2 Inorganic Compounds

Biological systems are dominated by organic molecules ranging from substrates to products. However, trace amounts of inorganic molecules exist in humans, which are crucial for maintaining genomic stability and for regulating most organic macromolecules such as enzymes.

2.6.2.1 Selenium

Selenium, an essential trace element, mediates metabolic pathways in conjunction with proteins, collectively called selenoproteins. So far, 25 selenoproteins have been discovered in humans (160). Most selenoproteins are involved in antioxidant function, including glutathione peroxidase-1 (GPX1) (161). GPX1 knockout mice exhibited increased susceptibility to H₂O₂-induced apoptosis (162), and accelerated accumulation of mutations (163), suggesting a potential role of selenium in genomic stability. When in excess, selenium metabolites can stimulate selenite-induced apoptosis and cell cycle arrest via the p53-dependent pathway (164) (165). Moreover, inorganic selenium sensitizes cancer cells to apoptotic inducers such as TRAIL through the p53-mediated mitochondrial pathway (166).

2.6.2.2 Copper

The balance of copper is important to maintain regular cell function. Cu²⁺ deficiency can cause myeloneuropathy, a fatal developmental disease (167). Conversely, the elevated serum level of copper observed in cancer patients (168) is caused by an excess of free Cu²⁺ radicals, which promotes oxidative stress, leading to genomic

instability (169). Surprisingly, when Cu^{2+} binds to its enzyme, CuZnSOD, the resultant complex reduces oxidative stress by eliminating O_2^- directly from mitochondria, preventing oxidative DNA damage (170).

2.6.2.3 Zinc

More than 300 enzymes and proteins require zinc as a cofactor for functional activity, including DNA the repair protein, p53. Under oxidative stress, the zinc finger-domain of p53 responds to DNA damage and assists in sequence-specific recognition of DNA repair machinery (171). Nevertheless, above a certain threshold, zinc inhibits DNA repair proteins such as DNA ligase I (170), which allows for the propagation of genomic mutations.

2.6.2.4 Iron

Most iron found in the body is present in hemoglobin in red blood cells or in myoglobin of muscle tissue. In terms of intracellular signaling, iron found in the cytochrome of mitochondria is directly involved in ROS formation, which can lead to oxidative stress. On the other hand, release of cytochrome c from the mitochondria activates the caspase cascade which leads to apoptosis. Additionally, iron is a cofactor of several DNA repair proteins, including α -ketoglutarate dependent DNA repair enzyme (A1KB), that showed reduced binding affinity to its substrate upon iron replacement with copper (172).

2.6.2.5 Calcium

Calcium is the most abundant metal in biological systems. Ca^{2+} is a highly versatile intracellular signaling molecule that ensures different cellular processes can respond precisely to diverse stimuli. For example, Ca^{2+} signals presynaptic neurons to release neurotransmitters in response to a nerve impulse, and the same Ca^{2+} also regulates actin for muscle contraction. The elaborate role of Ca^{2+} connects the entire signaling network, which makes it a perfect target for cancer to reprogram many metabolic pathways. Ca^{2+} plays a significant role in the metastatic behavior of cancer cells. In order to be invasive, cancer cells require focal detachment and proteolysis of the extracellular matrix for migration. Ca^{2+} binds to myosin light chain kinase (MLCK) for myosin II phosphorylation, and degrades focal adhesion proteins, resulting in focal detachment for migration (173). Moreover, upon binding to S1004A (EF-hand calcium binding protein) Ca^{2+} exposes the interacting domain to interact with cytoskeleton proteins, which has been implicated to be important for cell migration and epithelial to mesenchymal transition (EMT) (174, 175).

2.7 The Cancer Microenvironment

As mentioned, cancer develops after two initiating events in succession (the "two-hit hypothesis" of tumor suppressor mutation (176)) or after a promoting event, which leads to genetic modifications (177) usually in tumor suppressor genes (see Figure 2.5A). Growth and invasion of the cancer is promoted by the tumor microenvironment, which develops as a result of crosstalk among different cell types. The microenvironment is formed and controlled by the tumor itself but also consists of the tumor stroma, blood

vessels, inflammatory cells and other associated cells (178) (including cancer-associated fibroblasts, vascular and lymphatic endothelial cells).

2.7.1 The Stroma and its Components

The stroma is the surrounding matrix that supports the tumor (179). The tumor stroma consists of the extracellular matrix (ECM) and the surrounding noncancerous cells (180). One of the most important types of cells in the stroma are cancer associated fibroblasts (CAFs; also known as activated fibroblasts or myofibroblasts). CAFs are spindle-shaped, mesenchymal cells with stress fibers and fibronexus (181), and may arise from epithelial cells through the epithelial to mesenchymal transition (EMT) (182). CAFs synthesize the ECM by producing fibrous proteins such collagens and fibronectin which are embedded in a glycosaminoglycan gel (183). CAFs not only secrete growth factors that impact cell motility, but also contribute to ECM remodeling by secreting matrix metalloproteinases (182). This may allow cancer cells to get across tissue boundaries, and create cancer cell niches and initiate angiogenesis (183). CAFs also secrete laminin and type IV collagen to make up the basement membrane (also known as the basal lamina).

Infiltrating inflammatory cells in the tumor microenvironment include those that mediate adaptive immunity, including tumor-infiltrating T lymphocytes, dendritic cells, and B cells (to a lesser extent), and those that mediate innate immunity, including tumor-associated macrophages, polymorphonuclear leukocytes (PMLs), and rare natural killer (NK) cells (178). Many tumor-infiltrating T lymphocytes are specific for tumor-associated antigens, implying host immune surveillance, but are incapable of halting tumor growth (178).

Tumor-associated macrophages (TAMs) are reprogrammed to inhibit lymphocyte functions (by the release of inhibitory cytokines) (184). A version of immature dendritic cells known as myeloid suppressor cells (MSCs) produces arginase 1, which facilitates tumor growth and suppresses immune cell functions (185). Important mediators of cancer are cytokines (and their cognate receptors), which may promote or inhibit cancer, and in general, regulate immunity and inflammation (186). Chemokines are chemoattractant cytokines that play important roles in allowing cells to traffic in and out of the tumor microenvironment. The chemokine system is subjugated by cancer cells for this purpose (187, 188). Interestingly, the chemokine receptor CXCR4 has been found to be overexpressed on many cancer cell types including breast, prostate, and pancreatic cancers; melanomas; and certain leukemias (187). Overall, the tumor subverts inflammatory cells which leads to tumor growth and evasion of the host immune system, allowing the tumor to proliferate.

Cells that form the tumor-associated vasculature (vascular endothelial cells) may have altered characteristics compared to normal vasculature, including differences in gene expression profiles and cell surface markers. On the other hand, the role of lymphatic endothelial cells (that form lymphatic vessels) is poorly understood in terms of tumor growth. Lymphatic vessels in the tumor itself are often collapsed and non-functional, while lymphangiogenesis is occurring on the periphery of the tumor and on adjacent normal cells. This suggests that these lymphatics form channels that allow seeding of metastasis (105).

Regardless, studies of proteins and factors involved in either vascular or lymphatic endothelial cells lead to identification of new therapeutic targets (anti-

angiogenic or anti-metastatic therapies). One key protein secreted by endothelial cells is SPARC (secreted protein acidic and rich in cysteine; also termed osteonectin), involved in cell-cell, and cell-matrix interaction without participating structurally in the ECM (189). SPARC can modulate focal-adhesion and metalloproteinase expression, and interact with growth factors such as vascular endothelial growth factor (VEGF) and platelet-derived growth factor (PDGF) (190) to determine cell shape, cytoskeleton architecture, and proliferation (191). Histological studies have also validated overexpression of SPARC (192), and its importance in epithelial-mesenchymal transition for metastasis (193, 194). In addition to endothelial cells, pericytes are another type of cell that wrap around the endothelium of blood vessels. Pericytes secrete antiproliferative signals, produce vascular endothelial growth factor (VEGF), and work with endothelial cells to stabilize vessel walls (195, 196). In tumors, pericytes help support the tumor endothelium, and are thus another target for pharmacological intervention (105). Some of the components of the tumor microenvironment are depicted in Figure 2.5C.

Paramount to tumor malignancy is the process of angiogenesis (197), where new blood vessels form to supply nutrients/oxygen to the existing tumor and allow for the removal of waste products (Figure 2.5C). Folkman and colleagues demonstrated the need for inducing and sustaining angiogenesis in tumors (105, 197, 198). In cancer, the angiogenic switch can be activated by altering the balance of angiogenic inducers and inhibitors. Angiogenic inducer and inhibitor prototypes include VEGF-A (vascular endothelial growth factor-A) and TSP-1 (thrombospondin-1), respectively (105, 199). In the last decade, many other angiogenic factors have been identified and summarized (200). Angiogenic inhibitors are being actively pursued for cancer therapy, with the

concept of cutting off the blood supply to the tumor (200, 201).

2.7.2 The Invasion-Metastasis Cascade

Further cancer progression into metastases involves the tumor cells' ability to 1) invade through the ECM and stromal cells, 2) intravasate into the blood vessel lumen, 3) survive in the bloodstream, 4) seed at an organ site, 5) extravasate into these organs, 6) survive and form micrometastases, and 7) form metastatic colonies (177, 202, 203). The end result is the spread of cancer to new sites/organs, or metastasis (204) (Figure 2.5).

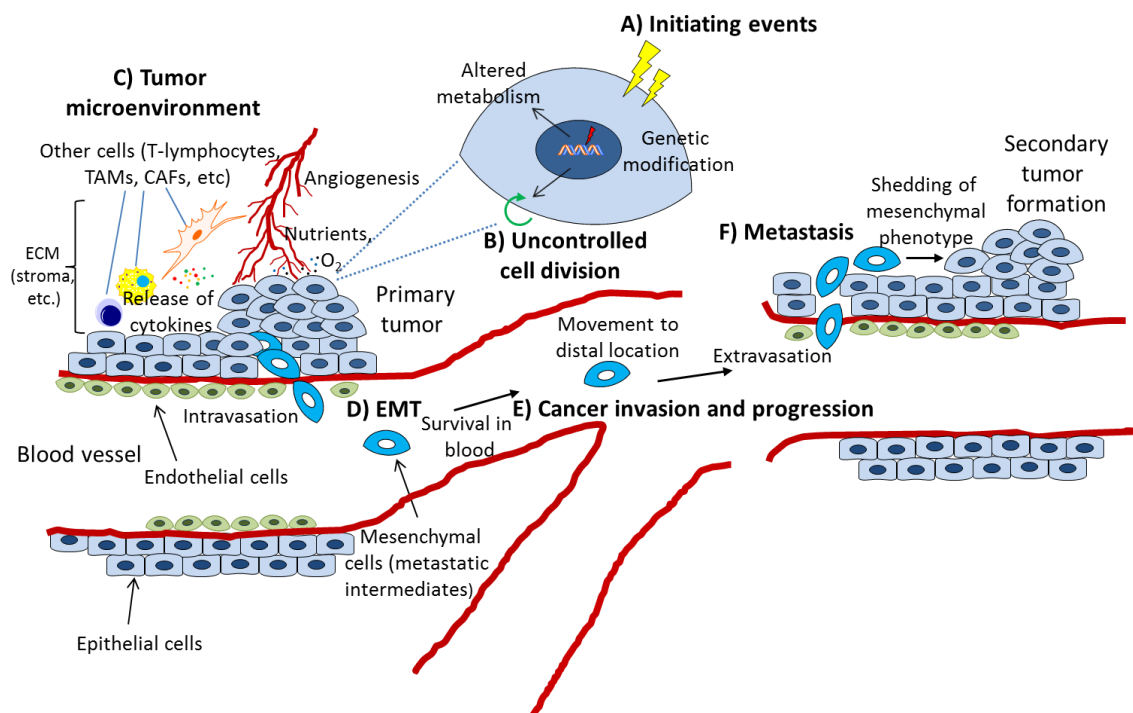


Figure 2.5 The major steps in cancer. A) Initiating events; B) Uncontrolled cell division; C) Tumor microenvironment; D) EMT; E) Cancer invasion and progression; F) Metastasis.

2.7.2.1 Epithelial-to-Mesenchymal Transition (EMT)

For the invasion through the ECM and stroma, tumor epithelial cells must undergo an epithelial-to-mesenchymal transition (205) which allows for an increased capacity to migrate, an enhanced resistance to apoptosis, increased invasiveness, and an ability to remodel the extracellular matrix (206-208).

Of the 2 types of EMTs, type 3 EMT is associated with cancer progression and metastasis (207). EMT may be the activating factor for acquisition of malignancy for epithelial cancers. These cancer cells appear to have a mesenchymal phenotype, express typical mesenchymal markers such as vimentin, desmin, FSP1 (fibroblast-specific protein 1), and α -SMA (smooth muscle α -actin) (209), and appear at the invasive front of tumors. After the invasion-metastasis cascade, to form a secondary tumor, these cells have to shed their mesenchymal phenotype and return to their epithelial phenotype (207) (Figure 2.5F). It is thought that EMT-inducing signals (including HGF; EGF, epidermal growth factor; PDGF; TGF- β) may emanate from tumor stroma, resulting in a complex cascade, starting with transcription factor activation (of Snail; Slug; ZEB1, zinc finger E-box binding homeobox 1; Twist; Goosecoid; FOXC2, Forkhead 1) followed by further signal transduction (by ras; c-Fos; LEF, lymphoid enhancer factor; ERK, extracellular signal-regulated kinase; MAPK, PI3K, Akt, Smads, RhoB, β -catenin). Cell surface proteins (integrins) are also activated which disrupt several cell-cell or cell-ECM junctions (207). Lastly, E-cadherin loss is central in the EMT program (210). TGF- β exposure induces transcription factors Snail, Slug, SIP1 (Smad-interacting protein 1), and E12 (E2A transcription factor family member), which in turn, repress E-cadherin expression. Lack of E-cadherin correlates with increased tumorigenicity and metastasis

in some models (211). Finally microRNAs miR-200 and miR-205 increase E-cadherin expression, and help maintain the epithelial phenotype, while miR-21 upregulation facilitates TGF- β -induced EMT (212). The EMT's role in cancer progression is depicted in Figure 2.5D.

2.7.2.2 Entering and Surviving the Circulation

Intravasation of cancer cells into the lymphatic lumen represents the main mechanism of dispersion of such cells (213). This process is facilitated by changes that allow these cancer cells to cross the pericytes and endothelial cells that make up the vessels (203). Tumor-associated blood vessels (neovasculature) are leaky and are continuously being reconfigured. These weak interactions between the endothelial cells and pericytes facilitate intravasation (214). Once in the bloodstream, these circulating tumor cells (CTCs) are thought of as “metastatic intermediates” (203) and use particular signaling pathways to avoid anoikis (a form of apoptosis caused by anchorage loss). These CTCs must also avoid damage by hemodynamic shear and attack by the immune system. They do so by using the blood coagulation process, forming microemboli, a process likely mediated by L- and P-selectins expressed by the CTCs (215). See Figure 2.5D and E.

2.7.2.3 Seeding, Extravasation, Micrometastasis, and Metastatic Colonization

CTCs may either be physically trapped in microvessels, or are “predetermined” to lodge in certain organs/tissues. Predetermined lodging is based on formation of specific

adhesive interactions between the CTC and the organ. After honing to a specific organ, CTCs may form microcolonies that disrupt the surrounding vessels, or extravasate by entering the vessel by penetrating the endothelial and pericytes in the stroma. To facilitate this process, primary tumors may secrete a number of factors that disrupt distant metastatic sites and induce permeability at these distant sites (203). Cancer cells may establish a “premetastatic niche” (216) where primary tumors secrete systemic signals that induce fibronectin expression from specific organs, which leads to mobilization of VEGFR-1 and its ligand, secretion of MMPs, integrins, and other ECM factors, prior to the arrival of the CTCs (203). Further stimulation of signaling allows the cells to survive in this foreign environment. Finally, colonization of large macrometastases occurs following Paget’s “seed and soil” hypothesis where the “soil” represents a hospitable tissue environment for the “seed” (micrometastases) to form (217). Recently, gene expression of factors that help metastatic colonization have been identified for bone, lung, liver, and brain (203). An example of the implication of this is that breast cancer cells that metastasize to the bone use different mechanisms for colonization than those that metastasize to the lung. The ability of cells to undergo high self-renewal (e.g., tumor initiating cells) are more likely to undergo metastatic colonization. Several transcription factors (EMT-inducing and those involved in inhibition of cell differentiation) have been implicated in this self-renewal process. The process of metastasis is depicted in Figure 2.5F. Factors involved in the metastatic process are indeed being actively pursued as cancer therapeutics as well.

2.8 Conclusion

In the late 1800s, since the “two-hit hypothesis” of cancer initiation was postulated, our understanding of cancer initiation and progression has truly evolved. A basic summary of events occurring in cancer is depicted in Figure 2.5. Initiating events trigger DNA damage, leading to genetic modification, and changes in the cell including altered metabolism (Figure 2.5A). Uncontrolled cell division leads to cell proliferation (Figure 2.5B). The tumor microenvironment depicts recruitment of other cells, and angiogenesis that occurs when tumors form. Nutrients, cytokines, etc. are released (Figure 2.5C). EMT is a program where proliferating cells undergo an epithelial to mesenchymal transition, and intravasate out of the primary locale (Figure 2.5D). Cancer invasion and progression continue, and cells extravasate (Figure 2.5E). Finally, metastasis occurs when cells extravasate to a new site, shed their mesenchymal phenotype, and form secondary tumors (Figure 2.5F). A fundamental understanding of tumor development has come from detailed investigation of cancer biology, and has identified many of the genes, proteins, signals, and other factors involved in cancer. With this arsenal of knowledge, scientists will continue to find ways to halt cancer in its tracks. Paramount to this will not only be the discovery of novel drug targets, but approaches to deliver new drugs specifically to tumor cells.

2.9 References

1. J.E. Visvader. Cells of origin in cancer. *Nat.* 469:314-322 (2011).
2. N.A. Lobo, Y. Shimono, D. Qian, and M.F. Clarke. The Biology of Cancer Stem Cells. *Annu Rev Cell Dev Biol.* 23:675-699 (2007).
3. L. Harrington. Does the reservoir for self-renewal stem from the ends? *Oncog.* 23:7283-7289 (2004).

4. T. Reya, S.J. Morrison, M.F. Clarke, and I.L. Weissman. Stem cells, cancer, and cancer stem cells. *Nat.* 414:105-111 (2001).
5. W.R. Bruce and H. Van Der Gaag. A Quantitative Assay for the Number of Murine Lymphoma Cells Capable of Proliferation in Vivo. *Nat Cell Biol.* 199:79-80 (1963).
6. D.E. Bergsagel and F.A. Valeriote. Growth characteristics of a mouse plasma cell tumor. *Cancer Res.* 28:2187-2196 (1968).
7. C.H. Park, D.E. Bergsagel, and E.A. McCulloch. Mouse myeloma tumor stem cells: a primary cell culture assay. *J Nat Cancer Inst.* 46:411-422 (1971).
8. W. Guo, J.L. Lasky, and H. Wu. Cancer Stem Cells. *Pediatr Res.* 59:59R-64R (2006).
9. C.T. Jordan, M.L. Guzman, and M. Noble. Cancer Stem Cells. *N Engl J Med.* 355:1253-1261 (2006).
10. T. Holyoake, X. Jiang, C. Eaves, and A. Eaves. Isolation of a highly quiescent subpopulation of primitive leukemic cells in chronic myeloid leukemia. *Blood.* 94:2056-2064 (1999).
11. N. Takahashi, I. Miura, K. Saitoh, and A.B. Miura. Lineage involvement of stem cells bearing the philadelphia chromosome in chronic myeloid leukemia in the chronic phase as shown by a combination of fluorescence-activated cell sorting and fluorescence in situ hybridization. *Blood.* 92:4758-4763 (1998).
12. R.P. Hill. Identifying cancer stem cells in solid tumors: case not proven. *Cancer Res.* 66:1891-1896 (2006).
13. T. Brabletz, A. Jung, S. Spaderna, F. Hlubek, and T. Kirchner. Opinion: migrating cancer stem cells - an integrated concept of malignant tumour progression. *Nat Rev Cancer.* 5:744-749 (2005).
14. M. Al-Hajj, M.S. Wicha, A. Benito-Hernandez, S.J. Morrison, and M.F. Clarke. Prospective identification of tumorigenic breast cancer cells. *PNAS.* 100:3983-3988 (2003).
15. S.K. Singh, C. Hawkins, I.D. Clarke, J.A. Squire, J. Bayani, T. Hide, R.M. Henkelman, M.D. Cusimano, and P.B. Dirks. Identification of human brain tumour initiating cells. *Nat.* 432:396-401 (2004).
16. N. Sanai, A. Alvarez-Buylla, and M.S. Berger. Neural stem cells and the origin of gliomas. *N Engl J Med.* 353:811-822 (2005).
17. D. Fang, T.K. Nguyen, K. Leishear, R. Finko, A.N. Kulp, S. Hotz, P.A. Van Belle, X. Xu, D.E. Elder, and M. Herlyn. A Tumorigenic subpopulation with stem cell properties in melanomas. *Cancer Res.* 65:9328-9337 (2005).
18. A.T. Collins, P.A. Berry, C. Hyde, M.J. Stower, and N.J. Maitland. Prospective identification of tumorigenic prostate cancer stem cells. *Cancer Res.* 65:10946-10951 (2005).

19. C.P. Gibbs, V.G. Kukekov, J.D. Reith, O. Tchigrinova, O.N. Suslov, E.W. Scott, S.C. Ghivizzani, T.N. Ignatova, and D.A. Steindler. Stem-like cells in bone sarcomas: implications for tumorigenesis. *Neoplasia*. 7:967-976 (2005).
20. D. Bonnet and J.E. Dick. Human acute myeloid leukemia is organized as a hierarchy that originates from a primitive hematopoietic cell. *Nat Med*. 3:730-737 (1997).
21. A. Castor, L. Nilsson, I. Astrand-Grundstrom, M. Buitenhuis, C. Ramirez, K. Anderson, B. Strombeck, S. Garwicz, A.N. Bekassy, K. Schmiegelow, B. Lausen, P. Hokland, S. Lehmann, G. Juliusson, B. Johansson, and S.E. Jacobsen. Distinct patterns of hematopoietic stem cell involvement in acute lymphoblastic leukemia. *Nat Med*. 11:630-637 (2005).
22. S.K. Singh, C. Hawkins, I.D. Clarke, J.A. Squire, J. Bayani, T. Hide, R.M. Henkelman, M.D. Cusimano, and P.B. Dirks. Identification of human brain tumour initiating cells. *Nature*. 432:396-401 (2004).
23. M.D. Taylor, H. Poppleton, C. Fuller, X. Su, Y. Liu, P. Jensen, S. Magdaleno, J. Dalton, C. Calabrese, J. Board, T. Macdonald, J. Rutka, A. Guha, A. Gajjar, T. Curran, and R.J. Gilbertson. Radial glia cells are candidate stem cells of ependymoma. *Cancer Cell*. 8:323-335 (2005).
24. M. Al-Hajj, M.S. Wicha, A. Benito-Hernandez, S.J. Morrison, and M.F. Clarke. Prospective identification of tumorigenic breast cancer cells. *Proceedings of the National Academy of Sciences of the United States of America*. 100:3983-3988 (2003).
25. D. Fang, T.K. Nguyen, K. Leishear, R. Finko, A.N. Kulp, S. Hotz, P.A. Van Belle, X. Xu, D.E. Elder, and M. Herlyn. A tumorigenic subpopulation with stem cell properties in melanomas. *Cancer Research*. 65:9328-9337 (2005).
26. M.S. Wicha, S. Liu, and G. Dontu. Cancer stem cells: an old idea—a paradigm shift. *Cancer Res*. 66:1883-1890 (2006).
27. J.C.Y. Wang and J.E. Dick. Cancer stem cells: lessons from leukemia. *Trends Cell Biol*. 15:494-501 (2005).
28. B.J.P. Huntly and D.G. Gilliland. Leukaemia stem cells and the evolution of cancer-stem-cell research. *Nat Rev Cancer*. 5:311-321 (2005).
29. C. Odoux, H. Fohrer, T. Hoppo, L. Guzik, D.B. Stolz, D.W. Lewis, S.M. Gollin, T.C. Gamblin, D.A. Geller, and E. Lagasse. A Stochastic model for cancer stem cell origin in metastatic colon cancer. *Cancer Res*. 68:6932-6941 (2008).
30. A.V. Krivtsov, D. Twomey, Z. Feng, M.C. Stubbs, Y. Wang, J. Faber, J.E. Levine, J. Wang, W.C. Hahn, D.G. Gilliland, T.R. Golub, and S.A. Armstrong. Transformation from committed progenitor to leukaemia stem cell initiated by MLL–AF9. *Nat*. 442:818-822 (2006).
31. R.W. Cho, X. Wang, M. Diehn, K. Shedden, G.Y. Chen, G. Sherlock, A. Gurney, J. Lewicki, and M.F. Clarke. Isolation and molecular characterization of cancer stem cells in MMTV-Wnt-1 murine breast tumors. *Stem Cells*. 26:364-371 (2008).

32. F. Vaillant, M.-L. Asselin-Labat, M. Shackleton, N.C. Forrest, G.J. Lindeman, and J.E. Visvader. The mammary progenitor marker CD61/ β 3 integrin identifies cancer stem cells in mouse models of mammary tumorigenesis. *Cancer Res.* 68:7711-7717 (2008).
33. M. Zhang, F. Behbod, R.L. Atkinson, M.D. Landis, F. Kittrell, D. Edwards, D. Medina, A. Tsimelzon, S. Hilsenbeck, J.E. Green, A.M. Michalowska, and J.M. Rosen. Identification of tumor-initiating cells in a p53-null mouse model of breast cancer. *Cancer Res.* 68:4674-4682 (2008).
34. I. Malanchi, H. Peinado, D. Kassen, T. Hussenet, D. Metzger, P. Chambon, M. Huber, D. Hohl, A. Cano, W. Birchmeier, and J. Huelsken. Cutaneous cancer stem cell maintenance is dependent on [bgr]-catenin signalling. *Nat.* 452:650-653 (2008).
35. A.P. Feinberg, R. Ohlsson, and S. Henikoff. The epigenetic progenitor origin of human cancer. *Nat Rev Genet.* 7:21-33 (2006).
36. C.A. Iacobuzio-Donahue. Epigenetic changes in cancer. *Annu Rev Pathol.* 4:229-249 (2009).
37. C.O. Nordling. A new theory on cancer-inducing mechanism. *Br J Cancer.* 7:68-72 (1953).
38. A.G. Knudson, Jr. Mutation and cancer: statistical study of retinoblastoma. *PNAS.* 68:820-823 (1971).
39. C. H. Tumor suppressor (TS) genes and the two-hit hypothesis. *Nat Educ:*1 (2008).
40. B.A. Lodish H, Zipursky SL, et al. . Section 24.2, Proto-Oncogenes and Tumor-Suppressor Genes. *Mol Cell Biol*, W. H. Freeman, New York, 2000.
41. S.P. Chellappan, S. Hiebert, M. Mudryj, J.M. Horowitz, and J.R. Nevins. The E2F transcription factor is a cellular target for the RB protein. *Cell.* 65:1053-1061 (1991).
42. N. Dyson, P.M. Howley, K. Munger, and E. Harlow. The human papilloma virus-16 E7 oncoprotein is able to bind to the retinoblastoma gene product. *Sci.* 243:934-937 (1989).
43. W. Jiang, S.M. Kahn, N. Tomita, Y.J. Zhang, S.H. Lu, and I.B. Weinstein. Amplification and expression of the human cyclin D gene in esophageal cancer. *Cancer Res.* 52:2980-2983 (1992).
44. R.A. Weinberg. The retinoblastoma protein and cell cycle control. *Cell.* 81:323-330 (1995).
45. A. Efeyan and M. Serrano. p53: guardian of the genome and policeman of the oncogenes. *Cell Cycle.* 6:1006-1010 (2007).
46. K. Vermeulen, D.R. Van Bockstaele, and Z.N. Berneman. The cell cycle: a review of regulation, deregulation and therapeutic targets in cancer. *Cell Prolif.* 36:131-149 (2003).

47. M. Mossalam, K.J. Matissek, A. Okal, J.E. Constance, and C.S. Lim. Direct induction of apoptosis using an optimal mitochondrially targeted p53. *Mol Pharm.* 9:1449-1458 (2012).
48. D.W. Meek. Tumour suppression by p53: a role for the DNA damage response? *Nat Rev Cancer.* 9:714-723 (2009).
49. J.M. Espinosa. Mechanisms of regulatory diversity within the p53 transcriptional network. *Oncog.* 27:4013-4023 (2008).
50. F. Murray-Zmijewski, E.A. Slee, and X. Lu. A complex barcode underlies the heterogeneous response of p53 to stress. *Nat Rev Mol Cell Biol.* 9:702-712 (2008).
51. C.J. Sherr and J.D. Weber. The ARF/p53 pathway. *Curr Opin Gen Amp.* 10:94-99 (2000).
52. Z.A. Stewart, S.D. Leach, and J.A. Pietsenpol. p21(Waf1/Cip1) inhibition of cyclin E/Cdk2 activity prevents endoreduplication after mitotic spindle disruption. *Mol Cell Biol.* 19:205-215 (1999).
53. C. Blanco-Aparicio, O. Renner, J.F. Leal, and A. Carnero. PTEN, more than the AKT pathway. *Carcinog.* 28:1379-1386 (2007).
54. A. Suzuki, J.L. de la Pompa, V. Stambolic, A.J. Elia, T. Sasaki, I.d.B. Barrantes, A. Ho, A. Wakeham, A. Itie, W. Khoo, M. Fukumoto, and T.W. Mak. High cancer susceptibility and embryonic lethality associated with mutation of the PTEN tumor suppressor gene in mice. *Curr Biol.* 8:1169-1178 (1998).
55. A.D. Cristofano, B. Pesce, C. Cordon-Cardo, and P.P. Pandolfi. Pten is essential for embryonic development and tumour suppression. *Nat Genet.* 19:348-355 (1998).
56. P.R. Kufe DW, Weichselbaum RR, et al. (ed.). *Holland-Frei Cancer Medicine*, BC Decker, Hamilton (ON), 2003.
57. J.L. Bos. ras oncogenes in human cancer: a review. *Cancer Res.* 49:4682-4689 (1989).
58. T. Minamoto, M. Mai, and Z. Ronai. K-ras mutation: early detection in molecular diagnosis and risk assessment of colorectal, pancreas, and lung cancers--a review. *Cancer Detect Prev.* 24:1-12 (2000).
59. D.M. Beaupre and R. Kurzrock. RAS and leukemia: from basic mechanisms to gene-directed therapy. *J Clin Oncol.* 17:1071-1079 (1999).
60. A.A. Adjei. Blocking Oncogenic Ras Signaling for Cancer Therapy. *J Natl Cancer Inst.* 93:1062-1074 (2001).
61. W. Kolch. Meaningful relationships: the regulation of the Ras/Raf/MEK/ERK pathway by protein interactions. *Biochem J.* 351 Pt 2:289-305 (2000).
62. S.K. Oster, C.S. Ho, E.L. Soucie, and L.Z. Penn. The myc oncogene: MarvelouslyY Complex. *Adv Cancer Res.* 84:81-154 (2002).

63. O. Brison. Gene amplification and tumor progression. *Biochimica et biophysica acta*. 1155:25-41 (1993).
64. G. Brodeur, R. Seeger, M. Schwab, H. Varmus, and J. Bishop. Amplification of N-myc in untreated human neuroblastomas correlates with advanced disease stage. *Sci*. 224:1121-1124 (1984).
65. D.A. Spandidos and M.L. Anderson. Oncogenes and onco-suppressor genes: their involvement in cancer. *J Pathol*. 157:1-10 (1989).
66. C. Bouchard, K. Thieke, A. Maier, R. Saffrich, J. Hanley-Hyde, W. Ansorge, S. Reed, P. Sicinski, J. Bartek, and M. Eilers. Direct induction of cyclin D2 by Myc contributes to cell cycle progression and sequestration of p27. *EMBO J*. 18:5321-5333 (1999).
67. J. van Riggelen, A. Yetil, and D.W. Felsher. MYC as a regulator of ribosome biogenesis and protein synthesis. *Nat Rev Cancer*. 10:301-309 (2010).
68. A.L. Gartel, X. Ye, E. Goufman, P. Shianov, N. Hay, F. Najmabadi, and A.L. Tyner. Myc represses the p21(WAF1/CIP1) promoter and interacts with Sp1/Sp3. *PNAS*. 98:4510-4515 (2001).
69. J.S. Ross and J.A. Fletcher. HER-2/neu (c-erb-B2) gene and protein in breast cancer. *Am J Clin Pathol*. 112:S53-67 (1999).
70. B. Falini and D.Y. Mason. Proteins encoded by genes involved in chromosomal alterations in lymphoma and leukemia: clinical value of their detection by immunocytochemistry. *Blood*. 99:409-426 (2002).
71. N.A. Heerema. Chromosomes in lymphomas and solid tumors. *Cancer Investig*. 16:183-187 (1998).
72. P. Blumberg and T. Hunter. Oncogenic kinase signalling. *Nat*. 411:355-365 (2001).
73. M.W.N. Deininger, J.M. Goldman, and J.V. Melo. The molecular biology of chronic myeloid leukemia. *Blood*. 96:3343-3356 (2000).
74. K. Grønhaug, C. Hother, and P.A. Jones. Epigenetic changes in cancer. *APMIS*. 115:1039-1059 (2007).
75. M. Ehrlich, M.A. Gama-Sosa, L.H. Huang, R.M. Midgett, K.C. Kuo, R.A. McCune, and C. Gehrke. Amount and distribution of 5-methylcytosine in human DNA from different types of tissues of cells. *Nucleic Acids Res*. 10:2709-2721 (1982).
76. W.M. Rideout, 3rd, G.A. Coetzee, A.F. Olumi, and P.A. Jones. 5-Methylcytosine as an endogenous mutagen in the human LDL receptor and p53 genes. *Sci*. 249:1288-1290 (1990).
77. M. Nakayama, M. Wada, T. Harada, J. Nagayama, H. Kusaba, K. Ohshima, M. Kozuru, H. Komatsu, R. Ueda, and M. Kuwano. Hypomethylation status of CpG sites at the promoter region and overexpression of the human MDR1 gene in acute myeloid leukemias. *Blood*. 92:4296-4307 (1998).

78. J.G. Herman and S.B. Baylin. Gene silencing in cancer in association with promoter hypermethylation. *N Engl J Med.* 349:2042-2054 (2003).
79. G. Egger, G. Liang, A. Aparicio, and P.A. Jones. Epigenetics in human disease and prospects for epigenetic therapy. *Nat.* 429:457-463 (2004).
80. M. Esteller. Aberrant DNA methylation as a cancer-inducing mechanism. *Annu Rev Pharm Toxicol.* 45:629-656 (2005).
81. M. Esteller and J.G. Herman. Cancer as an epigenetic disease: DNA methylation and chromatin alterations in human tumours. *J Pathol.* 196:1-7 (2002).
82. S.K. Kurdistani. Histone modifications in cancer biology and prognosis. *Prog Drug Res.* 67:91-106 (2011).
83. M. Lachner, D. O'Carroll, S. Rea, K. Mechtler, and T. Jenuwein. Methylation of histone H3 lysine 9 creates a binding site for HP1 proteins. *Nat.* 410:116-120 (2001).
84. H. Santos-Rosa, R. Schneider, A.J. Bannister, J. Sherriff, B.E. Bernstein, N.C. Emre, S.L. Schreiber, J. Mellor, and T. Kouzarides. Active genes are trimethylated at K4 of histone H3. *Nat.* 419:407-411 (2002).
85. R. Margueron, P. Trojer, and D. Reinberg. The key to development: interpreting the histone code? *Curr Opin Gen Dev.* 15:163-176 (2005).
86. S.B. Baylin, M. Esteller, M.R. Rountree, K.E. Bachman, K. Schuebel, and J.G. Herman. Aberrant patterns of DNA methylation, chromatin formation and gene expression in cancer. *Hum Mol Genet.* 10:687-692 (2001).
87. D.P. Bartel. MicroRNAs: Target Recognition and Regulatory Functions. *Cell.* 136:215-233 (2009).
88. A.C. Siva, L.J. Nelson, C.L. Fleischer, M. Majlessi, M.M. Becker, R.L. Vessella, and M.A. Reynolds. Molecular assays for the detection of microRNAs in prostate cancer. *Mol Cancer.* 8:17 (2009).
89. M.E. Jung, J.A. Berliner, L. Koroniak, B.G. Gugiu, and A.D. Watson. ChemInform Abstract: Improved Synthesis of the Epoxy Isoprostane Phospholipid PEIPC and Its Reactivity with Amines. *ChemInform.* 40:no-no (2009).
90. W.C.S. Cho. MicroRNAs: Potential biomarkers for cancer diagnosis, prognosis and targets for therapy. *Int J of Biochem amp.* 42:1273-1281 (2010).
91. E. Bandres, N. Bitarte, F. Arias, J. Agorreta, P. Fortes, X. Agirre, R. Zarate, J.A. Diaz-Gonzalez, N. Ramirez, J.J. Sola, P. Jimenez, J. Rodriguez, and J. Garcia-Foncillas. microRNA-451 Regulates Macrophage Migration Inhibitory Factor Production and Proliferation of Gastrointestinal Cancer Cells. *Clin Cancer Res.* 15:2281-2290 (2009).
92. E. Bandres, N. Bitarte, F. Arias, J. Agorreta, P. Fortes, X. Agirre, R. Zarate, J.A. Diaz-Gonzalez, N. Ramirez, J.J. Sola, P. Jimenez, J. Rodriguez, and J. Garcia-Foncillas. microRNA-451 Regulates Macrophage Migration Inhibitory Factor

- Production and Proliferation of Gastrointestinal Cancer Cells. *Clinical Cancer Research*. 15:2281-2290 (2009).
93. T. Greither, L.F. Grochola, A. Udelnow, C. Lautenschläger, P. Würfl, and H. Taubert. Elevated expression of microRNAs 155, 203, 210 and 222 in pancreatic tumors is associated with poorer survival. *Int J Cancer*. 126:73-80 (2010).
 94. G.A. Calin and C.M. Croce. MicroRNA signatures in human cancers. *Nat Rev Cancer*. 6:857-866 (2006).
 95. L. Dyrskjøt, M.S. Ostensfeld, J.B. Bramsen, A.N. Silahatoglu, P. Lamy, R. Ramanathan, N. Frstrup, J.L. Jensen, C.L. Andersen, K. Zieger, S. Kauppinen, B.P. Ulhøi, J. Kjems, M. Borre, and T.F. Ørntoft. Genomic Profiling of MicroRNAs in Bladder Cancer: miR-129 Is Associated with Poor Outcome and Promotes Cell Death In vitro. *Cancer Res*. 69:4851-4860 (2009).
 96. A.B.Y. Hui, W. Shi, P.C. Boutros, N. Miller, M. Pintilie, T. Fyles, D. McCready, D. Wong, K. Gerster, I. Jurisica, L.Z. Penn, and F.-F. Liu. Robust global micro-RNA profiling with formalin-fixed paraffin-embedded breast cancer tissues. *Lab Invest*. 89:597-606 (2009).
 97. J. Li, H. Huang, L. Sun, M. Yang, C. Pan, W. Chen, D. Wu, Z. Lin, C. Zeng, Y. Yao, P. Zhang, and E. Song. MiR-21 Indicates Poor Prognosis in Tongue Squamous Cell Carcinomas as an Apoptosis Inhibitor. *Clin Cancer Res*. 15:3998-4008 (2009).
 98. H.C. Chen, G.H. Chen, Y.H. Chen, W.L. Liao, C.Y. Liu, K.P. Chang, Y.S. Chang, and S.J. Chen. MicroRNA deregulation and pathway alterations in nasopharyngeal carcinoma. *Br J Cancer*. 100:1002-1011 (2009).
 99. J.H. Gibcus, L.P. Tan, G. Harms, R.N. Schakel, D. De Jong, T. Blokzijl, P. Möller, S. Poppema, B.J. Kroesen, and A. Van Den Berg. Hodgkin lymphoma cell lines are characterized by a specific miRNA expression profile. *Neoplasia*. 11:167-176 (2009).
 100. T. Greither, L.F. Grochola, A. Udelnow, C. Lautenschläger, P. Würfl, and H. Taubert. Elevated expression of microRNAs 155, 203, 210 and 222 in pancreatic tumors is associated with poorer survival. *International Journal of Cancer*. 126:73-80 (2010).
 101. A.B. Hui, W. Shi, P.C. Boutros, N. Miller, M. Pintilie, T. Fyles, D. McCready, D. Wong, K. Gerster, I. Jurisica, L.Z. Penn, and F.F. Liu. Robust global micro-RNA profiling with formalin-fixed paraffin-embedded breast cancer tissues. *Lab Invest*. 89:597-606 (2009).
 102. M.N. Jung, J.E. Koo, S.J. Oh, B.W. Lee, W.J. Lee, S.H. Ha, Y.R. Cho, and J.H. Chang. Influence of growth mode on the structural, optical, and electrical properties of In-doped ZnO nanorods. *Appl Phys Lett*. 94: (2009).
 103. T.W. Grunt, A. Lametschwandtner, and O. Staindl. The vascular pattern of basal cell tumors: light microscopy and scanning electron microscopic study on vascular corrosion casts. *Microvascular Research*. 29:371-386 (1985).

104. J.M. Brown and A.J. Giaccia. The unique physiology of solid tumors: opportunities (and problems) for cancer therapy. *Cancer Res.* 58:1408-1416 (1998).
105. D. Hanahan and R.A. Weinberg. Hallmarks of cancer: the next generation. *Cell.* 144:646-674 (2011).
106. R.J. Deberardinis, N. Sayed, D. Ditsworth, and C.B. Thompson. Brick by brick: metabolism and tumor cell growth. *Curr Opin Genet Dev.* 18:54-61 (2008).
107. L.M. Ferreira, A. Hebrant, and J.E. Dumont. Metabolic reprogramming of the tumor. *Oncog* (2012).
108. R. Diaz-Ruiz, S. Uribe-Carvajal, A. Devin, and M. Rigoulet. Tumor cell energy metabolism and its common features with yeast metabolism. *Biochim Biophys Acta.* 1796:252-265 (2009).
109. N. Marty, M. Dallaporta, and B. Thorens. Brain glucose sensing, counterregulation, and energy homeostasis. *Physiol.* 22:241-251 (2007).
110. O. Warburg, F. Wind, and E. Negelein. The Metabolism of tumors in the body. *The Journal of general physiology.* 8:519-530 (1927).
111. M.E. Phelps. PET: the merging of biology and imaging into molecular imaging. *Journal of nuclear medicine : official publication, Society of Nuclear Medicine.* 41:661-681 (2000).
112. V. Ganapathy, M. Thangaraju, and P.D. Prasad. Nutrient transporters in cancer: relevance to Warburg hypothesis and beyond. *Pharmacology & therapeutics.* 121:29-40 (2009).
113. S.N. Reske, K.G. Grillenberger, G. Glatting, M. Port, M. Hildebrandt, F. Gansauge, and H.G. Beger. Overexpression of glucose transporter 1 and increased FDG uptake in pancreatic carcinoma. *Journal of nuclear medicine : official publication, Society of Nuclear Medicine.* 38:1344-1348 (1997).
114. B. Thorens and M. Mueckler. Glucose transporters in the 21st Century. *American journal of physiology Endocrinology and metabolism.* 298:E141-145 (2010).
115. M. Uldry and B. Thorens. The SLC2 family of facilitated hexose and polyol transporters. *Pflugers Archiv : European Journal of Physiology.* 447:480-489 (2004).
116. M. Mueckler, C. Caruso, S.A. Baldwin, M. Panico, I. Blench, H.R. Morris, W.J. Allard, G.E. Lienhard, and H.F. Lodish. Sequence and structure of a human glucose transporter. *Sci.* 229:941-945 (1985).
117. F. Schwartzenberg-Bar-Yoseph, M. Armoni, and E. Karnieli. The tumor suppressor p53 down-regulates glucose transporters GLUT1 and GLUT4 gene expression. *Cancer Res.* 64:2627-2633 (2004).
118. M. Tsukioka, Y. Matsumoto, M. Noriyuki, C. Yoshida, H. Nobeyama, H. Yoshida, T. Yasui, T. Sumi, K. Honda, and O. Ishiko. Expression of glucose

- transporters in epithelial ovarian carcinoma: correlation with clinical characteristics and tumor angiogenesis. *Oncol Rep.* 18:361-367 (2007).
119. T. Tohma, S. Okazumi, H. Makino, A. Cho, R. Mochizuki, K. Shuto, H. Kudo, K. Matsubara, H. Gunji, H. Matsubara, and T. Ochiai. Overexpression of glucose transporter 1 in esophageal squamous cell carcinomas: a marker for poor prognosis. *Diseases of the esophagus : official journal of the International Society for Diseases of the Esophagus / ISDE.* 18:185-189 (2005).
 120. S.S. Kang, Y.K. Chun, M.H. Hur, H.K. Lee, Y.J. Kim, S.R. Hong, J.H. Lee, S.G. Lee, and Y.K. Park. Clinical significance of glucose transporter 1 (GLUT1) expression in human breast carcinoma. *Japanese Journal of Cancer Research : Gann.* 93:1123-1128 (2002).
 121. S.U. Berlangieri and A.M. Scott. Metabolic staging of lung cancer. *N Engl J Med.* 343:290-292 (2000).
 122. T. Suzuki, A. Iwazaki, H. Katagiri, Y. Oka, J.L. Redpath, E.J. Stanbridge, and T. Kitagawa. Enhanced expression of glucose transporter GLUT3 in tumorigenic HeLa cell hybrids associated with tumor suppressor dysfunction. *Eur J Biochem.* 262:534-540 (1999).
 123. J.W. Kim, I. Tchernyshyov, G.L. Semenza, and C.V. Dang. HIF-1-mediated expression of pyruvate dehydrogenase kinase: a metabolic switch required for cellular adaptation to hypoxia. *Cell Metabolism.* 3:177-185 (2006).
 124. H. Shim, C. Dolde, B.C. Lewis, C.S. Wu, G. Dang, R.A. Jungmann, R. Dalla-Favera, and C.V. Dang. c-Myc transactivation of LDH-A: implications for tumor metabolism and growth. *PNAS.* 94:6658-6663 (1997).
 125. M. Reinacher and E. Eigenbrodt. Immunohistological demonstration of the same type of pyruvate kinase isoenzyme (M2-Pk) in tumors of chicken and rat. *Virchows Archiv B, Cell Pathology Including Molecular Pathology.* 37:79-88 (1981).
 126. S. Mazurek, C.B. Boschek, F. Hugo, and E. Eigenbrodt. Pyruvate kinase type M2 and its role in tumor growth and spreading. *Seminars in Cancer Biology.* 15:300-308 (2005).
 127. O. Feron. Pyruvate into lactate and back: from the Warburg effect to symbiotic energy fuel exchange in cancer cells. *Radiotherapy and oncology : journal of the European Society for Therapeutic Radiology and Oncology.* 92:329-333 (2009).
 128. S. Mazurek, H. Grimm, M. Oehmke, G. Weisse, S. Teigelkamp, and E. Eigenbrodt. Tumor M2-PK and glutaminolytic enzymes in the metabolic shift of tumor cells. *Anticancer Res.* 20:5151-5154 (2000).
 129. A. Hoshino, J.A. Hirst, and H. Fujii. Regulation of cell proliferation by interleukin-3-induced nuclear translocation of pyruvate kinase. *J Biol Chem.* 282:17706-17711 (2007).
 130. S.J. Bensinger and H.R. Christofk. New aspects of the Warburg effect in cancer cell biology. *Seminars in Cell & Developmental Biology* (2012).

131. A.P. Halestrap and D. Meredith. The SLC16 gene family-from monocarboxylate transporters (MCTs) to aromatic amino acid transporters and beyond. *Pflugers Archiv : European Journal of Physiology*. 447:619-628 (2004).
132. M.S. Ullah, A.J. Davies, and A.P. Halestrap. The plasma membrane lactate transporter MCT4, but not MCT1, is up-regulated by hypoxia through a HIF-1 α -dependent mechanism. *J Biol Chem*. 281:9030-9037 (2006).
133. H. Li, L. Myeroff, D. Smiraglia, M.F. Romero, T.P. Pretlow, L. Kasturi, J. Lutterbaugh, R.M. Rerko, G. Casey, J.P. Issa, J. Willis, J.K. Willson, C. Plass, and S.D. Markowitz. SLC5A8, a sodium transporter, is a tumor suppressor gene silenced by methylation in human colon aberrant crypt foci and cancers. *PNAS*. 100:8412-8417 (2003).
134. P. Swietach, R.D. Vaughan-Jones, and A.L. Harris. Regulation of tumor pH and the role of carbonic anhydrase 9. *Cancer metastasis reviews*. 26:299-310 (2007).
135. H.S. Waagepetersen, U. Sonnewald, O.M. Larsson, and A. Schousboe. A possible role of alanine for ammonia transfer between astrocytes and glutamatergic neurons. *J Neurochem*. 75:471-479 (2000).
136. K.M. Kennedy and M.W. Dewhirst. Tumor metabolism of lactate: the influence and therapeutic potential for MCT and CD147 regulation. *Future Oncol*. 6:127-148 (2010).
137. S. Walenta and W.F. Mueller-Klieser. Lactate: mirror and motor of tumor malignancy. *Seminars in Radiation Oncology*. 14:267-274 (2004).
138. K. Fischer, P. Hoffmann, S. Voelkl, N. Meidenbauer, J. Ammer, M. Edinger, E. Gottfried, S. Schwarz, G. Rothe, S. Hoves, K. Renner, B. Timischl, A. Mackensen, L. Kunz-Schughart, R. Andreesen, S.W. Krause, and M. Kreutz. Inhibitory effect of tumor cell-derived lactic acid on human T cells. *Blood*. 109:3812-3819 (2007).
139. J. Heitman, N.R. Movva, and M.N. Hall. Targets for cell cycle arrest by the immunosuppressant rapamycin in yeast. *Sci*. 253:905-909 (1991).
140. N. Hayand N. Sonenberg. Upstream and downstream of mTOR. *Genes Dev*. 18:1926-1945 (2004).
141. H. Nojima, C. Tokunaga, S. Eguchi, N. Oshiro, S. Hidayat, K. Yoshino, K. Hara, N. Tanaka, J. Avruch, and K. Yonezawa. The mammalian target of rapamycin (mTOR) partner, raptor, binds the mTOR substrates p70 S6 kinase and 4E-BP1 through their TOR signaling (TOS) motif. *J Biol Chem*. 278:15461-15464 (2003).
142. D.D. Sarbassov, S.M. Ali, S. Sengupta, J.H. Sheen, P.P. Hsu, A.F. Bagley, A.L. Markhard, and D.M. Sabatini. Prolonged rapamycin treatment inhibits mTORC2 assembly and Akt/PKB. *Mol Cell*. 22:159-168 (2006).
143. L.J. Saucedo, X. Gao, D.A. Chiarelli, L. Li, D. Pan, and B.A. Edgar. Rheb promotes cell growth as a component of the insulin/TOR signalling network. *Nat Cell Biol*. 5:566-571 (2003).

144. P.G. Charest, Z. Shen, A. Lakoduk, A.T. Sasaki, S.P. Briggs, and R.A. Firtel. A Ras signaling complex controls the RasC-TORC2 pathway and directed cell migration. *Developmental Cell*. 18:737-749 (2010).
145. R.J. Dowling, I. Topisirovic, T. Alain, M. Bidinosti, B.D. Fonseca, E. Petroulakis, X. Wang, O. Larsson, A. Selvaraj, Y. Liu, S.C. Kozma, G. Thomas, and N. Sonenberg. mTORC1-mediated cell proliferation, but not cell growth, controlled by the 4E-BPs. *Sci*. 328:1172-1176 (2010).
146. X.M. Ma and J. Blenis. Molecular mechanisms of mTOR-mediated translational control. *Nat Rev Mol Cell Biol*. 10:307-318 (2009).
147. K.F. Wilson, W.J. Wu, and R.A. Cerione. Cdc42 stimulates RNA splicing via the S6 kinase and a novel S6 kinase target, the nuclear cap-binding complex. *J Biol Chem*. 275:37307-37310 (2000).
148. C. Mayer, J. Zhao, X. Yuan, and I. Grummt. mTOR-dependent activation of the transcription factor TIF-IA links rRNA synthesis to nutrient availability. *Genes Dev*. 18:423-434 (2004).
149. Y. Kamada, T. Funakoshi, T. Shintani, K. Nagano, M. Ohsumi, and Y. Ohsumi. Tor-mediated induction of autophagy via an Apg1 protein kinase complex. *J Cell Biol*. 150:1507-1513 (2000).
150. R. Zoncu, A. Efeyan, and D.M. Sabatini. mTOR: from growth signal integration to cancer, diabetes and ageing. *Nat Rev Mol Cell Biol*. 12:21-35 (2011).
151. V. Facchinetti, W. Ouyang, H. Wei, N. Soto, A. Lazorchak, C. Gould, C. Lowry, A.C. Newton, Y. Mao, R.Q. Miao, W.C. Sessa, J. Qin, P. Zhang, B. Su, and E. Jacinto. The mammalian target of rapamycin complex 2 controls folding and stability of Akt and protein kinase C. *EMBO J*. 27:1932-1943 (2008).
152. D.D. Sarbassov, D.A. Guertin, S.M. Ali, and D.M. Sabatini. Phosphorylation and regulation of Akt/PKB by the rictor-mTOR complex. *Sci*. 307:1098-1101 (2005).
153. J.R. Sabine, S. Abraham, and I.L. Chaikoff. Control of lipid metabolism in hepatomas: insensitivity of rate of fatty acid and cholesterol synthesis by mouse hepatoma BW7756 to fasting and to feedback control. *Cancer Res*. 27:793-799 (1967).
154. M. Ookhtens, R. Kannan, I. Lyon, and N. Baker. Liver and adipose tissue contributions to newly formed fatty acids in an ascites tumor. *The American Journal of Physiology*. 247:R146-153 (1984).
155. F.P. Kuhajda. Fatty-acid synthase and human cancer: new perspectives on its role in tumor biology. *Nutr*. 16:202-208 (2000).
156. C.D. Young and S.M. Anderson. Sugar and fat - that's where it's at: metabolic changes in tumors. *Breast Cancer Res*. 10:202 (2008).
157. E.S. Pizer, F.D. Wood, G.R. Pasternack, and F.P. Kuhajda. Fatty acid synthase (FAS): a target for cytotoxic antimetabolites in HL60 promyelocytic leukemia cells. *Cancer Res*. 56:745-751 (1996).

158. W.B. Kinlaw, J.L. Quinn, W.A. Wells, C. Roser-Jones, and J.T. Moncur. Spot 14: A marker of aggressive breast cancer and a potential therapeutic target. *Endocrinol.* 147:4048-4055 (2006).
159. D.K. Nomura, J.Z. Long, S. Niessen, H.S. Hoover, S.W. Ng, and B.F. Cravatt. Monoacylglycerol lipase regulates a fatty acid network that promotes cancer pathogenesis. *Cell.* 140:49-61 (2010).
160. G.V. Kryukov, S. Castellano, S.V. Novoselov, A.V. Lobanov, O. Zehtab, R. Guigo, and V.N. Gladyshev. Characterization of mammalian selenoproteomes. *Sci.* 300:1439-1443 (2003).
161. W.H. Cheng, Y.S. Ho, D.A. Ross, B.A. Valentine, G.F. Combs, and X.G. Lei. Cellular glutathione peroxidase knockout mice express normal levels of selenium-dependent plasma and phospholipid hydroperoxide glutathione peroxidases in various tissues. *The Journal of Nutrition.* 127:1445-1450 (1997).
162. J.B. de Haan, C. Bladier, M. Lotfi-Miri, J. Taylor, P. Hutchinson, P.J. Crack, P. Hertzog, and I. Kola. Fibroblasts derived from Gpx1 knockout mice display senescent-like features and are susceptible to H₂O₂-mediated cell death. *Free Radic Biol Med.* 36:53-64 (2004).
163. D.H. Lee, R.S. Esworthy, C. Chu, G.P. Pfeifer, and F.F. Chu. Mutation accumulation in the intestine and colon of mice deficient in two intracellular glutathione peroxidases. *Cancer Res.* 66:9845-9851 (2006).
164. C.L. Shen, W. Song, and B.C. Pence. Interactions of selenium compounds with other antioxidants in DNA damage and apoptosis in human normal keratinocytes. *Cancer epidemiology, biomarkers & prevention : a publication of the American Association for Cancer Research, cosponsored by the American Society of Preventive Oncology.* 10:385-390 (2001).
165. R. Zhao, F.E. Domann, and W. Zhong. Apoptosis induced by selenomethionine and methioninase is superoxide mediated and p53 dependent in human prostate cancer cells. *Mol Cancer Ther.* 5:3275-3284 (2006).
166. H. Hu, C. Jiang, T. Schuster, G.X. Li, P.T. Daniel, and J. Lu. Inorganic selenium sensitizes prostate cancer cells to TRAIL-induced apoptosis through superoxide/p53/Bax-mediated activation of mitochondrial pathway. *Mol Cancer Ther.* 5:1873-1882 (2006).
167. E. Madsen and J.D. Gitlin. Copper deficiency. *Current Opinion in Gastroenterology.* 23:187-192 (2007).
168. S. Inutsuka and S. Araki. Plasma copper and zinc levels in patients with malignant tumors of digestive organs: clinical evaluation of the C1/Zn ratio. *Cancer.* 42:626-631 (1978).
169. M.C. Linder. Copper and genomic stability in mammals. *Mutation Research.* 475:141-152 (2001).
170. W.H. Cheng. Impact of inorganic nutrients on maintenance of genomic stability. *Environmental and Molecular Mutagenesis.* 50:349-360 (2009).

171. N.P. Pavletich, K.A. Chambers, and C.O. Pabo. The DNA-binding domain of p53 contains the four conserved regions and the major mutation hot spots. *Genes Dev.* 7:2556-2564 (1993).
172. B. Bleijlevens, T. Shivarattan, B. Sedgwick, S.E. Rigby, and S.J. Matthews. Replacement of non-heme Fe(II) with Cu(II) in the alpha-ketoglutarate dependent DNA repair enzyme AlkB: spectroscopic characterization of the active site. *Journal of Inorganic Biochemistry.* 101:1043-1048 (2007).
173. A.J. Ridley, M.A. Schwartz, K. Burridge, R.A. Firtel, M.H. Ginsberg, G. Borisy, J.T. Parsons, and A.R. Horwitz. Cell migration: integrating signals from front to back. *Sci.* 302:1704-1709 (2003).
174. G. Giannone, P. Ronde, M. Gaire, J. Beaudouin, J. Haiech, J. Ellenberg, and K. Takeda. Calcium rises locally trigger focal adhesion disassembly and enhance residency of focal adhesion kinase at focal adhesions. *J Biol Chem.* 279:28715-28723 (2004).
175. M. Schneider, J.L. Hansen, and S.P. Sheikh. S100A4: a common mediator of epithelial-mesenchymal transition, fibrosis and regeneration in diseases? *J Mol Med (Berl).* 86:507-522 (2008).
176. A.G. Knudson, Jr. Mutation and cancer: statistical study of retinoblastoma. *Proc Natl Acad Sci U S A.* 68:820-823 (1971).
177. F. Mbeunkui and D.J. Johann, Jr. Cancer and the tumor microenvironment: a review of an essential relationship. *Cancer Chemother Pharmacol.* 63:571-582 (2009).
178. T.L. Whiteside. The tumor microenvironment and its role in promoting tumor growth. *Oncog.* 27:5904-5912 (2008).
179. T.D. Tlsty and L.M. Coussens. Tumor stroma and regulation of cancer development. *Annu Rev Pathol.* 1:119-150 (2006).
180. M. Sundand R. Kalluri. Tumor stroma derived biomarkers in cancer. *Cancer metastasis reviews.* 28:177-183 (2009).
181. O. De Wever, P. Demetter, M. Mareel, and M. Bracke. Stromal myofibroblasts are drivers of invasive cancer growth. *Int J Cancer.* 123:2229-2238 (2008).
182. F. Xing, J. Saidou, and K. Watabe. Cancer associated fibroblasts (CAFs) in tumor microenvironment. *Front Biosci.* 15:166-179 (2010).
183. R. Kalluri and M. Zeisberg. Fibroblasts in cancer. *Nat Rev Cancer.* 6:392-401 (2006).
184. A. Mantovani, S. Sozzani, M. Locati, P. Allavena, and A. Sica. Macrophage polarization: tumor-associated macrophages as a paradigm for polarized M2 mononuclear phagocytes. *Trends in Immunology.* 23:549-555 (2002).
185. A.C. Ochoa, A.H. Zea, C. Hernandez, and P.C. Rodriguez. Arginase, prostaglandins, and myeloid-derived suppressor cells in renal cell carcinoma. *Clin Cancer Res.* 13:721s-726s (2007).

186. M.J. Smyth, E. Cretney, M.H. Kershaw, and Y. Hayakawa. Cytokines in cancer immunity and immunotherapy. *Immunol Rev.* 202:275-293 (2004).
187. F.R. Balkwill. The chemokine system and cancer. *J Pathol.* 226:148-157 (2012).
188. F. Balkwill. Cancer and the chemokine network. *Nat Rev Cancer.* 4:540-550 (2004).
189. P. Bornstein and E.H. Sage. Matricellular proteins: extracellular modulators of cell function. *Curr Opin Cell Biol.* 14:608-616 (2002).
190. E.W. Raines, T.F. Lane, M.L. Iruela-Arispe, R. Ross, and E.H. Sage. The extracellular glycoprotein SPARC interacts with platelet-derived growth factor (PDGF)-AB and -BB and inhibits the binding of PDGF to its receptors. *PNAS.* 89:1281-1285 (1992).
191. P. Hasselaar and E.H. Sage. SPARC antagonizes the effect of basic fibroblast growth factor on the migration of bovine aortic endothelial cells. *J Cell Biochem.* 49:272-283 (1992).
192. P.L. Porter, E.H. Sage, T.F. Lane, S.E. Funk, and A.M. Gown. Distribution of SPARC in normal and neoplastic human tissue. *J Histochem Cytochem.* 43:791-800 (1995).
193. S.R. Alonso, L. Tracey, P. Ortiz, B. Perez-Gomez, J. Palacios, M. Pollan, J. Linares, S. Serrano, A.I. Saez-Castillo, L. Sanchez, R. Pajares, A. Sanchez-Aguilera, M.J. Artiga, M.A. Piris, and J.L. Rodriguez-Peralto. A high-throughput study in melanoma identifies epithelial-mesenchymal transition as a major determinant of metastasis. *Cancer Res.* 67:3450-3460 (2007).
194. D.J. Smit, B.B. Gardiner, and R.A. Sturm. Osteonectin downregulates E-cadherin, induces osteopontin and focal adhesion kinase activity stimulating an invasive melanoma phenotype. *Int J Cancer.* 121:2653-2660 (2007).
195. G. Bergers and S. Song. The role of pericytes in blood-vessel formation and maintenance. *Neuro Oncol.* 7:452-464 (2005).
196. K. Gaengel, G. Genove, A. Armulik, and C. Betsholtz. Endothelial-mural cell signaling in vascular development and angiogenesis. *Arteriosclerosis, thrombosis, and vascular biology.* 29:630-638 (2009).
197. J. Folkman. Tumor angiogenesis: therapeutic implications. *N Engl J Med.* 285:1182-1186 (1971).
198. D. Hanahan and R.A. Weinberg. The hallmarks of cancer. *Cell.* 100:57-70 (2000).
199. R.T. Poon, S.T. Fan, and J. Wong. Clinical implications of circulating angiogenic factors in cancer patients. *J Clin Oncol.* 19:1207-1225 (2001).
200. E.M. Bridges and A.L. Harris. The angiogenic process as a therapeutic target in cancer. *Biochem Pharmacol.* 81:1183-1191 (2011).
201. G. Tortora, D. Melisi, and F. Ciardiello. Angiogenesis: a target for cancer therapy. *Current Pharmaceutical Design.* 10:11-26 (2004).

202. R.A. Weinberg. *The Biology of Cancer*, Garland Science, Taylor & Francis Group, 2007.
203. S. Valastyan and R.A. Weinberg. Tumor metastasis: molecular insights and evolving paradigms. *Cell*. 147:275-292 (2011).
204. A.C. Chiang and J. Massague. Molecular basis of metastasis. *N Engl J Med*. 359:2814-2823 (2008).
205. E.D. Hay. An overview of epithelio-mesenchymal transformation. *Acta Anat (Basel)*. 154:8-20 (1995).
206. R. Kalluri and E.G. Neilson. Epithelial-mesenchymal transition and its implications for fibrosis. *J Clin Invest*. 112:1776-1784 (2003).
207. R. Kalluri and R.A. Weinberg. The basics of epithelial-mesenchymal transition. *J Clin Invest*. 119:1420-1428 (2009).
208. D.C. Radisky. Epithelial-mesenchymal transition. *J Cell Sci*. 118:4325-4326 (2005).
209. J. Yang and R.A. Weinberg. Epithelial-mesenchymal transition: at the crossroads of development and tumor metastasis. *Developmental cell*. 14:818-829 (2008).
210. D. Medici, E.D. Hay, and B.R. Olsen. Snail and Slug promote epithelial-mesenchymal transition through beta-catenin-T-cell factor-4-dependent expression of transforming growth factor-beta3. *Mol Biol Cell*. 19:4875-4887 (2008).
211. S. Hirohashi. Inactivation of the E-cadherin-mediated cell adhesion system in human cancers. *Am J Pathol*. 153:333-339 (1998).
212. J. Zavadil, M. Narasimhan, M. Blumenberg, and R.J. Schneider. Transforming growth factor-beta and microRNA:mRNA regulatory networks in epithelial plasticity. *Cells, tissues, organs*. 185:157-161 (2007).
213. G.P. Gupta and J. Massague. Cancer metastasis: building a framework. *Cell*. 127:679-695 (2006).
214. P. Carmeliet and R.K. Jain. Principles and mechanisms of vessel normalization for cancer and other angiogenic diseases. *Nature reviews Drug discovery*. 10:417-427 (2011).
215. J.A. Joyce and J.W. Pollard. Microenvironmental regulation of metastasis. *Nat Rev Cancer*. 9:239-252 (2009).
216. B. Psaila and D. Lyden. The metastatic niche: adapting the foreign soil. *Nat Rev Cancer*. 9:285-293 (2009).
217. S. Paget. The distribution of secondary growths in cancer of the breast. *Lancet*. 133:571-573 (1889).

CHAPTER 3

A CHIMERIC P53 EVADES MUTANT P53 TRANSDOMINANT INHIBITION IN CANCER CELLS

3.1 Abstract

Due to the dominant negative effect of mutant p53, there has been limited success with wild-type (wt) p53 cancer gene therapy. Therefore, an alternative oligomerization domain for p53 was investigated to enhance the utility of p53 for gene therapy. The tetramerization domain of p53 was substituted with the coiled-coil (CC) domain from Bcr (breakpoint cluster region). Our p53 variant (p53-CC) maintains proper nuclear localization in breast cancer cells detected via fluorescence microscopy and shows similar expression profile of p53 target genes as wt-p53. Additionally, similar tumor suppressor activities of p53-CC and wt-p53 were detected by TUNEL, annexin-V, 7-AAD, and colony forming assays. Furthermore, p53-CC was found to cause apoptosis in 4 different cancer cell lines, regardless of endogenous p53 status. Interestingly, the transcriptional activity of p53-CC was higher than wt-p53 in 3 different reporter gene assays. We hypothesized that the higher transcriptional activity of p53-CC over wt-p53 was due to the sequestration of wt-p53 by endogenous mutant p53 found in cancer cells. Co-immunoprecipitation revealed that wt-p53 does indeed interact with endogenous mutant p53 via its tetramerization domain, while p53-CC escapes this interaction.

Therefore, we investigated the impact of the presence of a transdominant mutant p53 on tumor suppressor activities of wt-p53 and p53-CC. Overexpression of a potent mutant p53 along with wt-p53 or p53-CC revealed that unlike wt-p53, p53-CC retains the same level of tumor suppressor activity. Finally, viral transduction of wt-p53 and p53-CC into a breast cancer cell line that harbors a tumor derived transdominant mutant p53 validated that p53-CC indeed evades sequestration and consequent transdominant inhibition by endogenous mutant p53.

3.2 Introduction

The tumor suppressor p53, a 393 amino acid sequence-specific transcription factor, stimulates a wide network of signals including cell cycle arrest, DNA repair, and apoptosis. p53-dependent apoptosis is achieved through two distinct apoptotic signaling pathways; the extrinsic pathway through death receptors and the intrinsic pathway through the mitochondria (1). While p53 is able to induce apoptosis when targeted to the mitochondria (2-4), its tumor suppressor function mainly depends on localization to the nucleus and formation of p53 tetramers leading to its function as a transcription factor of several target genes (5). The p53 protein is commonly divided into three regions: an acidic N-terminal region (codons 1-101), a DNA binding domain (DBD, codons 102-292), and a basic C-terminal region (codons 293-393) (6). The C-terminus contains three nuclear localization signals (NLSs), a nuclear export signal (E), and a tetramerization domain (TD) (Figure 3.1A). In response to cellular stimuli such as DNA damage and oncogene activation (7), the MDM2-p53 degradation pathway is inactivated leading to increased concentration of p53 followed by rapid accumulation in the nucleus, which is

essential for regulating cell cycle arrest, DNA repair, senescence, and apoptosis (8, 9).

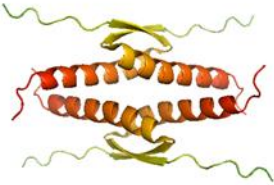
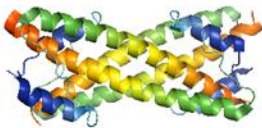
Current strategies to enhance the anti-cancer/tumor-suppressor function of p53 are focused on introducing additional wt-p53 to the affected cells or tumor. This treatment modality introduces wt-p53 as a gene into cancer cells using various delivery vehicles. Wild-type p53 is a currently approved gene therapeutic for head and neck cancer in China (10). While a promising approach, there are significant limitations to the efficacy of this method, namely the presence of mutations in the endogenous p53 molecule.

The tumor suppressor p53 is inactivated in more than half of all human tumors (11). Acquisition of missense mutations in the *TP53* gene results in aberrant p53 that is transcriptionally inactive (12-14). Mutant p53 can also contribute to cancer drug resistance due to its inhibition of wild-type (wt) p53 via a dominant negative effect and the acquisition of gain of function properties (15). Since p53 binds DNA as a tetramer consisting of a dimer of dimers (16), when endogenous mutant p53 oligomerizes with exogenous wt-p53 the resulting tetramer is inactive (17-19). Such hetero-tetramerization is possible as the TD retains functionality in mutant p53. This dominant negative effect, wherein mutant p53 inactivates therapeutic wt-p53, represents a key problem with using wt-p53 for gene therapy. The dominant negative effect of p53 has shown to be operative *in vivo* using knock-in mice expressing mutant p53 (20).

Because sequestration of wt-p53 into inactive hetero-tetramers with mutant p53 forms a critical barrier to the efficacy of utilizing p53 for cancer therapy, improvements to advance the efficacy of this therapy even in the presence of p53 mutants is needed (11). Our approach to bypass the dominant negative effect of tumor-derived p53 is to engineer a p53 variant that relies on a different oligomerization motif to prevent hetero-

oligomer formation. To our knowledge, only one attempt has been made to eliminate the dominant negative effect of mutant p53 in hetero-tetramers via substituting its TD, with marginal success (21). Whereas the native TD of p53 drives the formation of *antiparallel* tetramers (21-23), this previous work utilized an oligomerization domain that led to *parallel* tetramer formation which resulted in a significant reduction in p53 function. We recognized that the oligomerization domain from breakpoint cluster region (Bcr) protein, a 72 amino acid coiled-coil (CC), tetramerizes as two dimers of two antiparallel-oriented monomers (24), in a similar fashion to the TD of wt-p53. This would be a suitable candidate for TD substitution (22), forming a chimeric p53-Bcr fusion. Table 3.1 depicts the oligomerization domains for p53 (TD) and the CC domain from Bcr.

Table 3.1 Comparison of the native TD from wt-p53 to the CC domain from Bcr. Snapshots were taken with molecular visualization software PyMOL (PyMOL Molecular Graphics System Version 1.5.0.4 Schrodinger, LLC.) initiated from the 1C26 for p53 TD (22) and 1K1F for Bcr CC (25) PDB structures.

	TD	CC
Sequence	31 amino acids	72 amino acids
Secondary Structure	Consists of a β strand, a tight turn followed by an α helix	Consists of two α helices
Orientation	Antiparallel	Antiparallel
Tetramer Formation	Dimer of dimers	Dimer of dimers
Structure		

This report demonstrates that our p53 variant, namely p53-CC, shows higher levels of transcriptional activity in reporter gene assays, and exhibits similar tumor suppressor activity compared to wt-p53 in cell lines with varying p53 status. Lastly, we show the ability of p53-CC to circumvent the dominant negative effect in cancer cells harboring a strong transdominant mutant p53.

3.3 Materials and Methods

3.3.1 Construction of Plasmids

To construct pEGFP-p53-CC (p53-CC), a truncated version of wt-p53 that lacks the tetramerization domain (amino acids 1-322) was amplified via PCR with primers 5'-gcgcgcgcgctccggaatggaggagccgcagtca-3' and 5'-gcgcgcgcgctccggatggttcttctttggctggggaga-3' using the previously cloned pEGFP-p53 (wt-p53) as the template DNA (4). The PCR product was then subcloned into the BspEI site of pEGFP-CC (CC) (26).

To create pEGFP-p53- Δ TDC (p53- Δ TDC), the same truncated version of wt-p53 (amino acids 1-322) was amplified via PCR with primers 5'-gcgcgcgcgctccggaatggaggagccgcagtca-3' and 5'-gcgcgcgcgcggtacctcatggttcttctttggctgggg-3' using pEGFP-p53 as the template DNA (4). The PCR product (insert) was then subcloned into the digested pEGFP-C1 vector (Clontech, Mountain View, CA) at the BspEI and KpnI sites.

To design pTagBFP-mut-p53, wt-p53 was amplified via PCR with primers 5'-gcgcgcgcgctccggagccatggaggagccgcagt-3', and 5'-gcgcgcgcgcggtacctcagtctgagtcaggcccttctgtc-3' using pEGFP-p53 as a template. This insert was then subcloned into the digested pTagBFP-C vector (Evrogen, Moscow, Russia) at the BspEI and KpnI sites. Three hot

spot mutations (R175H, R248W, and R273H) (27, 28) were then introduced into pTagBFP-p53 via QuikChange II XL Site-Directed Mutagenesis Kit (Agilent, Santa Clara, CA). The following primers were used: for the R175H mutation, 5'-tgacggaggtgtgaggcactgccccaccatgagcgc-3' and 5'-gcgctcatggtggggcagtgccctcacaacctccgtca-3'; for R248W, 5'-ctgcatggcgcatgaactggaggccatcctcacca-3' and 5'-tggtgaggatgggcctccagttcatgccgcccag-3'; and for R273H, 5'-ggaacagctttgaggtgcatgtttgtcctgtcctggg-3' and 5'-cccaggacaggcacaacatgcacctcaaagctgttc-3'.

3.3.2 Cell Lines and Transient Transfection

T47D human ductal breast epithelial tumor cells (ATCC, Manassas, VA), MCF-7 human breast adenocarcinoma cells (ATCC), HeLa human epithelial cervical adenocarcinoma cells (ATCC), H1373 human non-small cell lung carcinoma cells (a kind gift from Dr. Andrea Bild, University of Utah), and MDA-MB-231 human breast adenocarcinoma cells (ATCC) were grown as monolayers in RPMI (Invitrogen, Carlsbad, CA) supplemented with 10% fetal bovine serum (Invitrogen), 1% penicillin-streptomycin-glutamine (Invitrogen), 0.1% gentamicin (Invitrogen). T47D and MCF-7 were also supplemented with 4 mg/L insulin (Sigma, St. Louis, MO). 1471.1 murine breast adenocarcinoma cells (gift of Dr. Gordon Hager, NCI, NIH), HEK293 human embryonic kidney (ATCC), MDA-MB-468 human breast adenocarcinoma cells (ATCC), and 4T1 murine breast carcinoma cells were grown as monolayers in DMEM (Invitrogen) supplemented with 10% fetal bovine serum, 1% penicillin-streptomycin-glutamine, and 0.1% gentamicin. MDA-MB-468 cells were also supplemented with 1% MEM non-essential amino acids (Invitrogen). All cells were incubated in 5% CO₂ at 37°C. The cells

were seeded at a density of 7.5×10^4 cells (for 1471.1, MDA-MB-231, HeLa, and 4T1 cells) and 3.0×10^5 cells (for MCF-7, T47D, HEK293, MDA-MB-468 and H1373 cells) in 6-well plates (Greiner Bio-One, Monroe, NC). Transfections of 1 pmol DNA were carried out 24 h after seeding using Lipofectamine 2000 (Invitrogen) following the manufacturer's recommendations (4).

3.3.3 Microscopy

All microscopy was performed using 1471.1 cells due to their ideal microscopic morphology (4). 24 h post transfection, media in 2-well live-cell chambers (Nalgene Nunc, Rochester, NY) was replaced with phenol red-free DMEM (Invitrogen). Cells were then incubated with 2 $\mu\text{g}/\text{mL}$ Hoechst 33342 nuclear stain (Invitrogen) for 30 minutes at 37°C. Images were taken using an Olympus IX71F fluorescence microscope (Scientific Instrument Company, Aurora, CO) with high-quality narrow band GFP filter (excitation, HQ480/20 nm; emission, HQ510/ 20 nm) to detect EGFP and cyan GFP v2 filter (excitation HQ436/20 nm, emission HQ480/40 nm, with beam splitter 455dclp) to detect H33342 as previously described (29).

3.3.4 qRT-PCR

Twenty-four h following transfection of T47D cells, mRNA from cell lysates was isolated using RNeasy[®] Mini Kit (Qiagen, Valencia, CA). cDNA was then obtained using RT²[®] First Strand Kit (Qiagen) and mixed with RT SYBR[®] Green qPCR Mastermix (Qiagen). Equal volumes were then aliquoted into a 384-well p53 Signaling Pathway PCR Array[®] (Qiagen). Roche LightCycler 480 was used for real-time PCR cycling.

Analysis of the PCR array was performed using the manufacturer's web-based analysis software (<http://pcrdataanalysis.sabiosciences.com/pcr/arrayanalysis.php>). Genes outside of a 2-fold range were considered to be statistically different per the manufacturer.

3.3.5 Western Blotting

Twenty-four h following transfection of T47D cells, EGFP-positive cells were sorted using the FACS Aria-II (BD-BioSciences). 3×10^5 cells were pelleted and resuspended in 200 μ L lysis buffer (62.5 mM Tris-HCl, 2% w/v SDS, 10% glycerol, 1 % protease inhibitor). Standard western blotting procedures (30) were followed using primary antibodies to detect p21/WAF1, Bax, and actin as a loading control. The primary antibodies anti-p21 (ab16767, Abcam, Cambridge, MA), anti-Bax (ab7977, Abcam), anti-actin (mouse, ab3280, Abcam), and anti-actin (rabbit, ab1801, Abcam) were detected with anti-rabbit (#7074S, Cell Signaling Technology, Danvers, MA) or anti-mouse (ab6814, Abcam) HRP-conjugated antibodies before the addition of SuperSignal West Pico chemiluminescent substrate (Thermo Scientific, Waltham, MA). Signals were detected using a FluorChem FC2 imager and software (Alpha Innotech, Sanata Clara, CA).

3.3.6 TUNEL Assay

As previously described (4), T47D cells were prepared 48 h after transfection using In Situ Death Detection Kit, TMR red (Roche, Mannheim, Germany). Cells were EGFP gated and analyzed using FACS Aria-II (BD-BioSciences, University of Utah Core Facility) and FACSDiva software. EGFP and TMR red were excited at 488 nm and 563

nm wavelengths and detected at 507 nm and 580 nm, respectively. The TUNEL assay was repeated three times (n=3) and analyzed using one-way ANOVA with Bonferroni's post hoc test.

3.3.7 Annexin-V Assay

The annexin-V assay was performed as before (4). Briefly, 48 h post transfection, T47D cells were suspended in 400 μ l annexin binding buffer (Invitrogen) and incubated with 5 μ l annexin-APC (annexin-V conjugated to allophycocyanin, Invitrogen) for 15 minutes. The incubated cells were EGFP gated and analyzed using FACSCanto-II. EGFP and APC were excited at 488 nm and 635 nm wavelengths and detected at 507 nm and 660 nm, respectively. Each construct was tested three times (n=3) and analyzed using one-way ANOVA with Bonferroni's post hoc test (4).

3.3.8 7-AAD Assay

As before (4), following manufacturer's instructions, T47D, MCF-7, H1373, and MDA-MB-468 cells were stained with 7-aminoactinomycin D (7-AAD, Invitrogen) 48 h after transfection. Since HeLa, MDA-MB-231, and 4T1 cells are highly proliferating cells, these cell lines were assayed 24 h post transfection. Cells were analyzed and gated for EGFP (with same fluorescence intensity to ensure equal expression of proteins) using the FACSCanto-II (BD-BioSciences, University of Utah Core Facility) and FACSDiva software. Excitation was set at 488 nm and detected at 507 nm and 660 nm for EGFP and 7-AAD, respectively. The means from three separate experiments (n=3) were analyzed using one-way ANOVA with Bonferroni's post hoc test.

3.3.9 Colony Forming Assay (CFA)

CFA was carried out using the Cytoselect[®] 96-well cell transformation assay (Cell Biolabs, San Diego, CA). A base agar layer was prepared per manufacturer's directions, and 50 μ L was transferred to each well of a clear-bottom 96-well plate. T47D cells were transfected as described above with wt-p53, p53-CC, or CC and harvested 24 h post transfection. The cells were resuspended in RPMI medium (Invitrogen) at a concentration of 3.0×10^5 cells/mL per the manufacturer's instructions. A cell agar layer was then prepared as recommended, and 75 μ L of the mixture was transferred to each well of the 96-well plate containing the base agar layer. To each well, 100 μ L of complete culture medium was added and plates were then incubated at 37°C and 5% CO₂ for 7 days. The culture medium was removed, solubilized, and lysed. Into a new black-bottom 96-well plate, 10 μ L of cell lysates were transferred. CyQuant GR dye working solution (1:400 in PBS) was added to each well (90 μ L) and incubated for 10 min at RT. A Spectra Max M2 plate reader (Molecular Devices, Sunnyvale, CA) was used to detect fluorescence using a 485/520 nm filter set. Independent transfections of each construct were tested three times (n=3) and analyzed using one-way ANOVA with Bonferroni's post hoc test.

3.3.10 Reporter Gene Assay

The following plasmids: wt-p53, p53-CC, CC, or EGFP (3.5 μ g of each construct) were co-transfected with 0.35 μ g of pRL-SV40 plasmid encoding for *Renilla* luciferase (Promega, Madison, WI) to normalize for transfection efficiency in T47D cells. In addition to *Renilla* luciferase, constructs were co-transfected with 3.5 μ g of p53-Luc Cis-Reporter (Agilent Technologies, Santa Clara, CA) (4), p21/WAF1 reporter (a generous

gift from Dr. Bert Vogelstein, Addgene plasmid 16451) (31), or PUMA reporter (from Dr. Vogelstein, Addgene plasmid 16591, Cambridge, MA) (32); all 3 reporters encode the firefly luciferase gene. The Dual-Glo Luciferase Assay System (Promega) was used to determine firefly luciferase activity and *Renilla* luciferase per manufacturer's instructions. Luminescence from active luciferase was then detected using PlateLumino (Strattec Biomedical Systems, Birkenfeld, Germany) as previously (4). *Renilla* luciferase activity was used to normalize the firefly luciferase values. The highest relative luminescence value was set at 100% and untreated cells were set at 0%. The means from triplicate samples were taken from 3 independent experiments and analyzed using one-way ANOVA with Bonferroni's post hoc test.

3.3.11 Co-Immunoprecipitation (co-IP)

The co-IP was performed using Dynabeads co-IP Kit (Invitrogen). T47D cells transfected with either EGFP-wt-p53 or EGFP-p53-CC were collected and weighed out (0.05 g) 20 h post transfection. Anti-GFP antibody (ab290, Abcam) was coupled to magnetic beads using Dynabeads Antibody Coupling Kit (Invitrogen). Approximately 0.2 g of cell pellet was lysed in 1.8 ml extraction buffer B (1x IP, 100 mM NaCl, 2 mM MgCl₂, 1 mM DTT, 1 % protease inhibitor). The lysate was incubated for 30 min at 4°C with 1.5 mg of the dynabeads coupled with anti-GFP antibody. The immune complexes were then collected by a magnet and washed three times with extraction buffer B and one time with last wash buffer (1x LWB, 0.02% Tween 20). Immune complexes were then eluted using 60 µl elution buffer. Finally, the eluted complexes were denatured and

blotted using anti-p53 antibody HRP-conjugated (sc-126 HRP, Santa Cruz Biotechnology, Santa Cruz, CA).

3.3.12 Overexpression of Mutant p53

H1373 cells were cotransfected with 1 pmol of the transdominant mutant pTagBFP-mut-p53 (R175H, R248W, and R273H) (27, 28) and 1 pmol of wt-p53, p53-CC, or CC fused to EGFP. Cells were stained as in the 7-AAD assay above 48 h post transfection and gated for EGFP and BFP using the FACSCanto-II (BD-BioSciences, University of Utah Core Facility) and FACSDiva software. Excitation for BFP was set at 405 nm and detected at 457 nm. The means from three separate experiments (n=3) were analyzed using one-way with Bonferroni's post hoc test and unpaired *t* test.

3.3.13 Recombinant Adenovirus Production

Replication-deficient recombinant adenovirus serotype 5 (Ad) constructs were generated using the Adeno-X[®] Adenoviral Expression System 3 (Clontech). Either wt-p53 or p53-CC was inserted into a cassette under the control of the CMV promoter. A separate CMV promoter controls the expression of ZsGreen1 for visualization. The empty virus (vector) was used as a negative control. Wt-p53 and p53-CC were PCR amplified with primers containing 15 base pair homology with a linearized pAdenoX vector (Clontech) based on an In-Fusion[®] HD Cloning Kit (Clontech). Stellar[®] competent cells (Clontech) were transformed with the adenoviral vector plasmids containing our constructs. Viral DNA was then purified, linearized and transfected into HEK293 cells for packaging and amplification. Viral particles were isolated from HEK293 cells by

freeze-thawing, purified using Adeno-X[®] Mega Purification Kit (Clontech), and dialyzed against storage and proper tonicity buffer (2.5% glycerol (w/v), 25 mM NaCl, and 20 mM Tris-HCl, pH 7.4). The viral titer was determined using flow cytometry per the manufacturer's recommendation.

3.4 Results

3.4.1 p53-CC Localizes to the Nucleus

Because the nuclear localization of p53 is important for anti-apoptotic function, we first chose to investigate if p53-CC also localized to the nucleus. Full length wt-p53 contains three NLSs encoded by amino acids 305-322, 370-376, and 380-386 (Figure 3.1A, top). Given that p53-CC (illustrated in Figure 3.1A) lacks most of the C-terminal domain (amino acids 323-393), which contains two NLSs, nuclear accumulation of p53-CC was verified using fluorescence microscopy (Figure 3.1B). Both wt-p53 and p53-CC were fused to EGFP to enable visualization of the subcellular localization of each protein. Figure 3.1B shows similar nuclear accumulation of p53-CC and wt-p53 in 1471.1 murine adenocarcinoma cells. CC alone fused to EGFP showed mostly cytoplasmic localization (data not shown). Similar results were obtained in T47D and MCF-7 breast cancer cells (data not shown).

3.4.2 Wt p53 and p53-CC Show Similar

Gene Expression Profiles

After verifying the nuclear localization of p53-CC via fluorescence microscopy, the activity of p53-CC was investigated next.

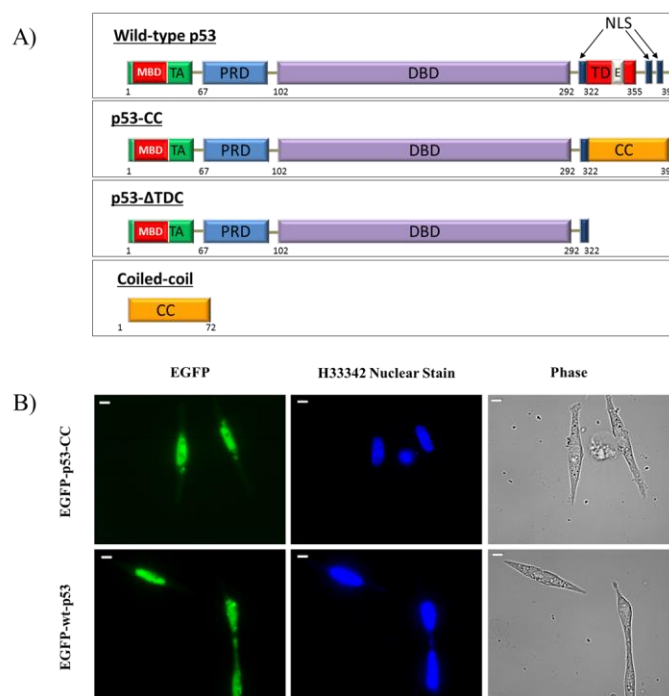


Figure 3.1 p53 domains and translocation to the nucleus. (A) Schematic representation of the experimental constructs and controls. Full length p53 (wt-p53) contains a MDM2 binding domain (MBD), a transactivation domain (TA) in the amino terminus, a proline-rich domain (PRD), a DNA binding domain (DBD), a strong nuclear localization signal (NLS), a tetramerization domain (TD) that also contains a nuclear export signal (E), and a carboxy terminus (C-terminus) that includes two weak NLSs. For p53-CC, the TD and C-terminus were replaced by the coiled-coil (CC) from Bcr. p53-ΔTDC lacks both the TD and the C-terminus. (B) Representative fluorescence microscopy images of 1471.1 cells confirm exclusive nuclear accumulation of EGFP-p53-CC similar to EGFP-wt-p53. EGFP Fluorescence, nuclear staining with H33342, and phase contrast images are shown, left to right. White scale bars on top left corners are 10 μ m.

The Human p53 Signaling Pathway RT² Profiler™ PCR Array (Qiagen, Valencia, CA) (33) was used to compare the transcription profiles between wt-p53 and p53-CC in T47D human breast cancer cells. T47D cells contain mutant p53 (a L194F mutation) that does not exhibit a strong transdominant effect (34). Exogenously added wt-p53 has been shown to be functional in this cell line (4, 30), and hence these cells can be used for comparing wt-p53 activity with p53-CC. The PCR array uses real-time PCR to measure the expression profiles of 84 genes directly related to p53-mediated signal transduction,

including genes involved in apoptosis, cell cycle, DNA repair, cell proliferation, and differentiation.

Analysis of the PCR array indicated that p53-CC showed a similar expression profile of 83 out of 84 genes compared to wt-p53 (Figure 3.2A), with the exception of the p53AIP1 gene (circled in black), whose protein product is one of many involved in the intrinsic apoptotic pathway. A tetramerization-deficient form of p53 (p53- Δ TDC) was included as a negative control in these assays to validate that the activity of p53-CC is due to proper tetramer formation, along with CC (also a negative control). As expected, both p53- Δ TDC and CC had significantly different expression profiles from wt-p53 (Supplementary Figures 3.1 and 3.2) in the p53 signaling pathway PCR array.

To verify the array results, the protein expression of two typical genes involved in two different pathways that are directly regulated by p53, Bax and p21/WAF1, were examined by western blotting. Bax is involved in the p53-dependent intrinsic apoptosis pathway (1), while p21/WAF1 is involved in cell cycle arrest (35). Figure 3.2B shows that T47D cells transfected with wt-p53 (first lane) or p53-CC (second lane) demonstrated overexpression of Bax and p21, while the monomeric form of p53 (p53- Δ TDC, third lane) and the CC (fourth lane) negative controls did not significantly induce expression of the Bax and p21/WAF1. Faint p21/WAF1 bands are observed with negative controls and represent background levels of this protein. Due to its inactivity, p53- Δ TDC was not included in the remaining apoptotic assays.

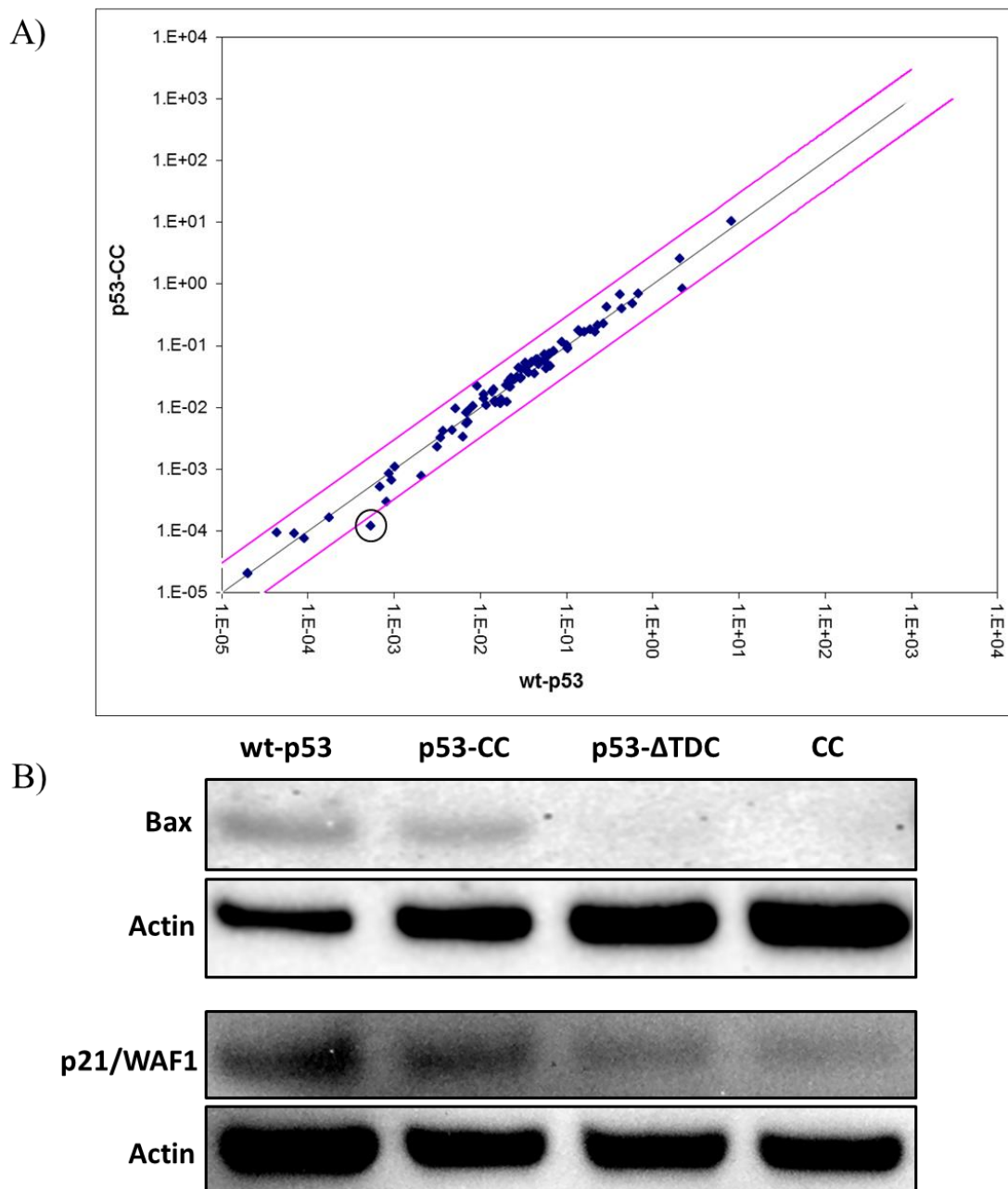


Figure 3.2 p53-CC is capable of transactivating several p53 target genes. (A) Scatter plot representation of mRNA levels of 84 p53 target genes in T47D cells transfected with wt-p53 or p53-CC. Each dot represents one of the 84 genes assayed in this PCR array. The two magenta lines represent a boundary of two fold upregulation or downregulation in mRNA levels. Cells treated with wt-p53 or p53-CC showed similar levels of mRNA for all 84 genes except for one, p53AIP1, which is circled on the scatter plot. (B) Representative cropped western blots of T47D cell lysates 24 h post transfection with wt-p53, p53-CC, p53-ΔTDC, or CC. Similar levels of Bax and p21/WAF1 protein expression were detected from cells treated with wt-p53 or p53-CC.

3.4.3 p53-CC Exhibits Tumor Suppressor Activity

To determine if the similar gene expression profiles between p53-CC and wt-p53 correlate with comparable tumor suppressor activity, the apoptotic potential (TUNEL, annexin V, 7-AAD) and transformative ability (colony formation) were tested in T47D cells. As mentioned before, T47D cells were chosen to compare the activity of p53-CC and wt-p53, since we have shown before that wt-p53 is active in these cells (4, 30).

The TUNEL (terminal deoxynucleotidyl transferase dUTP nick end labeling) assay, which measures DNA fragmentation into nucleosomal segments, is a hallmark of apoptosis (36). Figure 3.3A shows that p53-CC has a similar ability to induce DNA fragmentation as wt-p53 compared to CC control. Next, the apoptotic potential of p53-CC was also validated in the annexin-V assay, which evaluates the externalization of phosphatidylserine on the cell surface of apoptotic cells (37, 38). Similar levels of annexin-V positive staining were detected between cells transfected with p53-CC and wt-p53 (Figure 3.3B), and were significantly higher than positive staining in cells transfected with CC negative control.

The last apoptotic assay tested was the 7-AAD viability assay. In apoptotic or necrotic cells, the plasma membrane is disrupted allowing intercalation of the 7-AAD stain into DNA in the nucleus of these damaged cells (39, 40). In this assay, p53-CC maintains the same level of apoptotic activity as wt-p53, and is able to induce higher levels of cell death compared to the control (CC). Finally, the decrease in transformative ability (or oncogenic potential) of cells treated with p53-CC or wt-p53 were tested via a colony forming assay. In this assay, treatment with a tumor suppressor would be expected to reduce the number of cell colonies formed in an agar matrix.

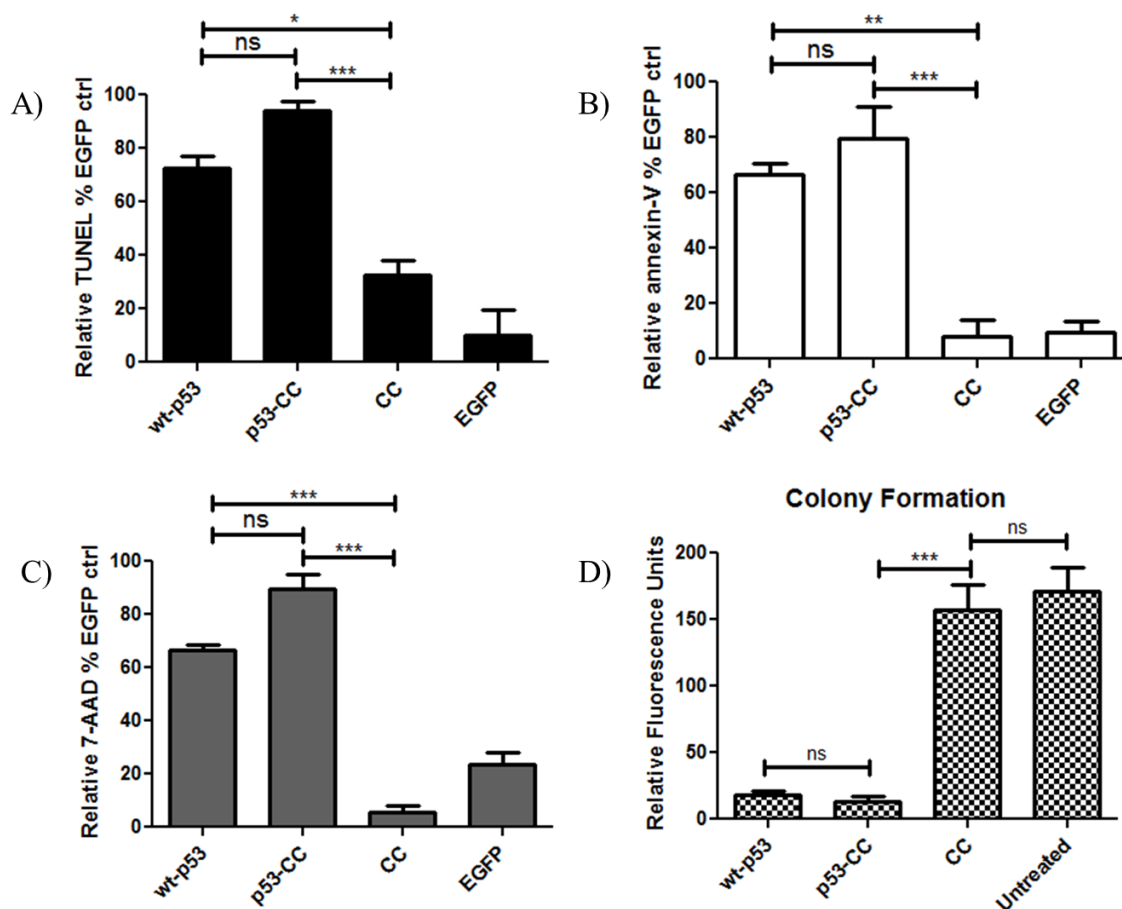


Figure 3.3 Apoptotic and cell proliferation assays were performed in T47D cells 48 h after transfection. (A) TUNEL assay shows similar apoptotic activity of p53-CC compared to wt-p53. Both p53-CC and wt-p53 demonstrate a significantly higher activity compared to CC negative control. Similar results were obtained from (B) annexin V staining and (C) 7-AAD staining. (D) The colony forming assay shows the transformative ability of T47D cells post treatment with wt-p53, p53-CC, and CC. Cells treated with wt-p53 and p53-CC show significant reduction in transformative ability (oncogenic potential) of T47D cells compared to untreated cells or cells treated with CC. Mean values were analyzed using one-way ANOVA with Bonferroni's post test; * $p < 0.05$, ** $p < 0.01$, and *** $p < 0.001$. Error bars represent standard deviations from at least three independent experiments ($n=3$).

Indeed, as shown in Figure 3.3D, both p53-CC (second bar) and wt-p53 (first bar) significantly reduced the number of colonies formed compared to the negative controls (CC and untreated cells, third and fourth bars, respectively). Overall, these results indicate that p53-CC shows similar ability to induce statistically significant levels of apoptosis and reduce oncogenic potential as wt-p53.

To ensure that the potential for p53-CC to induce apoptosis is neither dependent on endogenous p53 status nor cancer cell line specific, p53-CC was tested in several different cell lines. Human epithelial cervical adenocarcinoma cells (HeLa), which express endogenous wt-p53 (41), MDA-MB-231 metastatic triple-negative breast cancer cells harboring mutant p53 (42), MCF-7 breast cancer cells with wild type but mislocalized p53 (43), and H1373 nonsmall cell lung carcinoma cells that are p53 null (44) (Table 3.2), were tested in the 7-AAD assay. In all four cell lines, p53-CC and wt-p53 were able to induce similar levels of apoptosis, and were higher than the negative control (CC), as shown in Figures 3.4A-D.

Table 3.2 Comparison of the four different cell lines (HeLa, MDA-MB-231, MCF-7 and H1373) in terms of p53 status and cancer type.

Cell Line	p53 Status	Cancer Type	Ref
HeLa	Wild-type	Cervical adenocarcinoma	[40]
MDA-MB-231	Mutated (R280K)	Triple-negative breast cancer	[41]
MCF-7	Mislocalized to cytoplasm	Breast cancer	[42]
H1373	Null	Nonsmall cell lung carcinoma	[43]

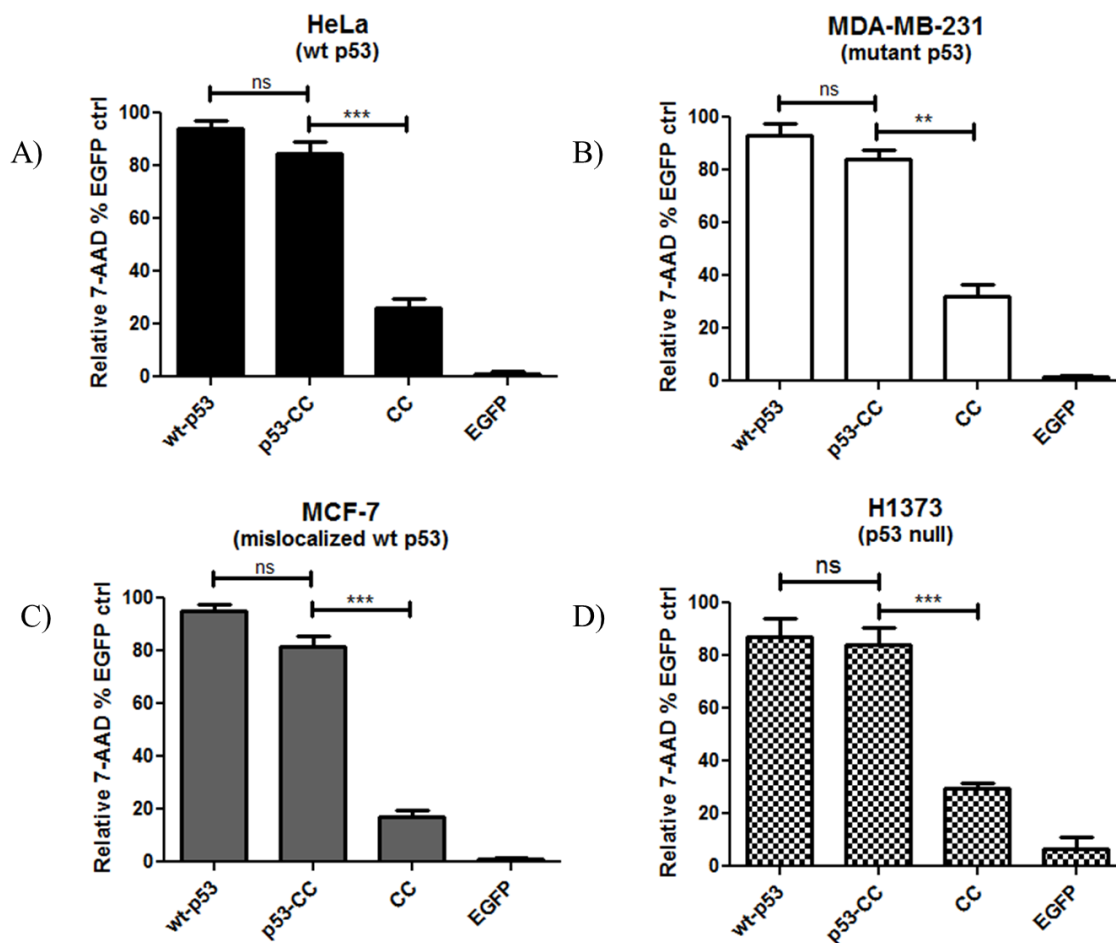


Figure 3.4 7-AAD assay was conducted in four different cell lines with varying p53 status (A) HeLa, (B) MDA-MB-231, (C) MCF-7, and (D) H1373. In all four cases, p53-CC is capable of inducing cell death in a similar fashion compared to wt-p53, regardless of the endogenous p53 status or the cancer cell line used. Statistical analysis was performed using one-way ANOVA with Bonferroni's post test; ** $p < 0.01$ and *** $p < 0.001$.

3.4.4 p53-CC Maintains Transcriptional

Activity of p53 Target Genes

While p53-CC exhibited similar apoptotic activity as wt-p53, we wanted to determine if p53-CC was capable of activating promoters of p53-dependent target genes. Tetramerization of p53 is a prerequisite to transcriptional activity, thus transcriptional activation will indicate tetramerization ability (of both wt-p53 and p53-CC) (45). The transcriptional activity of p53-CC was tested in T47D cells using three different reporter gene assays. The first was the p53 cis-reporter system, a common reporter for measuring p53 activity, which relies on a synthetic promoter consisting of repeats of the transcription recognition consensus for p53 (TGCCTGGACTTGCCTGG)₁₄ (46). The second and third reporter systems utilized the binding consensus sequences from p21/WAF1 and PUMA promoters, respectively. p21/WAF1 is a cyclin-dependent kinase inhibitor that mediates p53-dependent G1 cell cycle arrest (31, 35), while PUMA translocates to the mitochondria, deactivates antiapoptotic Bcl-2 and Bcl-XL proteins and induces p53-dependent apoptosis (47). In all three reporter gene assays, p53-CC showed higher transcriptional activity compared to wt-p53, and both were higher than the negative controls CC and EGFP (Figures 3.5A-C) in T47D cells.

3.4.5 p53-CC Avoids Interaction with Endogenous p53

We hypothesized that the higher level of transcriptional activity of p53-CC over wt-p53 was due to the possible hetero-oligomerization of wt-p53 with endogenous mutant p53 in this cell line. Therefore, a co-IP assay was performed to determine if exogenously added wt-p53 interacts with mutant p53 present in these cells.

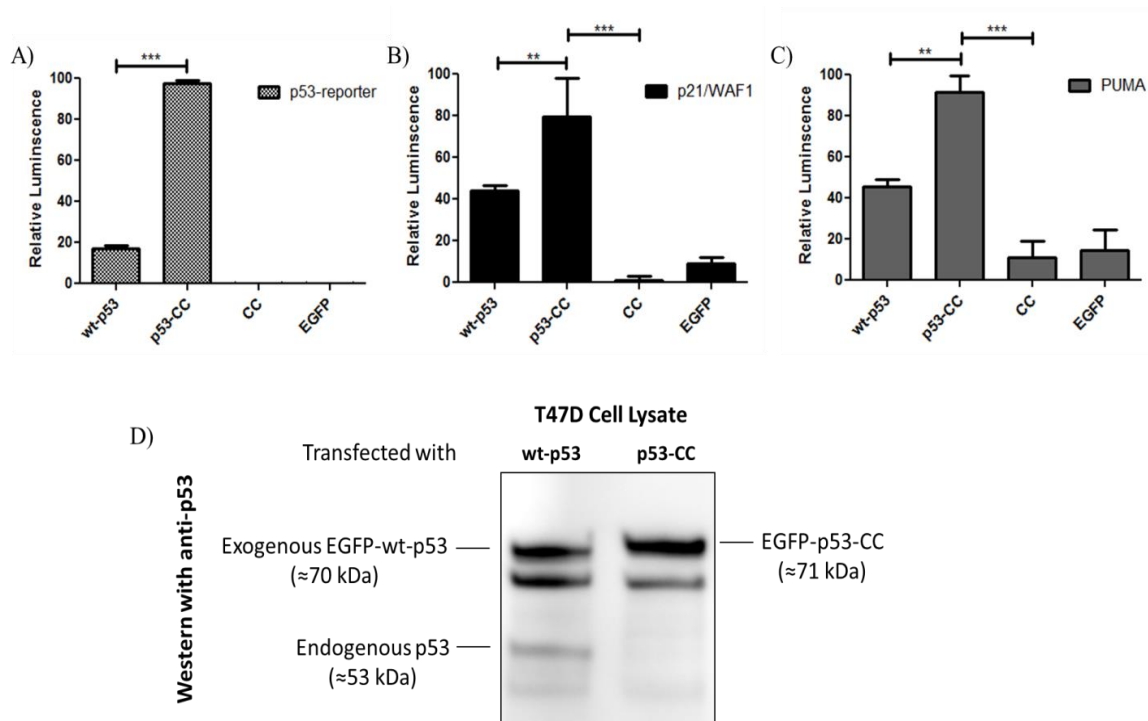


Figure 3.5 Relative luminescence represents the activation of (A) the p53-cis reporter, (B) the p21/WAF1 reporter, and (C) the PUMA reporter in T47D cells. The ability of p53-CC to transactivate these promoters is higher than wt-p53. In all three cases, 3.5 μ g of construct (wt-p53, p53-CC, CC, or EGFP) was co-transfected with 0.35 μ g of pRL-SV40 plasmid encoding for *Renilla* luciferase to normalize for transfection efficiency. In addition to *Renilla* luciferase, constructs were co-transfected with 3.5 μ g of p53-Luc Cis-Reporter, p21/WAF1 reporter, or PUMA reporter encoding for firefly luciferase. Mean values were analyzed using one-way ANOVA with Bonferroni's post test; ** $p < 0.01$, and *** $p < 0.001$. Error bars represent standard deviations from three independent experiments ($n=3$). (D) Interaction of endogenous p53 with exogenous wt-p53 or p53-CC was investigated in T47D via co-IP. A representative cropped western blot of protein complexes co-immunoprecipitated using anti-GFP antibody is shown. Left lane, endogenous p53 (53 kDa) co-immunoprecipitates with exogenous EGFP-wt-p53 (70 kDa). Right lane, endogenous p53 fails to co-immunoprecipitate with exogenous EGFP-p53-CC (71 kDa).

To this end, mutant p53 in T47D cells would not be expected to co-immunoprecipitate with p53-CC. Cell lysates transfected with either EGFP-wt-p53 or EGFP-p53-CC were incubated with anti-GFP antibody to selectively immunoprecipitate our fusion EGFP proteins (Figure 3.5D). Endogenous p53 that could potentially co-immunoprecipitate with either exogenous EGFP-wt-p53 or EGFP-p53-CC was probed using anti-p53 antibody. Figure 3.5D shows that endogenous p53 (53 kDa) co-immunoprecipitates with exogenous wt-p53 (left lane, 70 kDa) but fails to immunoprecipitate with p53-CC (right lane, 71 kDa). These findings indicate that endogenous p53 interacts directly with exogenous wt-p53, which is presumably due to hetero-oligomerization via their TDs. As expected, p53-CC, which lacks the native TD, evaded binding to endogenous p53. It should be noted that a prominent secondary band is normally detected by this anti-p53 antibody at about 69 kDa (per Santa Cruz Biotechnology).

3.4.6 Bypassing the Dominant Negative Effect

Since p53-CC did not interact with endogenous wt-p53 in the co-IP assay, the ability of p53-CC to bypass the dominant negative effect was tested, first using overexpression of a dominant negative mutant p53 in H1373 cells (p53 null), and second, in MDA-MB-468 cells that harbor a strong dominant negative p53 mutant (48). The ability of p53-CC to “rescue” the loss of apoptotic activity induced by an inactive mutant p53 in H1373 (p53 null) cells was tested; Figure 3.6A shows that in the absence of the inactive mutant p53 (first 3 sets of bars), both p53-CC and wt-p53 can similarly induce apoptosis (measured by 7-AAD) compared to the negative CC control.

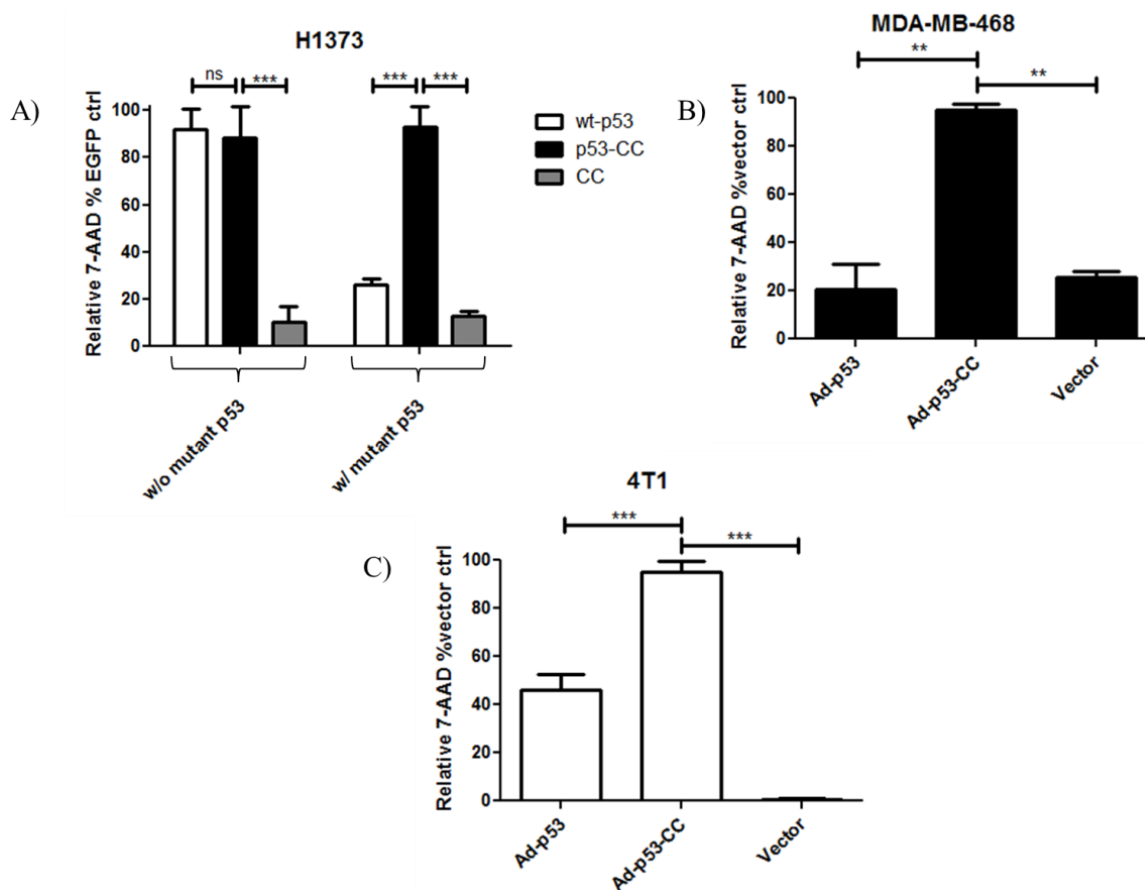


Figure 3.6 p53-CC circumvents transdominant inhibition by mutant p53. (A) Overexpression of mutant p53 reduces the activity of exogenous wt-p53 but has no influence on exogenous p53-CC activity. H1373 cells were chosen for this experiment since they are p53 null and hence there will be no additional p53 activity from the cells due to lack of endogenous p53. (B) 7-AAD assay was conducted 48 h post transducing MDA-MB-468 cells, which harbor a potent transdominant mutant p53 (R273H), with adenoviral vectors expressing either wt-p53 or p53-CC with a multiplicity of infection (MOI) of 200. As expected, exogenous wt-p53 (Ad-p53) activity is limited in this cell line due to the presence of endogenous transdominant tumor derived p53. (C) 7-AAD assay was also performed 48 h post transducing 4T1 cells (MOI 250). Interestingly, p53-CC is more active than wt-p53 in this particular cell line. The adenoviral vector alone was used as a negative control. Mean values were analyzed using one-way ANOVA with Bonferroni's post test; ** <math>p < 0.01</math>, and *** <math>p < 0.001</math>. Error bars represent standard deviations from three independent experiments (n=3).

However, when a transdominant mutant p53 is added (bars 4-6), only p53-CC is able to rescue apoptotic activity, while wt-p53 cannot. We engineered this transdominant mutant p53 by combining three hotspot mutations (R175H, R248W, and R273H) that are known to exhibit a dominant negative effect (27, 28). This supports the notion that p53-CC can bypass the dominant negative effect of a transdominant mutant p53.

To further investigate this, the ability of p53-CC to induce apoptosis was tested in a cell line known to contain an endogenous strong transdominant mutant form of p53, MDA-MB-468 (49). The endogenous p53 in MDA-MB-468 contains the R273H point mutation that is known to exhibit transdominant inhibition of wt-p53, so exogenous wt-p53 in this case would be expected to have limited activity. MDA-MB-468 cells are resistant to transient transfection with lipofectamine (used in the majority of these studies), so instead, they were transduced with adenovirus (Ad) constructs carrying the wt-p53 or p53-CC as genetic cargo. Figure 3.6B shows that indeed, only Ad-p53-CC (second bar) is able to significantly induce apoptotic activity measured by 7-AAD compared to wt-p53 and empty Ad vector (bars 1 and 3). This suggests that the transdominant effect of endogenous mutant p53 found in MDA-MB-468 cells can be circumvented by using an oligomerization variant of p53, namely p53-CC.

Finally, we also tested adenovirally delivered p53-CC in a p53 null cell line (Figure 3.6C), where both wt-p53 and p53-CC should be active. Indeed, as shown in Figure 3.6C, both constructs are active in this cell line. Interestingly, p53-CC is more active than wt-p53 in this particular cell line.

3.5 Discussion

To summarize, our data show that a version of p53 with an alternative tetramerization domain localizes to the correct subcellular compartment (the nucleus, Figure 3.1B), and shows a similar gene expression profile as wt-p53 (Figure 3.2A). Two genes regulated by p53, Bax and p21/WAF1, also showed similar protein expression levels when induced by p53-CC or wt-p53, as demonstrated by western blotting (Figure 3.2B). Tumor suppressor activity, measuring apoptotic activity (by TUNEL, annexin V, and 7-AAD) and reduced oncogenic potential (reduced number of colonies), Figure 3.3 A-D, was similar between p53-CC and wt-p53. Importantly, p53-CC was found to induce statistically significant levels of apoptosis in 4 different cell lines (Figure 3.4A-D), regardless of p53 status, indicating that p53-CC activity is not dependent on p53 status, nor is it cell-line specific (see Table 3.2). The transcriptional activity of p53-CC was tested using 3 reporter gene assays in Figures 3.5A-C (a standard p53 reporter gene, a p21/WAF1 reporter involved in cell cycle arrest, and a PUMA reporter involved in apoptosis), and in all 3 cases, was higher than wt-p53. In T47D cells, the transcriptional activity of p53-CC was higher than wt-p53 in these reporter gene assays (Figures 3.5A-C), while the apoptotic activity of p53-CC was similar to wt-p53 (Figures 3.3A-C). This is not unexpected, since transcriptional activity does not necessarily linearly correlate with apoptotic activity. Transcriptional activity of target genes is a prerequisite step prior to the apoptotic cascade; if a threshold of transcriptional activity is met, the downstream measure of apoptosis may not change significantly. Interestingly, the negative controls (p53 Δ TDC and CC) did not have activity in binding, nor were they able to express apoptotic or cell cycle arrest genes.

A co-IP was performed and showed that p53-CC did not interact with endogenous p53 (Figure 3.5D). Since there was no interaction between p53-CC and endogenous p53, the ability of p53-CC to bypass the dominant negative effect was tested, first with transdominant mutant p53 overexpression (Figure 3.6A), and second, in MDA-MB-468 cells that harbor a tumor-derived endogenous transdominant negative p53 mutant (Figure 3.6B). In both cases, p53-CC appears to not be effected by this endogenous transdominant inhibition. Finally, adenovirally delivered p53-CC was also tested in a p53 null cell line, and was active, as expected (Figure 3.6C).

Mutant p53 retains its tetramerization capability since its TD remains intact, and can form inactive p53 tetramers upon the introduction of exogenous wt-p53 in cancer cells (Figure 3.7, left side). These hetero-tetramers have a significantly reduced transcriptional activity compared to homo-tetramers of p53-CC. Such a phenomenon gives rise to a great barrier that limits the utility of p53 for cancer therapy (11).

As an approach to prevent hetero-oligomerization, we investigated swapping the TD with an alternative oligomerization domain (Table 3.1). The CC from Bcr tetramerizes in a similar fashion as the TD; both form dimers of two antiparallel-oriented monomers (50). To our knowledge, only one attempt at substituting the TD of p53 to eliminate the dominant negative effect of mutant p53 in hetero-tetramers has been made, with marginal success (21). This previous work utilized an oligomerization domain that leads to *parallel* tetramer formation, whereas the native TD of p53 drives the formation of *antiparallel* tetramers (21-23). This might offer an explanation to the significant reduction in p53 function observed in their published activity assays (21) compared to wt-p53.

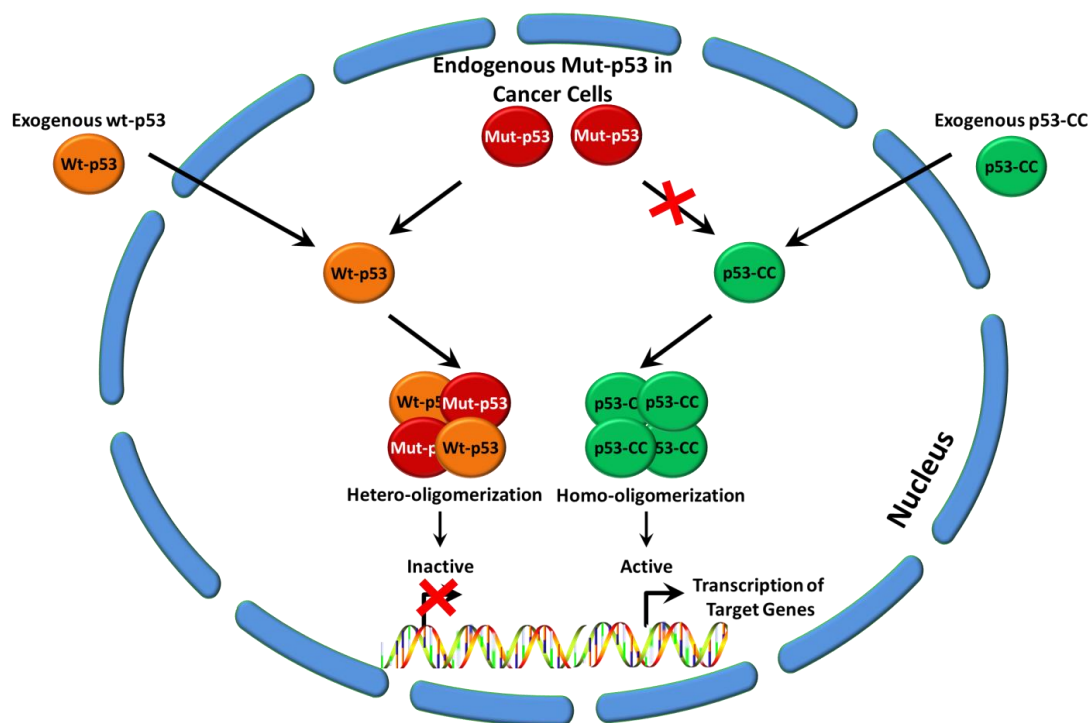


Figure 3.7 Proposed mechanism of p53-CC activity. Left side of figure: exogenously added wt-p53 can still form hetero-tetramers with mutant p53 due to the presence of the TD, and becomes inactivated. Right side of figure: p53-CC can bypass transdominant inhibition by mutant p53 in cancer cells, and still exhibit tumor suppressor activity.

On the other hand, our results show that p53-CC evades hetero-oligomerization with mutant p53, allowing it to retain the full tumor suppressor function of wt-p53. Figure 3.7 illustrates our hypothesis of bypassing the dominant negative effect with p53-CC (right side), which maintains functional tumor suppressor activity.

Bcr, from which the CC was obtained, is a ubiquitous eukaryotic phosphotransferase protein that may have a role in general cell metabolism. Theoretically, p53-CC could interact with Bcr via its CC domain. While this is a possibility, this may be unlikely due to the compartmentation of Bcr (found in the cytoplasm) (51) vs. p53-CC (found in the nucleus, shown in Figure 3.1B). Bcr-knockout

mice still survive; the major defect in these mice was reduced intimal proliferation in low-flow carotid arteries compared to wt mice (52).

Bcr has mostly been studied in the context of chronic myeloid leukemia (CML) where a reciprocal chromosomal translocation with Abl results in the fusion protein Bcr-Abl, the causative agent of CML (53). The activity of Bcr-Abl is largely due to the constitutive activation of the Abl portion of the molecule (54). Generally, Bcr may be involved in inflammatory pathways and cell proliferation (52). We have previously reported that the isolated Bcr coiled-coil does not in itself induce apoptosis (26). Nevertheless, potential inadvertent interaction with the CC oligomerization domain of Bcr via any introduced p53-CC is currently being addressed in our lab by introducing mutations in the CC domain of p53-CC that will disfavor interactions with Bcr-CC.

Besides not interacting with endogenous p53, the elevation in p53-CC transcriptional activity could also be due to a higher stability of the p53-CC tetramer compared to wt-p53 tetramer. We have reported that melting temperature (T_m) for CC is about 83°C (26), which is slightly higher than the T_m for TD around 75°C at physiological pH (55). In fact, our lab has shown previously that CC forms homo-dimers in thermal denaturation studies (26). However, further experiments would be needed to definitively prove the biochemical tetramerization of p53-CC.

Our results corroborate our hypothesis that unlike wt-p53, p53-CC can circumvent transdominant inhibition of mutant p53, illustrating the potential of using p53-CC as an alternative to wt-p53 for cancer gene therapy. Since the dominant negative effect of mutant p53 in cancer cells is currently one of the barriers limiting the use of p53 in cancer gene therapy (11), our approach offers an alternative to overcome this barrier

by swapping the TD of p53 with an alternative oligomerization domain while maintaining the tumor suppressor activity. Our designed p53-CC is expected to cause apoptosis in many types of cancers, especially in tumors with transdominant mutant p53, where wt-p53 has proven to be ineffective. Ultimately, we plan on utilizing the p53-CC construct as a gene therapeutic delivered using an adenoviral vector that could replace the current limited utility of wild-type p53 as a cancer therapeutic.

3.6 References

1. S. Haupt, M. Berger, Z. Goldberg, and Y. Haupt. Apoptosis - the p53 network. *J Cell Sci.* 116:4077-4085 (2003).
2. N.D. Marchenko, A. Zaika, and U.M. Moll. Death signal-induced localization of p53 protein to mitochondria. A potential role in apoptotic signaling. *J Biol Chem.* 275:16202-16212 (2000).
3. M. Mihara, S. Erster, A. Zaika, O. Petrenko, T. Chittenden, P. Pancoska, and U.M. Moll. p53 has a direct apoptogenic role at the mitochondria. *Mol Cell.* 11:577-590 (2003).
4. M. Mossalam, K.J. Matissek, A. Okal, J.E. Constance, and C.S. Lim. Direct induction of apoptosis using an optimal mitochondrially targeted p53. *Mol Pharm.* 9:1449-1458 (2012).
5. K.G. McLure and P.W. Lee. How p53 binds DNA as a tetramer. *EMBO J.* 17:3342-3350 (1998).
6. M. Lacroix, R.A. Toillon, and G. Leclercq. p53 and breast cancer, an update. *Endocr Relat Cancer.* 13:293-325 (2006).
7. A. Willis, E.J. Jung, T. Wakefield, and X. Chen. Mutant p53 exerts a dominant negative effect by preventing wild-type p53 from binding to the promoter of its target genes. *Oncogene.* 23:2330-2338 (2004).
8. G. Shaulsky, N. Goldfinger, M.S. Tosky, A.J. Levine, and V. Rotter. Nuclear localization is essential for the activity of p53 protein. *Oncogene.* 6:2055-2065 (1991).
9. N. Baptiste and C. Prives. p53 in the cytoplasm: a question of overkill? *Cell.* 116:487-489 (2004).
10. Z. Peng. Current status of gendicine in China: recombinant human Ad-p53 agent for treatment of cancers. *Human Gene Therapy.* 16:1016-1027 (2005).

11. A. de Vries, E.R. Flores, B. Miranda, H.M. Hsieh, C.T. van Oostrom, J. Sage, and T. Jacks. Targeted point mutations of p53 lead to dominant-negative inhibition of wild-type p53 function. *Proc Natl Acad Sci U S A.* 99:2948-2953 (2002).
12. T. Soussi. p53 alterations in human cancer: more questions than answers. *Oncogene.* 26:2145-2156 (2007).
13. T. Soussi, C. Ishioka, M. Claustres, and C. Beroud. Locus-specific mutation databases: pitfalls and good practice based on the p53 experience. *Nat Rev Cancer.* 6:83-90 (2006).
14. T. Soussi and K.G. Wiman. Shaping genetic alterations in human cancer: the p53 mutation paradigm. *Cancer Cell.* 12:303-312 (2007).
15. A.M. Goh, C.R. Coffill, and D.P. Lane. The role of mutant p53 in human cancer. *J Path.* 223:116-126 (2011).
16. R.L. Weinberg, S.M. Freund, D.B. Veprintsev, M. Bycroft, and A.R. Fersht. Regulation of DNA binding of p53 by its C-terminal domain. *J Mol Biol.* 342:801-811 (2004).
17. J. Milner and E.A. Medcalf. Cotranslation of activated mutant p53 with wild type drives the wild-type p53 protein into the mutant conformation. *Cell.* 65:765-774 (1991).
18. S. Srivastava, S. Wang, Y.A. Tong, Z.M. Hao, and E.H. Chang. Dominant negative effect of a germ-line mutant p53: a step fostering tumorigenesis. *Canc Res.* 53:4452-4455 (1993).
19. S.E. Kern, J.A. Pietenpol, S. Thiagalingam, A. Seymour, K.W. Kinzler, and B. Vogelstein. Oncogenic forms of p53 inhibit p53-regulated gene expression. *Science.* 256:827-830 (1992).
20. Ming K. Lee, Wei W. Teoh, Beng H. Phang, Wei M. Tong, Zhao Q. Wang, and K. Sabapathy. Cell-type, dose, and mutation-type specificity dictate mutant p53 functions in vivo. *Cancer Cell.* 22:751-764 (2012).
21. M.J. Waterman, J.L. Waterman, and T.D. Halazonetis. An engineered four-stranded coiled coil substitutes for the tetramerization domain of wild-type p53 and alleviates transdominant inhibition by tumor-derived p53 mutants. *Cancer Res.* 56:158-163 (1996).
22. P.D. Jeffrey, S. Gorina, and N.P. Pavletich. Crystal structure of the tetramerization domain of the p53 tumor suppressor at 1.7 angstroms. *Science.* 267:1498-1502 (1995).
23. W. Lee, T.S. Harvey, Y. Yin, P. Yau, D. Litchfield, and C.H. Arrowsmith. Solution structure of the tetrameric minimum transforming domain of p53. *Nat Struct Biol.* 1:877-890 (1994).
24. C. Wichmann, Y. Becker, L. Chen-Wichmann, V. Vogel, A. Vojtkova, J. Herglotz, S. Moore, J. Koch, J. Lausen, W. Mantele, H. Gohlke, and M. Grez. Dimer-tetramer transition controls RUNX1/ETO leukemogenic activity. *Blood.* 116:603-613 (2010).

25. X. Zhao, S. Ghaffari, H. Lodish, V.N. Malashkevich, and P.S. Kim. Structure of the Bcr-Abl oncoprotein oligomerization domain. *Nat Struct Biol.* 9:117-120 (2002).
26. A.S. Dixon, S.S. Pendley, B.J. Bruno, D.W. Woessner, A.A. Shimpi, T.E. Cheatham, 3rd, and C.S. Lim. Disruption of Bcr-Abl coiled coil oligomerization by design. *J Biol Chem.* 286:27751-27760 (2011).
27. C.J. Di Como, C. Gaiddon, and C. Prives. p73 function is inhibited by tumor-derived p53 mutants in mammalian cells. *Molecular and Cellular Biology.* 19:1438-1449 (1999).
28. P. Dong, M. Tada, J. Hamada, A. Nakamura, T. Moriuchi, and N. Sakuragi. p53 dominant-negative mutant R273H promotes invasion and migration of human endometrial cancer HHUA cells. *Clin Exp Metastasis.* 24:471-483 (2007).
29. A.S. Dixon, M. Kakar, K.M. Schneider, J.E. Constance, B.C. Paullin, and C.S. Lim. Controlling subcellular localization to alter function: sending oncogenic Bcr-Abl to the nucleus causes apoptosis. *J Control Release.* 140:245-249 (2009).
30. S. Reaz, M. Mossalam, A. Okal, and C.S. Lim. A single mutant, A276S of p53, turns the switch to apoptosis. *Mol Pharm* (2013).
31. W.S. el-Deiry, T. Tokino, V.E. Velculescu, D.B. Levy, R. Parsons, J.M. Trent, D. Lin, W.E. Mercer, K.W. Kinzler, and B. Vogelstein. WAF1, a potential mediator of p53 tumor suppression. *Cell.* 75:817-825 (1993).
32. J. Yu, L. Zhang, P.M. Hwang, K.W. Kinzler, and B. Vogelstein. PUMA induces the rapid apoptosis of colorectal cancer cells. *Mol Cell.* 7:673-682 (2001).
33. C. Brockschmidt, H. Hirner, N. Huber, T. Eismann, A. Hillenbrand, G. Giamas, B. Radunsky, O. Ammerpohl, B. Bohm, D. Henne-Bruns, H. Kalthoff, F. Leithauser, A. Trauzold, and U. Knippschild. Anti-apoptotic and growth-stimulatory functions of CK1 delta and epsilon in ductal adenocarcinoma of the pancreas are inhibited by IC261 in vitro and in vivo. *Gut.* 57:799-806 (2008).
34. Y. Tomita, N. Marchenko, S. Erster, A. Nemajerova, A. Dehner, C. Klein, H. Pan, H. Kessler, P. Pancoska, and U.M. Moll. WT p53, but not tumor-derived mutants, bind to Bcl2 via the DNA binding domain and induce mitochondrial permeabilization. *The Journal of Biological Chemistry.* 281:8600-8606 (2006).
35. T. Waldman, K.W. Kinzler, and B. Vogelstein. p21 is necessary for the p53-mediated G1 arrest in human cancer cells. *Cancer Res.* 55:5187-5190 (1995).
36. D.T. Loo and J.R. Rillema. Measurement of cell death. *Methods Cell Biol.* 57:251-264 (1998).
37. G. Koopman, C.P. Reutelingsperger, G.A. Kuijten, R.M. Keehnen, S.T. Pals, and M.H. van Oers. Annexin V for flow cytometric detection of phosphatidylserine expression on B cells undergoing apoptosis. *Blood.* 84:1415-1420 (1994).
38. I. Vermes, C. Haanen, H. Steffens-Nakken, and C. Reutelingsperger. A novel assay for apoptosis. Flow cytometric detection of phosphatidylserine expression

- on early apoptotic cells using fluorescein labelled Annexin V. *J Immun Meth.* 184:39-51 (1995).
39. I. Schmid, W.J. Krall, C.H. Uittenbogaart, J. Braun, and J.V. Giorgi. Dead cell discrimination with 7-amino-actinomycin D in combination with dual color immunofluorescence in single laser flow cytometry. *Cytometry.* 13:204-208 (1992).
 40. M.J. Serrano, P. Sanchez-Rovira, I. Algarra, A. Jaen, A. Lozano, and J.J. Gaforio. Evaluation of a gemcitabine-doxorubicin-paclitaxel combination schedule through flow cytometry assessment of apoptosis extent induced in human breast cancer cell lines. *Jap J Cancer Res.* 93:559-566 (2002).
 41. F.D. Goodrum and D.A. Ornelles. p53 status does not determine outcome of E1B 55-kilodalton mutant adenovirus lytic infection. *J Virol.* 72:9479-9490 (1998).
 42. J. Bartek, R. Iggo, J. Gannon, and D.P. Lane. Genetic and immunochemical analysis of mutant p53 in human breast cancer cell lines. *Oncogene.* 5:893-899 (1990).
 43. L.M. Mooney, K.A. Al-Sakkaf, B.L. Brown, and P.R. Dobson. Apoptotic mechanisms in T47D and MCF-7 human breast cancer cells. *Br J Cancer.* 87:909-917 (2002).
 44. S.M. Bodner, J.D. Minna, S.M. Jensen, D. D'Amico, D. Carbone, T. Mitsudomi, J. Fedorko, D.L. Buchhagen, M.M. Nau, A.F. Gazdar, and et al. Expression of mutant p53 proteins in lung cancer correlates with the class of p53 gene mutation. *Oncogene.* 7:743-749 (1992).
 45. T. Kawaguchi, S. Kato, K. Otsuka, G. Watanabe, T. Kumabe, T. Tominaga, T. Yoshimoto, and C. Ishioka. The relationship among p53 oligomer formation, structure and transcriptional activity using a comprehensive missense mutation library. *Oncogene.* 24:6976-6981 (2005).
 46. N. Yahagi, H. Shimano, T. Matsuzaka, Y. Najima, M. Sekiya, Y. Nakagawa, T. Ide, S. Tomita, H. Okazaki, Y. Tamura, Y. Iizuka, K. Ohashi, T. Gotoda, R. Nagai, S. Kimura, S. Ishibashi, J. Osuga, and N. Yamada. p53 Activation in adipocytes of obese mice. *J Biol Chem.* 278:25395-25400 (2003).
 47. J.K. Brunelle and A. Letai. Control of mitochondrial apoptosis by the Bcl-2 family. *J Cell Sci.* 122:437-441 (2009).
 48. W. Wang, B. Cheng, L. Miao, Y. Mei, and M. Wu. Mutant p53-R273H gains new function in sustained activation of EGFR signaling via suppressing miR-27a expression. *Cell Death & Disease.* 4:e574 (2013).
 49. L.Y. Lim, N. Vidnovic, L.W. Ellisen, and C.O. Leong. Mutant p53 mediates survival of breast cancer cells. *British Journal of Cancer.* 101:1606-1612 (2009).
 50. C.M. Taylor and A.E. Keating. Orientation and oligomerization specificity of the Bcr coiled-coil oligomerization domain. *Biochem.* 44:16246-16256 (2005).
 51. Y. Maru and O.N. Witte. The BCR gene encodes a novel serine/threonine kinase activity within a single exon. *Cell.* 67:459-468 (1991).

52. J.D. Alexis, N. Wang, W. Che, N. Lerner-Marmarosh, A. Sahni, V.A. Korshunov, Y. Zou, B. Ding, C. Yan, B.C. Berk, and J. Abe. Bcr kinase activation by angiotensin II inhibits peroxisome-proliferator-activated receptor gamma transcriptional activity in vascular smooth muscle cells. *Circ Res.* 104:69-78 (2009).
53. D.W. Woessner, C.S. Lim, and M.W. Deininger. Development of an effective therapy for chronic myelogenous leukemia. *Cancer J.* 17:477-486 (2011).
54. J.V. Melo and D.J. Barnes. Chronic myeloid leukaemia as a model of disease evolution in human cancer. *Nat Rev Cancer.* 7:441-453 (2007).
55. C. Galea, P. Bowman, and R.W. Kriwacki. Disruption of an intermonomer salt bridge in the p53 tetramerization domain results in an increased propensity to form amyloid fibrils. *Protein Sci.* 14:2993-3003 (2005).

CHAPTER 4

RE-ENGINEERED p53 ACTIVATES APOPTOSIS IN VIVO AND CAUSES PRIMARY TUMOR REGRESSION IN A DOMINANT NEGATIVE BREAST CANCER XENOGRAFT MODEL

4.1 Abstract

Inactivation of p53 pathway is reported in more than half of all human tumors and can be correlated to malignant development. Missense mutation in the DNA binding region (DBD) of p53 is the most common mechanism of p53 inactivation in cancer cells. The resulting tumor-derived p53 variants, similar to wild-type (wt) p53, retain their ability to oligomerize via the tetramerization domain (TD). Upon hetero-oligomerization, mutant p53 enforces a dominant negative effect over active wt-p53 in cancer cells. To overcome this barrier, we have previously designed a chimeric superactive p53 (p53-CC) with an alternative oligomerization domain capable of escaping transdominant inhibition by mutant p53 *in vitro*. In this report, we demonstrate the superior tumor suppressor activity of p53-CC and its ability to cause tumor regression of the MDA-MB-468 aggressive p53-dominant negative breast cancer tumor model *in vivo*. In addition, we illustrate the profound effects of the dominant negative effect of endogenous mutant p53 over wt-p53 in cancer cells. Finally, we investigate the underlying differential

mechanisms of activity for p53-CC and wt-p53 delivered using viral-mediated gene therapy approach in the MDA-MB-468 tumor model.

4.2 Introduction

The ability of p53 to achieve tumor suppressor function depends on formation of p53 tetramers to act as a transcription factor of several target genes (1, 2). Once activated, p53 stimulates a wide network of signals including DNA repair, cell cycle arrest, and apoptosis (3). The significance of p53 function is highlighted by the correlation of its inactivity and malignant development. Inactivation of p53 pathway is reported in more than half of all human tumors and can be achieved via several mechanisms including nuclear exclusion and hyperactivation of MDM2, the main regulator of p53 function (4-6). However, acquisition of missense mutations in one or both alleles of the *TP53* gene remains the most common mechanism of p53 inactivation (7). The majority of these mutations take place in the DNA binding domain (DBD) which is responsible for p53 interaction with DNA. Although mutant p53 in cancer cells may have impaired tumor suppressor function and transcriptional activity, it retains its ability to oligomerize with other mutant or wild-type (wt) p53 via the tetramerization domain (TD) (8, 9). When mutant p53 oligomerizes with wt-p53 through hetero-oligomerization, the resulting tetramer has impaired function in most cases due to *transdominant inhibition* by mutant p53 (Figure 4.1). The outcome of this transdominant inhibition varies significantly based on the type of mutant p53 present in cells (10). This phenomenon is known as the dominant negative effect of mutant p53 and gives rise to a critical barrier to utilizing wt-p53 for cancer gene therapy (11).

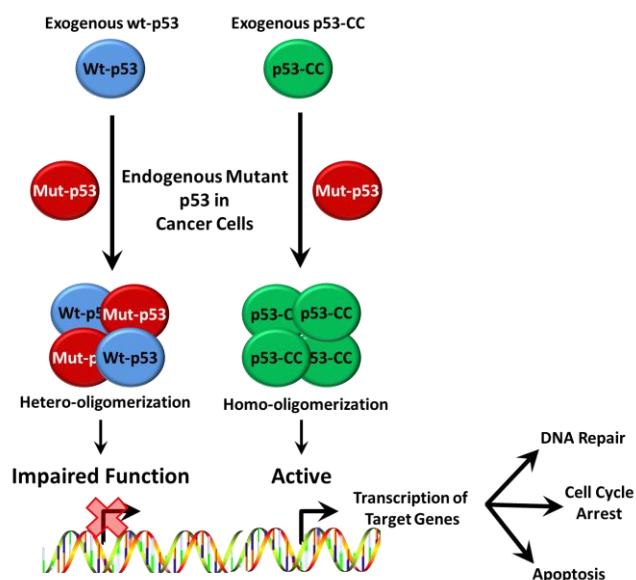


Figure 4.1 Schematic representation of the fates of wt-p53 (left) and p53-CC (right) in the presence of endogenous mutant p53 in cancer cells. Wt-p53 (left) is sequestered into hetero-oligomers that have an impaired transcription function, while p53-CC (right) can exclusively form homo-oligomers that retain full tumor suppressor activity.

Our goal was to design a new, chimeric superactive p53 with the following activity: wt-p53 like functional transcriptional activity; promotion of improved, highly potent p53-dependent apoptosis; and circumvention of the dominant negative inactivating effect of endogenous mutant p53 in cancer cells. To this end, we engineered a chimeric p53 (p53-CC) that has an alternative tetramerization domain and showed its ability to escape transdominant inhibition by mutant p53 *in vitro* (12). The Bcr coiled-coil (CC) alternative oligomerization domain of p53-CC evades hetero-oligomerization with endogenous mutant p53, and hence, bypasses the dominant negative effect reported in cancer cells. The CC domain itself was tested as a control previously, and was found to be nontoxic (12). p53-CC activity was found to retain similar tumor suppressor activity compared to exogenous wt-p53 in several cancer cell lines harboring different p53

statuses (null, wt, wt mislocalized, and mutant nondominant). Finally, we investigated potential transdominant inhibition of p53-CC and wt-p53 via co-expression of a potent dominant negative mutant p53. As hypothesized, p53-CC retained the same levels of activity regardless of the presence of transdominant mutant p53, while wt-p53 showed loss of activity (12).

In this report, we demonstrate the superior tumor suppressor activity of p53-CC *in vitro* and *in vivo* in MDA-MB-468, an aggressive p53-dominant negative breast cancer cell line. Furthermore, we investigate the underlying differential mechanisms of activity for p53-CC and wt-p53 in the MDA-MB-468 tumor model. Our viral-mediated gene therapy approach succeeds in demonstrating the effects of the transdominant effect of endogenous mutant p53 over p53-CC and wt-p53.

4.3 Materials and Methods

4.3.1 Recombinant Adenovirus Production

Replication-deficient recombinant adenovirus serotype 5 (Ad) constructs were generated using the Adeno-X[®] Adenoviral Expression System 3 (Clontech, Mountain View, CA) As we have done before .(12) Either wt-p53 or p53-CC was inserted into a cassette under the control of the CMV promoter. A separate CMV promoter controls the expression of ZsGreen1 fluorescent protein for visualization. The empty virus (vector) was used as a negative control. Wt-p53 and p53-CC were PCR amplified with primers containing 15 base pair homology with a linearized pAdenoX vector (Clontech) based on an In-Fusion[®] HD Cloning Kit (Clontech). Stellar[®] competent cells (Clontech) were transformed with the adenoviral vector plasmids containing our constructs. Viral DNA

was then purified, linearized and transfected into HEK293 cells for packaging and amplification. Viral particles were isolated from HEK293 cells by freeze-thawing, purified using Adeno-X[®] Mega Purification Kit (Clontech), and dialyzed against storage and proper tonicity buffer (2.5% glycerol (w/v), 25 mM NaCl, and 20 mM Tris-HCl, pH 7.4). The viral titer was determined using flow cytometry per the manufacturer's recommendation.

4.3.2 Cell Lines and Viral Transductions

HEK293 human embryonic kidney cells (ATCC, Manassas, VA) were used for viral production and MDA-MB-468 human breast adenocarcinoma cells (ATCC) harboring a dominant negative mutant p53 were grown as monolayers in DMEM (Invitrogen, Carlsbad, CA) supplemented with 10% fetal bovine serum, 1% penicillin-streptomycin-glutamine, and 0.1% gentamicin. MDA-MB-468 cells were also supplemented with 1% MEM non-essential amino acids (Invitrogen). All cells were incubated in 5% CO₂ at 37°C. The cells were seeded at a density of 3.0×10^5 cells in 6-well plates (Greiner Bio-One, Monroe, NC). Viral transductions were carried out immediately after seeding the cells at multiplicity of infection (MOI) of 200.

4.3.3 7-AAD Assay

Following manufacturer's instructions and as previously described, (13) MDA-MB-468 cells were stained with 7-aminoactinomycin D (7-AAD, Invitrogen) 48 h after transfection. Cells were analyzed and gated for ZsGreen1 (with same fluorescence intensity to ensure equal expression of proteins) using the FACSCanto-II (BD-

BioSciences, University of Utah Core Facility) and FACSDiva software. Excitation was set at 488 nm and detected at 507 nm and 780 nm for ZsGreen1 and 7-AAD, respectively. The means from three separate experiments ($n=3$) were analyzed using one-way ANOVA with Bonferroni's post-hoc test.

4.3.4 TMRE Assay

MDA-MB-468 cells were incubated with 100 nM tetramethylrhodamine ethyl ester (TMRE) (Invitrogen) for 30 min at 37 °C 36 h after infection. (14) The time point was determined to be 36 h as a result of several optimization pilot studies for the TMRE assay, and since mitochondrial outer membrane permeabilization occurs prior to caspase-3/7, annexin-V, and 7-AAD detection (48 h). MDA-MB-468 cells were pelleted and resuspended in 300 μ L of annexin-V binding buffer (Invitrogen). Only ZsGreen1 positive cells were analyzed by using the FACS Canto-II (BD BioSciences, University of Utah Core Facility) with FACS Diva software. ZsGreen1 was excited with the 488 nm laser with emission filter 530/35, and TMRE was excited with the 561 nm laser with the emission filter 585/15. Mitochondrial depolarization (loss in TMRE intensity) correlates with an increase in MOMP (15). Independent transfections of each construct were tested three times ($n = 3$).

4.3.5 Caspase-3/7 Assay

MDA-MB-468 cells were probed 48 h after treatment using FLICA® 660 Caspase-3/7 Assay Kit (Immunochemistry Technologies, Bloomington, MN). Cells were pelleted, resuspended in 300 μ L of 1 \times wash buffer (Immunochemistry Technologies),

and incubated with FLICA® 660 Caspase-3/7 reagent for 45 min per the manufacturer's recommendations. Only ZsGreen1 positive cells were analyzed using the FACS Canto-II (BD BioSciences, University of Utah Core Facility) with FACS Diva software. ZsGreen1 and FLICA® 660 were excited with the 488 nm (emission filter 530/35) and the 635 laser (emission filter 670/30), respectively. Independent transfections of each construct were tested three times (n = 3).

4.3.6 Annexin-V Assay

The annexin-V assay was performed as before (12, 13). Briefly, 48 h post infection, MDA-MB-468 cells were suspended in 400 µl annexin binding buffer (Invitrogen) and incubated with 5 µl annexin-APC (annexin-V conjugated to allophycocyanin, Invitrogen) for 15 minutes. The incubated cells were ZsGreen1 gated and analyzed using FACSCanto-II. ZsGreen1 and APC were excited at 488 nm and 635 nm wavelengths and detected at 507 nm and 660 nm, respectively. Each construct was tested three times (n=3) and analyzed using one-way ANOVA with Bonferroni's post hoc test (13).

4.3.7 *In Vivo* Study

The experimental protocol was approved by the Institutional Animal Care and Use Committee (IACUC) at the University of Utah. All experiments were performed in Female nu/nu athymic mice (6-8 weeks old, Jackson Laboratories, Bar Harbor, ME). Human MDA-MB-468 cells (1×10^7 cells/mouse in 100 µl of serum-free RPMI-1640 medium) were injected subcutaneously into the mammary fat pad located in the right

inguinal area. When tumors reached a mean size of 50mm^3 , animals were randomized into 4 treatment groups and received single peritumoral injections of adenoviral constructs (5.0×10^8 pfu) in a 50 μl volume prepared fresh on days 0-4 and 7-11. Twenty-four hours after the last injection the mice were sacrificed and the tumors as well as the organs were harvested for analyses. Tumor volumes were measured daily using Vernier calipers along the longest width (W) and the corresponding perpendicular length (L). The tumor volume was calculated using $V = (L \times W \times 0.5W)$. All procedures were performed according to established NIH guidelines and University of Utah Institutional Animal Care and Use Committee approved protocols.

4.3.8 Histology

Animal tumor tissue samples and organs were fixed in 10% formalin for 24 h followed by tissue preparation and embedded in paraffin. Embedded tissues were then sectioned to cut at 4 μm thick sections and mounted on plus slides. Slides from each tumor tissue from all mice in the three treatment groups as well as the untreated group were stained using hematoxylin and eosin and p21 immunohistochemistry stain. Tissue and histological slide preparation was conducted in collaboration with ARUP Laboratories (Salt Lake City, Utah) (16).

4.3.9 Western Blotting

In vivo: fresh tumor tissue samples from animals of each treatment group were collected, snap-frozen in liquid nitrogen, ground with mortar and pestle, resuspended in 200 mL lysis buffer (62.5 mM Tris-HCl, 2% w/v SDS, 10% glycerol, 1 % protease

inhibitor) followed by sonication on ice. Recovered tissue lysates were then centrifuged for 45 min at 14,000 rpm and the supernatants were used for immunoblotting. Standard western blotting procedures (12, 17) were followed using primary antibodies to detect p21/WAF1, cleaved caspase-3, and actin as a loading control. The primary antibodies anti-p21 (ab16767, Abcam, Cambridge, MA), anti-cleaved caspase-3 (#9665P, Cell Signaling Technology, Danvers, MA), anti-actin (mouse, ab3280, Abcam), and anti-actin (rabbit, ab1801, Abcam) were detected with anti-rabbit (#7074S, Cell Signaling Technology) or anti-mouse (ab6814, Abcam) HRP-conjugated antibodies before the addition of SuperSignal West Pico chemiluminescent substrate (Thermo Scientific, Waltham, MA). Signals were detected using a FluorChem FC2 imager and software (Alpha Innotech, Sanata Clara, CA). All experiments were conducted in triplicates.

In vitro: 24 h following infection of MDA-MB-468 cells, 3×10^5 cells were pelleted and resuspended in 200 μ L lysis buffer (62.5 mM Tris-HCl, 2% w/v SDS, 10% glycerol, 1 % protease inhibitor), sonicated on ice, and centrifuged for 15 min at 14,000 rpm. The supernatants were used for immunoblotting as described above and densitometry analysis was performed as described before (18).

4.3.10 Statistical Analysis

One-way ANOVA with Bonferroni's post test was used to compare the different treatment groups and controls. A value of $p < 0.05$ was considered statistically significant. Error bars represent standard deviations from at least three independent experiments ($n = 3$) except for the animal study ($n=6$).

4.4 Results

4.4.1 p53-CC Induces Higher Levels of Cell Death Compared to Wt-p53

We (12) and others (19, 20) have shown that the MDA-MB-468 human breast adenocarcinoma cell line serves as a suitable dominant negative mutant p53 model for testing the effect of p53-CC and wt-p53. The endogenous p53 in MDA-MB-468 contains the R273H point mutation, which is known to exhibit a dominant negative effect over wt-p53.(12, 20) As we have shown previously, p53-CC is capable of inducing cell death in this as well as other cancer cell lines, regardless of endogenous p53 status. Figure 4.2 illustrates the superior tumor suppressor function of p53-CC over wt-p53 in a 7-AAD viability assay which stains apoptotic and necrotic cells (21, 22) (compare Figure 4.2A vs 2B). Wt-p53 activity is not significantly different from that achieved by the negative control Ad-ZsGreen1 (Figure 4.2B vs 2C). This observation illustrates the dominant negative effect of endogenous mutant p53 over wt-p53 in cancer cells and highlights the significance of our approach to escape transdominant inhibition. These results are summarized in Figure 4.2D.

4.4.2 p53-CC Caused Cell Death via the Apoptotic Pathway

Figure 4.2 suggests that the MDA-MB-468 cell line is a suitable tumor model to test the impact of the dominant negative effect of mutant p53 *in vivo*. In preceding animal studies, we explored the mechanism of cell death, and hypothesized that it occurs via an apoptotic pathway.

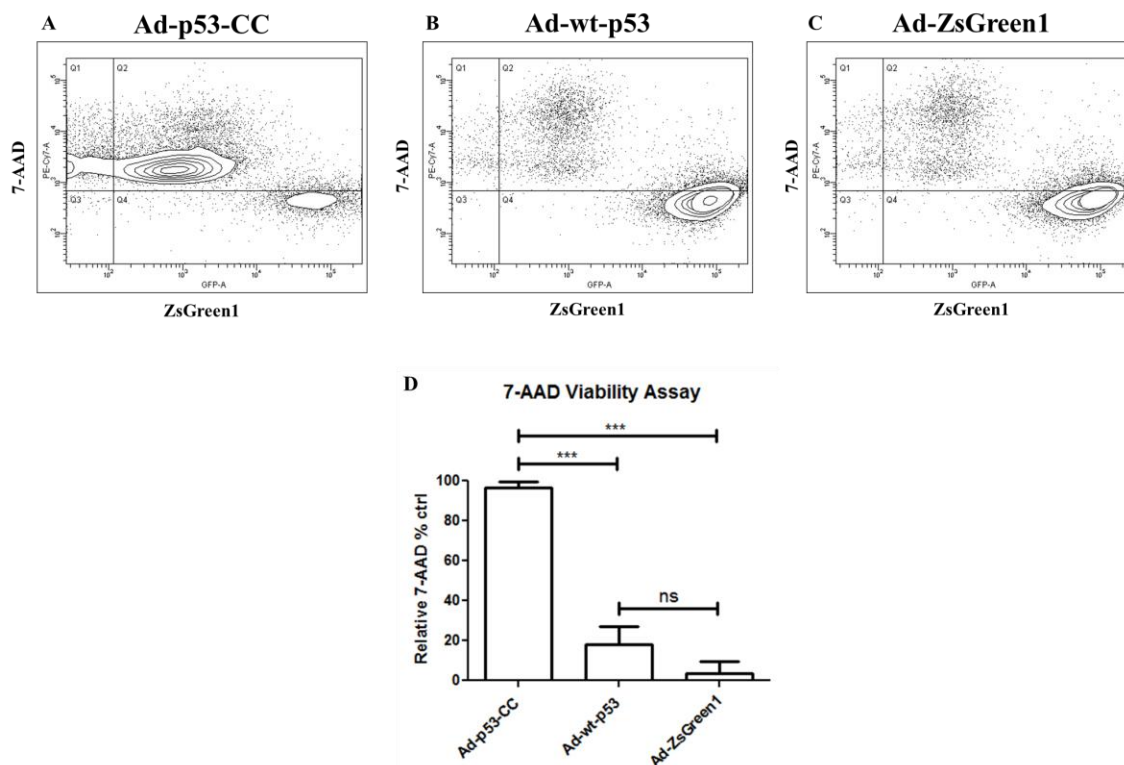


Figure 4.2 7-AAD staining of apoptotic and necrotic cells was performed. 48 h after viral transfection, cells were analyzed and gated for ZsGreen1. (A-C) Representative individual contour plots from each transfection and treatment group showing only ZsGreen1-gated cells. Q1&Q2= 7-AAD positive cells; Q3&Q4= 7-AAD negative cells. (D) Percentage of cell death induced by each transfection and treatment group. Mean values were analyzed using one-way ANOVA with Bonferroni's post test; ns= non-significant, *** $p < 0.001$. Error bars represent standard deviations from at least three independent experiments ($n = 3$).

Thus, three different apoptosis assays, the TMRE assay (analogous to the JC-1 assay), activated caspase-3/7 assay, and annexin-V staining were carried out. Mitochondrial depolarization as measured by loss in TMRE intensity correlates with an increase in mitochondrial outer membrane permeabilization (MOMP) (15). TMRE is a cationic, cell-permeant, and fluorescent dye that rapidly accumulates in mitochondria of living cells due to the negative mitochondrial membrane potential ($\Delta\Psi_m$) of intact mitochondria compared to cytosol (23, 24). Mitochondrial depolarization results in loss

of TMRE from mitochondria and a decrease in mitochondrial fluorescence intensity (FI)⁷, illustrated as %MOMP induction in Figure 4.3A. Figure 4.3A demonstrates that p53-CC induced significantly higher levels of mitochondrial membrane permeabilization, a hallmark of intrinsic apoptosis, compared to wt-p53. Wt-p53 also induced mitochondrial membrane permeabilization, although not to the same extent as p53-CC. MOMP indicates that cells are transitioning to an apoptotic state (25).

To further investigate the potential apoptotic activity of p53-CC and wt-p53, we carried out a flow cytometry-based assay to detect the levels of activated caspase-3/7 in MDA-MB-468 cells (Figure 4.3B). Caspase-3/7 activation is downstream from mitochondrial outer membrane permeabilization in the intrinsic apoptotic pathway and plays a central role at the execution-phase of cell apoptosis.(26-28) Figure 4.3B shows that cells treated with p53-CC display increased levels of active caspase-3/7 compared to those treated with wt-p53 or the negative control Ad-ZsGreen1.

Finally, annexin-V staining was performed, which measures externalization of phosphatidylserine on the cell surface of apoptotic cells specifically (29, 30). Figure 4.3C shows higher levels of annexin-V positive staining in cells treated with Ad-p53-CC compared to Ad-wt-p53; wt-p53 apoptotic activity was not significantly different from the negative control Ad-ZsGreen1. Cellular apoptosis as indicated in Figure 4.3C parallel the results from the 7-AAD staining in Figure 4.2.

To summarize, Figures 4.3 A, B, and C show MDA-MB-468 cells treated with Ad-p53-CC undergo significant apoptosis, validating p53-CC as a potent candidate for gene therapy.

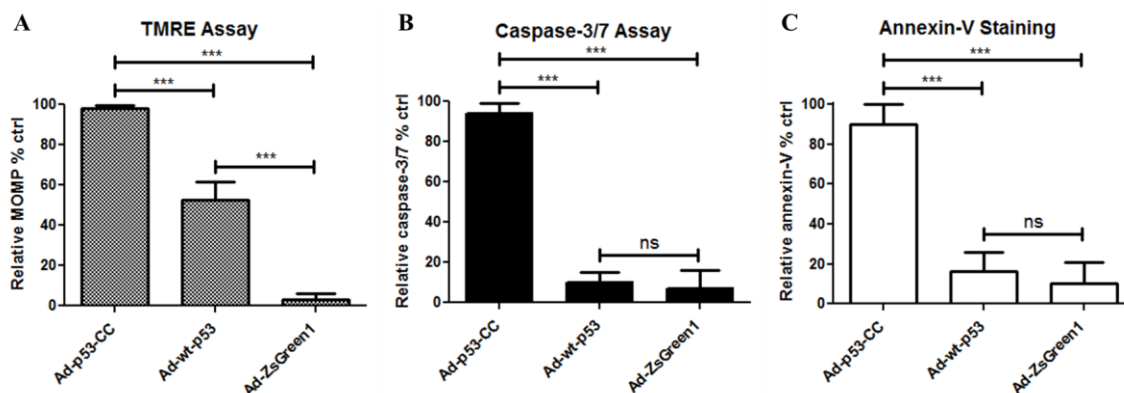


Figure 4.3 Induction of apoptosis is measured by (A) TMRE, (B) Caspase-3/7, and (C) Annexin-V. In all three assays, MDA-MB-468 cells treated with Ad-p53-CC undergo higher levels of apoptosis compared to cells infected with Ad-wt-p53 or the negative control Ad-ZsGreen1. Mean values were analyzed using one-way ANOVA with Bonferroni's post test; ns= nonsignificant, *** $p < 0.001$. Error bars represent standard deviations from at least three independent experiments ($n = 3$).

The levels of apoptosis induced by Ad-p53-CC are statistically significant compared to that of Ad-wt-p53 or Ad-ZsGreen1 in all three apoptosis assays (Figure 4.3) in addition to the 7-AAD assay (Figure 4.2).

4.4.3 *In vivo* Efficacy in a Dominant Negative

Breast Cancer Animal Model

MDA-MB-468 human breast adenocarcinoma represents an aggressive breast cancer cell line characterized as triple negative due to the absence of molecular targets including estrogen receptor, progesterone receptor, and human epidermal growth factor receptor 2 (ref. (31)). In addition, MDA-MB-468 cells harbor a dominant negative mutant p53 capable of impairing the function of wt-p53 (12, 19, 20). We therefore used this cell line to induce orthotopic breast tumors in mice to compare the impact of the dominant negative effect of mutant p53 on the biological activity of p53-CC and wt-p53 in viral-

mediated gene therapy. Because of the presence of the coxsackievirus and adenovirus receptor (CAR), MDA-MB-468 cells can be transfected by adenovirus (32).

Induced in the mammary fat pad of female athymic nu/nu mice, MDA-MB-468 tumors orthotopic engraftment fosters tumorigenesis to occur in the appropriate macro- as well as microenvironment mimicking the environment of human MDA-MB-468 tumors (33, 34). Due to this, MDA-MB-468 is a commonly used xenograft model for triple negative breast cancer (35, 36). Tumors were allowed to grow to approximately 50 mm³ prior to randomization of treatment groups which received intratumoral injections of Ad-p53-CC or Ad-wt-p53. The empty viral vector (Ad-ZsGreen1) served as a negative control in addition to an untreated control. Injections were made on days 0-4 and 7-11 for optimal efficacy(37) and consisted of 5.0x10⁸ PFU of the viral constructs in a 50 µl volume. All procedures were performed according to established NIH guidelines and followed University of Utah Institutional Animal Care and Use Committee approved protocols. Figure 4.4A shows a representative image of a tumor bearing mouse with the mammary tumor located in the right inguinal area, while Figure 4.4B shows images of representative excised tumors from each treatment group.

The tumor size reduction expected with these treatments served as a direct measure of the tumor suppressor function of our p53 variants. As expected, the Ad-p53-CC treatment group achieved statistically significant ($p < 0.001$) reduction in mean tumor size compared to Ad-wt-p53, Ad-ZsGreen1, and untreated groups (Figure 4.4C). Although tumor reduction induced by Ad-wt-p53 is not statistically significant compared to the Ad-ZsGreen1 or untreated groups, Ad-wt-p53 treatment resulted in stable disease, halting tumor progression.

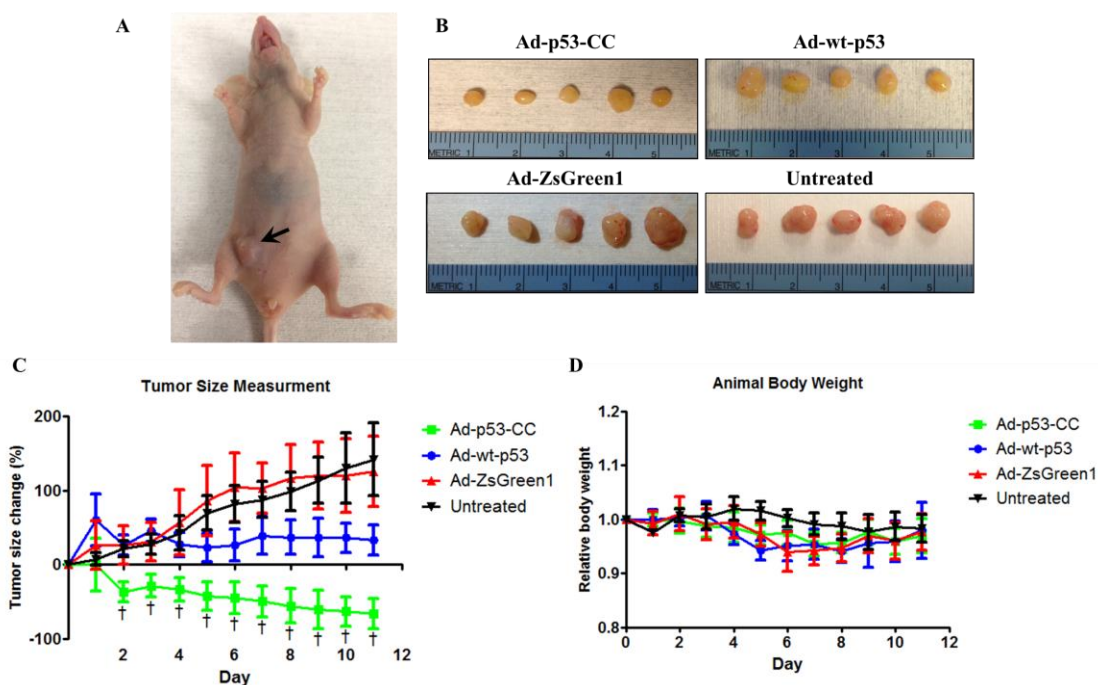


Figure 4.4 Effect of viral gene therapy using p53-CC and wt-p53 on the aggressive p53-dominant negative MDA-MB-468 human breast adenocarcinoma in female athymic nu/nu mice. (A) A representative image of a mouse in the study. For tumor inductions, MDA-MB-468 cells were injected in the right mammary fat pad of the inguinal area (highlighted by the black arrow). (B) Representative images of the excised tumors from each treatment group scaled to the same ratios. (C) Tumor size measured with calipers daily and normalized to Day 0. (D) Animal weights as measured daily and normalized relative to weights from Day 0. Six mice per group were used for this study. Mean values were analyzed using one-way ANOVA with Bonferroni's post test; † $p < 0.001$. Error bars represent standard deviations.

The findings from Figure 4.4C reveal that p53-CC can achieve tumor *regression* of an aggressive p53-dominant negative breast cancer model *in vivo*, while wt-p53 is only capable of halting tumor progression. In addition, the excised tumors from the Ad-ZsGreen1 negative control and untreated groups appeared to be more vascularized compared to tumors derived from the treatment groups Ad-p53-CC and Ad-wt-p53 (Figure 4.4B), potentially implying an additional anti-angiogenic effect of p53-CC and wt-p53 *in vivo*.

Animal body weights were regularly monitored throughout the study and no significant weight loss in animals was observed in any of the groups (Figure 4.4D) rendering the treatment as well as the viral carrier safe. Throughout the study, the Ad-p53-CC treatment group maintained the smallest mean tumor size compared to all other groups. Both control groups (Ad-ZsGreen1 and untreated) exhibited the largest mean tumor size compared to all other groups throughout the entire study.

4.4.4 Histopathological Evaluation of Tumor Tissues and Evidence for Tumor Suppressor Activity

The tumor size reduction observed in Figure 4.4C indicates tumor suppressor functionality of Ad-p53-CC as well as Ad-wt-p53 *in vivo*. To verify if this activity is indeed p53-dependent, we carried out immunohistochemical staining of p21 as it is one of the best characterized bona fide p53 target genes. (38) Photomicrographs of representative sections from harvested tumor tissues from each group are displayed in Figure 4.5A.

The left column in Figure 4.5A exhibits hematoxylin and eosin (H&E) staining, while the middle column represents p21 immunohistochemical staining for each group. In addition, the right column in Figure 4.5A shows the intratumoral expression of our gene load (i.e., p53-CC or wt-p53) as a function of the ZsGreen1 fluorescent protein co-expressed with our genes of interest. Microscopic examination of H&E staining revealed higher levels of necrosis (solid arrows, necrosis; open arrows, nonnecrotic areas) in all tumors harvested from mice injected with Ad-p53-CC compared to the Ad-wt-p53, Ad-ZsGreen1, or untreated groups (Figure 4.5A).

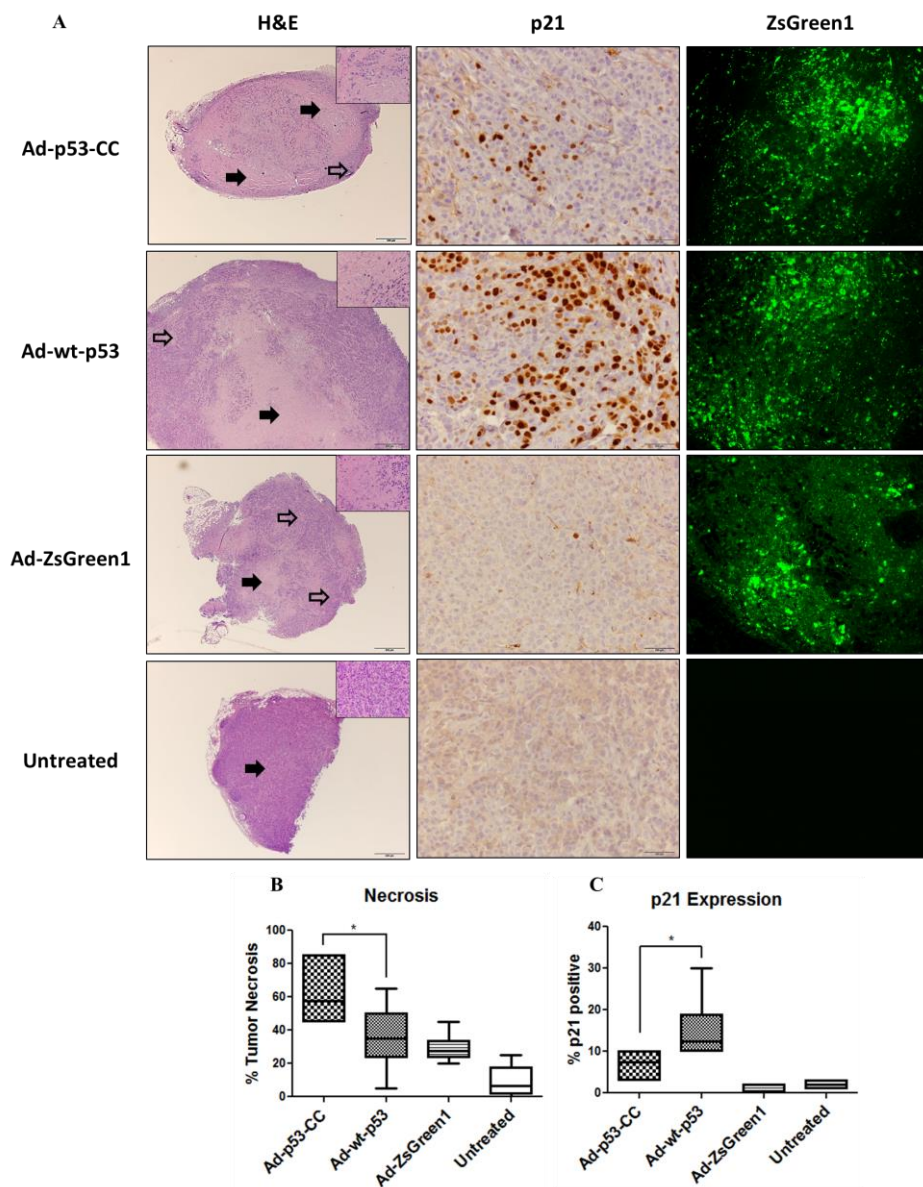


Figure 4.5 Representative photomicrographs showing the effects of the different treatment groups on tumor tissues visualized via H&E staining (A) left column, p21 immunohistochemistry staining (A) middle column, and ZsGreen1 fluorescence (A) right column. (A) Solid black arrows (left column) indicate necrotic cells, while open arrows indicate nonnecrotic areas. 3,3' diaminobenzidine (DAPI) stains the nuclei of p21-positive cells brown (middle column). Examination of the H&E staining microscopically revealed higher levels of necrosis in all tumor tissues from mice injected with Ad-p53-CC compared to the Ad-wt-p53, Ad-ZsGreen1, or untreated groups. p21 immunohistochemistry staining revealed higher levels of p21 induction in the Ad-wt-p53 treatment group compared to the Ad-p53-CC treatment group. Semiquantitative histoscore analyses of (B) tumor necrosis and (C) p21 up-regulation in the excised tumors from all groups is shown. Mean values were analyzed using one-way ANOVA with Bonferroni's post test; * $p < 0.05$. Error bars represent standard deviations ($n=6$).

This implies the detected necrosis may be due to the tumor suppressor activity of p53-CC since the tumors did not reach a large enough size to develop a necrotic core, and as such the observed necrosis was due to treatment, not hypoxia. 3,3' diaminobenzidine (DAB) stains the nuclei of p21-positive cells brown, as shown in photomicrographs (middle column, Figure 4.5A). Unexpectedly, p21 immunohistochemistry staining revealed higher levels of p21 induction in the Ad-wt-p53 treatment group compared to the Ad-p53-CC treatment group. p21 is one of the key factors by which p53 enforces cell cycle arrest. The induction of cell cycle arrest by p21 converges with findings from Figure 4.4C where tumors from the Ad-wt-p53 treatment group show a halt (arrest) in tumor growth. As expected, p21 expression was not detected in the Ad-ZsGreen1 negative control or untreated groups, which validates that p21 expression is linked to direct p53 activation. Similar expression of ZsGreen1 across the different groups (Ad-p53-CC, Ad-wt-p53, and Ad-ZsGreen1) in the right column of Figure 4.5A indicates comparable intratumoral expression of our viral constructs. In addition, p53 immunohistochemistry staining was performed and equal levels of total (i.e., endogenous and exogenous) p53 expression were detected across all groups, including the untreated group, which relates to the known presence of endogenous p53 in MDA-MB-468 cells (data not shown). Figures 4.5 B and C represent semiquantitative histoscore analyses of tumor necrosis and p21 upregulation in the excised tumors from all groups.

Tissues from additional organs (liver, kidney, spleen, heart, and lungs) harvested from animals of all treatment groups showed normal physiology and no abnormalities or signs of pathology (data not shown). However, metastases of tumor cells to the gastrointestinal region were noted in 2 out of 6 mice in the Ad-ZsGreen1 group and 3 out

of 6 mice in the untreated group (data not shown). This may imply an anti-metastatic function of p53-CC as well as wt-p53 in this tumor model although further examination is necessary.

4.4.5 Detection of Pathway-Specific Markers for Cell Cycle Arrest and Apoptosis

Based on our observations, we postulate that p53-CC is capable of causing tumor size reduction *in vivo* by favoring the apoptotic pathway, while wt-p53 activity is biased towards inducing cell cycle arrest. To further investigate this hypothesis, we carried out immunoblotting of cleaved (activated) caspase-3 and p21 on samples from *in vitro* and *in vivo*. It is well known that all apoptotic pathways converge on caspase-3 (the main executioner caspase) (39, 40), whereas p21 induction by p53 causes cells to undergo cell cycle G₁ phase arrest (41-43). Therefore, detection of activated caspase-3 and p21 are acceptable biomarkers for apoptosis and cell cycle arrest, respectively. Figure 4.6A shows a representative western blot analyses of p21 (middle band) and caspase-3 (bottom band) of MDA-MB-468 cells *in vitro*. MDA-MB-468 cells treated with Ad-p53-CC express lower levels of p21 compared to cells treated with Ad-wt-p53 (Figure 4.6B), a clear indication of a cell cycle arrest activity of wt-p53. However, higher levels of activated caspase-3 are detected in cells treated with Ad-p53-CC compared to Ad-wt-p53 (Figure 4.6C, a hallmark of apoptosis induction).

Part of the excised tumor tissues from each animal was homogenized and lysed for western blotting. Figure 4.6D shows representative western blotting of MDA-MB-468 *in vivo* tumor tissue lysates.

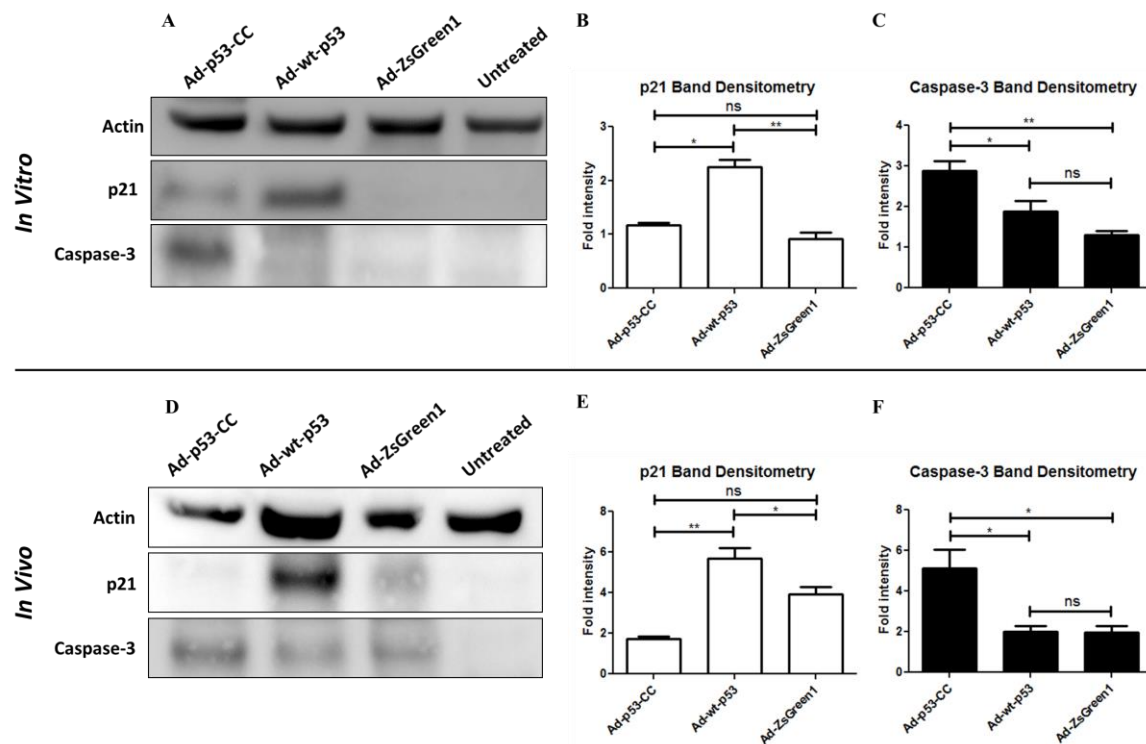


Figure 4.6 Representative cropped western blots of MDA-MB-468 (A-C) *in vitro* cell lysates and (D-F) homogenized tumors from the *in vivo* study treated with Ad-p53-CC, Ad-wt-p53, Ad-ZsGreen1, or untreated. Western analyses show that MDA-MB-468 cells (A) and tumor tissues (D) treated with Ad-p53-CC both express lower levels of p21, but higher levels of activated (cleaved) caspase-3 compared to cells treated with Ad-wt-p53. No significant levels of p21 or cleaved caspase-3 induction were observed in cells (A) or tumors (D) injected with Ad-ZsGreen1 or untreated. Semiquantitative densitometric analyses was carried out as described before(18) to evaluate p21 (B) and cleaved caspase-3 (C) expression *in vitro* as well as expression of p21 (E) and cleaved caspase-3 (F) expression *in vivo*. Mean values were analyzed using one-way ANOVA with Bonferroni's post test; * $p < 0.05$, ** $p < 0.01$, and *** $p < 0.001$. Error bars represent standard deviations (n=3).

Similar to the findings obtained from *in vitro* western blotting (Figures 4.6A-C), tumor tissues from the Ad-p53-CC treatment group showed lower p21 expression (Figure 4.6E) but higher caspase-3 induction (Figure 4.6F).

Results from Figure 4.6 corroborate our hypothesis that p53-CC favors induction of apoptosis *in vitro* and *in vivo*, while wt-p53 is biased towards inducing cell cycle arrest.

4.5 Discussion

The data obtained in this report support our hypothesis that chimeric p53-CC has superior tumor suppressor function compared to wt-p53 *in vitro* and *in vivo* using a dominant negative mutant p53 model. Although the concept of a “superactive” p53 was reported in 2010 (44), there are no known reports of constructing a p53 capable of bypassing the dominant negative effect of mutant p53 in cancer cells and increases apoptosis (over wt-p53). p53-CC induces higher levels of cell death *in vitro* compared to wt-p53 in the 7-AAD assay (Figure 4.2) as well as in the apoptosis assays: TMRE, caspase-3/7, and annexin-V (Figure 4.3). To validate if the superior activity of p53-CC *in vitro* translates *in vivo*, we carried out animal studies using an orthotopic MDA-MB-468 xenograft breast cancer model in mouse mammary fat pads. Indeed, intratumoral injections with Ad-p53-CC achieved substantial tumor regression that is statistically significant compared to the Ad-wt-p53, Ad-ZsGreen1, and untreated groups (Figure 4.4C), without any sign of treatment toxicity (Figure 4.4D). H&E staining of tumor tissues revealed higher levels of necrosis in all tumor tissues from mice injected with Ad-p53-CC compared to the Ad-wt-p53, Ad-ZsGreen1, or untreated groups.

To test if the observed tumor suppressor activity of p53-CC *in vivo* is p53-dependent, immunohistochemistry staining of p21, the most well studied p53 target gene (38), was conducted. As expected, p21-positive staining was observed only in the Ad-p53-CC and Ad-wt-p53 treatment groups (Figure 4.5) with higher p21 staining with Ad-wt-p53 treatment.

Since p53-CC was able to induce apoptosis (including caspase 3/7), and wt-p53 increased p21 expression, we explored a possible differential mechanism of p53-CC (favoring apoptosis) and wt-p53 (favoring cell cycle arrest) in MDA-MB-468 cells. To test this premise, immunoblotting was carried out on samples from *in vitro* (Figures 4.6A-C) and *in vivo* (Figures 4.6D-F) to detect expression levels of p21, which induces cell cycle arrest, and caspase-3, a major executor of apoptosis. Figure 4.6 revealed that tumor tissues treated with Ad-p53-CC expressed low levels of p21 (reduced cell cycle arrest) but high levels of active caspase-3 (increased apoptosis). In contrast, tumor tissues injected with Ad-wt-p53 expressed high levels of p21 (increased cell cycle arrest) but low levels of caspase-3 (decreased apoptosis).

The transdominant mutant p53 found endogenously in MDA-MB-468 cells retains the ability to hetero-oligomerize with exogenous wt-p53, since its tetramerization domain remains intact (10). We and others have shown previously that upon hetero-oligomer formation, the activity of exogenous wt-p53 is impaired due to the dominant negative effect of mutant p53 in cancer cells (12, 19, 20). Our chimeric p53-CC was designed to overcome this barrier with a use of an alternative oligomerization domain, a coiled-coil from Bcr (CC). This CC is known to tetramerize as an antiparallel dimer of dimers, similar to the tetramerization domain of wt-p53 (12, 45).

The use of this alternative oligomerization domain allows p53-CC to escape any possible hetero-oligomerization with mutant p53 and consequent transdominant inhibition. Indeed, our previous work validated the ability of p53-CC to exclusively form homo-oligomers. From a gene therapy point of view, the ability of p53-CC to evade transdominant inhibition gives it an advantage over wt-p53 in dominant mutant p53 cancer cells such as MDA-MB-468. Our viral-mediated gene therapy *in vivo* studies show that p53-CC has superior tumor suppressor activity compared to wt-p53 in the MDA-MB-468 aggressive p53-dominant negative breast cancer model. In fact, p53-CC was capable of achieving significant tumor *regression*, while wt-p53 is only capable of halting tumor *progression* (Figure 4.4C).

Upon further investigation, we discovered that the difference in outcome of the tumor size reduction was due to the ability of p53-CC to activate the apoptotic pathway, whereas wt-p53 activates cell cycle arrest via p21 induction (Figure 4.7). These findings are supported by western blot analyses from *in vitro* (Figure 4.6A-C) and *in vivo* (Figure 4.6D-F) MDA-MB-468 cells/tumors. Analysis of p53-regulated gene expression patterns may possibly offer an explanation for differential pathway activation between p53-CC and wt-p53 (apoptosis vs. cell cycle arrest). It has been shown that p53-responsive gene expression patterns are highly variable, depending on the p53 protein levels in the cell (46). It is also known that higher levels of active p53 lead to activation of apoptotic genes, while lower levels of p53 activate cell cycle regulator genes (47). In cells treated with p53-CC vs. wt-p53, higher levels of the chimeric p53-CC protein exist compared to levels of active wt-p53 protein in cells, due to the ability of p53-CC to escape sequestration by mutant p53.

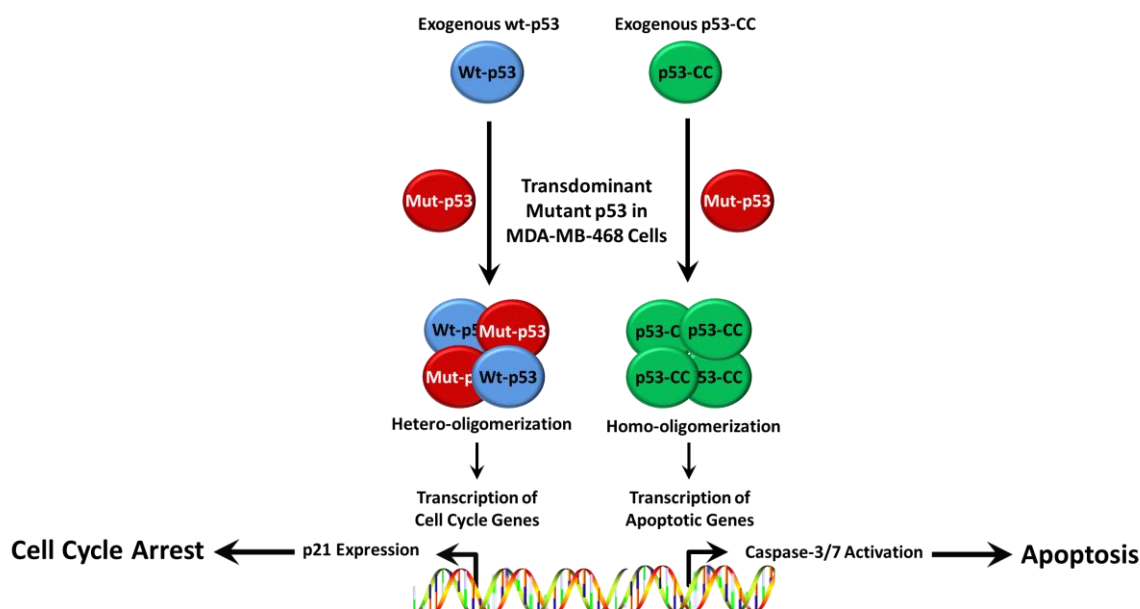


Figure 4.7 Schematic representation of the outcomes of wt-p53 (left) and p53-CC (right) activation. Wt-p53 induces cell cycle arrest via p21 expression (left), while p53-CC induces cell death via the apoptotic pathway (right).

Unlike p53-CC, substantial amounts of the wt-p53 protein are forced into inactive hetero-oligomers with endogenous mutant p53 (the dominant negative effect). This reduction in ‘available’ active wt-p53 could lead to failure in binding promoters of apoptotic genes that require higher active p53 protein levels in the cell. Cell cycle regulator genes, such as p21, would be activated instead, since wt-p53 possess higher binding affinities to these promoters (i.e., requires less p53 to bind and activate). In contrast, abundance in active chimeric p53-CC protein levels is found in cells treated with p53-CC, which would lead to binding and activation of apoptotic genes promoters. The variability of pathway activation (i.e. p53-CC, apoptosis vs wt-p53, cell cycle arrest) may be specific to this tumor model due to the dominant negative mutant p53 endogenously found in MDA-MB-468 cells/tumors. This is because we have shown previously (12) that p53-CC and wt-p53 induce similar levels of apoptosis in four

different non-p53-dominant negative breast cancer cell lines with varying endogenous p53 statuses (H1373 cells: p53 null, HeLa cells: wt-p53, T47D cells: wt-p53 mislocalized, and MDA-MB-231 cells: mutant p53) (12). Furthermore, qRT-PCR analyses and western blotting showed that p53-CC and wt-p53 induced similar levels of p21 gene expression in T47D breast carcinoma cells.

In summary, we have shown for the first time, use of a version of p53 that overcomes the limitations of using wt-p53 for gene therapy. A chimeric superactive p53 has been described as the ‘ultimate cancer therapeutic’ (48). Our p53-CC demonstrates comparable functional transcriptional activity to wt p53 (12), shows significantly improved apoptosis (Figures 4.2 and 4.33), and successfully circumvents the dominant negative inactivating effect of endogenous mutant p53 *in vitro* (12). Importantly, our compelling *in vivo* data (Figure 4.4) demonstrates that p53-CC is more effective than wt p53, and may serve as a more potent and reliable novel anticancer therapeutic.

4.6 References

1. W. Guand R.G. Roeder. Activation of p53 sequence-specific DNA binding by acetylation of the p53 C-terminal domain. *Cell*. 90:595-606 (1997).
2. B. Vogelstein and K.W. Kinzler. p53 function and dysfunction. *Cell*. 70:523-526 (1992).
3. B. Vogelstein, D. Lane, and A.J. Levine. Surfing the p53 network. *Nature*. 408:307-310 (2000).
4. A.J. Levine, J. Momand, and C.A. Finlay. The p53 tumour suppressor gene. *Nature*. 351:453-456 (1991).
5. U.M. Moll, G. Riou, and A.J. Levine. Two distinct mechanisms alter p53 in breast cancer: mutation and nuclear exclusion. *PNAS*. 89:7262-7266 (1992).
6. P.H. Kussie, S. Gorina, V. Marechal, B. Elenbaas, J. Moreau, A.J. Levine, and N.P. Pavletich. Structure of the MDM2 oncoprotein bound to the p53 tumor suppressor transactivation domain. *Science*. 274:948-953 (1996).

7. A. Okal, S. Reaz, and C. Lim. Cancer biology: some causes for a variety of different diseases. In Y.H. Bae, R.J. Mrsny, and K. Park (eds.), *Cancer Targeted Drug Delivery*, Springer New York, 2013, pp. 121-159.
8. M.J. Waterman, J.L. Waterman, and T.D. Halazonetis. An engineered four-stranded coiled coil substitutes for the tetramerization domain of wild-type p53 and alleviates transdominant inhibition by tumor-derived p53 mutants. *Cancer Res.* 56:158-163 (1996).
9. A. Willis, E.J. Jung, T. Wakefield, and X. Chen. Mutant p53 exerts a dominant negative effect by preventing wild-type p53 from binding to the promoter of its target genes. *Oncogene.* 23:2330-2338 (2004).
10. W.M. Chan, W.Y. Siu, A. Lau, and R.Y. Poon. How many mutant p53 molecules are needed to inactivate a tetramer? *Molecular and Cellular Biology.* 24:3536-3551 (2004).
11. A.G. Zeimet and C. Marth. Why did p53 gene therapy fail in ovarian cancer? *The Lancet Oncology.* 4:415-422 (2003).
12. A. Okal, M. Mossalam, K.J. Matissek, A.S. Dixon, P.J. Moos, and C.S. Lim. A chimeric p53 evades mutant p53 transdominant inhibition in cancer cells. *Mol Pharm.* 10:3922-3933 (2013).
13. M. Mossalam, K.J. Matissek, A. Okal, J.E. Constance, and C.S. Lim. Direct induction of apoptosis using an optimal mitochondrially targeted p53. *Mol Pharm.* 9:1449-1458 (2012).
14. A.J. Krohn, T. Wahlbrink, and J.H. Prehn. Mitochondrial depolarization is not required for neuronal apoptosis. *The Journal of Neuroscience : the official journal of the Society for Neuroscience.* 19:7394-7404 (1999).
15. K.J. Matissek, M. Mossalam, A. Okal, and C.S. Lim. The DNA binding domain of p53 is sufficient to trigger a potent apoptotic response at the mitochondria. *Mol Pharm.* 10:3592-3602 (2013).
16. M.E. Salama, M. Rajan Mariappan, K. Inamdar, S.R. Tripp, and S.L. Perkins. The value of CD23 expression as an additional marker in distinguishing mediastinal (thymic) large B-cell lymphoma from Hodgkin lymphoma. *Int J Surg Pathol.* 18:121-128 (2010).
17. S. Reaz, M. Mossalam, A. Okal, and C.S. Lim. A single mutant, A276S of p53, turns the switch to apoptosis. *Mol Pharm* (2013).
18. D.W. Woessner and C.S. Lim. Disrupting BCR-ABL in combination with secondary leukemia-specific pathways in CML cells leads to enhanced apoptosis and decreased proliferation. *Mol Pharm.* 10:270-277 (2013).
19. D.J. Junk, L. Vrba, G.S. Watts, M.M. Oshiro, J.D. Martinez, and B.W. Futscher. Different mutant/wild-type p53 combinations cause a spectrum of increased invasive potential in nonmalignant immortalized human mammary epithelial cells. *Neoplasia.* 10:450-461 (2008).

20. L.Y. Lim, N. Vidnovic, L.W. Ellisen, and C.O. Leong. Mutant p53 mediates survival of breast cancer cells. *British Journal of Cancer*. 101:1606-1612 (2009).
21. I. Schmid, W.J. Krall, C.H. Uittenbogaart, J. Braun, and J.V. Giorgi. Dead cell discrimination with 7-amino-actinomycin D in combination with dual color immunofluorescence in single laser flow cytometry. *Cytometry*. 13:204-208 (1992).
22. M.J. Serrano, P. Sanchez-Rovira, I. Algarra, A. Jaen, A. Lozano, and J.J. Gaforio. Evaluation of a gemcitabine-doxorubicin-paclitaxel combination schedule through flow cytometry assessment of apoptosis extent induced in human breast cancer cell lines. *Japanese Journal of Cancer Research : Gann*. 93:559-566 (2002).
23. C.M. O'Reilly, K.E. Fogarty, R.M. Drummond, R.A. Tuft, and J.V. Walsh, Jr. Quantitative analysis of spontaneous mitochondrial depolarizations. *Biophys J*. 85:3350-3357 (2003).
24. J.E. Ricci, R.A. Gottlieb, and D.R. Green. Caspase-mediated loss of mitochondrial function and generation of reactive oxygen species during apoptosis. *J Cell Biol*. 160:65-75 (2003).
25. J.E. Chipuk and D.R. Green. How do BCL-2 proteins induce mitochondrial outer membrane permeabilization? *Trends in Cell Biology*. 18:157-164 (2008).
26. M. Mossalam, K.J. Matissek, A. Okal, J.E. Constance, and C.S. Lim. Direct induction of apoptosis using an optimal mitochondrially targeted p53. *Mol Pharm*. 9:1449-1458 (2012).
27. E.A. Slee, C. Adrain, and S.J. Martin. Executioner caspase-3, -6, and -7 perform distinct, non-redundant roles during the demolition phase of apoptosis. *The Journal of Biological Chemistry*. 276:7320-7326 (2001).
28. S.A. Lakhani, A. Masud, K. Kuida, G.A. Porter, Jr., C.J. Booth, W.Z. Mehal, I. Inayat, and R.A. Flavell. Caspases 3 and 7: key mediators of mitochondrial events of apoptosis. *Science*. 311:847-851 (2006).
29. G. Koopman, C.P. Reutelingsperger, G.A. Kuijten, R.M. Keehnen, S.T. Pals, and M.H. van Oers. Annexin V for flow cytometric detection of phosphatidylserine expression on B cells undergoing apoptosis. *Blood*. 84:1415-1420 (1994).
30. I. Vermes, C. Haanen, H. Steffens-Nakken, and C. Reutelingsperger. A novel assay for apoptosis. Flow cytometric detection of phosphatidylserine expression on early apoptotic cells using fluorescein labelled Annexin V. *J Immunol Methods*. 184:39-51 (1995).
31. O. Metzger-Filho, A. Tutt, E. de Azambuja, K.S. Saini, G. Viale, S. Loi, I. Bradbury, J.M. Bliss, H.A. Azim, Jr., P. Ellis, A. Di Leo, J. Baselga, C. Sotiriou, and M. Piccart-Gebhart. Dissecting the heterogeneity of triple-negative breast cancer. *J Clin Oncol*. 30:1879-1887 (2012).
32. R. Price, J. Gustafson, K. Greish, J. Cappello, L. McGill, and H. Ghandehari. Comparison of silk-elastinlike protein polymer hydrogel and poloxamer in matrix-mediated gene delivery. *Int J Pharm*. 427:97-104 (2012).

33. J. Killion, R. Radinsky, and I. Fidler. Orthotopic models are necessary to predict therapy of transplantable tumors in mice. *Cancer and Metastasis Reviews*. 17:279-284 (1998).
34. M.C. Bibby. Orthotopic models of cancer for preclinical drug evaluation: advantages and disadvantages. *Eur J Cancer*. 40:852-857 (2004).
35. S. Vantuyghem, A. Allan, C. Postenka, W. Al-Katib, M. Keeney, A. Tuck, and A. Chambers. A new model for lymphatic metastasis: development of a variant of the MDA-MB-468 human breast cancer cell line that aggressively metastasizes to lymph nodes. *Clin Exp Metastasis*. 22:351-361 (2005).
36. J.R. Garlich, P. De, N. Dey, J.D. Su, X. Peng, A. Miller, R. Murali, Y. Lu, G.B. Mills, V. Kundra, H.K. Shu, Q. Peng, and D.L. Durden. A vascular targeted pan phosphoinositide 3-kinase inhibitor prodrug, SF1126, with antitumor and antiangiogenic activity. *Cancer Research*. 68:206-215 (2008).
37. L.L. Nielsen, P. Lipari, J. Dell, M. Gurnani, and G. Hajjan. Adenovirus-mediated p53 gene therapy and paclitaxel have synergistic efficacy in models of human head and neck, ovarian, prostate, and breast cancer. *Clinical Cancer Research : an official journal of the American Association for Cancer Research*. 4:835-846 (1998).
38. O. Laptenko, R. Beckerman, E. Freulich, and C. Prives. p53 binding to nucleosomes within the p21 promoter in vivo leads to nucleosome loss and transcriptional activation. *Proceedings of the National Academy of Sciences of the United States of America*. 108:10385-10390 (2011).
39. S.W. Tait and D.R. Green. Mitochondria and cell death: outer membrane permeabilization and beyond. *Nature Reviews Molecular Cell Biology*. 11:621-632 (2010).
40. S. Fulda and K.M. Debatin. Extrinsic versus intrinsic apoptosis pathways in anticancer chemotherapy. *Oncogene*. 25:4798-4811 (2006).
41. W.S. el-Deiry, J.W. Harper, P.M. O'Connor, V.E. Velculescu, C.E. Canman, J. Jackman, J.A. Pietenpol, M. Burrell, D.E. Hill, Y. Wang, et al. WAF1/CIP1 is induced in p53-mediated G1 arrest and apoptosis. *Cancer Research*. 54:1169-1174 (1994).
42. T. Waldman, K.W. Kinzler, and B. Vogelstein. p21 is necessary for the p53-mediated G1 arrest in human cancer cells. *Cancer Research*. 55:5187-5190 (1995).
43. T. Waldman, Y. Zhang, L. Dillehay, J. Yu, K. Kinzler, B. Vogelstein, and J. Williams. Cell-cycle arrest versus cell death in cancer therapy. *Nature Medicine*. 3:1034-1036 (1997).
44. D.P. Lane, C.F. Cheok, and S. Lain. p53-based cancer therapy. *Cold Spring Harb Perspect Biol*. 2:a001222 (2010).
45. C. Wichmann, Y. Becker, L. Chen-Wichmann, V. Vogel, A. Vojtkova, J. Herglotz, S. Moore, J. Koch, J. Lausen, W. Mantele, H. Gohlke, and M. Grez.

- Dimer-tetramer transition controls RUNX1/ETO leukemogenic activity. *Blood*. 116:603-613 (2010).
46. T. Yamada, Y. Hiraoka, M. Ikehata, K. Kimbara, B.S. Avner, T.K. Das Gupta, and A.M. Chakrabarty. Apoptosis or growth arrest: modulation of tumor suppressor p53's specificity by bacterial redox protein azurin. *Proceedings of the National Academy of Sciences of the United States of America*. 101:4770-4775 (2004).
 47. X. Chen, L.J. Ko, L. Jayaraman, and C. Prives. p53 levels, functional domains, and DNA damage determine the extent of the apoptotic response of tumor cells. *Genes & Development*. 10:2438-2451 (1996).
 48. D.P. Lane, C.F. Cheok, and S. Lain. p53-based cancer therapy. *Cold Spring Harb Perspect Biol*. 2:a001222 (2010).

CHAPTER 5

A RE-ENGINEERED p53 CHIMERA WITH ENHANCED HOMO-OLIGOMERIZATION THAT MAINTAINS TUMOR SUPPRESSOR ACTIVITY

5.1 Abstract

The use of the tumor suppressor p53 for gene therapy of cancer is limited by the dominant negative inactivating effect of mutant endogenous p53 in cancer cells. We have shown previously that swapping the tetramerization domain (TD) of p53 with an alternative oligomerization domain, the coiled-coil from Bcr, allows evasion of hetero-oligomerization with endogenous p53. This enhances the utility of this construct, p53-CC, for cancer gene therapy. Since domain swapping to create p53-CC could result in p53-CC interacting with endogenous Bcr, which is ubiquitous in cells, modifications on the CC domain are necessary to minimize potential interactions with Bcr. Hence, we investigated the possible design of mutations that will improve homo-dimerization of CC

Adapted from a manuscript submitted to *Molecular Pharmaceutics*. Abood Okal, Sean Cornillie, Stephan J. Matissek, Karina J. Matissek, Thomas E. Cheatham III, Carol S. Lim.

A.O. carried out the *in vitro* 7-AAD, mammalian two-hybrid, and co-immunoprecipitation assays. S.C. and T.E.C. III carried out all *in silico* design, simulations, and analyses. K.J.M. carried out 7-AAD assay in MCF-7 cells while S.J.M carried out 7-AAD assay in SKOV3.ip1 cells.

mutants and disfavor hetero-oligomerization with wild-type CC (CCwt), with the goal of minimizing potential interactions with endogenous Bcr in cells. This involved integrated computational and experimental approaches to rationally design an enhanced version of our chimeric p53-CC tumor suppressor. Indeed, the resulting lead candidate p53-CCmutE34K-R55E avoids binding to endogenous Bcr and retains p53 tumor suppressor activity. Specifically, p53-CCmutE34K-R55E exhibits potent apoptotic activity in a variety of cancer cell lines, regardless of p53 status (in cells with mutant p53, wild-type p53, or p53-null cells). This construct overcomes the limitations of wt p53, and has high significance for future gene therapy for treatment of cancers characterized by p53 dysfunction, which represent over half of all human cancers.

5.2 Introduction

The tumor suppressor p53 is the most commonly mutated gene of all human cancers, making it an ideal therapeutic target (1, 2). However, the diversity of p53 mutations precludes finding a single drug that hits all possible variants of the protein (3). In cancer cells, mutant p53 may not only impair tumor suppressor function and transcriptional activity, but effectively deplete wild-type p53 (wt-p53) since mutant p53 retains its ability to oligomerize with other p53 via the tetramerization domain (TD) (4, 5). Upon hetero-oligomerization of mutant and wt-p53 in cancer cells, mutant p53 exerts a dominant negative effect over wt-p53 and leads to its inactivation as a therapeutic (6-8). To overcome these issues, our alternative approach has been to engineer a chimeric version of p53 for cancer gene therapy that can be used universally, regardless of p53 mutational status in cancer (9). To create this chimeric, transcriptionally active version

p53 that can only form homo-tetramers, we searched for possible domain swapping motifs, and chose to replace the 31 amino acid TD of p53 (10) with the 72 amino acid coiled-coil (CC) of Bcr (breakpoint cluster region protein) (11). Superficially, these motifs may appear structurally dissimilar, but both the TD and CC contain a main α -helix that orients in an antiparallel fashion and forms a dimer of dimers (10, 11). Due to their similar orientation and ability to form tetramers, the CC motif from Bcr was a reasonable starting point for domain swapping. We have shown previously (9) that swapping the tetramerization domain of p53 with the CC domain enhances the utility of p53 for cancer gene therapy in p53-dominant negative breast cancer cells. This alteration of the oligomerization motif of the tumor suppressor allowed for our chimeric p53, namely p53-CC, to evade hetero-oligomerization with endogenous mutant p53 commonly found in cancer cells while retaining the tumor suppressor function of p53. This proves to be critical since mutant p53 has a transdominant inhibitory effect over wild-type p53 upon hetero-oligomerization.

Bcr, from which the CC was obtained, is a ubiquitous eukaryotic phosphotransferase, and has mostly been studied in the context of chronic myeloid leukemia (CML) where a reciprocal chromosomal translocation with Abl results in the fusion protein Bcr-Abl, the causative agent of CML (12, 13). Generally, Bcr may be involved in inflammatory pathways and cell proliferation (14). Although it has been shown that Bcr-knockout mice still survive, one of the major defects in these mice was reduced intimal proliferation in low-flow carotid arteries compared to wild-type mice (14). In addition, Bcr plays a role in arterial proliferative disease *in vivo* as well as differentiation and inflammatory responses of vascular smooth muscle cells (15, 16).

Since domain swapping to create p53-CC could result in p53-CC interacting with endogenous Bcr, modifications on the CC domain are necessary to minimize potential interactions with Bcr. Hence, the purpose of this work is to modify the CC domain in p53-CC to reduce potential interactions with endogenous Bcr.

Coiled-coil domains are characterized by heptad repeats of amino acids (denoted by letters for each residue, **(abcdefg)_n**, for n repeats) that control the specificity and orientation of the oligomerization motif (17, 18). Distinct interaction profiles exist between the different residues based on the orientation (parallel or antiparallel) of the coiled-coil (17, 19). Surface interactions between positions **e** to **e'** (where the ' denotes a residue on the opposing coiled-coil in the dimer) and **g** to **g'** are known to be essential in antiparallel coiled-coils, whereas interactions between positions **g** to **e'** are the most critical for parallel coiled-coils (17, 19). The coiled-coil domain from Bcr is assembled as two 36-residue helices antiparallel to each other (Figure 5.1A) (20, 21). This antiparallel orientation gives rise to the aforementioned **e** to **e'** and **g** to **g'** interactions that can be utilized to potentially modify electrostatic interactions within a dimer. We investigated the possible design of mutations that will form opposing charges on residues **e** to **e'** and **g** to **g'** to increase salt bridge formation (see Figure 5.1) in order to improve homodimerization of CC mutants and disfavor hetero-oligomerization with wild-type (CCwt), with the goal of minimizing potential interactions with endogenous Bcr in cells. *In silico* examination of CCwt (Figure 5.1A) revealed that Bcr has uncharged Ser-41 at position **g** and Glu-48 (acidic) representing **g'** that are within proximity for salt bridge formation. Similarly, CCwt has uncharged Gln-60 at position **e** and Lys-39 (basic) at position **e'** which are also within proximity for salt bridge formation.

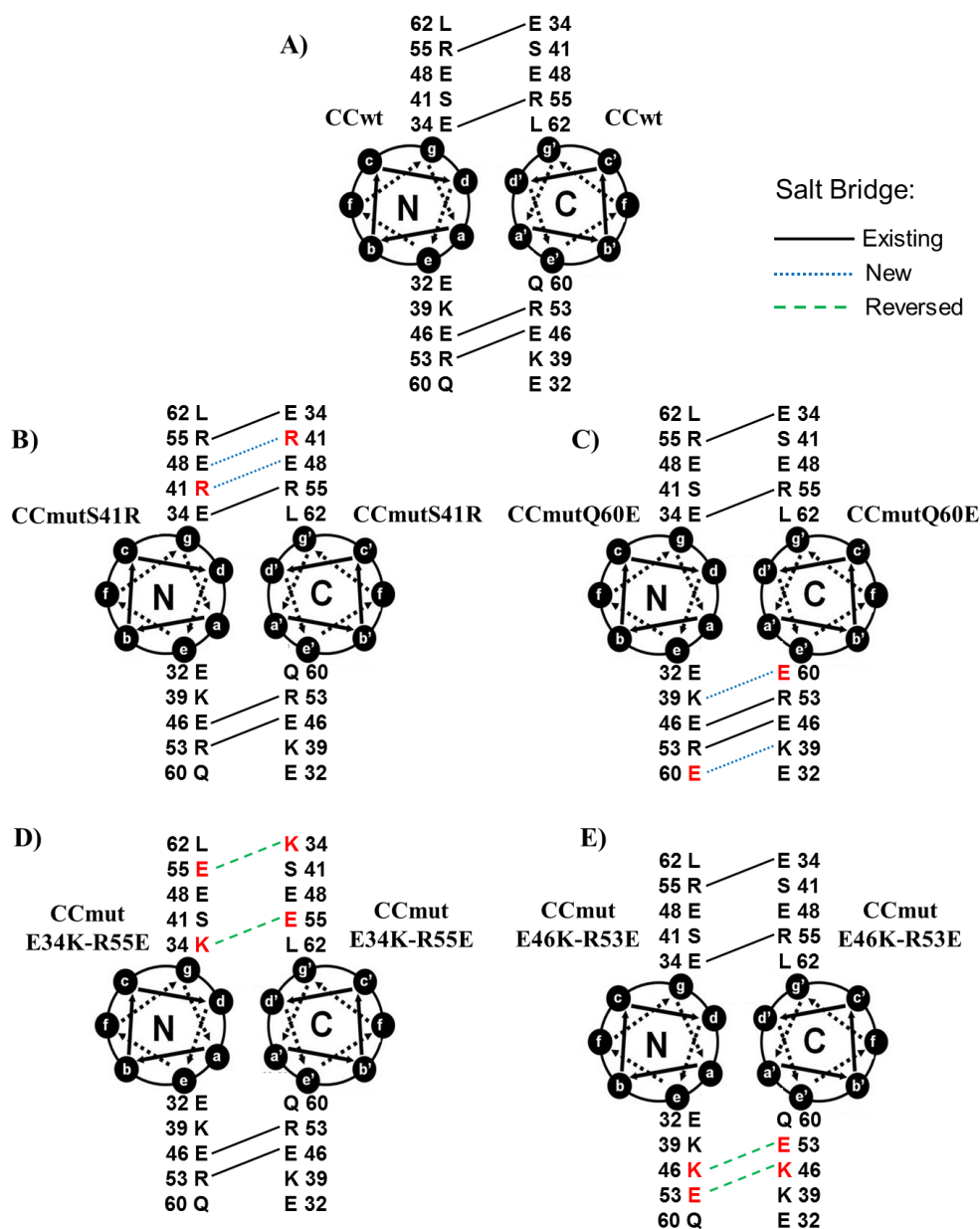


Figure 5.1 Helical wheel diagrams of wild-type CC homo-dimers (CCwt) (A), CCmutS41R homo-dimers (B), CCmutQ60E homo-dimers (C), CCmutE34K-R55E homo-dimers (D), and CCmutE46K-R53E homo-dimers (E). Solid lines indicate possible ionic interactions already existing in the wild-type coiled-coil. Dotted (blue) lines represent newly formed ionic interactions. Dashed (green) lines indicate reversed ionic interactions existing in the wild-type coiled-coil.

Therefore, we hypothesized that introducing S41R (Arg, basic) and Q60E (Glu, acidic) mutations separately, would potentially form two extra salt bridges per mutation (Figure 5.1B and 1C, respectively). These two mutant candidates are referred to as CCmutS41R and CCmutQ60E.

In addition, examination of the coiled-coil interchain salt bridges indicate that two more potential compound mutants (i.e., more than one mutation per candidate) could be made to improve homo-dimerization of CC mutants. Mutation of Glu-34 to Lys and Arg-55 to Glu (CCmutE34K-R55E) will preserve all four stabilizing salt bridges found in CCwt in the case of CCmut homo-oligomerization (Figure 5.1D).

However, in the case of CCmutE34K-R55E hetero-oligomerization with CCwt, only two stabilizing salt bridges are maintained while two destabilizing charge-charge repulsions are formed (further discussed in the results). This allows for increased specificity for CCmutE34K-R55E towards homo-oligomerization over hetero-oligomerization with CCwt. Similarly, introducing the E46K and R53E compound mutation (CCmutE46K-R53E) results in favoring homo-oligomerization (Figure 5.1E). Disfavoring hetero-oligomer formation with CCwt represents minimizing interactions with endogenous Bcr in cells.

The resulting designed four mutant candidates: p53-CCmutS41R, p53-CCmutQ60E, p53-CCmutE34K-R55E, and p53-CCmutE46K-R53E, are listed in Table 5.1 and were further assessed computationally and tested *in vitro* for their ability to retain apoptotic activity and minimize any possible interaction with endogenous Bcr.

Table 5.1 Mutant candidates and the rationale of the design for each mutation.

Mutations CCmut	Purpose	Rationale	Net Ionic Interactions
S41R	Increase binding stability	Two new salt bridges	6
Q60E	Increase binding stability	Two new salt bridges	6
E34K-R55E	Increase binding specificity (homo-dimers)	Reverse an existing salt bridge	4
E46K-R53E	Increase binding specificity (homo-dimers)	Reverse an existing salt bridge	4

5.3 Materials and Methods

5.3.1 Computational Modeling and Simulation

Models of the Bcr CC domain were built starting with the crystal structure of the N-terminal oligomerization domain of Bcr-Abl (Protein Data Bank code 1K1F, choosing residues 1-67 in each of chains A and B). Using the *swapaa* tool in Chimera (22), selenomethionine residues were reverted back to methionine, and residue 38 was mutated back to cysteine, consistent with the wild-type structures. Models of the mutant coiled-coils were built using the *swapaa* tool which facilitates placement of modified side chains by sourcing the Dunbrack backbone-dependent rotamer library to predict the most accurate side-chain rotamers (23). Models were built using ff12SB (24, 25) force field parameters and explicitly solvated in truncated octahedron with at least a 10 Å surrounding buffer of TIP3P water (26). Net-neutralizing counter-ions (Na^+/Cl^-) were incorporated using the Joung & Cheatham ion parameters (27), and 52 additional Na^+/Cl^- atoms were added to achieve an approximate ion concentration of 200 mM. All models were subjected to an extensive minimization and equilibration protocol to relax and steer systems towards energetically-favored conformations prior to production molecular dynamics (MD). An initial minimization was performed (500 steps of steepest descent,

500 steps of conjugate gradient) prior to heating of the system to 300 K. A 25 kcal/mol-Å² restraint was placed upon backbone C_α atoms throughout the initial minimization and heating step. Following the initial minimization and heating, systems were subjected to five cycles of minimization (500 steps of steepest descent, 500 steps of conjugate gradient) and equilibration, in which restraint weights were lifted sequentially from 5 kcal/mol-Å² to 1 kcal/mol-Å² following each cycle. A final equilibration was performed for 500 ps with a restraint weight of 0.5 kcal/mol-Å² prior to production MD. Constant temperature and pressure were controlled throughout the minimization protocol using a Berendsen thermostat (28) with a 0.2 coupling time.

All production MD simulations were carried out with the AMBER 12.0 modeling code suite (29, 30) for 200 ns (using a 2 fs time step) in explicit solvent, using a Langeven thermostat (31) with a collision frequency of 1 ps⁻¹ to control constant temperature and pressure (32), a 10 Å nonbonded cutoff, default particle mesh Ewald treatment of electrostatics (33) and SHAKE applied to bonds to hydrogens (34).

Analysis of the MD trajectories was performed using the PTRAJ and CPPTRAJ analysis tools (35) available in the AmberTools 12.0 and 13.0 distributions: RMSD and 2D-RMS analyses were employed to monitor if the protein structure retained the expected structure, and clustering analysis of the structures sampled during the MD (using the average linkage algorithm) (36) was used to identify the most frequently sampled protein conformations of each MD trajectory. Additionally, a DSSP analysis (37) of secondary structure was performed to determine the percent helicity of each mutant, and α-helical specific hydrogen bonds were recorded by monitoring hydrogen bonding interactions between peptide backbone atoms of *i* and *i*+4 residues. The atomic

positional fluctuations of C α backbone atoms were recorded to identify regions of flexibility in response to the induced mutations. An MM-PBSA energetic analysis was performed to assess the relative binding energies of each mutant (38, 39).

5.3.2 Cell Lines and Transient Transfections

T47D human ductal breast epithelial tumor cells (ATCC, Manassas, VA), COS-7 monkey kidney fibroblast cells (ATCC), SKOV-3.ip1 human ovarian adenocarcinoma cells (a kind gift from Dr. Margit Janát-Amsbury, University of Utah), and MCF-7 human breast adenocarcinoma cells (ATCC) were cultured in RPMI 1640 (T47D, COS-7, MCF-7) or DMEM (SKOV-3.ip1) (Invitrogen, Carlsbad, CA) supplemented with 10% FBS (Invitrogen), 1% penicillin-streptomycin (Invitrogen), 1% glutamine (Invitrogen) and 0.1% gentamycin (Invitrogen). Additionally, T47D and MCF-7 cells were supplemented with 4 mg/L insulin (Sigma, St. Louis, MO). Cells were maintained in a 5% CO $_2$ incubator at 37°C. For all assays, 3.0 x 10 5 cells for T47D and MCF-7 cells, 2.0 x 10 5 for COS-7 and SKOV-3.ip1 cells were seeded in 6-well plates (Greiner Bio-One, Monroe, NC). Approximately 24 h after seeding, transfection was performed using 1 pmol of DNA per well and Lipofectamine 2000 (Invitrogen) following the manufacturer's recommendations.

5.3.3 Plasmid Construction

The plasmids pEGFP-wt-p53 (wt-p53), pEGFP-p53-CC (p53-CCwt), and pEGFP-CC (CCwt) were subcloned as previously (9, 40). pEGFP-p53-CCmutS41R (p53-CCmutS41R), pEGFP-p53-CCmutQ60E (p53-CCmutQ60E), pEGFP-p53-CCmutE34K-

R55E (p53-CCmutE34K-R55E), and pEGFP-p53-CCmutE46K-R53E (p53-CCmutE46K-R53E) were created through site directed mutagenesis using pEGFP-p53-CC as the template.

The following primers were used for the p53-CCmutS41R mutation: 5'-ggagcgtgcaaggccCGCtccattcggcgctgg-3' and 5'-ccaggcgccgaatggaGCGggccttgacgctcc-3'; for the p53-CCmutQ60E mutation, 5'-tccgatgatctacgtggagacgttgctggccaag-3' and 5'-ctggccagcaactctccaggtagatcatgcggA-3' primers were used.

For the p53-CCmutE34K-R55E compound mutant, sequential site directed mutagenesis was carried out using the following primers: for the E34K mutation, 5'-gtggcgacatcgagcagAagctggagcgtgcaagg-3' and 5'-ccttgacgctccagctTctgctgatgctgcccac-3'; for the R55E mutation, 5'-aggtgaaccaggagcgttcGAGatgatctacgtcagacgtt-3' and 5'-aacgtctgcaggtagatcatCTCgaagCgctcctggtcacct-3' primers were used.

For the p53-CCmutE46K-R53E compound mutant, sequential site directed mutagenesis was carried out using the following primers: for the E46K mutation, 5'-gcctcattcggcgctgAagcaggaggtgaaccagg-3' and 5'-CCTGGTTCACCTCCTGCTTCAGGCGCCGAATG-GAGGC-3', for the R53E mutation, primers 5'-agcaggaggtgaaccaggagttccgatgatctactgca-3' and 5'-tgcaggtagatcatgcggaactcctggtcacctcctgct-3' were used for deletion of R53; primers 5'-gcaggaggtgaaccaggagGAGttccgatgatctactgc-3' and 5'-gcaggtagatcatgcggaaCTCctcctggtcacctcctgc-3' were used for insertion of 53E.

The plasmids pBIND-p53-CCwt, pBIND-p53CCmutE34K-R55E, pACT-p53-CCwt, and pACT-p53-CCmutE34K-R55E were cloned for the mammalian two-hybrid assay. For pBIND-p53-CCwt and pBIND-p53-CCmutE34K-R55E, DNA encoding p53-CCwt and p53-CCmutE34K-R55E was digested from the pEGFP-p53-CC and pEGFP-

p53-CCmutE34K-R55E vectors respectively, using the *Bam*HI and *Kpn*I restriction enzymes and subcloned into the pBIND vector (Promega, Madison, WI) at the *Bam*HI and *Kpn*I sites. Similarly, to clone pACT-p53-CCwt and pACT-p53-CCmutE34K-R55E, DNA encoding p53-CCwt and p53-CCmutE34K-R55E was also digested from the pEGFP-p53-CC and pEGFP-p53-CCmutE34K-R55E vectors respectively, using the *Bam*HI and *Kpn*I restriction enzymes and subcloned into the pACT vector (Promega) at the *Bam*HI and *Kpn*I sites.

5.3.4 7-AAD Assay

Following manufacturer's instructions and as previously described (41), T47D, SKOV-3.ip1, and MCF-7 cells were pelleted and resuspended in 500 μ L PBS (Invitrogen) containing 1 μ M 7-aminoactinomycin D (7-AAD) (Invitrogen) for 30 min prior to analysis by flow cytometry. The assay was performed 48 h after transfection for T47D and MCF-7 (42) and 24 h for SKOV-3.ip1. Cells were analyzed and gated for EGFP (with same fluorescence intensity to ensure equal expression of proteins) using the FACSCanto-II (BD-BioSciences, University of Utah Core Facility) and FACSDiva software. Excitation was set at 488 nm and detected at 507 nm and 660 nm, respectively. Each construct was tested three times (n=3).

5.3.5 Mammalian Two-Hybrid Assay

The pBIND-p53-CCwt (or pBIND-p53-CCmutE34K-R55E) containing the *Renilla reniformis* luciferase gene for normalization, pACT-p53-CCwt (or pACT-p53-CCmutE34K-R55E), and pG5luc (containing firefly luciferase gene, Promega) plasmids

were cotransfected using 3.5 μg of each plasmid following the manufacturer's recommendations. The pBIND-Id and pACT-MyoD (Promega) plasmids were used for the positive control, and pBIND vector lacking the coiled-coil gene was used as the negative control. Approximately 24 h after transfection, the Dual-Glo Luciferase Assay (Promega) was used to detect both firefly and renilla luminescence as previously (40). The means from duplicate transfections were taken from three separate experiments ($n=3$). As per the manufacturer's protocol, a relative response ratio was calculated using the firefly luciferase values normalized to the renilla luciferase values: $(\text{sample} - \text{ctrl}^-)/(\text{ctrl}^+ - \text{ctrl}^-)$ (43).

5.3.6 Coimmunoprecipitation (Co-IP)

Co-IP was performed as we have done before (9). Briefly, T47D cells treated with p53-CCmutE34K-R55e or p53-CCwt were prepared using the Dynabeads Co-Immunoprecipitation Kit (Invitrogen) 24 h post transfection. Approximately 0.2 g of T47D treated cell pellet was lysed in 1.8 mL of extraction buffer B (1 x IP, 100 mM NaCl, 2 mM MgCl_2 , 1 mM DTT, 1% protease inhibitor). The lysate was incubated for 30 min at 4°C with 1.5 mg of dynabeads coupled with anti-GFP antibody (ab290, Abcam). Immune complexes were then collected on a magnet, washed, and eluted using 60 μL of elution buffer. Finally, the eluted complexes were denatured and western blots were carried out as described before (9). The coiled-coil domain was probed using anti-Bcr (sc-885, Santa Cruz Biotechnology, Santa Cruz, CA). The primary antibody was detected with anti-rabbit HRP-conjugated (#7074S, Cell Signaling Technology, Danvers, MA) antibody before the addition of SuperSignal West Pico chemiluminescent substrate (Thermo

Scientific, Waltham, MA). Signals were detected using a FluorChem FC2 imager and software (Alpha Innotech, Santa Clara, CA). Each co-IP was repeated at least three times. A semi-quantitative densitometry analysis was carried out by normalizing the detected Bcr band to either p53-CCwt or p53-CCmutE34K-R55E as described before (44).

5.3.7 Statistical Analysis

For *in vitro* experiments, one-way ANOVA with Bonferroni's post test was used to compare the different groups and controls. A value of $p < 0.05$ was considered statistically significant. Error bars represent standard deviations from at least three independent experiments ($n = 3$).

5.4 Results

5.4.1 *In Silico* Modeling of Coiled-Coil Structures

and Estimation of Binding Free Energies

Computational modeling and atomistic biomolecular simulations were employed to facilitate the design of coiled-coil mutations which serve to enhance homo-oligomerization of the modified coils while disrupting hetero-oligomerization with the native coiled-coil region of Bcr. Initial simulations estimated differences in relative binding free energy of the modified coils to predict the most effective coiled-coil design (Table 5.2). All four mutants from Table 5.1 were rationally designed based on optimization of the electrostatic interactions and the potential for salt bridge formation identified in the helical wheel structure of the CC motif (helical wheel characterized previously by Taylor et al.) (20).

Table 5.2 Relative Energetic analysis of p53-CC wild type and mutants coiled-coil dimers as obtained by MM-PBSA.

Mutations	$\Delta\Delta G_{\text{binding}}$	S.E.
None (CCwt)	<i>kcal/mol</i>	
<i>Homo-dimer</i>	0	
p53-CCmutE34K-R55E		
<i>Homo-dimer</i>	7.6	0.8
<i>Hetero-dimer</i>	22.0	0.8
p53-CCmutE46K-R53E		
<i>Homo-dimer</i>	1.3	0.7
<i>Hetero-dimer</i>	8.5	0.7
p53-CCmutS41R		
<i>Homo-dimer</i>	-20.5	0.8
<i>Hetero-dimer</i>	4.7	0.8
p53-CCmutQ60E		
<i>Homo-dimer</i>	-17.1	0.7
<i>Hetero-dimer</i>	-0.1	0.7

The designed mutations aimed to enhance homo-oligomerization by either enhancement of the binding interaction between modified coiled-coils (CCmutS41R and CCmutQ60E), or disruption of the interaction between mutant and wild-type coiled-coils (CCmutE34K-R55E and CCmutE46K-R53E). Production molecular dynamics were carried out on a total of nine independent simulations, in which trajectories were generated for each of the modified coils paired with either itself (homo-dimer) or CCwt (hetero-dimer). A wild-type coiled-coil homo-dimer was used as a control.

An MM-PBSA postprocessing energetic analysis of the MD trajectories of the dimers (38, 39) was performed on each independent simulation to identify the optimal modifications to enhance self-oligomerization (see Table 5.2). Modified coiled-coils

which were designed to promote self-oligomerization by increasing the binding stability (p53-CCmutS41R and p53-CCmutQ60E) significantly enhanced the binding affinities of the homo-dimers (Table 5.2, $\Delta\Delta G = -20.5$ kcal/mol and $\Delta\Delta G = -17.1$ kcal/mol, respectively) relative to the affinity of the wt/wt homodimers. However, the modified coils failed to disrupt binding to the native CCwt (Table 5.2, $\Delta\Delta G = -4.7$ kcal/mol and $\Delta\Delta G = -0.1$ kcal/mol, respectively), suggesting that creating additional salt bridges *will not* prevent p53-CC from binding to endogenous Bcr. Results (Table 5.2) suggest that the best approach to increase self-oligomerization among the modified coiled-coils while minimizing hetero-oligomerization with Bcr is to increase the binding specificity of the coiled-coil for itself through the reversing of existing salt bridges (resembled by CCmutE34K-R55E and CCmutE46K-R53E). Energetic analyses of the modified coiled-coils featuring a reversal of salt bridges (p53-CCmutE34K-R55E and p53-CCmutE46K-R53E) revealed minimal de-stabilization of the homo-dimers p53-CCmutE34K-R55E and p53-CCmutE46K-R53E (Table 5.2, $\Delta\Delta G = 7.6$ kcal/mol and $\Delta\Delta G = 1.3$ kcal/mol, respectively) relative to the wt homodimer, and in the case of the p53-CCmutE34K-R55E mutant, a significant de-stabilization of the hetero-dimer with CCwt (Table 5.2, $\Delta\Delta G = 22.0$ kcal/mol). The p53-CCmutE46K-R53E mutant hetero-dimer with CCwt was minimally destabilized ($\Delta\Delta G = 8.5$ kcal/mol) when compared with the wt homodimer. Therefore, of the four rationally designed mutants, p53-CCmutE34K-R55E is the only variant which displays both of the desired characteristics of homo-dimer stabilization and disruption of CCwt binding, suggesting that the CCmutE34K-R55E mutant provides the most effective strategy to promote self-oligomerization and prevent interaction with native Bcr.

5.4.2 Initial Screening for *In Vitro* Activity

Next, we carried out initial *in vitro* screening of the activity of each p53-CCmut to examine if our proposed mutations abrogate the tumor suppressor function of p53-CC. Active p53-CC has been shown previously to induce significant levels of cell death in T47D breast cancer cells (9). Hence, the 7-AAD assay, which stains apoptotic and necrotic cells (45, 46), served as a screening tool to measure tumor suppressor function of the different p53-CC mutants (Figure 5.2). Surprisingly, all of the designed mutations led to abolishment of p53-CC function, except for the CCmutE34K-R55E compound mutation.

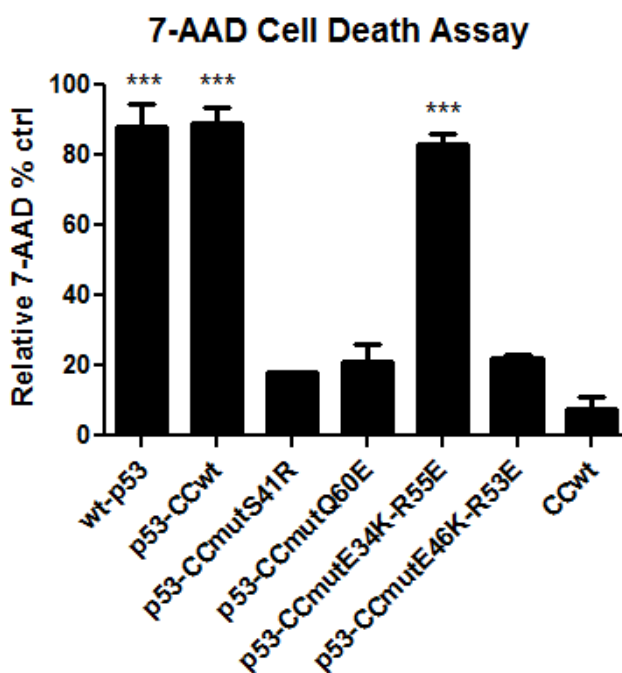


Figure 5.2 Tumor suppressor activity screening using the 7-AAD assay was conducted in T47D cells 48 h post transfection. p53-CCmutE34K-R55E is the only candidate that retains the ability to induce cell death in a similar way to p53-CCwt and the wt-p53 control. CCwt was used as a negative control. Statistical analysis was performed using one-way ANOVA with Bonferroni's post test; *** $p < 0.001$ compared to CCwt. Error bars represent standard deviations (n=3).

Figure 5.2 illustrates that p53-CCmutE34K-R55E (fifth bar) retains the apoptotic activity of p53-CCwt and wt-p53 (first two bars). As expected, the negative control CCwt alone shows no apoptotic activity in the 7-AAD assay (last bar). These findings suggest that the S41R, Q60E, and E46K-R53E mutations may disrupt the oligomerization of CC, lead to instability of the coiled-coil domain, or alter the conformation of p53, resulting in loss of tumor suppressor function (third, fourth and sixth bars, respectively).

Although computational design and modeling implies that S41R, Q60E, and E46K-R53E may be candidates for increasing salt bridge formation and binding stability, the data in Figure 5.2 illustrate that introducing any of these mutations on the CC domain leads to biological inactivation of the chimeric p53-CC. Therefore, we narrowed down our mutant candidate to p53-CCmutE34K-R55E, which favors homo-oligomer formation over hetero-dimerization with CCwt of Bcr (Table 5.2), while retaining the biological activity of p53-CCwt (Figure 5.2). Figure 5.3 shows ribbon diagrams with corresponding helical wheels (below) of CCwt homo-dimer (Figure 5.3A), CCwt:CCmutE34K-R55E hetero-dimer (Figure 5.3B), and CCmutE34K-R55E homo-dimer (Figure 5.3C). As expected from our computational design, the compound mutant CCmutE34K-R55E does not lead to formation of new additional ionic interactions (salt bridges). Instead, the same two salt bridges found in the CCwt:CCwt homo-dimer (Figure 5.3A) are preserved (but reversed) in CCmutE34K-R55E:CCmutE34K-R55E homo-dimer (Figure 5.3C). However, Figure 5.3B illustrates that two possible charge-charge repulsions in the CCwt:CCmutE34K-R55E hetero-dimer could form, which have the potential to reduce p53-CCmutE34K-R55E interaction with Bcr (aka CCwt). Results were obtained using MM-PBSA functionality of the AmberTools suite of programs (29).

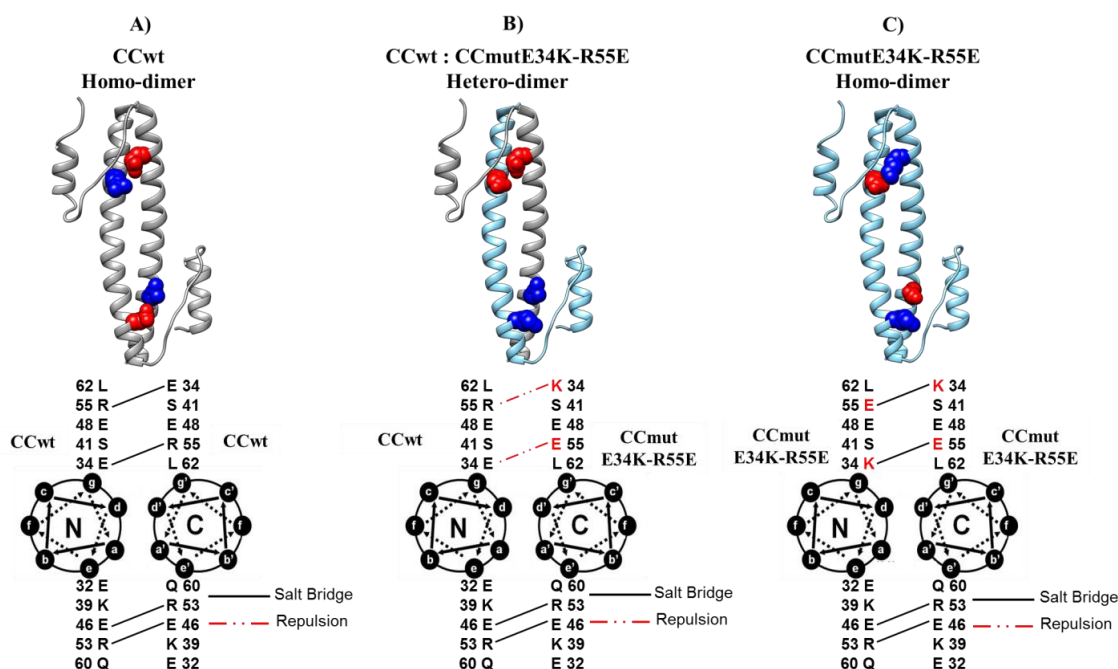


Figure 5.3 Ribbon diagrams with corresponding helical wheels of CCwt homo-dimer (A), CCwt-CCmutE34K-R55E hetero-dimer (B), and CCmutE34K-R55E homo-dimer (C). Gray ribbons represent the CCwt domain, and cyan ribbons represent the CCmutE34K-R55E domain. The side chains of key residues (Glu/Lys-34 and Arg/Glu-55) are shown as red (acidic) or blue (basic). Solid lines indicate salt bridges, while the long dash double dotted line represents charge-charge repulsions.

Every 20 ns of simulation time, energetic analyses were performed on 5 ns snapshots of simulation (0-5 ns, 20-25ns, 40-45 ns, etc.) at 25 ps intervals to examine the evolution of relative free binding energies of each system over time. The results reflect the lowest calculated free energies of the nine different MD trajectories relative to the CCwt homo-dimers (See Supporting Information 1 for more information).

5.4.3 Global Stability of p53-CCmutE34K-R55E

Several analyses were performed to evaluate the stability of CCmutE34K-R55E homo-dimer relative to the CCwt homo-dimer and the CCwt:CCmutE34K-R55E hetero-

dimer. RMSD analyses of the MD sampled structures to the initial structures revealed that both the mutant homo-dimer and mutant hetero-dimers remained close to their initial structures, as was observed with the CCwt homo-dimer (Figure 5.4).

The atomic positional fluctuations (Supporting Information 2) of C_{α} backbone atoms were recorded to identify regions of flexibility in response to the induced mutations, revealing an increase in flexibility of the CCmutE34K-R55E mutant when paired to CCwt, in the region of the E34K-R55E mutations. This can be attributed to the destabilization of the coiled-coils by the unfavorable electrostatic interactions occurring between the mutant and wild-type coiled-coils. A slight increase in the flexibility of the CCmutE34K-R55E homo-dimer is observed at N-termini and C-termini α -helical regions (Residues 1-10 & 124-134, respectively); however a DSSP secondary structure analysis (37) revealed no loss in coiled-coil helicity in the CCmutE34K-R55E homo-dimer relative to the CCwt homo-dimer (Table 5.3, helicity= 71.8% and 71.6%, respectively), suggesting that the α -helical dimerization interface remains stable.

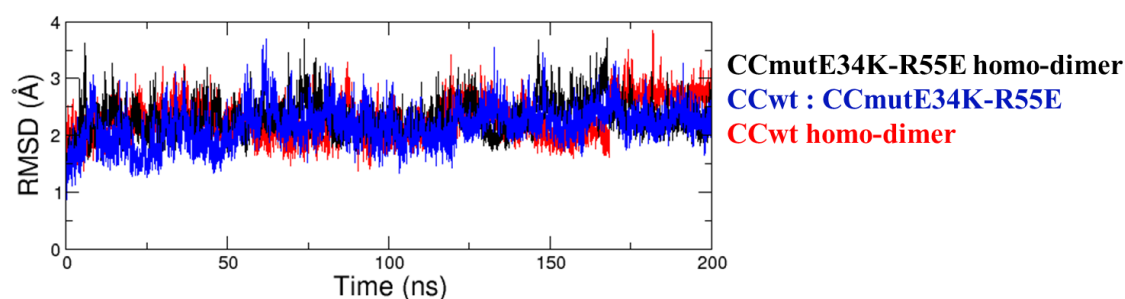


Figure 5.4 Time course of the deviation of the MD structures of the Bcr coiled-coil region (CCwt) and CCmut E34K-R55E to the experimental reference structure. One-dimensional RMSD analyses was performed to monitor the structural variance of the mutant CCmutE34K-R55E homo-dimer (*black*) and the CCwt:CCmutE34K-R55E (*blue*) relative to the CCwt homo-dimer (*red*).

Table 5.3 Relative helicity of the modified coiled-coil region CCmutE34K-R55E relative to the native coiled-coil from Bcr (CCwt).

Mutations	Secondary Structure		Hydrogen Bonds	
	Helicity	S.D.	i, i + 4 hb	S.D.
	%		%	
None (CCwt)				
<i>Homo-dimer</i>	71.6	9.6	32.1	3.7
CCmutE34K-R55E				
<i>Homo-dimer</i>	71.8	10.6	31.3	3.6
<i>Hetero-dimer</i>	71.1	11.5	31.3	3.7

Analysis of α -helical specific hydrogen bonding interactions (between backbone atoms of i and $i+4$ residues) revealed no significant difference in hydrogen bonding patterns between the CCmutE34K-R55E and CCwt homo-dimers (Table 5.3; i and $i + 4$ hydrogen bond = 33.1% and 32.1%, respectively) to indicate a loss of coiled-coil stability due to the observed atomic positional fluctuations.

Together, these results suggest that the compound mutation E34K-R55E does not affect the stability of the coiled-coil, supporting the existing evidence (Figure 5.2) that p53-CCmutE34K-R55E forms active oligomers, retaining transcriptional and tumor suppressor activity of p53.

5.4.6 Binding Assay Validates Design

To specifically address whether our lead mutant compound CCmutE34K-R55E limited hetero-oligomerization with CCwt (found in endogenous Bcr), the widely accepted mammalian two-hybrid binding assay (43) was carried out. Figure 5.5 demonstrates that formation of CCmutE34K-R55E homo-oligomers (third bar) is more favored than CCwt:CCmutE34K-R55E hetero-oligomerization (middle bar).

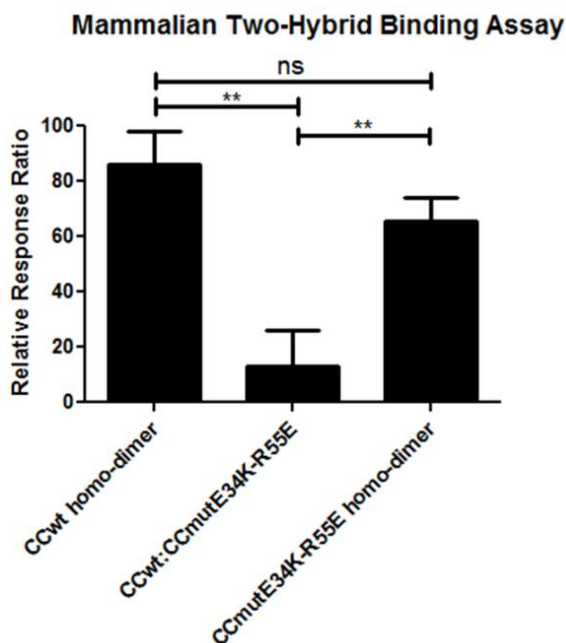


Figure 5.5 Binding of CCmutE34K-R55E homo- and hetero-dimers with CCwt tested using the mammalian two-hybrid assay. The assay was carried out in COS-7 cells 24 h post transfection. Both CCwt and CCmutE34K-R55E have similar binding as indicated by the first and third bar, respectively. The mammalian two-hybrid assay revealed weak binding of CCmutE34K-R55E hetero-dimerization with CCwt. Statistical analysis was performed using one-way ANOVA with Bonferroni's post test; ** $p < 0.01$, ns = not significant. Error bars represent standard deviations (n=3).

While CCmutE34K-R55E homo-dimerization leads to preserving all 4 possible salt bridges that normally exist in the CCwt homo-dimer (see Figure 5.3, C vs A), CCmutE34K-R55E hetero-dimerization with CCwt may produce two new possible charge-charge repulsions (see Figure 5.3B). In addition, Figure 5.5 shows no significant difference in the binding between CCwt and CCmutE34K-R55E homo-dimers (first and third bars), as expected. This similarity in binding between CCwt vs CCmutE34K-R55E homo-dimers converges with the data obtained from our computational modeling of binding energies (Table 5.2; also illustrated in Figure 5.3), in which no change of the total number of salt bridges occur as a consequence of introducing the E34K-R55E mutation

to the coiled-coil domain.

A DSSP secondary structure analysis was performed on each of the nine MD trajectories, characterizing the phi (ϕ) and psi (Ψ) backbone dihedral torsions of each residue to calculate the percentage of coiled-coil residues defined as alpha-helical. The percentage of interhelical hydrogen bonds between i and $i+4$ residues (specific to alpha-helices) formed throughout the trajectory was compared to the total number of potential i , $i+4$ hydrogen bonding interactions (total number of residues in each coiled-coil minus four).

5.4.7 p53-CCmutE34K-R55E Interaction

with Endogenous Bcr

The mammalian two-hybrid assay illustrates the ability of our CCmutE34K-R55E compound mutation in limiting the interaction of p53-CCmutE34K-R55E with the CCwt domain of endogenous Bcr in cells. To substantiate the mammalian two-hybrid assay data, a coimmunoprecipitation assay was performed to determine if exogenously added p53-CCmutE34K-R55E has limited interaction with the CCwt domain of endogenous Bcr compared to p53-CCwt. Cell lysates transfected with either p53-CCmutE34K-R55E or p53-CCwt were immunoprecipitated as we have done before (9). Endogenous Bcr that could potentially coimmunoprecipitate was probed using anti-CCwt antibody. Figure 5.6A shows that endogenous Bcr coimmunoprecipitates (i.e., interacts) with p53-CCmutE34K-R55E to a lesser extent compared to p53-CCwt. Furthermore, we carried out Bcr mean band densitometry analyses from three separate coimmunoprecipitation assays.

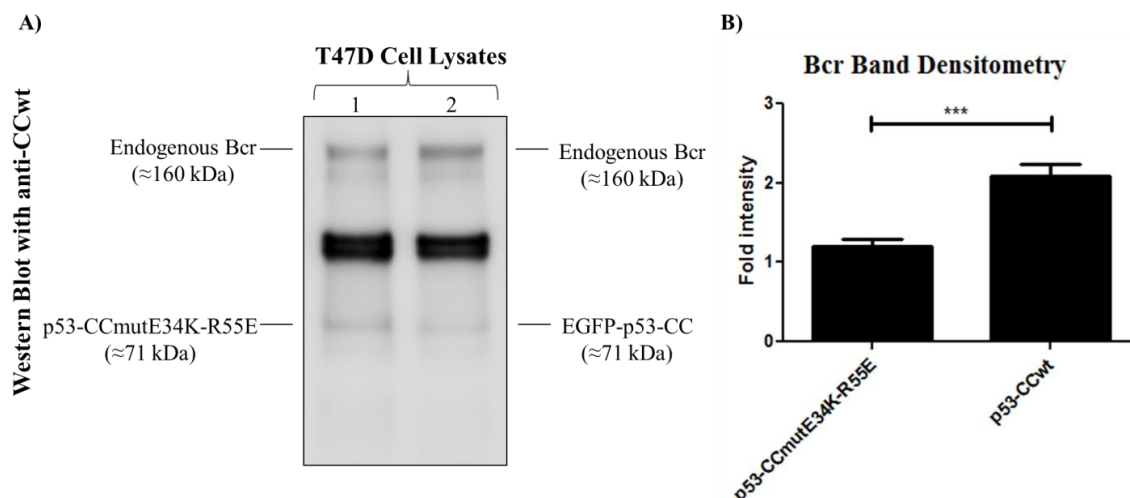


Figure 5.6 Interaction of p53-CCmutE34K-R55E and p53-CC with endogenous Bcr was investigated in T47D cells via co-IP. A) A representative cropped western blot of protein complexes coimmunoprecipitated using anti-GFP antibody is shown. Left lane, endogenous Bcr (160 kDa) coimmunoprecipitates with p53-CCmutE34K-R55E (71 kDa) to a lesser extent compared to that with p53-CC (71 kDa) in the right lane. B) Semi-quantitative densitometric analyses was carried out as described before (44) to evaluate Bcr interaction with p53-CCmutE34K-R55E and p53-CC. Mean values were analyzed using one-way ANOVA with Bonferroni's post test; *** $p < 0.001$. Error bars represent standard deviations (n=3).

Figure 5.6B shows that p53-CCwt hetero-oligomerization with endogenous Bcr is two-fold higher than the p53-CCmutE34K-R55E interaction with Bcr. These findings indicate that the E34K-R55E compound mutation reduces hetero-oligomerization with endogenous Bcr compared to CCwt interaction with Bcr, presumably due to the formation of charge-charge repulsions (see Figure 5.3B). It should be noted that prominent double secondary bands are detected by this anti-CCwt antibody even in untreated cell lysates (data not shown).

5.4.8 p53-CCmutE34K-R55E Induces Apoptosis Regardless of the p53 Status or Cancer Cell Type

To ensure that the ability of p53-CCmutE34K-R55E to induce cell death is neither dependent on endogenous p53 status nor cancer cell line specific, its apoptotic activity was tested in three different cancer cell lines; SKOV-3.ip1 human ovarian cancer cells (p53-null) (47), MCF-7 human breast cancer cells (wild type but mislocalized p53) (48), and T47D human breast carcinoma cells (mutant p53) (49). Figure 5.7 A-C demonstrates that p53-CCmutE34K-R55E is capable of inducing cell death similarly to p53-CCwt and wt-p53, regardless of the endogenous p53 status or cancer cell line.

5.5 Discussion

Since domain swapping to create p53-CC could result in p53-CC interacting with endogenous Bcr, we mutated p53-CC to avoid this. The implications of possible binding of endogenous Bcr are unknown, but may be undesired, as Bcr is a ubiquitous protein involved in inflammatory pathways and cell proliferation (14).

Since no other proteins in cells contain the Bcr CCwt motif, the sequence-specific interaction with Bcr CCwt is the only one we need be concerned with eliminating. In this report, we designed mutations in our alternative oligomerization domain, the coiled-coil, to avoid interaction with Bcr. Computationally designed and modeled mutations in the CC domain (40) were developed to minimize interactions with native endogenous Bcr. Based on initial examination of the CC motif, several possible mutation sites were identified and summarized in Table 5.1 with the rationale behind designing each mutation.

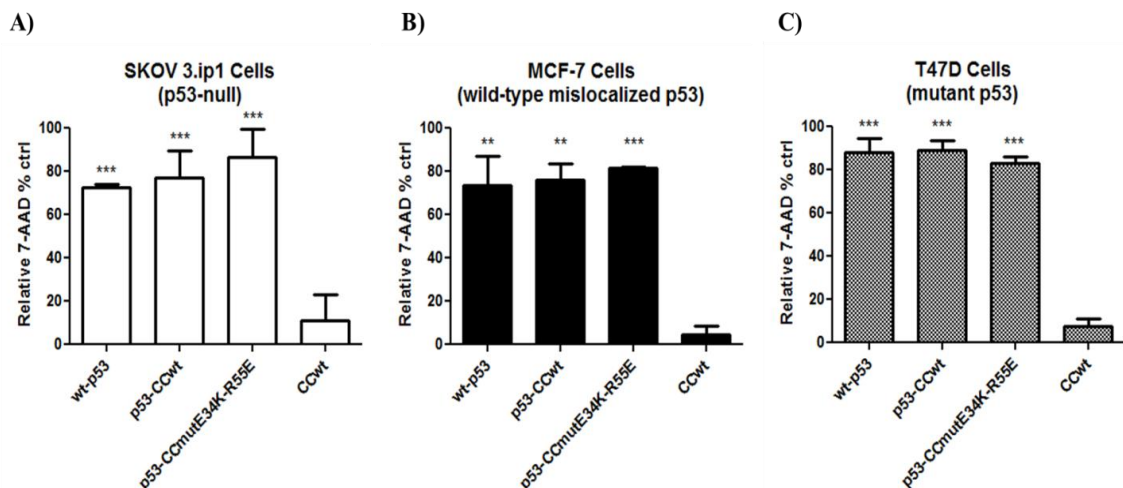


Figure 5.7 7-AAD assay was conducted in three different cell lines with varying p53 status (A) SKOV 3.ip1, (B) MCF-7, and (C) T47D cells. In all three cases, p53-CCmutE34K-R55E was capable of inducing cell death in a similar fashion compared to p53-CC and wt-p53, regardless of the endogenous p53 status or the cancer cell line used. Statistical analysis was performed using one-way ANOVA with Bonferroni's post test; ** $p < 0.01$ and *** $p < 0.001$.

In addition, Figure 5.1 shows helical diagrams representing the CCwt, the modified CC domain (CCmut), and the hypothesized changes in electrostatic interactions (salt bridges).

Two different modified coiled-coils with a single point mutation each were designed to enhance self-oligomerization. Residues Ser-41 and Gln-60 are arranged opposite of charged residues Glu-48 and Lys-39, such that the mutations S41R and Q60E serve to create additional salt bridges in the coiled-coil dimers. In the first mutant, Ser-41 was mutated to Arg, creating two new salt bridges via interaction with Glu-48 (Figure 5.1B). In the second mutant, Gln-60 was mutated to Glu, creating two new salt bridges via interaction with Lys-39 (Figure 5.1C).

Furthermore, two different modified coiled-coils with two point mutations each (compound mutants) were designed to increase binding specificity of the modified

coiled-coil for itself by disrupting affinity for CCwt. By reversing the charge of existing salt bridges (dashed line highlighted in green in Figure 5.1 D and E), a scenario is created in which charge repulsion disrupts the binding of the CCwt to the modified coiled-coils. In the p53-CCmutE34K-R55E mutant, the salt bridge between Glu-34 and Arg-55 is effectively reversed by introducing the mutations E34K and R55E. Similarly, the p53-CCmutE46K-R53E mutant features the mutations E46K and R53E to reverse the salt bridge between Glu-46 and Arg-53.

Molecular modeling, MD simulation, and free energy analysis revealed the ranking of our different modifications in terms of minimizing CCwt-CCmut hetero-oligomerization (Table 5.2). On one hand, free binding energy analysis by MM-PBSA revealed that CCmutS41R and CCmutQ60E may both have strong homo-oligomer binding stability (Table 5.2, $\Delta\Delta G = -20.5$ kcal/mol and $\Delta\Delta G = -17.1$ kcal/mol, respectively) relative to the wt homo-dimer. However, the same analysis revealed that both, CCmutS41R and CCmutQ60E, also have similar or increased relative binding affinities for the CCwt coil (Table 5.2, $\Delta\Delta G = 4.7$ kcal/mol and $\Delta\Delta G = -0.1$ kcal/mol, respectively). In addition, there is no significant difference in relative binding energies between CCmutE46K-R53E homo-dimers and hetero-dimers (Table 5.2, $\Delta\Delta G = 1.3$ kcal/mol and $\Delta\Delta G = 8.5$ kcal/mol, respectively). On the other hand, the free energy analyses showed that CCmutE34K-R55E may be a suitable candidate for minimizing interactions with CCwt, with CCmutE34K-R55E disfavoring interaction with CCwt. A significant difference in binding energies exists between the CCmutE34-R55E homo-dimer and hetero-dimer with CCwt (Table 5.2, $\Delta\Delta G = 7.6$ kcal/mol and $\Delta\Delta G = 22.0$ kcal/mol, respectively). This result suggests that CCmutE34K-R55E favors homo-

oligomerization over hetero-oligomerization with CCwt of Bcr. Furthermore, the binding of the CCmutE34K-R55E hetero-dimer with CCwt is less favored (Table 5.2, $\Delta\Delta G= 22.0$ kcal/mol) compared to that of CCwt homo-oligomer (Table 5.2, $\Delta\Delta G= 7.6$ kcal/mol). To test if our possible mutations led to any abrogation in p53-CC activity, we carried out an *in vitro* cell death assay in which p53-CC has been proven previously to induce cell death (in T47D cells) (9). Figure 5.2 showed that all mutants (p53-CCmutS41R, p53-CCmutQ60E, and p53-CCmutE46K-R53E) have lost the tumor suppressor activity of p53-CC except for the compound mutant p53-CCmutE34K-R55E. Thus, p53-CCmutE34K-R55E was the lead, eliminating the need to test the inactive mutants in the remaining experiments.

Both the mammalian two-hybrid assay (Figure 5.5) and the co-immunoprecipitation experiment (Figure 5.6) validate the computational modeling and strongly indicate that p53-CCmutE34K-R55E minimize interaction with CCwt of endogenous Bcr in cells, suggesting that our hypothesized interactions are indeed occurring. Finally, we confirmed that the tumor suppressor activity (measured by apoptotic activity) of p53-CCmutE34K-R55E remains consistent regardless of endogenous p53 status or the type of cancer cell line as shown in Figure 5.7.

This study showed how *in silico* modeling can guide experimental design (as we have done before) (50) and that further iterations of *in vitro* design resulted in an enhanced version of our chimeric p53 (9). The resulting rationally designed p53-CCmutE34K-R55E avoids binding to endogenous Bcr and yet retains potent apoptotic activity in a variety of cancer cell lines, regardless of p53 status. This construct will be used for future gene therapy experiments for treatment of cancers characterized by p53

dysfunction, which represent over half of all human cancers.

5.5.1 Explanation of the Potential Deviation between

Results Obtained *In Silico* and *In Vitro*

In silico and *in vitro* studies correlate in terms of describing overall binding trends observed of our mutant candidates and endogenous Bcr. However, the results obtained from relative energetic analysis of p53-CC wild type and mutant coiled-coil dimers obtained by MM-PBSA may not be representative of the full interactions taking place in the cellular environment, which may explain the partial deviation between the two sets of data. Although *in silico* estimations (Table 5.2) of relative free binding energies suggest disfavored hetero-oligomerization between our lead candidate p53-CCmutE34K-R55E and endogenous Bcr ($\Delta\Delta G_{\text{binding}} = 22.0$ kcal/mol), actual binding evaluation *in vitro* revealed that introduction of the E34K-R55E reduces potential interaction with endogenous Bcr by 2 fold (co-immunoprecipitation, Figure 5.6). Some of the reasons that may help explain the deviation between *in silico* and *in vitro* estimations of relative binding are discussed below:

- I. While the calculations of relative binding energies *in silico* are based on estimations of the dimeric interphase binding of each mutant to itself (homo-oligomerization) or endogenous Bcr (hetero-oligomerization) relative to the wild type coiled-coil dimer, actual evaluation of binding *in vitro* via co-immunoprecipitation accounts for the interaction on a tetrameric scale as well as the dimeric interphase. Hence, it is logical to observe differences between *in silico* and *in vitro* evaluation of mutant coiled-coil binding to endogenous Bcr since

- interactions in the tetrameric interphase are not accounted for in the relative free binding energy estimations.
- II. Another factor that may contribute to the observed difference in disfavoring hetero-oligomerization of CCmutE34K-R55E *in silico* vs. *in vitro* could be attributed to the fact that the conditions used for *in silico* simulations do not fully represent the actual intracellular environment where these interactions actually take place. For instance, although net-neutralizing counter-ions (Na^+/Cl^-) were incorporated using the Joung & Cheatham ion parameters (27), and 52 additional Na^+/Cl^- atoms were added to achieve an approximate ion concentration of 200 mM, there are other ions (including divalent ions such Ca^{++}) that are present in the cells that may affect the overall interaction. Furthermore, since the rationale behind our modifications on the coiled-coil domain is based on altering the ionic salt bridges that form in the dimeric interphase, these divalent ions present in cells and not accounted for in the relative free binding energy calculations *in silico* may screen the charged residues responsible for salt bridge formation, leading to a decrease in overall binding *in vitro* compared to *in silico* estimations.
- III. Although solute entropy is accounted for in the relative free energies calculated according to standard formulas in order to obtain more representative approximation of relative binding energies, the full entropic contributions to the relative free binding energies calculated may be different than what exists in reality in cells. This can cause further deviations between *in silico* estimations and *in vitro* measurements of the reduction in hetero-oligomerization between our lead candidate p53-CCmutE34K-R55E and endogenous Bcr.

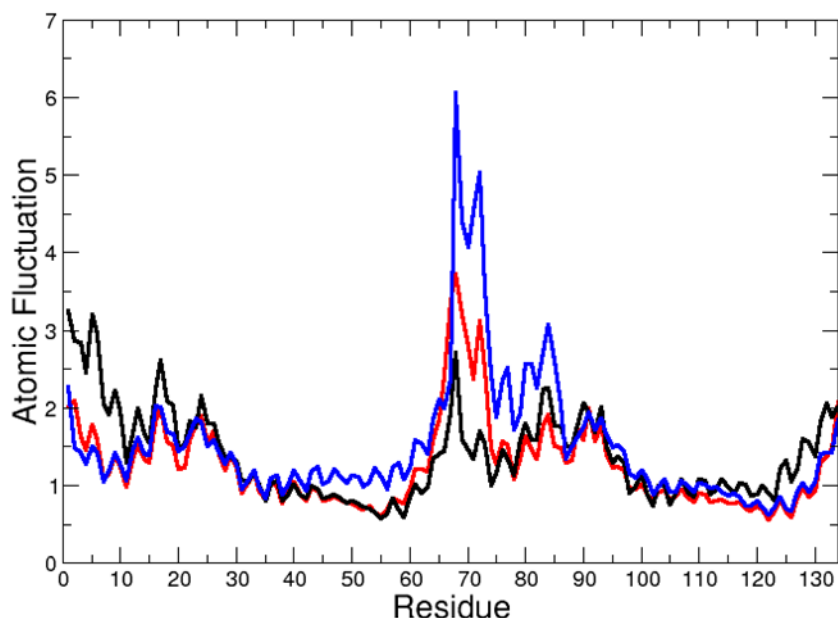
Additionally, the potential reason for lack of activity of the mutant candidates p53-CCmutE46K-R53E, p53-CCmutS41R, and p53-CCmutQ60E must be addressed. Although estimations of relative free binding energies of p53-CCmutE46K-R53E heterodimers may suggest that introduction of the E46K-R53E mutations may favor homodimerization over hetero-oligomerization with endogenous Bcr, our activity assays (Figure 5.2) revealed that introduction of the E46K-R53E resulted in complete abolishment of activity. Similarly, introduction of S41R and Q60E also resulted in complete loss of activity compared to p53-CCwt. We speculate that introduction of these mutations may disrupt the overall conformation and stability of the coiled-coil domain, leading to loss of the oligomerization required for transcriptional activation and tumor suppressor function. We also postulate that this structural instability may be in the context of fully formed tetramers, since the relative free binding energies estimated *in silico* appear to support stable formation of coiled-coil dimers. However, to fully investigate the actual significance of these residues (S41, Q60, E46, R53) for proper tetramer formation and oligomerization, a better computational model must be utilized that has the potential to investigate the tetrameric coiled-coil interphase on full scale rather than dimeric interphase only. This is beyond the scope of this dissertation work, but is a potential new area for computational exploration. Finally, *in silico* experiments were not designed for one to obtain a single absolute free energy for which to compare with a single free energy obtained experimentally. Instead, the *in silico* experiments were viewed as an ensemble, and are relevant only when viewed in this manner. Further, the *in silico* free energy calculations were used in this case to obtain a baseline comparison of what might work out experimentally, not to provide absolute free binding energy values.

5.6 Supporting Information

MM-PBSA Energetic Analysis at 5 ns Snapshots (kcal/mol)

System	0-5 ns	20-25 ns	40-45 ns	60-65 ns	80-85 ns	100-105 ns	120-125 ns	140-145 ns	160-165 ns	180-185 ns	195-200 ns
CCwt <i>Homo</i>	-39.6	-58.8	-50.1	-52.2	-52.5	-59.5	-52.8	-55.0	-37.8	-42.3	-45.4
CCmutE34K-R55E <i>Homo</i>	-23.7	-23.6	-32.3	-28.1	-31.2	-37.5	-51.9	-41.8	-35.8	-39.9	-28.0
CCmutE34K-R55E <i>Hetero</i>	-11.5	-20.2	-23.9	-22.4	-22.8	-6.7	-35.9	-28.8	-20.5	-37.5	-35.6
CCmutE46K-R53E <i>Homo</i>	-25.7	-14.8	-14.6	-58.2	-32.8	-34.6	-35.8	-35.3	-33.4	-38.5	-31.5
CCmutE46K-R53E <i>Hetero</i>	-22.9	-22.1	-37.7	-42.7	-45.2	-41.1	19.2	-51.0	-42.7	-48.0	-35.1
CCmutS41R <i>Homo</i>	-51.5	-34.7	-72.2	-70.4	-64.1	-64.5	-64.6	-80.0	-62.8	-54.4	-62.3
CCmutS41R <i>Hetero</i>	-52.9	-54.8	-49.9	-37.2	-39.8	-52.7	-40.8	-35.0	-39.3	-40.1	-14.8
CCmutQ60E <i>Homo</i>	-53.2	-63.2	-68.4	-54.5	-54.6	-63.4	-62.5	-65.1	-64.8	-63.2	-76.6
CCmutQ60E <i>Hetero</i>	-43.0	-59.6	-58.5	-55.2	-47.1	-35.1	-46.0	-47.3	-43.9	-37.9	-44.1

Supporting Information 5.1 MM-PBSA energetic analysis at 5 ns snapshots. At 20 ns intervals, an MM-PBSA energetic analysis was performed (over a 5 ns window sampled at 25 ps intervals) to uncover the most energetically favorable conformations of each system. Because each simulation will sample its most favorable conformation independently and at varying time points throughout the simulation, it is beneficial to perform the energetic analyses at various time points in order to build a profile of the relative binding free energies of each of the different systems as the energies evolve over time. Highlighted are the most favorable relative binding free energies of each system as they occur at various points in time throughout the 200 ns trajectory.



Supporting Information 5.2 Atomic positional fluctuations of the E34K-R55E compound mutant relative to the wild-type homo-dimer. Atomic fluctuations of C_{α} backbone atoms were recorded to identify changes in coil flexibility among p53-CCmutE34K-R55E homo-dimer (*black*) and hetero-dimer (complexed with wild-type) (*blue*) relative to the wild-type coiled-coil homo-dimer (*red*). Residues 1-67 correspond to chain A, while residues 68-134 correspond to chain B.

5.7 References

1. A.J. Levine and M. Oren. The first 30 years of p53: growing ever more complex. *Nat Rev Cancer*. 9:749-758 (2009).
2. M. Hollstein, D. Sidransky, B. Vogelstein, and C.C. Harris. p53 mutations in human cancers. *Science*. 253:49-53 (1991).
3. N. Turner, E. Moretti, O. Siclari, I. Migliaccio, L. Santarpia, M. D'Incalci, S. Piccolo, A. Veronesi, A. Zambelli, G. Del Sal, and A. Di Leo. Targeting triple negative breast cancer: Is p53 the answer? *Cancer Treat Rev*. 39:541-550 (2013).
4. M.J. Waterman, J.L. Waterman, and T.D. Halazonetis. An engineered four-stranded coiled coil substitutes for the tetramerization domain of wild-type p53 and alleviates transdominant inhibition by tumor-derived p53 mutants. *Cancer Res*. 56:158-163 (1996).

5. A. Willis, E.J. Jung, T. Wakefield, and X. Chen. Mutant p53 exerts a dominant negative effect by preventing wild-type p53 from binding to the promoter of its target genes. *Oncogene*. 23:2330-2338 (2004).
6. S. Kern, K. Kinzler, A. Bruskin, D. Jarosz, P. Friedman, C. Prives, and B. Vogelstein. Identification of p53 as a sequence-specific DNA-binding protein. *Science*. 252:1708-1711 (1991).
7. J. Milner and E.A. Medcalf. Cotranslation of activated mutant p53 with wild type drives the wild-type p53 protein into the mutant conformation. *Cell*. 65:765-774 (1991).
8. S. Srivastava, S. Wang, Y.A. Tong, Z.M. Hao, and E.H. Chang. Dominant negative effect of a germ-line mutant p53: a step fostering tumorigenesis. *Cancer Research*. 53:4452-4455 (1993).
9. A. Okal, M. Mossalam, K.J. Matissek, A.S. Dixon, P.J. Moos, and C.S. Lim. A chimeric p53 evades mutant p53 transdominant inhibition in cancer cells. *Mol Pharm*. 10:3922-3933 (2013).
10. P. Jeffrey, S. Gorina, and N. Pavletich. Crystal structure of the tetramerization domain of the p53 tumor suppressor at 1.7 angstroms. *Science*. 267:1498-1502 (1995).
11. X. Zhao, S. Ghaffari, H. Lodish, V.N. Malashkevich, and P.S. Kim. Structure of the Bcr-Abl oncoprotein oligomerization domain. *Nat Struct Biol*. 9:117-120 (2002).
12. M.W. Deininger, J.M. Goldman, and J.V. Melo. The molecular biology of chronic myeloid leukemia. *Blood*. 96:3343-3356 (2000).
13. D.W. Woessner, C.S. Lim, and M.W. Deininger. Development of an effective therapy for chronic myelogenous leukemia. *Cancer J*. 17:477-486 (2011).
14. J.D. Alexis, N. Wang, W. Che, N. Lerner-Marmarosh, A. Sahni, V.A. Korshunov, Y. Zou, B. Ding, C. Yan, B.C. Berk, and J. Abe. Bcr kinase activation by angiotensin II inhibits peroxisome-proliferator-activated receptor gamma transcriptional activity in vascular smooth muscle cells. *Circ Res*. 104:69-78 (2009).
15. S.J. Yi, J. Groffen, and N. Heisterkamp. Bcr is a substrate for Transglutaminase 2 cross-linking activity. *BMC Biochem*. 12:8 (2011).
16. J.D. Alexis, N. Wang, W. Che, N. Lerner-Marmarosh, A. Sahni, V.A. Korshunov, Y. Zou, B. Ding, C. Yan, B.C. Berk, and J. Abe. Bcr kinase activation by angiotensin II inhibits peroxisome-proliferator-activated receptor gamma transcriptional activity in vascular smooth muscle cells. *Circ Res*. 104:69-78 (2009).
17. J.M. Mason and K.M. Arndt. Coiled coil domains: stability, specificity, and biological implications. *ChemBiochem*. 5:170-176 (2004).
18. A. Lupas. Coiled coils: new structures and new functions. *Trends Biochem Sci*. 21:375-382 (1996).

19. P. Burkhard, J. Stetefeld, and S.V. Strelkov. Coiled coils: a highly versatile protein folding motif. *Trends in Cell Biology*. 11:82-88 (2001).
20. C.M. Taylor and A.E. Keating. Orientation and oligomerization specificity of the Bcr coiled-coil oligomerization domain. *Biochemistry*. 44:16246-16256 (2005).
21. J.R. McWhirter, D.L. Galasso, and J.Y. Wang. A coiled-coil oligomerization domain of Bcr is essential for the transforming function of Bcr-Abl oncoproteins. *Molecular and Cellular Biology*. 13:7587-7595 (1993).
22. E.F. Pettersen, T.D. Goddard, C.C. Huang, G.S. Couch, D.M. Greenblatt, E.C. Meng, and T.E. Ferrin. UCSF Chimera--a visualization system for exploratory research and analysis. *Journal of Computational Chemistry*. 25:1605-1612 (2004).
23. M.V. Shapovalov and R.L. Dunbrack, Jr. A smoothed backbone-dependent rotamer library for proteins derived from adaptive kernel density estimates and regressions. *Structure*. 19:844-858 (2011).
24. V. Hornak, R. Abel, A. Okur, B. Strockbine, A. Roitberg, and C. Simmerling. Comparison of multiple Amber force fields and development of improved protein backbone parameters. *Proteins*. 65:712-725 (2006).
25. W.D. Cornell, P. Cieplak, C.I. Bayly, I.R. Gould, K.M. Merz, D.M. Ferguson, D.C. Spellmeyer, T. Fox, J.W. Caldwell, and P.A. Kollman. A second generation force field for the simulation of proteins, nucleic acids, and organic molecules. *Journal of the American Chemical Society*. 117:5179-5197 (1995).
26. W.L. Jorgensen, J. Chandrasekhar, J.D. Madura, R.W. Impey, and M.L. Klein. Comparison of simple potential functions for simulating liquid water. *The Journal of Chemical Physics*. 79:926-935 (1983).
27. I.S. Joung and T.E. Cheatham, 3rd. Determination of alkali and halide monovalent ion parameters for use in explicitly solvated biomolecular simulations. *J Phys Chem B*. 112:9020-9041 (2008).
28. H.J.C. Berendsen, J.P.M. Postma, W.F. van Gunsteren, A. DiNola, and J.R. Haak. Molecular dynamics with coupling to an external bath. *The Journal of Chemical Physics*. 81:3684-3690 (1984).
29. T.A.D. D.A. Case, T.E. Cheatham, III, C.L. Simmerling, J. Wang, R.E. Duke, R. Luo, R.C. Walker, W. Zhang, K.M. Merz, B. Roberts, S. Hayik, A. Roitberg, G. Seabra, J. Swails, A.W. Goetz, I. Kolossváry, K.F. Wong, F. Paesani, J. Vanicek, R.M. Wolf, J. Liu, X. Wu, S.R. Brozell, T. Steinbrecher, H. Gohlke, Q. Cai, X. Ye, J. Wang, M.-J. Hsieh, G. Cui, D.R. Roe, D.H. Mathews, M.G. Seetin, R. Salomon-Ferrer, C. Sagui, V. Babin, T. Luchko, S. Gusarov, A. Kovalenko, and P.A. Kollman (2012), AMBER 12, University of California, San Francisco.
30. D.A. Pearlman, D.A. Case, J.W. Caldwell, W.S. Ross, T.E. Cheatham III, S. DeBolt, D. Ferguson, G. Seibel, and P. Kollman. AMBER, a package of computer programs for applying molecular mechanics, normal mode analysis, molecular dynamics and free energy calculations to simulate the structural and energetic properties of molecules. *Computer Physics Communications*. 91:1-41 (1995).

31. R. Zwanzig. Nonlinear generalized Langevin equations. *J Stat Phys.* 9:215-220 (1973).
32. R.J. Loncharich, B.R. Brooks, and R.W. Pastor. Langevin dynamics of peptides: the frictional dependence of isomerization rates of N-acetylalanyl-N'-methylamide. *Biopolymers.* 32:523-535 (1992).
33. U. Essmann, L. Perera, M.L. Berkowitz, T. Darden, H. Lee, and L.G. Pedersen. A smooth particle mesh Ewald method. *The Journal of Chemical Physics.* 103:8577-8593 (1995).
34. J.-P. Ryckaert, G. Ciccotti, and H.J.C. Berendsen. Numerical integration of the cartesian equations of motion of a system with constraints: molecular dynamics of n-alkanes. *Journal of Computational Physics.* 23:327-341 (1977).
35. D.R. Roe and T.E. Cheatham. PTRAJ and CPPTRAJ: Software for processing and analysis of molecular dynamics trajectory data. *Journal of Chemical Theory and Computation.* 9:3084-3095 (2013).
36. J. Shao, S.W. Tanner, N. Thompson, and T.E. Cheatham. Clustering Molecular Dynamics Trajectories: 1. Characterizing the performance of different clustering algorithms. *Journal of Chemical Theory and Computation.* 3:2312-2334 (2007).
37. B. Rost and C. Sander. Prediction of protein secondary structure at better than 70% accuracy. *Journal of Molecular Biology.* 232:584-599 (1993).
38. B.R. Miller, T.D. McGee, J.M. Swails, N. Homeyer, H. Gohlke, and A.E. Roitberg. MMPBSA.py: An efficient program for end-state free energy calculations. *Journal of Chemical Theory and Computation.* 8:3314-3321 (2012).
39. P.A. Kollman, I. Massova, C. Reyes, B. Kuhn, S. Huo, L. Chong, M. Lee, T. Lee, Y. Duan, W. Wang, O. Donini, P. Cieplak, J. Srinivasan, D.A. Case, and T.E. Cheatham, 3rd. Calculating structures and free energies of complex molecules: combining molecular mechanics and continuum models. *Acc Chem Res.* 33:889-897 (2000).
40. A.S. Dixon, S.S. Pendley, B.J. Bruno, D.W. Woessner, A.A. Shimpi, T.E. Cheatham, 3rd, and C.S. Lim. Disruption of Bcr-Abl coiled coil oligomerization by design. *J Biol Chem.* 286:27751-27760 (2011).
41. M. Mossalam, K.J. Matissek, A. Okal, J.E. Constance, and C.S. Lim. Direct induction of apoptosis using an optimal mitochondrially targeted p53. *Mol Pharm.* 9:1449-1458 (2012).
42. M. Mossalam, K.J. Matissek, A. Okal, J.E. Constance, and C.S. Lim. Direct induction of apoptosis using an optimal mitochondrially targeted p53. *Mol Pharm.* 9:1449-1458 (2012).
43. A.S. Dixon, G.D. Miller, B.J. Bruno, J.E. Constance, D.W. Woessner, T.P. Fidler, J.C. Robertson, T.E. Cheatham, and C.S. Lim. Improved coiled-coil design enhances interaction with Bcr-Abl and induces apoptosis. *Mol Pharm.* 9:187-195 (2012).

44. D.W. Woessner and C.S. Lim. Disrupting BCR-ABL in combination with secondary leukemia-specific pathways in CML cells leads to enhanced apoptosis and decreased proliferation. *Mol Pharm.* 10:270-277 (2013).
45. I. Schmid, W.J. Krall, C.H. Uittenbogaart, J. Braun, and J.V. Giorgi. Dead cell discrimination with 7-amino-actinomycin D in combination with dual color immunofluorescence in single laser flow cytometry. *Cytometry.* 13:204-208 (1992).
46. M.J. Serrano, P. Sanchez-Rovira, I. Algarra, A. Jaen, A. Lozano, and J.J. Gaforio. Evaluation of a gemcitabine-doxorubicin-paclitaxel combination schedule through flow cytometry assessment of apoptosis extent induced in human breast cancer cell lines. *Japanese Journal of Cancer Research : Gann.* 93:559-566 (2002).
47. L. Emdad, D. Sarkar, I.V. Lebedeva, Z.Z. Su, P. Gupta, P.J. Mahareshti, P. Dent, D.T. Curiel, and P.B. Fisher. Ionizing radiation enhances adenoviral vector expressing mda-7/IL-24-mediated apoptosis in human ovarian cancer. *Journal of Cellular Physiology.* 208:298-306 (2006).
48. L.M. Mooney, K.A. Al-Sakkaf, B.L. Brown, and P.R. Dobson. Apoptotic mechanisms in T47D and MCF-7 human breast cancer cells. *Br J Cancer.* 87:909-917 (2002).
49. Y. Tomita, N. Marchenko, S. Erster, A. Nemajerova, A. Dehner, C. Klein, H. Pan, H. Kessler, P. Pancoska, and U.M. Moll. WT p53, but not tumor-derived mutants, bind to Bcl2 via the DNA binding domain and induce mitochondrial permeabilization. *J Biol Chem.* 281:8600-8606 (2006).
50. A.S. Dixon, S.S. Pendley, B.J. Bruno, D.W. Woessner, A.A. Shimpi, T.E. Cheatham, and C.S. Lim. Disruption of BCR-ABL coiled-coil oligomerization by design. *Journal of Biological Chemistry* (2011).

CHAPTER 6

CONCLUSIONS AND FUTURE WORK

6.1 Conclusions

This dissertation described the design of a novel p53-based gene therapeutic that is capable of inducing cell death in several types of cancer, regardless of p53 mutation, mislocalization, deletion, or malfunction occurring in these cancer cells. The main theme of the work is to overcome the limitations of using wt p53 in cancer gene therapy, and creating an enhanced version of the tumor suppressor. Hence, we designed the chimeric p53-CC for the purpose of evading interaction with mutant p53 and consequently, bypassing transdominant inhibition in cancer cells. These approaches lead to the hypothesis that *swapping the oligomerization domain of p53 with an alternative oligomerization domain will prevent transdominant inhibition by mutant p53 in cancer cells*. The activity of p53-CC was investigated *in vitro* for proof-of-concept and to validate its tumor suppressor functions. The chimeric p53-CC was then tested in an orthotopic breast cancer mouse model to investigate if the activity observed *in vitro* translates *in vivo*. Aided by computational design, we then investigated possible alterations and mutations that can be introduced on our chimeric p53-CC to enhance its specificity.

6.1.1 Chimeric p53-CC Maintains Tumor Suppressor Function

Due to the dominant negative effect of mutant p53, there has been limited success with wt p53 cancer gene therapy. Therefore, an alternative oligomerization domain for p53 was investigated to enhance the utility of p53 for gene therapy. The tetramerization domain of p53 was substituted with the CC domain from Bcr. Our chimeric p53-CC localized to the nucleus successfully upon expression and in fact showed a similar expression profile of p53 target genes relative to wt p53. Our apoptosis assays revealed that p53-CC was capable of inducing cell death similar to wt p53 in nondominant negative cancer cells, regardless of endogenous p53 status or cancer cell type. Additionally, we confirmed via reporter gene assays that p53-CC is indeed transcriptionally active. Because p53 transcriptional activity is dependent on tetrameric formation of the protein, this in fact suggests that our alternative oligomerization domain (CC) is capable of driving tetramerization of p53-CC. Since we hypothesized that swapping the TD of p53 with CC will allow for our p53-CC chimera to evade hetero-oligomerization with mutant p53, we carried out co-immunoprecipitation studies to detect any possible interaction with endogenous p53. As expected, p53-CC escaped any hetero-oligomerization with endogenous p53, while wt p53 showed significant levels of interaction with endogenous mutant p53. The biological outcomes of the ability of p53 to escape transdominant inhibition was then tested, first with transdominant mutant p53 overexpression, and second, in MDA-MB-468 cells that harbor a tumor-derived endogenous transdominant negative p53 mutant. In both cases, p53-CC appears to not be affected by this endogenous transdominant inhibition. Finally, adenoviral delivery of

p53-CC was tested in MDA-MB-468 cells as well as a p53-null cell line to determine feasibility of *in vivo* studies.

6.1.2 Validation of p53-CC Tumor Suppressor

Function *In Vivo*

Since we validated that the chimeric superactive p53-CC with an alternative oligomerization domain is capable of escaping transdominant inhibition by mutant p53 *in vitro*, we initiated animal studies to examine the activity of p53-CC *in vivo*. MDA-MB-468 human breast adenocarcinoma cells represent an aggressive breast cancer cell line characterized as triple negative due to the absence of molecular targets including estrogen receptor, progesterone receptor, and human epidermal growth factor receptor 2 (1). Importantly, MDA-MB-468 cells harbor a dominant negative mutant p53 capable of impairing the function of wt-p53 (2-4). We therefore used this cell line to induce orthotopic breast tumors in mice to compare the impact of the dominant negative effect of mutant p53 on the biological activity of p53-CC and wt p53 in viral-mediated gene therapy. As expected, p53-CC treatment group achieved significant reduction in mean tumor size compared to wt p53 and control groups. Interestingly, wt p53 treatment resulted in stable disease and halted tumor progression. Our findings from the *in vivo* efficacy study revealed that p53-CC could achieve tumor *regression* of an aggressive p53-dominant negative breast cancer model *in vivo*, while wt p53 is only capable of halting tumor progression. This is a critical breakthrough in p53 gene therapy not achieved before. Furthermore, we investigated the underlying differential mechanisms of activity for p53-CC and wt p53 in the MDA-MB-468 tumor model. We discovered that

the difference in outcome of the tumor size reduction was due in part to the ability of p53-CC to activate the apoptotic pathway, whereas wt p53 activates cell cycle arrest via p21 induction. These findings are supported by immunohistochemistry staining and western blot analyses from *in vitro* as well as *in vivo* MDA-MB-468 cells and tumor tissue samples. Therefore, our compelling *in vivo* data demonstrates that p53-CC is more effective than wt p53 in inducing apoptosis, and may serve as a potent and reliable novel anticancer therapeutic.

6.1.3 Altering the Design of the p53-CC Chimera to Minimize Interaction with Bcr

Since domain swapping to create the p53-CC chimera could result in p53-CC interacting with endogenous Bcr, modifications on the CC domain are necessary to minimize potential interactions with Bcr. Hence, we hypothesized that certain modifications to the CC domain in p53-CC could reduce potential interactions with endogenous Bcr in cells. We investigated the possible design of mutations that will form opposing charges on residues **e** to **e'** and **g** to **g'** of the coiled-helices (where the ' denotes a residue on the opposing coiled-coil in the dimer). This could lead to an increase in salt bridge formation, which has the potential to improve homo-dimerization of CC mutants and disfavor hetero-oligomerization with CCwt, with the goal of minimizing potential interactions with endogenous Bcr in cells. *In silico* examination of CCwt revealed that introducing S41R (Arg, basic) and Q60E (Glu, acidic) mutations separately, would potentially form two extra salt bridges per mutation. These two mutant candidates are referred to as CCmutS41R and CCmutQ60E. In addition, examination of the coiled-coil

interchain salt bridges indicated that two more potential compound mutants (i.e., more than one mutation per candidate) could be made to improve homo-dimerization of CC mutants. Mutation of Glu-34 to Lys and Arg-55 to a Glu (CCmutE34K-R55E) will preserve all 4 stabilizing salt bridges found in CCwt in the case of CCmut homo-oligomerization. However, in the case of CCmutE34K-R55E hetero-oligomerization with CCwt, only 2 stabilizing salt bridges are maintained while 2 destabilizing charge-charge repulsions are formed. Similarly, another mutant can be created by introducing the E46K and R53E compound mutation (CCmutE46K-R53E), which results in favoring homo-oligomerization over hetero-oligomerization with CCwt. Computational and *in vitro* assessment of the 4 designed mutants revealed that p53-CCmutE34K-R55E is the only candidate that maintains the tumor suppressor function of p53, and hence was considered the lead compound. An *in vitro* protein binding assay (mammalian two-hybrid) as well as coimmunoprecipitation analyses validated that p53-CCmutE34K-R55E succeeds at minimizing interactions with endogenous Bcr compared to p53-CC. Therefore, this construct will be used for future gene therapy experiments for treatment of cancers characterized by p53 dysfunction, which represent over half of human cancers.

6.2 Future Studies

6.2.1 Exploring the Differential in Target Gene

Regulation by p53-CC vs. Wt p53

In Chapter 4, we suggested that p53-CC favors induction of apoptosis, while wt p53 favors induction of cell cycle arrest, in the MDA-MB-468 breast cancer animal model. Immunohistochemistry staining and western blot analysis from tumor tissues

treated with Ad-p53-CC expressed low levels of p21 (reduced cell cycle arrest) but high levels of active caspase-3 (increased apoptosis). In contrast, tumor tissues injected with Ad-wt-p53 expressed high levels of p21 (increased cell cycle arrest) but low levels of caspase-3 (decreased apoptosis). To further explore this differential mechanism of activity for p53-CC (or p53-CCmutE34K-R55E) and wt p53 and their abilities to regulate transcription of target genes, chromatin immunoprecipitation (chIP) analysis will be conducted (5, 6). A chIP will allow for us to further investigate whether the ability of p53-CC to induce higher levels of apoptosis in the MDA-MB-468 breast cancer model is due to increased binding and transcriptional activation of apoptotic target genes. Additionally, this assay may offer insights into how p53-CC and wt-p53 differ in binding and activating various p53 target genes. Finally, the data obtained from the chIP assay conducted in MDA-MB-468 cells and/or tumor tissues will be compared with data from chIP assays carried out in other cell lines. This comparison will allow for identification of the difference in target gene activation by p53-CC chimeras and wt p53. In addition, efficacy data shown in our studies (Chapters 3, 4, and 5) in multiple cell lines (MCF-7, T47D, H1373, HeLa, MDA-MB-468, SKOV-3ip1, MDA-MB-231 and others) isolated from different types of cancer (breast cancer, lung cancer, ovarian cancer) suggest that the tumor suppressor function of our chimeric p53 is universal, and is independent of the endogenous p53 status or the cancer type.

6.2.2 Further Optimizations of Our Chimeric p53

Since our main goal is to create a chimeric p53 that will be an effective therapeutic for TNBC and virtually all other types of cancers, we continue to pursue

enhancement and optimization of our p53-CC chimera. One such enhancement is achieved by introducing mutations on p53-CC that can result in increased induction of apoptosis. This can be highly beneficial since cell death induction is one of the main purposes for development of a successful cancer therapeutic. To increase apoptosis, we have explored introducing mutations in the DBD of p53 to favor apoptosis over DNA repair (7); DNA repair is undesired since it runs counter to cell-killing. The selection of these functions depends on sequence-specific recognition of p53 to a target decameric sequence of gene promoters. For most apoptotic and cell cycle gene promoters, position 9 of the target DNA decameric sequence is a cytosine (C9) while for DNA repair gene promoters; thymine (T9) is found instead. Therefore, selective binding to the C9 cytosine may transcribe apoptotic gene promoters and induce apoptosis and cell cycle arrest. Molecular modeling indicated that substitution of a hydrophilic residue, A276S, would prefer binding to C9 of the target DNA whereas substitution of a hydrophobic residue (A276F) would fail to do so (8). Indeed, A276S-p53 showed higher transcription of apoptotic (PUMA, PERP) and cell cycle arrest promoters (p21WAF1/CIP1) containing a C9 and lower transcription of a DNA repair promoter (GADD45) containing a T9 compared to wild-type p53. Apoptotic assays and cell cycle analysis also proved the superiority of A276S over wt p53 for inducing apoptosis of cancer cells (7). Therefore, we will introduce the A276S mutation on our lead candidate p53-CCmutE34K-R55E chimera, and further test this will lead to an increase in apoptotic activity.

We will also computationally design and model more mutations in the CC domain (9) which will be designed to: 1) strengthen dimer/tetramer binding that may lead to an increase in activity, and 2) examine the CC domain for other possible mutations that can

result in enhanced ‘knobs-into-holes’ packing originally proposed by Crick in 1952 (10). So far, we have only introduced mutations to enhance the stability and specificity of the dimeric interaction interface of the coiled-coil domain. We hypothesize that further examination of the essential residues involved in the interactions responsible for the tetramerization of the coiled-coil may offer additional mutation sites that could increase the stability, and consequently the activity, of our chimeric p53. Lastly, since our coiled-coil domain adopts an α -helical secondary structure, we can use nearest-neighbor analysis coupled with computational modeling to rationally substitute residues that will lead to increased stabilization of our p53 chimeras (11-13).

6.2.3 Test the Activity of the Enhanced

Version of p53-CC *In Vivo*

Further *in vitro* activity studies are needed to validate the tumor suppressor function of our lead mutant candidate p53-CCmutE34K-R55E. The following apoptotic and cell proliferation assays will be performed: caspase-3, TUNEL, Annexin-V, 7-AAD, and colony forming assay. Once the activity of p53-CcmutE34K-R55E is validated, we will compare its activity with that of p53-CC *in vivo* in the same MDA-MB-468 orthotopic breast cancer tumor model as we have done before. However, prior to starting the animal studies, the p53-CcmutE34K-R55E will be cloned into an adenoviral vector (Ad-p53-CcmutE34K-R55E).

If initial tumor regression studies here are successful, we will use the well-established HCI-003 patient graft model (14) with mutant p53, and additional mutant p53 tumor grafts that may become available later. The patient-derived tumor graft models will

be used to determine if Ad-p53-CcmutE34K-R55E can prevent tumor recurrence, and prevent metastases. Although the HCI-003 patient graft model is not characterized as a triple negative breast cancer, it is an aggressive and highly metastatic breast cancer model that is clinically relevant. While metastases have been found at 4-5 months for most tumors in this bank, the minimum latency required for detectable metastases has not yet been determined (14). Furthermore, this tumor graft spontaneously metastasizes to clinically relevant sites and is therefore an ideal model in which to test the efficacy of our constructs.

In addition, co-engraftment of the original tumor mesenchymal stem cells will maintain natural angiogenesis and hence, phenotypic tumor growth of the primary human tumor (14). These types of experiments may require additional adenovirus construct dosing and some empirical determination of onset/determination metastases. Finally, the effect of p53-CcmutE34K-R55E on mice bearing patient grafts derived from *metastatic* pleural effusions (14) would be tested as well. Toxicity, efficacy, and biodistribution studies will be carried out as well to determine the feasibility and safety of using our lead therapeutic (p53-CcmutE34K-R55E) in the clinic. Since it has been shown before that adenovirus delivery of wt-p53 (Advexin™) has a proven record of safety but marginal therapeutical success for cancer gene therapy in humans, adenoviral delivery of p53-CcmutE34K-R55E will be used in a clinical trial following the *in vivo* studies.

Similar to Advexin™, our biological therapeutic Ad-p53-CcmutE34K-R55E can be used both as monotherapy and in combination with radiation and/or chemotherapy agents (15-17). However, we expect our therapeutic candidate (p53-CcmutE34K-R55E) to exceed the efficacy observed with Advexin™ in the Phase III clinical trials due to its

ability to evade transdominant inhibition, while maintaining a safe profile in for clinical use in cancer patients. In addition, we may consider other viral vectors (e.g., adeno-associated virus) as well as other nonviral vectors (e.g., WSLP) with better safety profiles in the clinic compared to adenoviral vectors for delivery of our therapeutics.

6.2.4 Combinational Gene Therapy with Proteasomal

Protein Switch and Chimeric p53-CC

Although the novel design of p53-CC chimera with an alternative oligomerization domain allows it to escape transdominant inhibition by mutant p53, certain types of mutant p53 exhibit ‘gain of function’ that can promote cancer cell survival (18-20). Hence, it is essential to address these oncogenic functions of mutant p53 in cancer cells. Our multitarget approach takes advantage of the combination therapy concept that has proven effective in cancer treatment. We will deliver a combination therapeutic consisting of two gene loads: 1) the chimeric p53-CC gene and 2) a gene encoding for proteasomal protein switch that is capable of targeting endogenous mutant p53 to the proteasome for degradation. This proteasomal protein switch was previously developed in our lab by Rian Davis (21). The starting point for this was our nuclear protein switch (PS), which consists of a ligand inducible nuclear import signal and an export signal to control the localization to the nucleus (22, 23). The localization is strictly controlled by a dexamethasone-specific ligand-binding domain from the glucocorticoid receptor (GR). Finally, to allow this protein switch to target the proteasome, the nuclear protein switch was fused to full-length p53. Upon ligand addition, the proteasomal protein switch translocates to the nucleus (as expected), and the p53 portion of it binds MDM2 found at

the nucleus. This p53-MDM2 binding allows the ubiquitination of the p53 segment of the proteasomal switch and targets the entire complex for degradation at the proteasome. Therefore, we can fuse our proteasomal protein switch (PS-p53) to the tetramerization domain of p53 (TD) and create a new version of proteasomal switch (PS-p53-TD). In theory, the PS-p53-TD should be able to interact with endogenous mutant p53 via the TD, and subsequently target it for proteasomal degradation. Hence, our combination therapy approach offers 1) introduction of the superactive tumor suppressor p53-CC chimera, and 2) targeting the oncogenic mutant p53 for proteasomal degradation and eliminating its 'gain of function.'

6.2.5 Using Chimeric p53-CC for Treatment of Cancers

in Patients with Li-Fraumeni Syndrome

Li-Fraumeni Syndrome (LFS) is a rare disorder that is characterized by genetic germline *TP53* mutation(s) that lead to inherited predisposition for cancer (24-26). Unlike other predisposition syndromes, LFS is not associated with site-specific cancers. Instead, LFS is linked with a variety of different tumors and leukemias, occurring over a wide age range. However, recent studies revealed that LFS can be correlated to increased disposition for acquiring sarcomas, lung, pancreatic, and premenopausal breast carcinoma. Therefore, individuals identified to have inherited LFS are recommended to undergo organ-targeted surveillance. Once diagnosed, treatment for cancer patients with LFS does not differ from those without LFS, except for an increased risk for radiation-induced cancer for individuals with LFS. Hence, radiation therapy is often avoided for individuals diagnosed with LFS.

Several reports have shown that tumor cells with dysfunctional p53 are very responsive to p53-based therapy aimed to reactivate the p53 pathway (27-29). Since patients with LFS carry a dysfunctional copy of the tumor suppressor p53, treatment of their cancers using our chimeric p53 should be extremely beneficial. For patients with solid tumors, adenoviral delivery of the chimeric p53-CC is feasible (15-17) and should lead to remission and/or stabilization of patients' cancers. To validate this, we would obtain LFS patients' tumor samples and test the efficacy of p53-CC *in vitro*. Furthermore, adenovirus gene therapy with chimeric p53-CC will then be tested *in vivo* using the p53^{+/-}, p53R270H⁻, and p53R172H⁻ well established LFS mouse models (29, 30). If this proves safe and effective, we will pursue first-in-man clinical trials of our chimeric p53-CC lead therapeutic candidates. Although beneficial mainly for solid tumors due to delivery hurdles (e.g., head and neck cancer), the chimeric p53-CC can be used in several other carcinomas with poor prognosis. If delivery issues can be overcome, p53-CC chimera gene therapy would have great potential for treating pancreatic cancer, ovarian cancer, and other incurable cancers.

6.3 References

1. O. Metzger-Filho, A. Tutt, E. de Azambuja, K.S. Saini, G. Viale, S. Loi, I. Bradbury, J.M. Bliss, H.A. Azim, Jr., P. Ellis, A. Di Leo, J. Baselga, C. Sotiriou, and M. Piccart-Gebhart. Dissecting the heterogeneity of triple-negative breast cancer. *J Clin Oncol.* 30:1879-1887 (2012).
2. D.J. Junk, L. Vrba, G.S. Watts, M.M. Oshiro, J.D. Martinez, and B.W. Futscher. Different mutant/wild-type p53 combinations cause a spectrum of increased invasive potential in nonmalignant immortalized human mammary epithelial cells. *Neoplasia.* 10:450-461 (2008).
3. L.Y. Lim, N. Vidnovic, L.W. Ellisen, and C.O. Leong. Mutant p53 mediates survival of breast cancer cells. *British Journal of Cancer.* 101:1606-1612 (2009).

4. A. Okal, M. Mossalam, K.J. Matissek, A.S. Dixon, P.J. Moos, and C.S. Lim. A chimeric p53 evades mutant p53 transdominant inhibition in cancer cells. *Mol Pharm.* 10:3922-3933 (2013).
5. C.-L. Wei, Q. Wu, V.B. Vega, K.P. Chiu, P. Ng, T. Zhang, A. Shahab, H.C. Yong, Y. Fu, Z. Weng, J. Liu, X.D. Zhao, J.-L. Chew, Y.L. Lee, V.A. Kuznetsov, W.-K. Sung, L.D. Miller, B. Lim, E.T. Liu, Q. Yu, H.-H. Ng, and Y. Ruan. A global map of p53 transcription-factor binding sites in the human genome. *Cell.* 124:207-219 (2006).
6. N.A. Barlev, L. Liu, N.H. Chehab, K. Mansfield, K.G. Harris, T.D. Halazonetis, and S.L. Berger. Acetylation of p53 activates transcription through recruitment of coactivators/histone acetyltransferases. *Molecular Cell.* 8:1243-1254 (2001).
7. S. Reaz, M. Mossalam, A. Okal, and C.S. Lim. A single mutant, A276S of p53, turns the switch to apoptosis. *Mol Pharm.* 10:1350-1359 (2013).
8. S. Reaz, M. Mossalam, A. Okal, and C.S. Lim. A single mutant, A276S of p53, turns the switch to apoptosis. *Mol Pharm* (2013).
9. A.S. Dixon, S.S. Pendley, B.J. Bruno, D.W. Woessner, A.A. Shimpi, T.E. Cheatham, 3rd, and C.S. Lim. Disruption of Bcr-Abl coiled coil oligomerization by design. *J Biol Chem.* 286:27751-27760 (2011).
10. F.H.C. Crick. {The packing of alpha-helices: simple coiled-coils}. *Acta Crystallographica.* 6:689-697 (1953).
11. A.K. Dunker and T.C. Jones. Proposed knobs-into-holes packing for several membrane proteins. *Molecular Membrane Biology.* 2:1-16 (1978).
12. D. Langosch and J. Heringa. Interaction of transmembrane helices by a knobs-into-holes packing characteristic of soluble coiled coils. *Proteins: Structure, Function, and Bioinformatics.* 31:150-159 (1998).
13. J.B.B. Ridgway, L.G. Presta, and P. Carter. 'Knobs-into-holes' engineering of antibody CH3 domains for heavy chain heterodimerization. *Protein Engineering.* 9:617-621 (1996).
14. Y.S. DeRose, G. Wang, Y.C. Lin, P.S. Bernard, S.S. Buys, M.T. Ebbert, R. Factor, C. Matsen, B.A. Milash, E. Nelson, L. Neumayer, R.L. Randall, I.J. Stijleman, B.E. Welm, and A.L. Welm. Tumor grafts derived from women with breast cancer authentically reflect tumor pathology, growth, metastasis and disease outcomes. *Nat Med.* 17:1514-1520 (2011).
15. J. Nemunaitis, G. Clayman, S.S. Agarwala, W. Hrushesky, J.R. Wells, C. Moore, J. Hamm, G. Yoo, J. Baselga, B.A. Murphy, K.A. Menander, L.L. Licato, S. Chada, R.D. Gibbons, M. Olivier, P. Hainaut, J.A. Roth, R.E. Sobol, and W.J. Goodwin. Biomarkers predict p53 gene therapy efficacy in recurrent squamous cell carcinoma of the head and neck. *Clinical Cancer Research.* 15:7719-7725 (2009).
16. D.I. Gabrilovich. INGN 201 (Advexin®): adenoviral p53 gene therapy for cancer. *Expert Opin Biol Ther.* 6:823-832 (2006).

17. N. Senzer and J. Nemunaitis. A review of contusugene ladenovec (Advexin) p53 therapy. *Curr Opin Mol Ther.* 11:54-61 (2009).
18. M. Oren and V. Rotter. Mutant p53 gain-of-function in cancer. *Cold Spring Harb Perspect Biol.* 2:a001107 (2010).
19. M.G.C.T. van Oijen and P.J. Slootweg. Gain-of-function mutations in the tumor suppressor gene p53. *Clinical Cancer Research.* 6:2138-2145 (2000).
20. M.V. Blagosklonny. p53 from complexity to simplicity: mutant p53 stabilization, gain-of-function, and dominant-negative effect. *The FASEB Journal.* 14:1901-1907 (2000).
21. J.R. Davis, M. Mossalam, and C.S. Lim. Controlled access of p53 to the nucleus regulates its proteasomal degradation by MDM2. *Mol Pharm.* 10:1340-1349 (2013).
22. T. Ylikomi, M.T. Bocquel, M. Berry, H. Gronemeyer, and P. Chambon. Cooperation of proto-signals for nuclear accumulation of estrogen and progesterone receptors. *The EMBO Journal.* 11:3681-3694 (1992).
23. E. Vegeto, G.F. Allan, W.T. Schrader, M.J. Tsai, D.P. McDonnell, and B.W. O'Malley. The mechanism of RU486 antagonism is dependent on the conformation of the carboxy-terminal tail of the human progesterone receptor. *Cell.* 69:703-713 (1992).
24. F.P. Li and J.F. Fraumeni, Jr. Soft-tissue sarcomas, breast cancer, and other neoplasms. A familial syndrome? *Ann Intern Med.* 71:747-752 (1969).
25. D. Malkin, F. Li, L. Strong, J. Fraumeni, C. Nelson, D. Kim, J. Kassel, M. Gryka, F. Bischoff, M. Tainsky, et al. Germ line p53 mutations in a familial syndrome of breast cancer, sarcomas, and other neoplasms. *Science.* 250:1233-1238 (1990).
26. M. Hisada, J.E. Garber, F.P. Li, C.Y. Fung, and J.F. Fraumeni. Multiple primary cancers in families with Li-Fraumeni syndrome. *Journal of the National Cancer Institute.* 90:606-611 (1998).
27. N. Senzer, J. Nemunaitis, M. Nemunaitis, J. Lamont, M. Gore, H. Gabra, R. Eeles, N. Sodha, F.J. Lynch, L.A. Zumstein, K.B. Menander, R.E. Sobol, and S. Chada. p53 therapy in a patient with Li-Fraumeni syndrome. *Molecular Cancer Therapeutics.* 6:1478-1482 (2007).
28. J.M. Nemunaitis and J. Nemunaitis. Potential of Advexin: a p53 gene-replacement therapy in Li-Fraumeni syndrome. *Future Oncology.* 4:759-768 (2008).
29. M. Olivier, A. Petitjean, V. Marcel, A. Petre, M. Mounawar, A. Plymoth, C.C. de Fromental, and P. Hainaut. Recent advances in p53 research: an interdisciplinary perspective. *Cancer Gene Therapy.* 16:1-12 (2009).
30. L.A. Donehower. The p53-deficient mouse: a model for basic and applied cancer studies. *Seminars in Cancer Biology.* 7:269-278 (1996).